Characterizations of and closed-form solutions for plain vanilla and exotic derivatives

Author:
Thul, Matthias

Publication Date:
2013

DOI:
https://doi.org/10.26190/unsworks/19425

Characterizations of and Closed-Form Solutions for Plain Vanilla and Exotic Derivatives

Matthias Thul

A thesis in partial fulfilment of the requirements for the degree of

Doctor of Philosophy (Ph.D.) in Finance

School of Banking and Finance

Australian School of Business

University of New South Wales

August 2013

To my parents Antje and Wolfgang Thul, for enabling me to embark on this journey.

To my fiancée Ally Quan Zhang, whose love and support made it even more enjoyable and helped me to conclude it.

THE UNIVERSITY OF NEW SOUTH WALES
Thesis/Dissertation Sheet

Surname or Family name: **Thul**

First name: **Matthias** Other name/s:

Abbreviation for degree as given in the University calendar: **PhD**

School: **School of Banking & Finance** Faculty: **Australian School of Business**

Title: **Characterizations of and Closed-Form Solutions for Plain Vanilla and Exotic Options**

Abstract 350 words maximum:

This dissertation is composed of three stand-alone research projects on the valuation of contingent claims.

The first essay proposes an extension of the Kou (2002) double exponential jump-diffusion model. Displacing the two exponential tails introduces additional degrees of asymmetry in the jump size distribution. The model dynamics are supported by a general equilibrium framework. Our main contribution is to derive closed-form solutions for European plain vanilla options. A further extension to displaced gamma tails is possible while retaining full analytical tractability. We propose an efficient routine to estimate the physical model parameters through maximum likelihood. Our empirical analysis covers a diverse sample of assets across equities, commodities and foreign exchange. We find that for the vast majority of assets, the original Kou (2002) model can be rejected in favour of our newly introduced displaced double exponential dynamics.

The second essay proposes an approach to valuation and risk management of deferred start barrier options within the Black and Scholes (1973) framework. We provide closed-form solutions which are functions of the implied volatility smile. Our barrier options are contingent claims on two perfectly correlated assets that diffuse with different volatilities. While the terminal payoff is a function of one of the assets, the barrier trigger is determined by the path of the other. To mitigate the dynamic hedging problems associated with large discontinuous sensitivities, we suggest the application of an additional exponential bending of the barrier close to maturity. By generalizing the method of images, we obtain closed-form solutions for both deferred start piecewise exponential barrier options and associated rebates.

The third essay models logarithmic asset prices under the physical probability measure as additive jump-diffusion processes. The corresponding risk-neutral probability measure is defined through an Esscher transform. We are interested in the conditions under which the jump size distributions under the two probability measures fall into the same parametric class. We show that it is both necessary and sufficient for the jump size distribution to follow a natural exponential mixture family at all points of time. Examples for applications of this result in financial engineering are provided.

FOR OFFICE USE ONLY Date of completion of requirements for Award:

Originality Statement

"I hereby declare that this submission is my own work and to the best of my knowledge it contains no materials previously published or written by another person, or substantial proportions of material which have been accepted for the award of any other degree or diploma at UNSW or any other educational institution, except where due acknowledgement is made in the thesis. Any contribution made to the research by others, with whom I have worked at UNSW or elsewhere, is explicitly acknowledged in the thesis. I also declare that the intellectual content of this thesis is the product of my own work, except to the extent that assistance from others in the project's design and conception or in style, presentation and linguistic expression is acknowledged."

Sydney, August 30, 2013 Matthias Thul

COPYRIGHT STATEMENT

AUTHENTICITY STATEMENT

Abstract

This dissertation is composed of three stand-alone research projects on the valuation of contingent claims.

The first essay proposes an extension of the Kou (2002) double exponential jump-diffusion model. Displacing the two exponential tails introduces additional degrees of asymmetry in the jump size distribution. The model dynamics are supported by a general equilibrium framework. Our main contribution is to derive closed-form solutions for European plain vanilla options. A further extension to displaced gamma tails is possible while retaining full analytical tractability. We propose an efficient routine to estimate the physical model parameters through maximum likelihood. Our empirical analysis covers a diverse sample of assets across equities, commodities and foreign exchange. We find that for the vast majority of assets, the original Kou (2002) model can be rejected in favour of our newly introduced displaced double exponential dynamics.

The second essay proposes an approach to valuation and risk management of deferred start barrier options within the Black and Scholes (1973) framework. We provide closed-form solutions which are functions of the implied volatility smile. Our barrier options are contingent claims on two perfectly correlated assets that diffuse with different volatilities. While the terminal payoff is a function of one of the assets, the barrier trigger is determined by the path of the other. To mitigate the dynamic hedging problems associated with large discontinuous sensitivities, we suggest the application of an additional exponential bending of the barrier close to maturity. By generalizing the method of images, we obtain closed-form solutions for both deferred start piecewise exponential barrier options and associated rebates.

The third essay models logarithmic asset prices under the physical probability measure as additive jump-diffusion processes. The corresponding risk-neutral probability measure is defined through an Esscher transform. We are interested in the conditions under which the jump size distributions under the two probability measures fall into the same parametric class. We show that it is both necessary and sufficient for the jump size

distribution to follow a natural exponential mixture family at all points of time. Examples for applications of this result in financial engineering are provided.

Bibliography

Black, Fischer and Myron S. Scholes (1973) "The Pricing of Options and Corporate Liabilities," *Journal of Political Economy*, Vol. 3, No. 3, pp. 637–654.

Kou, Steven G. (2002) "A Jump-Diffusion Model for Option Pricing," *Management Science*, Vol. 48, No. 8, pp. 1086–1101.

Acknowledgements

This dissertation would not have been completed without the support of many people. I would like to take the opportunity to express my gratitude to those who helped and supported me through the journey of my PhD study.

Foremost, I would like to express my deepest gratitude to my advisors, Dr. David Colwell and Prof. David Feldman, for their critical guidance and continuous support throughout my studies. They both always had an open-door policy and I thank them for the many hours that they dedicated to discussing my research. This dissertation strongly benefited from their constructive comments.

I would like to thank Prof. Wolfgang Bühler, whose extraordinary scholarship never failed to inspire me. Being his teaching assistant for both an undergraduate and postgraduate course was an invaluable experience. He set an example for me through his attention for detail and deep economic understanding.

This dissertation benefited from editing services by Elite Editing, Adelaide. Dr. Colwell and Ally Quan Zhang both meticulously worked through the mathematical derivations and proofread the entire dissertation.

I appreciate the friendship and support from my fellow PhD students, in particular Sarah Azzi-Södergren, Pavle Radicevic, Lee Smales and Sidharth Sahgal. They also never failed to provide some welcome distraction from my research.

I am grateful to my former and future colleagues in the equity derivatives trading team at Commerzbank AG in Frankfurt am Main. The motivation for Chapter III is based on insights that I gained through my work experience.

Prof. Wolfgang Schmidt and Prof. Uwe Wystup deserve my special thanks. Their lectures at Frankfurt School of Finance & Management sparked my passion for financial engineering and motivated me to pursue further postgraduate studies.

I am grateful to the two external examiners of this thesis, Prof. Uwe Wystup and Prof. Alexandre Ziegler. They provided highly valuable comments and suggestions that helped to further improve it.

I am grateful for the financial support that I received from the Australian School of Business and the University of New South Wales. The empirical results in this dissertation could not have been obtained without access to the university's cluster computing resources. I would also like to express my gratitude to the administrative staff at the School of Banking & Finance, in particular Ashley Coull, Stephanie Osborne, Marie Simmons and Shirley Webster.

Lastly and most importantly, I would like to thank my fiancée Ally Quan Zhang and my parents Antje Thul and Wolfgang Thul. Without their love and unconditional support, this endeavour would have not been possible. This dissertation is dedicated to them.

Contents

List of Tables

List of Figures

Chapter I

Introduction

The recent decades since the opening of the Chicago Board Options Exchange (CBOE) in 1973 have seen a substantial increase of the global turnover in contingent claims. The Bank for International Settlement (2013) reports a total notional amount outstanding of 685,039 billion USD as of December 2012, 92.34% of which is attributed the over-the-counter (OTC) market. This amounts to a more than fourfold increase over a period of ten years, despite the global financial crisis of 2007 and 2008 which had a particularly strong and negative impact on the market for credit derivatives. Figure I.1 shows the corresponding time series for equity, commodity and foreign exchange underlying assets. This increased trading volume can be both attributed to a higher liquidity in standard derivative products, such as forwards and plain vanilla options, and the increased popularity of more exotic payoff profiles.

These developments represent major challenges to academics and practitioners alike.

(i) First, they necessitate the development of consistent valuation frameworks that are both able to reflect the stylized empirical facts of the historical time series of returns and jointly explain the cross section of observable contingent claim prices. In particular, this commonly involves a calibration of the risk-neutral model dynamics to the Black and Scholes (1973) implied volatility surface for plain vanilla options.

(ii) Second, the increased liquidity in so-called flow derivatives, which are traded in continuous markets and include, among others, plain vanilla, binary and barrier options, creates a need for pricing functions that are numerically stable and fast to evaluate. As computational resources are limited, this objective is usually conflicting with the one previously mentioned. Often, model complexity is sacrificed for the ability to price contingent claims in closed-form.

(iii) Lastly, they demand for a robust dynamic hedging and risk management. This is especially crucial for contingent claims that exhibit discontinuities in their payoff profile.

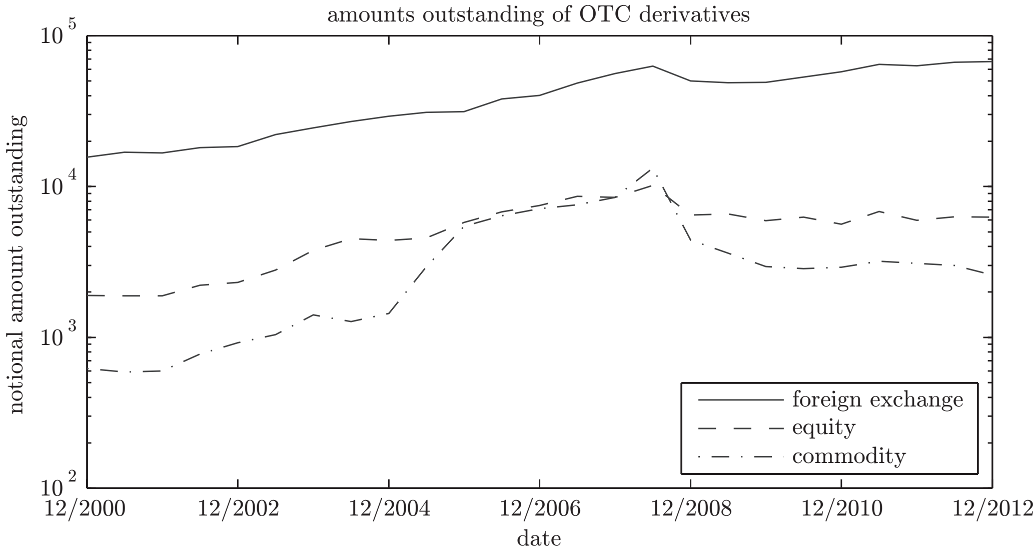

Figure I.1: Total amounts outstanding of OTC derivatives on foreign exchange, equities and commodities in billion USD. The y-axis is scaled logarithmically. Source: Bank for International Settlement quarterly reviews.

This dissertation is composed of three independent research projects, each of which is concerned with one or more of the above objectives. Our analysis applies to equity, commodity and foreign exchange markets alike. In what follows we briefly outline the research questions in Chapters II through IV. Each chapter is self-contained and presents a more detailed motivation as well as an extensive literature review. Chapter V briefly concludes this dissertation, summarizes its main contributions and discusses potential avenues of future research.

In Chapter II, we expand on previous work by Kou (2002) and propose a novel jump-diffusion model for asset prices. One of the key feature of our dynamics is their highly flexible jump size distribution, which generalizes the Kou (2002) double exponential model in two directions. First, it independently displaces the two exponential tails away from the origin. Second, it allows for each of the displaced tails to follow a gamma distribution with an integer-valued shape parameter. The newly introduced degrees of freedom represent additional means to control the higher moments of the corresponding logarithmic return distribution. Despite its increased complexity, our model still admits closed-form solutions for European plain vanilla options, thus pushing the boundary of the aforementioned trade-off between Objectives (i) and (ii). To provide an economic foundation of our proposed dynamics, we show that they are supported by an equilibrium economy in which a representative agent faces a infinite horizon consumption and portfolio choice problem.

This equilibrium also implies a risk-neutral probability measure under which both the diffusion and jump risk are priced.

This extension is not only academically interesting but succeeds at capturing statistical properties that are consistently present in asset returns. We advocate the use of maximum likelihood estimation to infer the physical model parameters from the historical time series of logarithmic returns due to its asymptotic efficiency. It furthermore requires no discretionary choices when defining the estimation objective. A computationally efficient routine to simultaneously evaluate the likelihood function for the full time series is discussed. Based on a diverse sample of assets, we find strong empirical support for non-zero displacements. The original Kou (2002) model can be rejected in favor of our newly introduced model dynamics in all cases.

Chapter III discusses the valuation and risk management of deferred start barrier options, where the monitoring window is limited to the some closed interval including the option maturity. It is related to the Objectives (ii) and (iii) above. When the underlying dynamics do not follow a constant coefficient Brownian motion, these contingent claims generally need to be priced through numerical approximation routines due to the complexity of their payoff profiles. However, even within the Black and Scholes (1973) setting, it is not clear how the diffusion coefficient should be chosen when the implied volatility exhibits a strike-dependent smile pattern. One remedy to this problem is to use an outside barrier option approach, where the terminal payoff and the barrier trigger are determined by two distinct but perfectly correlated assets that diffuse at different volatilities. We show that this is equivalent to valuing a deferred start exponential barrier option on a single asset.

While this so-called two-volatility approach yields a smile adjusted pricing, it does not by itself improve the robustness of the corresponding replication portfolios in real-world markets. The dynamic risk-management of reverse knock-out barrier options is particularly challenging due to the discontinuity in their payoff profiles. They exposes the holder of the short position to a substantial gap risk when the underlying asset price does not evolve as a pure diffusion process but exhibits jumps. To mitigate this problem, we suggest to employ a functional form for the barrier shift that explicitly takes the time-dependent nature of the risk exposure into account. We show that there again exists an equivalent single asset valuation problem in terms of a deferred start piecewise exponential barrier option.

The second half of Chapter III derives the prices for these types of contingent claims and their associated rebates. It represents our main contribution. The valuation problem is simplified considerable by introducing the image operator for exponentially bent barriers. We explicitly establish its connection to an appropriately chosen coordinate transformation applied to the Black and Scholes (1973) partial differential equation and the evaluation of a risk-neutral conditional expectation. By considering the contingent claims as nested compound options, we can iteratively derive their valuation functions, moving backwards in time. We obtain closed-form solutions in terms of higher-order binary options and their respective images that can be readily evaluated using standard statistical libraries. A Monte Carlo simulation study confirms that a time-dependent barrier shift *ceteris paribus* yields more robust dynamic hedges.

Chapter IV considers a model-independent question related to the class of additive jump-diffusion dynamics. It is linked to Objective (i) above. We consider logarithmic asset prices that follow a jump-diffusion process with a possibly time-dependent jump intensity and jump size distribution. The corresponding risk-neutral measure is generally not unique, if it exists. A common construction is to define the Radon-Nikodým derivative process through an Esscher transform of the logarithmic return process; see for example Gerber and Shiu (1994). We are interested in conditions under which the jump size distributions under the two probability measures fall into the same parametric class. We argue that this is not only a desirable property from a modeling point of view but it also simplifies the valuation problem for European plain vanilla options considerably. Our main finding is that additive jump-diffusion processes whose jump sizes follow a natural exponential mixture distribution at all points in time are closed under an Esscher transform measure change. Furthermore, we fully characterize the dynamics under the new probability measure and illustrate our results through various examples.

Bibliography

Bank for International Settlement (2013) "Statistical Annex to June 2013 Quarterly Review," Jun. available at http://www.bis.org/.

Black, Fischer and Myron S. Scholes (1973) "The Pricing of Options and Corporate Liabilities," *Journal of Political Economy*, Vol. 3, No. 3, pp. 637–654.

Gerber, Hans U. and Elias S. W. Shiu (1994) "Option Pricing by Esscher Transforms," *Transactions of Society of Actuaries*, Vol. 46, pp. 99–191.

Kou, Steven G. (2002) "A Jump-Diffusion Model for Option Pricing," *Management Science*, Vol. 48, No. 8, pp. 1086–1101.

Chapter II

Analytical Option Pricing under a Displaced Double Exponential Jump-Diffusion Model

We propose an extension of the Kou (2002) jump-diffusion model. By independently displacing each of the two exponential tails of the jump size distribution away from the origin, we introduce additional flexibility in the tails of the corresponding return distribution. Our model is supported by an equilibrium economy and we obtain closed-form solutions for European plain vanilla options. Our solution is computationally fast to evaluate and robust across the full parameter space. We further allow generalization to displaced gamma tails while retaining full analytical tractability. We propose an efficient routine to estimate the physical model parameters through maximum likelihood. Our empirical analysis covers a diverse sample of equities, commodities and exchange rates. For all assets, the original Kou (2002) model can be rejected in favor of our newly introduced asymmetrically displaced double exponential dynamics.

Keywords: displaced double exponential, jump-diffusion, option pricing, maximum likelihood estimation

JEL Classification: C13, G13
MS Classification (2010): 60G51

II.1 Introduction

Over the 40 odd years since the publication of the seminal articles by Black and Scholes (1973) and Merton (1973), a large strand of the option pricing literature has been devoted to generalizing the mostly unrealistic assumption of the underlying asset price following a geometric Brownian motion and the corresponding normal distribution of logarithmic returns. This misspecification is unveiled in the model's strong pricing biases first reported by Rubinstein (1985); see also the review in Bates (1996a). The central issue in this field is thus to develop price dynamics that are both consistent with the observed option prices and the empirical properties of the return distribution.

While option valuation through Monte Carlo simulation is possible even under very general assumptions, the availability of computational fast and numerically stable algorithms is crucial for their practical applicability. Computational speed is particularly important for the class of European plain vanilla options, as these are usually liquidly traded and serve as the reference prices that the risk-neutral model parameters are calibrated against. It is thus of high interest to develop generalized model dynamics that still admit a (quasi-)analytical solution for European plain vanilla call and put options.

Analytical or closed-form solutions are those, where the option price can be expressed in terms of a (possibly infinite) series of elementary and special functions. We explicitly distinguish analytical solutions from quasi-analytical ones, which might also involve limits of some kind. In particular, this excludes expressions in terms of integrals which have to be evaluated through numerical quadrature routines. The distinction, though essential, is often ignored in the literature. In what follows, we briefly discuss the most important models and classify them accordingly. This overview is by no means exhaustive.

II.1.1 Literature Review

Very few non-trivial models admit genuine analytical solutions. First among these is Merton (1976), who extends the geometric Brownian motion by introducing normally distributed compound Poisson jumps to the logarithmic stock price process. The jumps are considered to represent purely idiosyncratic shocks and are thus not priced. European plain vanilla options can be valued analytically through an infinite summation over Black and Scholes (1973) prices with exponentially decaying summands. Cox and Ross (1976) consider various alternative pure diffusion and pure jump models, where the jump size is a non-random function of the stock price immediately preceding it. This assumption renders the contingent claims redundant assets and allows for perfect replication. The authors obtain closed-form solutions in the special cases of proportional jumps, constant volatility and proportional variance. Kou (2002) introduces asymmetry to the discontinuous return component by modeling the jumps to follow a double exponential (DE) distribution. He derives closed-form expressions for the tail probabilities under the two relevant pricing measures; see also Kou and Wang (2003, 2004).

To account for the heteroscedasticity observed in empirical returns, several different stochastic volatility models have been suggested. Wiggins (1987) models the logarithmic volatility as an Ornstein-Uhlenbeck process correlated with the underlying asset and relies on a two-dimensional finite difference scheme for pricing. Hull and White (1987) show that when volatility risk is non-systematic, the values of European plain vanilla option can be expressed in a quasi-analytical fashion as the Black and Scholes (1973) price integrated over the distribution of the mean variance until maturity, given that at least the latter is known in closed-form. Stein and Stein (1991) also consider the case of independent spot and volatility dynamics and show that while the density of the mixing distribution is not available when the volatility follows an Ornstein-Uhlenbeck process, its characteristic function can be obtained in closed-form. This allows the authors to price general European contingent claims through Fourier inversion in terms of a double integral, which has to be evaluated numerically.

In a seminal paper, Heston (1993) models the stock price as a diffusion process whose variance itself follows a Cox et al. (1985) square-root process. Given closed-form expressions for the characteristic functions of the logarithmic terminal spot price under the two relevant numéraires, he obtains the corresponding exercise probabilities through a numerical Fourier inversion. This model independent approach yields European plain vanilla option pricing formulas, which are very similar in structure to the ones obtained by Black and Scholes (1973). Quasi-analytical Fourier techniques have since been widely applied to contingent claim valuation since the characteristic function of the logarithmic asset prices is often available under more complex underlying dynamics. We refer to Carr and Madan (1999), Lewis (2001) and Attari (2004) for alternative pricing representations. Bakshi and Madan (2000) provide an economic foundation for valuation using the characteristic function, by showing that it represents an equivalent basis for spanning the payoff universe of most contingent claims. Bates (1996b) adds independent Merton (1973) type jumps to the spot price process. Scott (1997) augments the Heston (1993) stochastic volatility model by a correlated Cox et al. (1985) process for the instantaneous risk-free interest rate and suggests a martingale approach for computing the characteristic functions. Based on these results, Schöbel and Zhu (1999) derive a solution to the characteristic function of the correlated Stein and Stein (1991) model. Bakshi et al. (1997) empirically test different special cases of the Bates (1996b) stochastic volatility and jump-diffusion model with an independent Cox et al. (1985) short-rate process. Duffie et al. (2000) unify much of the previous theoretical work by showing that an affine structure of the drift, covariance matrix, jump intensity and instantaneous interest rate allows us to obtain the Fourier transforms of the relevant random variables in terms of a system of ordinary differential equations (ODEs).

The main limitation of the approaches discussed above is their sole reliance on compound Poisson processes as the sources of jumps. An alternative strand of the literature focuses on modeling the logarithmic stock prices as Lévy processes, which encompass time-homogeneous jump-diffusions as special cases. All relevant models within this class also admit closed-form solutions for the corresponding characteristic functions. Thus, quasi-analytical Fourier techniques can be applied to price European plain vanilla options. Madan et al. (1998) model logarithmic stock prices through a variance gamma process; see also Madan and Senata (1990) and Milne and Madan (1991). They subject a drifted Brownian motion to an independent random time-change given by a gamma process. Barndorff-Nielsen (1998) discusses normal inverse Gaussian processes, where the time-change is given by an independent inverse Gaussian process. Barndorff-Nielsen and Shephard (2001a,b) propose a stochastic volatility model where the instantaneous variance follows a non-Gaussian Ornstein-Uhlenbeck process driven by an independent Lévy subordinator. It allows for simultaneous jumps in the logarithmic return and the volatility processes. Non-Gaussian Ornstein-Uhlenbeck processes are characterized by their stationary distribution; common choices are the inverse Gaussian and the gamma distributions. Geman et al. (2001) consider asset prices driven by purely discontinuous time-changed Brownian motions. Carr et al. (2003) incorporate volatility clustering effects by subjecting various Lévy processes to a stochastic clock whose instantaneous activity follows either a Cox et al. (1985) square-root process or a non-Gaussian Ornstein-Uhlenbeck process. Carr and Wu (2004) capture the leverage effect in equity markets by correlating the Lévy process and the time-change. They retain analytical tractability of characteristic functions by introducing a complex-valued auxiliary measure under which the leverage effect vanishes.

We emphasize that, despite its fairly general applicability and widespread use, a numerical implementation of the Fourier inversion technique that is both fast and stable for the whole parameter space is very intricate. Nevertheless, or maybe even because of its non-trivial nature, most authors avoid an explicit discussion of this issue. The first remark hinting at its inherent complexity can be found in Footnote 7 of Schöbel and Zhu (1999), p. 28. In what follows, we present a brief overview of three typical numerical issues encountered when implementing this approach. While focusing on the representation proposed by Carr and Madan (1999), similar problems arise in alternative formulations of the pricing equations such as in for example Heston (1993), Lewis (2001) or Attari (2004).

First, and as already noted by Carr and Madan (1999), the integrand in their approach becomes highly oscillatory for options that are far out-of-the-money relative to their maturity, thus exacerbating the pricing problem. To circumvent this issue, they consider the Fourier transform of the time value only. Alternatively, Andersen and Andreasen (2002) and Joshi and Yang (2011) suggest to employ the Black and Scholes (1973) model as a control variate, thus stabilizing the numerical Fourier inversion.

Second, the lack of integrability of the European call option price as a function of the logarithmic strike price requires the use of either a dampening factor as in Carr and Madan (1999) or the generalized Fourier transform as in Lewis (2001), where the integration is carried out along a horizontal strip of regularity in the complex plane. As shown by Lord and Kahl (2007), there exists an optimal choice for this contour of integration. It is chosen to minimize the cancellation error that arises due to the limited machine precision when numerically evaluating the integral for far out-of-the-money options; see also Lee (2004), who suggests to minimize the total error from both the numerical evaluation and the necessary truncation of the upper limit of integration.

Finally, the computation of the characteristic functions themselves is not as straightforward as it may seem due to the presence of complex logarithms and square roots. As first explicitly discussed in Schöbel and Zhu (1999), always evaluating the complex logarithms at their principal branch leads to discontinuities. Kahl and Jäckel (2005) propose a rotation-count algorithm that keeps track of the number of crossings of the negative real axis to overcome this problem; see also Lord and Kahl (2006). Albrecher et al. (2007) obtain a representation of the Heston (1993) characteristic function which is numerically stable in an unrestricted parameter space. Lord and Kahl (2010) generalize this result by showing that there exists a formulation of the characteristic function for affine jump-diffusion models where the principal branch is the correct choice.

Lastly, we briefly review some classes of models within which European plain vanilla options need to be priced through purely numerical methods. The most important of these are the local volatility or implied diffusion models proposed by Dupire (1994), Rubinstein (1994), Derman et al. (1995) and Derman et al. (1996). Here, the underlying asset price follows an Itō process. Dupire (1994) shows that an arbitrage-free continuum of European plain vanilla option prices implies a unique time-and-state-dependent diffusion coefficient. While this model perfectly matches any market implied volatility surface, its assumptions about the underlying dynamics largely contradict empirical evidence and yield unrealistic forward implied volatility smiles. Andersen and Brotherton-Ratcliffe (1997) propose an unconditionally stable finite difference lattice for the corresponding partial differential equation. It is first calibrated through forward induction and subsequently evaluated subject to contract-specific terminal and boundary conditions.

II.1.2 Contribution

The previous survey highlights the apparent trade-off between the generality of the model dynamics and the computational tractability of the associated valuation functions. While analytical expressions for the prices of plain vanilla options are often hard to derive in the first place, their numerical implementation is usually straightforward. Besides its preference independence, this is one of the major reasons for the success of the Black and Scholes (1973) option pricing model. Despite their usually faster computational speed, analytical solutions are also superior in terms of numerical stability over the full range of model parameter values. As discussed in Section II.1.1 above, there are many intricacies to be considered in the implementation of quasi-analytical or purely numerical techniques. Closed-form solutions for special cases of these models can serve as pricing benchmarks for their implementation. The higher the complexity of the benchmark dynamics is, the larger the parameter space is which can be used for testing the numerical results.

The contribution of this chapter to the literature is fourfold. First, we introduce a new generalization of the Kou (2002) model that allows for the jump sizes to follow an asymmetrically displaced double exponential (AD-DE) distribution. We derive the statistical properties and propose two approaches to obtain the spot price dynamics under a martingale measure. Second, we show that the model still admits genuinely closed-form solutions for the prices of European plain vanilla options. Although our valuation function appears quite formidable, it is composed entirely of elementary functions that can be readily implemented. Third, we demonstrate that these results can be further generalized to an asymmetrically displaced double gamma (AD-DG) distribution for the jump sizes while still maintaining full analytical tractability. Fourth, we estimate the model parameters under the physical probability measure through maximum likelihood (ML) estimation and based on the historical time series of returns. Our empirical analysis covers a diverse sample of assets, from equity indices over commodity indices to foreign exchange. Statistical tests confirm that for all assets, the asymmetric displacements provide a significantly better fit to the data than both the models with symmetric and no displacements.

The motivation for the generalizations introduced in this chapter is based on the symmetrically displaced double exponential (SD-DE) jump-diffusion dynamics considered by Weber and Wystup (2008) and Detering et al. (2011, 2013). These authors are interested in the performance of different investment strategies for equity-linked retirement plans. They do not consider the valuation problem for European plain vanilla options but instead analyze path-dependent payoff structures under stochastic interest rates. This necessitates the valuation through Monte Carlo simulations. In contrast, this chapter's main contributions is to show that a closed-form solution for European plain vanilla options can be obtained even when considering two further generalizations of their dynamics, asymmetric displacements and gamma tails, both of which are novel. This key property sets our model dynamics apart from other possible parametrizations that might find equal empirical support.

The remainder of this chapter is organized as follows. Section II.2 defines the physical dynamics of the AD-DE jump-diffusion model and derives its statistical properties. Section II.3 discusses two possible constructions of the risk-neutral probability measure. In Section II.4, we show that there exists a model economy such that the asset price follows the postulated dynamics in equilibrium. Section II.5 derives closed-form solutions for European plain vanilla options. Section II.6 further generalizes the model dynamics to jump sizes that follow an AD-DG distribution. Section II.7 discusses alternative estimation approaches based on the time series of logarithmic returns. In Section II.8, we describe the data set and apply ML estimation to infer the physical model parameters. Statistical tests confirm that the newly introduced displacement terms are significant for a wide variety of underlying assets. Finally, Section II.9 summarizes and concludes the chapter. The appendices provide the derivations of various technical results and present the empirical estimation results.

II.2 Model Setup

Let $W = \{W_t : t \in [0, T^*]\}$ be a standard one-dimensional Brownian motion, $N = \{N_t : t \in [0, T^*]\}$ be a one-dimensional Poisson process and $(Y_i)_{i\in\mathbb{N}}$ be a sequence of independent and identically distributed (i.i.d.) random variables on a complete filtered probability space $(\Omega, \mathfrak{F}, \mathbb{F}, \mathbb{P})$. We interpret $\mathbb{P}$ to be the physical or real-world probability measure, and we consider continuous trading in the interval $[0, T^*]$ for a fixed terminal time $0 < T^* < \infty$. The filtration $\mathbb{F} = (\mathfrak{F}_t)_{t\in[0,T^*]}$ is the $\mathbb{P}$-augmentation of the natural filtration induced by the processes W and N and the sequence of random variables $(Y_i)_{i\in\mathbb{N}}$, that is

$$\mathfrak{F}_t = \sigma\left(W_u, N_u : u \in [0, t]; Y_i : i \in \{1, 2, \ldots, N_t\}\right) \vee \mathcal{N},$$

where $\mathcal{N}$ are the corresponding $\mathbb{P}$-null sets. This construction ensures the right-continuity of $\mathbb{F}$; see for example Proposition II.7.7 in Karatzas and Shreve (1991), p. 90. We further assume that the processes W and N as well as the sequence of random variables $(Y_i)_{i\in\mathbb{N}}$ are independent. The Poisson process N has a constant intensity of $\lambda \in \mathbb{R}_+$, and each random variable Y_i follows the probability density function (PDF) $f(x)$.

The frictionless market consists of two assets. The first is a non-dividend paying limited liability spot asset $S = \{S_t : t \in [0, T^*]\}$, which later serves as the underlying asset for contingent claims. In the empirical analysis of Section II.7, we consider S to be the spot or futures price of an equity (index) and a commodity as well as the spot exchange rate between two currencies. The second asset is a money market account $B = \{B_t : t \in [0, T^*]\}$ with non-random dynamics

$$\mathrm{d}B_t = rB_t\mathrm{d}t,$$

where the risk-free interest rate $r \in \mathbb{R}$ is a constant and $B_0 = 1$. Imposing non-random interest rates is necessary to obtain a tractable closed-form solution. As shown by Scott (1997), the variability of actual interest rates has very little impact on the prices of short-term options. Due to the presence of the randomly distributed jumps, this market is in general incomplete in the Harrison and Pliska (1981) sense. Consequently, contingent claims are not redundant assets and cannot be priced by pure no-arbitrage arguments.

II.2.1 Physical Spot Price Dynamics

The logarithmic yield $X_t = \ln(S_t/S_0)$ with $S_0 > 0$ follows a time-homogeneous jump-diffusion process of the form

$$X_t = \gamma t + \sigma W_t + \sum_{i=1}^{N_t} Y_i \tag{II.1}$$

under $\mathbb{P}$, where the drift term $\gamma \in \mathbb{R}$ and the diffusion coefficient $\sigma \in \mathbb{R}_+$ are constants. The random variables Y_i follow an AD-DE distribution defined by

$$Y_i \sim \begin{cases} \xi^+ & \text{with probability } p \in [0,1] \\ -\xi^- & \text{with probability } 1-p \end{cases},$$

where $\xi^+ - \kappa_+$ and $\xi^- + \kappa_-$ are exponential random variables with means $1/\eta_+$ and $1/\eta_-$ respectively. We require that the two parameters controlling the tail behavior of the jumps satisfy $\eta_+ > 1$ and $\eta_- > 0$. The former condition is necessary to be able to compute the drift-compensator in Section II.3. However, since X is the logarithmic asset return, it corresponds to the mean size of an upward jump being less than 100%. Consequently, this restriction should not be binding in any real-world implementation in equity, commodity or foreign exchange markets. The displacement terms satisfy $\kappa_- \leq 0 \leq \kappa_+$ and each jump is positive with probability $p \in [0,1]$. The corresponding jump size density is given by

$$f(x) = p\eta_+ \mathrm{e}^{-\eta_+(x-\kappa_+)} 1\{x \geq \kappa_+\} + (1-p)\eta_- \mathrm{e}^{\eta_-(x-\kappa_-))} 1\{x \leq \kappa_-\},$$

with mean

$$\mathbb{E}[Y_i] = p\left(\kappa_+ + \frac{1}{\eta_+}\right) + (1-p)\left(\kappa_- - \frac{1}{\eta_-}\right).$$

We refer to Appendix II.B.1 for details. This parametrization nests the original Kou (2002) double exponential jump size distribution as a special case when $\kappa_+ = \kappa_- = 0$. Ramezani and Zeng (1999) independently propose the same model dynamics as Kou (2002). However, the authors are solely interested in estimation and do not obtain closed-form solutions for the corresponding transition densities. We obtain the Weber and Wystup (2008) and Detering et al. (2011, 2013) model with symmetric displacements by imposing $\kappa_- = -\kappa_+$. Figure II.1 shows a sample AD-DE jump size density.

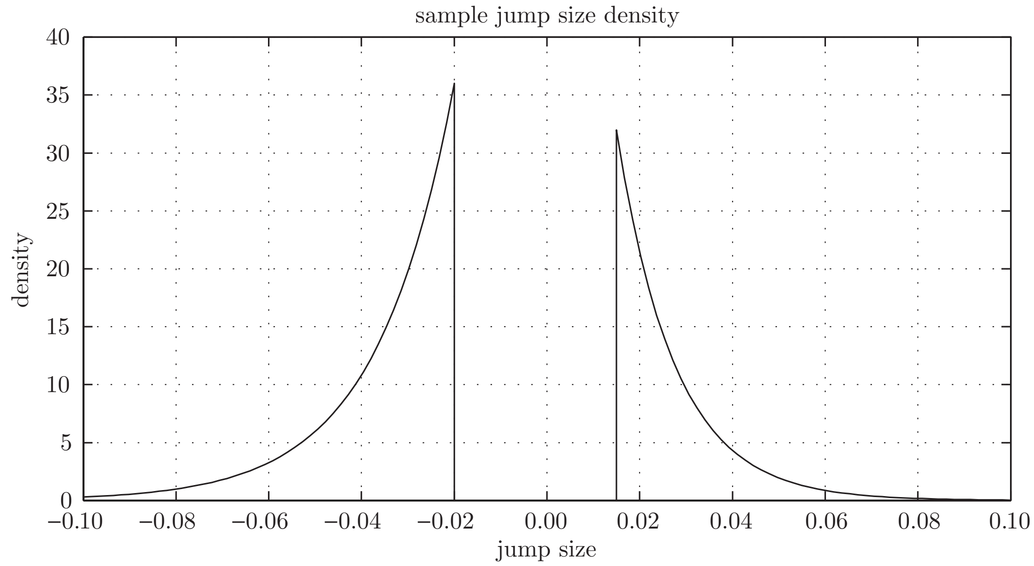

Figure II.1: Sample AD-DE jump size density for $p = 40\%$, $\eta_+ = 80$, $\eta_- = 60$, $\kappa_+ = +1.50\%$ and $\kappa_- = -2.00\%$.

Introducing the additional displacement terms allows us to better disentangle the price fluctuations caused by the diffusion and jump components, respectively, over discrete time intervals. While jumps can be clearly identified as a discontinuity in continuous observations, the effect of the two driving sources of uncertainty blends when samples are discrete. In the original DE model, the jumps not only account for large changes in the asset price but also contribute to the small noise in returns. This contradicts our intuition that jumps are relatively rare events with significant absolute returns. Furthermore, the displacements introduce an additional degree of asymmetry between jumps corresponding to good and bad news, respectively, which is one of the main motivations that leads Ramezani and Zeng (1999) to introduce two distinct exponential tails in the first place.

Lemma II.1 (Spot Price Dynamics).
The spot price dynamics are given by

$$\frac{\mathrm{d}S_t}{S_{t-}} = \left(\gamma + \frac{1}{2}\sigma^2\right)\mathrm{d}t + \sigma\mathrm{d}W_t + \left(\mathrm{e}^{Y_{N_t}} - 1\right)\mathrm{d}N_t.$$

Proof This follows immediately from applying the Itō formula for jump-diffusion processes to the function $f(t, X_t) = \mathrm{e}^{X_t}$; see for example Proposition 8.14 in Cont and Tankov (2004), p. 275. □

As will be shown in Section II.3, the drift can be expressed in terms of the instantaneous mean return $\mu \in \mathbb{R}$ as

$$\frac{\mathrm{d}S_t}{S_{t-}} = \left(\mu - \lambda \left(p\frac{\eta_+}{\eta_+ - 1}\mathrm{e}^{\kappa_+} + (1-p)\frac{\eta_-}{\eta_- + 1}\mathrm{e}^{\kappa_-} - 1\right)\right) \mathrm{d}t + \sigma \mathrm{d}W_t + \left(\mathrm{e}^{Y_{N_t}} - 1\right) \mathrm{d}N_t,$$

where the additional term is a compensator for the expected price change due to jumps.

It is instructive to discuss how we expect the parameters of the AD-DE model and the original parameterization to relate to each other, when estimated based on the same data set. Our analysis rests on the assumption that the newly introduced displacement terms are both non-zero. First consider the special case where (i) the displacements are symmetric around the origin and (ii) the two tail parameters coincide, that is $\kappa_+ = -\kappa_-$ and $\eta_+ = \eta_-$. Our objective is to keep the Lévy measure on the set $\mathcal{A} = (-\infty, \kappa_-] \cup [\kappa_+, \infty)$ unchanged when moving from the AD-DE to the DE model. The assumption behind this is, that the tails of the return distribution can be well approximated by a linear exponential decay. It requires that the two parameters controlling the tail decay agree under the two models. In the special case where both (i) and (ii) hold, we then obtain

$$\begin{aligned} \hat{p} &= p, \\ \hat{\lambda} &= \lambda \mathrm{e}^{\kappa_+ \eta_+}. \end{aligned}$$

While the probability of an upward jump stays unchanged, the jump frequency increases. Next, we analyze the effect of dropping only Assumption (i). We assume without loss of generality (w.l.o.g.) that the lower displacement is larger in absolute terms, that is $\kappa_+ < -\kappa_-$. The corresponding DE model parameters are given by

$$\begin{aligned} \hat{p} &= p\mathrm{e}^{\kappa_+ \eta_+} / \left(p\mathrm{e}^{\kappa_+ \eta_+} + (1-p)\mathrm{e}^{-\kappa_- \eta_-}\right), \\ \hat{\lambda} &= \lambda \left(p\mathrm{e}^{\kappa_+ \eta_+} + (1-p)\mathrm{e}^{-\kappa_- \eta_-}\right). \end{aligned}$$

We find that the probability of an upward jump decreases and the jump frequency increases. Next, we drop only Assumption (ii) and assume w.l.o.g. that the lower tail in the AD-DE model is longer, that is $\eta_- < \eta_+$. The expressions for the two free parameters in the absence of displacements are the same as before. Now, both the probability of an upward jump and the jump frequency increase. Note that it is in general not possible to relax both Assumptions (i) and (ii) simultaneously while still keeping the Lévy measure on the set $\mathcal{A}$ unchanged. In actual estimations, we thus expect a trade-off between the

Table II.1: The upper panel shows the parameters of the AD-DE model and the corresponding estimated parameters of the original Kou (2002) DE model including standard errors. The lower panel compares the cumulative distributions for daily returns at different levels.

Parameter	σ	λ	p	η_+	η_-	κ_+	κ_-
AD-DE	20.00%	15.00	40.00%	80.00	60.00	1.50%	-2.00%
DE	19.48%	44.19	42.12%	76.41	57.34	-	-
	(0.08%)	(2.21)	(0.73%)	(2.09)	(1.45)	-	-

Return	-4.50%	-3.00%	-1.50%	0.00%	+1.50%	+3.00%	+4.50%
AD-DE	1.05%	2.87%	14.07%	50.63%	87.24%	98.25%	99.64%
DE	1.02%	2.88%	14.24%	51.10%	87.60%	98.29%	99.62%

two effects. While the jump frequency always increases, the sign of the change in the probability of an upward jump might be both positive and negative. As argued before, small jumps and diffusive changes are hard to distinguish on discrete time scales and thus the diffusion coefficient should be lower in the DE model.

We sum up the preceding discussion on the differences in estimated model parameters in the following three hypotheses. We expect these to hold for all markets under consideration, conditional on the newly introduced displacement terms being statistically significant in the AD-DE model. Their empirical validation is presented in Section II.8.

Hypothesis II.1. *Compared to the AD-DE model, the empirical estimate of the diffusion coefficient σ is smaller under DE model.*

Hypothesis II.2. *Compared to the AD-DE model, the empirical estimate of the arrival rate λ is larger under the DE model.*

Hypothesis II.3. *Assume that the empirical estimate of the AD-DE model parameters satisfy $\kappa_+ > -\kappa_-$ ($\kappa_+ < -\kappa_-$) and $\eta_+ > \eta_-$ ($\eta_+ < \eta_-$). Then the empirical estimate of the probability of an upward jump is larger (smaller) under the DE model.*

Hypothesis II.4. *The empirical estimate of the tail parameters η_+ and η_- agree under the AD-DE and the DE model.*

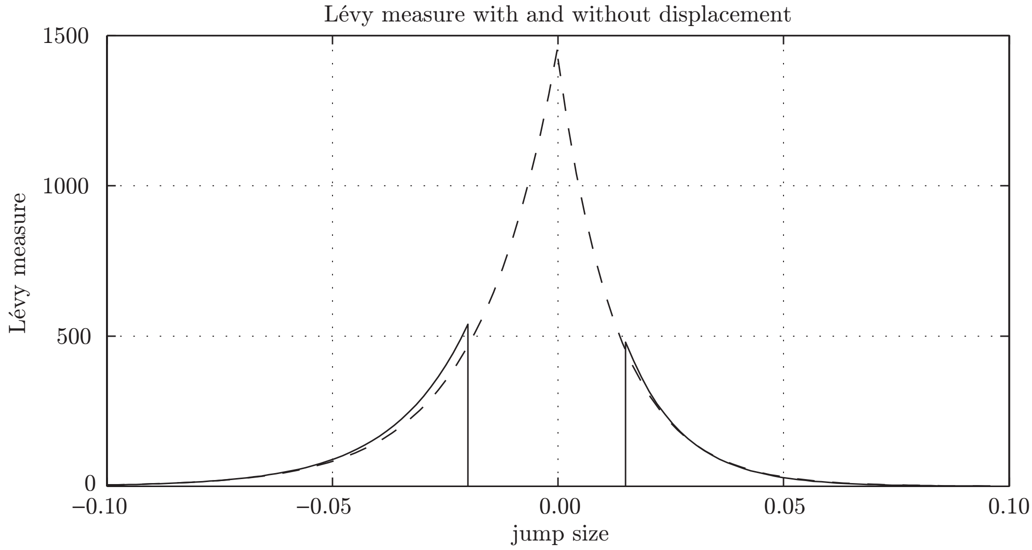

Figure II.2: Jump size densities for the AD-DE model (solid) and the corresponding DE model (dashed). The parameters are given in Table II.1.

We illustrate these hypotheses using a numerical example. We assume that the risk-neutral parameters of the AD-DE model are given by the values in the first row of the upper panel of Table II.1. We then estimate the corresponding parameters of the DE model using the ML routine described in Section II.7. The inference is based on a simulated time series of daily logarithmic returns of length $T = 100,000$. The estimated parameters and their corresponding standard errors are given in the second and third rows of the upper panel in Table II.1. In accordance with Hypotheses II.1 II.2, the diffusion coefficient is lower and the jump frequency is higher under in the restricted model. Both differences are significant at the 1% level. While the assumptions of Hypothesis II.3 are not met, we observe that the exponential tails decay slower under the DE model with both difference being significant at the 10% level. Figure II.2 compares the two Lévy measures that correspond to the jump size density scaled by the respective jump intensity. We observe that the Lévy measure of the DE model closely resembles that of the AD-DE model on the set $\mathcal{A} = (-\infty, -2.00\%] \cup [1.50\%, \infty)$.

While the dynamics proposed in this chapter aim at providing a realistic model for the jump size distribution, they do not capture other empirical features that are typically observed in asset returns. This is a deliberate modeling choice, as incorporating additional effects would prevent us from obtaining closed-form solutions for European plain vanilla options. Here, we briefly discuss the empirical shortcomings of our model. In all cases, it presents no difficulty to augment the model dynamics, while at least preserving a closed-form solution for the corresponding characteristic function. Like in any pure Lévy model, logarithmic returns are stationary and thus do not exhibit volatility clustering. Similarly, the market prices of diffusion and jump risk are constant. Furthermore, as will be discussed in Section II.2.2, the return distribution converges to a normal distribution as the time horizon increases. Consequently, the model implied volatility smile for long times to maturities flattens out and is unable to match the pronounced skew pattern observed in equity (index) option markets. However, the flexibility of the jump size distribution allows for a good calibration to the market prices of options with short times-to-maturity. Furthermore, while the model can be reasonably well calibrated to option prices with a common maturity date, the aforementioned effects prevent it from fitting the term-structure of implied volatilities.

II.2.2 Return Density, Characteristic Function & Moments

The following result will be used repeatedly throughout this chapter.

Lemma II.2 (Characteristic Exponent).
The characteristic exponent of X under $\mathbb{P}$ is given by

$$\psi_{X_1}(\omega) = \ln\left(\mathbb{E}\left[\mathrm{e}^{\mathrm{i}\omega X_1}\right]\right) = \mathrm{i}\omega\gamma - \frac{1}{2}\omega^2\sigma^2 + \lambda\left(\phi_{Y_1}(\omega) - 1\right).$$

Here, $\phi_{Y_1}(\omega)$ is the characteristic function of the sequence of random variables $(Y_i)_{i\in\mathbb{N}}$ under $\mathbb{P}$ given by

$$\phi_{Y_1}(\omega) = p\frac{\eta_+}{\eta_+ - \mathrm{i}\omega}\mathrm{e}^{\mathrm{i}\omega\kappa_+} + (1-p)\frac{\eta_-}{\eta_- + \mathrm{i}\omega}\mathrm{e}^{\mathrm{i}\omega\kappa_-}.$$

Proof This is a direct consequence of the Lévy-Khintchine representation for finite activity Lévy processes; see for example Theorems 1.2.14 and 1.3.3 in Applebaum (2004), pp. 28, 41, or Proposition 3.4 in Cont and Tankov (2004), p. 74. We refer to Appendix II.A.1 for details. □

Remark. The generalized characteristic function with $\omega \in \mathbb{C}$ is then defined in the strip of regularity $-\eta_+ < \mathfrak{Im}(\omega) < \eta_-$.

Having an analytical expression for the characteristic function of logarithmic returns allows us to compute the corresponding cumulants.

Lemma II.3 (Cumulants of the Logarithmic Return Process).
The n-th cumulant of the logarithmic return process X is given by

$$c_n\left(X_t\right) = t\left(\gamma 1\{n=1\} + \sigma^2 1\{n=2\} + \lambda n!\left(p\sum_{i=0}^{n}\frac{\kappa_+^i}{\eta_+^{n-i}i!} + (1-p)\sum_{i=0}^{n}\frac{\kappa_-^i}{\left(-\eta_-\right)^{n-i}i!}\right)\right).$$

Proof The n-th cumulant is defined as the n-th derivative of the cumulant generating function with respect to the transform parameter evaluated at zero, that is

$$c_n\left(X_t\right) = \frac{1}{\mathrm{i}^n}\frac{\partial^n\psi_{X_t}}{\partial\omega^n}(0);$$

see for example Theorem 2.3.1 in Lukacs (1970), pp. 20–21. The result then immediately follows from carefully differentiating $\psi_{X_t}(\omega)$. $\square$

Remark. While the first two cumulants are equal to the mean and variance, we can obtain the skewness and excess kurtosis of the logarithmic returns through normalization

$$\gamma_1\left(X_t\right) = \frac{c_3\left(X_t\right)}{c_2\left(X_t\right)^{3/2}}, \qquad \gamma_2\left(X_t\right) = \frac{c_4\left(X_t\right)}{c_2\left(X_t\right)^2};$$

see for example Section 2.4 in Lukacs (1970), pp. 26–27.

We observe that the skewness can be both positive and negative depending on the particular parameters, but the excess kurtosis is always non-negative and strictly positive for $\lambda > 0$.

Remark. Given closed-form expressions for the cumulants of all orders, we can also compute all corresponding central moments. The second to fourth central moments are given by

$$\begin{aligned}
\mu_2\left(X_t\right) &= c_2\left(X_t\right),\\
\mu_3\left(X_t\right) &= c_3\left(X_t\right),\\
\mu_4\left(X_t\right) &= c_4\left(X_t\right) + 3c_2^2\left(X_t\right).
\end{aligned}$$

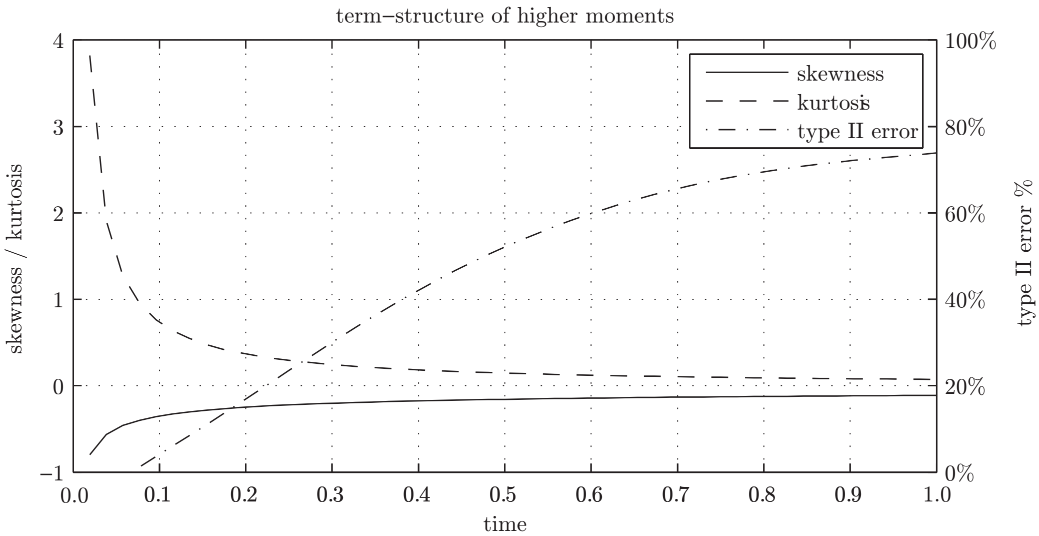

Figure II.3: Term-structure of skewness and excess kurtosis for $\lambda = 15$, $p = 40\%$, $\eta_+ = 80$, $\eta_- = 60$, $\kappa_+ = +1.50\%$, $\kappa_- = -2.00\%$. The right y-axis shows the percentage of type II errors of a Jarque-Bera test for normality at the 5% level based on a simulated time series of length 10,000.

Section 3.14 in Stuart and Ord (1994), pp. 85–89, provides a general result that links the n-th central moment to the cumulants $i = 2, 3, \ldots, n$.

In Section II.7, we advocate to infer the physical model parameters through ML estimation. However, the availability of closed-form expressions of central moments of all orders alternatively permits an estimation through the generalized method of moments (GMM). In this case, moment conditions can be constructed from matching the i-th empirical central moment to the i-th central moment implied by a certain parameter vector.

As for all Lévy processes with finite variance, the Lindeberg-Lévy central limit theorem implies that X_t converges in distribution to a normal random variable as $t \to \infty$. Consequently, the impact of the jumps is averaged out and asymptotically vanishes. The i-th standardized moment decays to zero at a rate of $t^{(i-2)/2}$. Figure II.3 illustrates this time-smoothing effect for the skewness and excess kurtosis based on our reference parameter set. In addition, we employ the Jarque-Bera test at the 5% level to test the null hypothesis that a simulated time series of 1,000 realizations for $X_{\Delta t}$ at various time horizons Δt is normally distributed. For each fixed Δt, we simulate 10,000 different such paths. The dash-dot line corresponding to the left y-axis represents the percentage of false

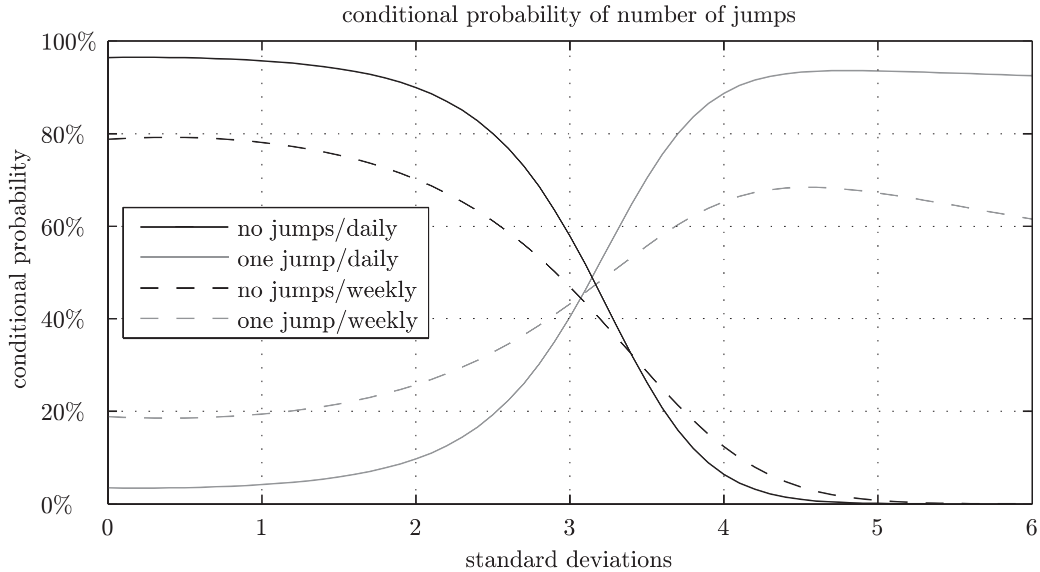

Figure II.4: Conditional probability of zero and one jump(s) for yields that correspond to standard deviations and sampling frequencies. The results are based on $\mu = 0\%$, $\sigma = 10\%$, $\lambda = 15$, $p = 40\%$, $\eta_+ = 80$, $\eta_- = 60$, $\kappa_+ = +1.50\%$, $\kappa_- = -2.00\%$.

acceptances of the null hypothesis, that is, type II errors. Already at $\Delta t = 0.50$ years, the rate of false acceptances is approximately 50%.

Figure II.4 illustrates the previous argument from a different viewpoint. It shows the conditional probability of a given yield resulting from either no jump or one jump. To normalize the results, the abscissa shows the corresponding number of standard deviations. Again, the computations are based on our standard sample parameter set and we consider both daily and weekly sampling frequencies. Note that the two probabilities do not add up to one due to the non-zero possibility of two or more jumps. For both time horizons, we observe that the conditional probability of no jumps is higher for returns below approximately three standard deviations and *vice versa*. However, while small daily returns below one standard deviation can be attributed to purely diffusive changes with a probability of approximately 96%, the same probability for weekly returns is only approximately 78%. This confirms our intuition that disentangling the contribution of the diffusion and jump components becomes harder as the time interval increases. Aït-Sahalia (2004), for example, discusses these issues in the context of the Merton (1973) jump-diffusion model. The implication of these findings is that any empirical estimation of the model has to be based on sufficiently frequent samples.

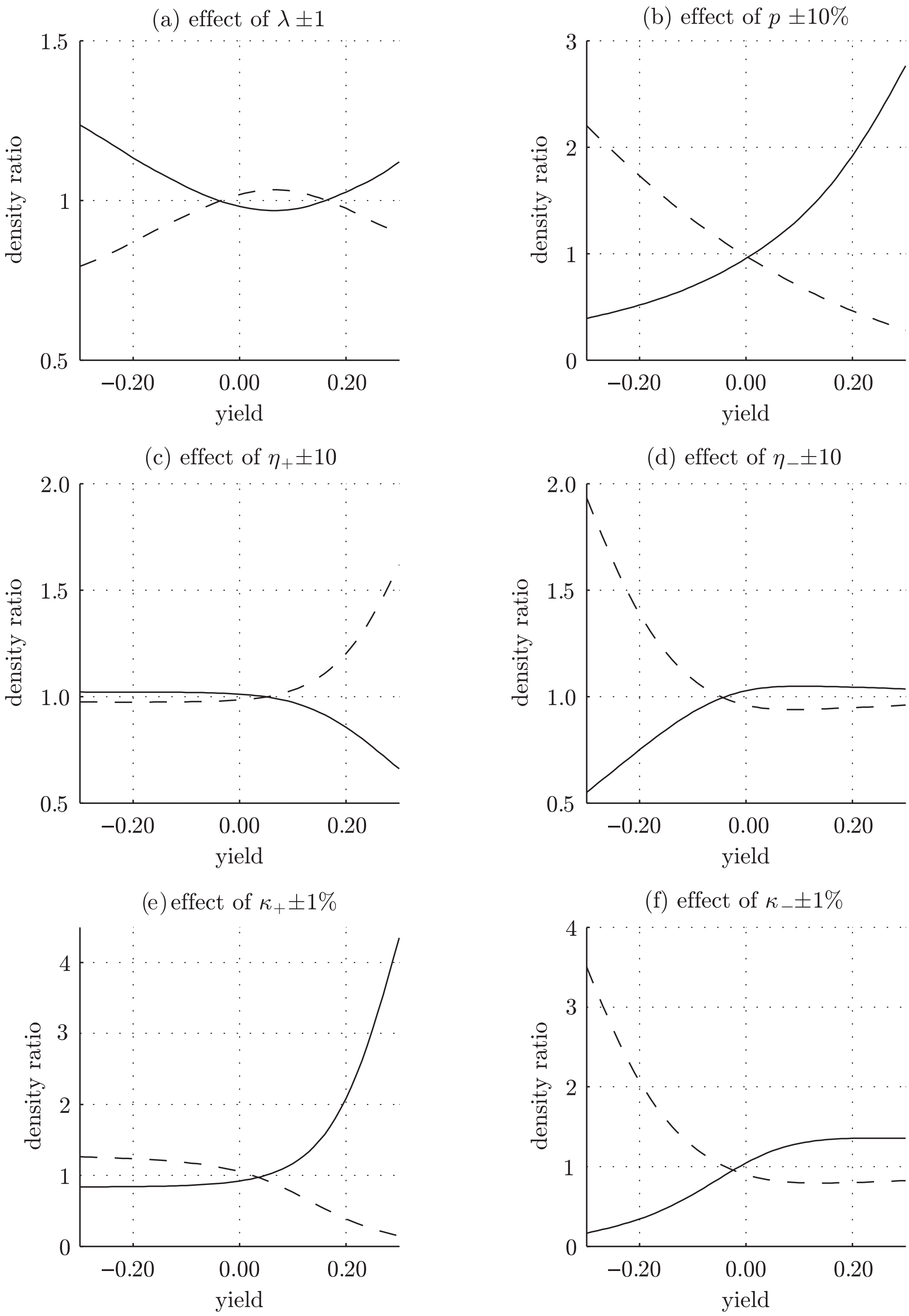

Figure II.5: Effect of changes of the jump parameters on the return density. The reference density is based on $\tau = 0.25$, $\mu = 0\%$, $\sigma = 10\%$, $\lambda = 15$, $p = 40\%$, $\eta_+ = 80$, $\eta_- = 60$, $\kappa_+ = +1.50\%$, $\kappa_- = -2.00\%$. The solid (dashed) line corresponds to the ratio of the density after an up (down) shift of one of the parameters, keeping all others constant, and the reference density.

Figure II.5 visualizes the *ceteris paribus* effect of changes of each individual jump parameter on the return density at a time-horizon of $\Delta t = 0.25$ years. Qualitatively, these results continue to hold for other maturities as well. In each subplot, the solid (dashed) line corresponds to an up (down) shift of the respective parameter, keeping all others constant. Instead of showing the changes in the densities directly, we plot the ratio between the density using the shifted parameters and the reference density using the original parameters. The reference density has been centered to have a mean of zero. Values above (below) one indicate that the shifted density has a higher (lower) likelihood of the respective yield occurring. Figure II.5.a shows that λ controls the tails of the distribution. Higher values for λ (increase) decrease the probability of large (small) absolute returns. The effect is more pronounced, when the initial value of λ is lower. It vanishes for large values due to a central limit argument. Thus, the kurtosis is increasing (decreasing) in λ when it is small (large). Figure II.5.b demonstrates that the probability p of an up-move mainly influences the skewness of returns. With higher values of p, the left (right) tail of the distribution decreases (increases). At the same time, there are more (less) small negative (positive) returns and thus the skewness increases. Figures II.5.c and II.5.d confirm our intuition that smaller values of η_+ and η_- lead to fatter right and left tails, respectively, and decrease the likelihood across all other returns. A decrease in η_+ or an increase in η_- alone mainly increases the skewness. The dominating effect of a simultaneous increase in both parameters is an increase in the kurtosis. Finally, Figures II.5.e and II.5.f show that increasing the absolute values of κ_+ and κ_- has a similar effect to that of decreasing η_+ and η_-.

II.3 Risk-Neutral Spot Price Dynamics

In this section, we discuss two possible constructions of the risk-neutral probability measure. The first one applies a simple drift change to the diffusion part in a rather ad-hoc way. However, it is a convenient choice when the $\mathbb{P}$-dynamics of the asset price are irrelevant. The second one defines the martingale measure through an Esscher transform of the logarithmic stock price process. As shown in Section II.4, this corresponds to the pricing kernel exhibited by an economy where agents have exponential utility. This approach is useful when a calibration to the market prices of plain vanilla options is not possible, but the $\mathbb{P}$-dynamics of the asset price process have been estimated from the time series of returns.

II.3.1 Drift Change Martingale Measure

We denote the drift-compensated return process by $\tilde{X}_t = X_t - t\psi_{X_1}(-\mathrm{i})$. Then $\tilde{S}_t = S_0 \mathrm{e}^{\tilde{X}_t}$ is a $(\mathbb{P}, \mathbb{F})$-martingale; see for example Proposition 2.1.3 in Applebaum (2004), pp. 72–73, or Proposition 3.17 in Cont and Tankov (2004), p. 97. Note, that this expression is only well-defined if $\eta_+ > 1$ as previously assumed. The characteristic exponent of $\tilde{X}_t$ is given by

$$\psi_{\tilde{X}_1}(\omega) = -\mathrm{i}\omega\tilde{\gamma} - \frac{1}{2}\omega^2\sigma^2 + \lambda\left(\phi_{Y_1}(\omega) - 1\right),$$

where

$$\begin{aligned}\tilde{\gamma} &= \frac{1}{2}\sigma^2 + \lambda\left(\phi_{Y_1}(-\mathrm{i}) - 1\right) \\ &= \frac{1}{2}\sigma^2 + \lambda\left(p\frac{\eta_+}{\eta_+ - 1}\mathrm{e}^{\kappa_+} + (1-p)\frac{\eta_-}{\eta_- + 1}\mathrm{e}^{\kappa_-} - 1\right).\end{aligned}$$

This allows us to define the mean logarithmic return of S under $\mathbb{P}$ as $\gamma = \mu - \tilde{\gamma}$, or equivalently $\mu = \gamma + \tilde{\gamma}$. We now formally define a new probability measure $\mathbb{P}^*$ equivalent to $\mathbb{P}$ on $[0, T^*]$ by

$$\frac{\mathrm{d}\mathbb{P}^*}{\mathrm{d}\mathbb{P}} = \exp\left\{-\alpha W_{T^*} - \frac{1}{2}\alpha^2 T^*\right\} \qquad \mathbb{P}\text{-a.s.},$$

In what follows, we interpret $\mathbb{P}^*$ to be the risk-neutral probability measure. The corresponding Radon-Nikodým derivative process $\nu(\mathbb{P}, \mathbb{P}^*) = \{\nu_t(\mathbb{P}, \mathbb{P}^*) : t \in [0, T^*]\}$ is given by

$$\nu_t(\mathbb{P}, \mathbb{P}^*) = \left.\frac{\mathrm{d}\mathbb{P}^*}{\mathrm{d}\mathbb{P}}\right|\mathfrak{F}_t = \exp\left\{-\alpha W_t - \frac{1}{2}\alpha^2 t\right\} \qquad \mathbb{P}\text{-a.s.}.$$

Here,

$$\alpha = \frac{\mu - r}{\sigma}$$

is the Sharpe ratio and it follows by Girsanov's theorem that the process $W^* = \{W_t^*, t \in [0, T^*)\}$ defined by

$$W_t^* = W_t + \alpha t$$

is a standard Brownian motion under $\mathbb{P}^*$; see for example Theorem III.5.1 in Karatzas and Shreve (1991), p. 191. Consequently, the discounted asset price is a $(\mathbb{P}^*, \mathbb{F})$-martingale and has the same distribution and characteristic exponent under $\mathbb{P}^*$ as the process $\tilde{S}$ under $\mathbb{P}$. Since the market is incomplete, this choice of the risk-neutral probability measure is not unique. However, it is convenient in that neither the jump intensity nor the jump size distribution changes. Instead, we only adjust the drift of the Brownian motion, just as in the standard geometric Brownian motion model. This approach is useful when the actual asset dynamics are irrelevant and our sole interest lies in pricing contingent claims. The risk-neutral parameters can then be directly calibrated to the market prices of plain vanilla options. Economically, α is the market price of Wiener risk with corresponding risk premium $\alpha\sigma$. The market price of jump risk is zero and thus jumps are assumed to represent a purely idiosyncratic risk source. This approach was first used by Merton (1976) in the context of normally distributed jumps in the logarithmic returns. While the assumption of idiosyncrasy is obviously unjustified when the underlying asset is a stock index, it is even difficult to argue in favor of the hypothesis that the jumps in single stocks are completely diversifiable.

II.3.2 Esscher Transform Martingale Measure

Alternatively to the pure drift adjustment, we can define the risk-neutral probability measure $\mathbb{P}^*$ through an Esscher transform of the logarithmic return process X. The Esscher transform is a tool originating from and widely used in the actuarial sciences. It refers to the exponential tilting and subsequent re-normalization of a PDF. The transform is due to Esscher (1932), who considers the problem of insurance pricing when the aggregate claim amount follows a non-negative compound Poisson random variable. Bühlmann (1980, 1984) economically develops the Esscher premium calculation principle. He shows that there exists an economy in which agents have exponential utility functions, such that the equilibrium price for some risk is given by the expected claim amount under the Esscher transformed probability measure. A survey on the origins and applications of the Esscher transform in the actuarial sciences can be found in Yang (2004).

In a seminal paper, Gerber and Shiu (1994) systematically develop the theory of using the Esscher transform to define an equivalent probability measure for exponential Lévy processes in the context of option pricing. To this end, they extend the Esscher transform from random variables to stochastic processes of the Lévy type and show that these constitute valid Radon-Nikodým derivative processes. The class of exponential Lévy models for the asset price in general, and jump-diffusion processes in particular, is closed under this measure change since both the independence and stationarity of increments are preserved. The Esscher transform martingale measure (ETMM) is obtained by uniquely choosing the transform parameter such that the asset price denominated in units of the money market account becomes a martingale. Again, this particular choice of the martingale measure is, apart from a few special cases, not unique and at first seems equally arbitrary. However, in the authors' response to the discussions following Gerber and Shiu (1994), they show that in an economy where the representative agent has power utility, the option is in zero net supply when its price is given by the discounted expected payoff under the Esscher transform martingale measure (ETMM). The transform parameter is closely linked to the coefficient of relative risk aversion. In Section II.4, we construct an economy based on the framework by Naik and Lee (1990), in which the equilibrium asset dynamics follow an exponential AD-DE jump-diffusion process and the change of measure can be represented as an Esscher transform.

Following Gerber and Shiu (1994), we define the equivalent risk-neutral probability measure $\mathbb{P}^*$ on $[0, T^*]$ through

$$\frac{\mathrm{d}\mathbb{P}^*}{\mathrm{d}\mathbb{P}} = \exp\left\{\beta X_{T^*} - T^* \psi_{X_1}(-\mathrm{i}\beta)\right\} \qquad \mathbb{P}\text{-a.s.},$$

with transform parameter $\beta \in \mathbb{R}$. As shown in Appendix II.B.1, the corresponding Radon-Nikodým derivative process $\nu(\mathbb{P}, \mathbb{P}^*) = \{\nu_t(\mathbb{P}, \mathbb{P}^*) : t \in [0, T^*])$ is given by

$$\begin{aligned} \nu_t(\mathbb{P}, \mathbb{P}^*) &= \left.\frac{\mathrm{d}\mathbb{P}^*}{\mathrm{d}\mathbb{P}}\right|\mathfrak{F}_t = \exp\left\{\beta X_t - t\psi_{X_1}(-\mathrm{i}\beta)\right\} \\ &= \exp\left\{\beta\sigma W_t - \frac{1}{2}\beta^2\sigma^2 t\right\} \exp\left\{\beta \sum_{i=1}^{N_t} Y_i - t\psi_{X_1^j}(-\mathrm{i}\beta)\right\} \qquad \mathbb{P}\text{-a.s.}, \qquad \text{(II.2)} \end{aligned}$$

where again Proposition 2.1.3 in Applebaum (2004), pp. 72–73, ensures that $\nu(\mathbb{P}, \mathbb{P}^*)$ is a $(\mathbb{P}, \mathbb{F})$-martingale; see also Proposition 3.17 in Cont and Tankov (2004), p. 97.

Proposition II.1 (Esscher Transform Dynamics).
For $\beta \in \mathcal{B} = (-\eta_-, \eta_+)$, the Esscher transform is well-defined. Under the new probability measure $\mathbb{P}^*$, X is also an AD-DE jump-diffusion process with parameters

$$\begin{aligned} \gamma^* &= \gamma + \beta\sigma^2, \\ \lambda^* &= \lambda\left(p\frac{\eta_+}{\eta_+^*}\mathrm{e}^{\beta\kappa_+} + (1-p)\frac{\eta_-}{\eta_-^*}\mathrm{e}^{\beta\kappa_-}\right), \\ f^*(x) &= p^*\eta_+^*\mathrm{e}^{-\eta_+^*(x-\kappa_+)}1\{x \geq \kappa_+\} + (1-p^*)\,\eta_-^*\mathrm{e}^{\eta_-^*(x-\kappa_-)}1\{x \leq \kappa_-\}, \\ p^* &= p\frac{\lambda\eta_+}{\lambda^*\eta_+^*}\mathrm{e}^{\beta\kappa_+}, \\ \eta_\pm^* &= \eta_\pm \mp \beta \end{aligned}$$

and characteristic exponent

$$\psi^*_{X_1}(\omega) = \mathrm{i}\omega\left(\gamma + \beta\sigma^2\right) - \frac{1}{2}\omega^2\sigma^2 + \lambda\int_{-\infty}^{+\infty}\left(\mathrm{e}^{\mathrm{i}\omega x} - 1\right) f(x)\mathrm{e}^{\beta x}\mathrm{d}x.$$

The diffusion coefficient σ and the two displacement terms κ_+ and κ_- are invariant under the measure change.

Proof Here, we present only an outline of the proof. All details are given in Appendix II.B.1. Again, it follows by Girsanov's theorem that the process W^* defined by

$$W^*_t = W_t - \beta\sigma t$$

is a standard Brownian motion under $\mathbb{P}^*$ and we obtain the new drift term γ^*; see for example Theorem III.5.1 in Karatzas and Shreve (1991), p. 191. The second factor of $\nu(\mathbb{P}, \mathbb{P}^*)$ in Equation II.2 can be rearranged to

$$\exp\left\{\beta\sum_{i=1}^{N_t} Y_i - t\psi_{X_1^j}(-\mathrm{i}\beta)\right\} = \exp\left\{\sum_{i=1}^{N_t}\ln\left(\frac{\lambda^* f^*(Y_i)}{\lambda f(Y_i)}\right) - (\lambda^* - \lambda)\,t\right\}.$$

The parameters determining the $\mathbb{P}^*$-dynamics of X^j are found by matching terms. We require that $\eta_+ > \beta$ and $\eta_- > -\beta$. Then η^*_+ and η^*_- are strictly positive and the PDF $f^*(x)$ is well-defined. It then follows by Girsanov's theorem for compound Poisson processes, see for example Proposition 9.6 in Cont and Tankov (2004), p. 305, that the process X^j is a compound Poisson process with intensity λ^* and jump size density $f^*(x)$ under $\mathbb{P}^*$. $\square$

Note, in particular, that the jump sizes still follow an AD-DE distribution. This is due to the parametric form of the AD-DE distribution in combination with the exponential tilting of the Lévy measure $\nu^*_X(\mathrm{d}x)$ of X under the Esscher transform, that is

$$\nu^*_X(\mathrm{d}x) = \nu_X(\mathrm{d}x)\mathrm{e}^{\beta x}.$$

This closedness result holds under more general conditions; see Chapter IV for details. The invariance of the two displacement terms κ_+ and κ_- is necessary for the equivalence of the two probability measures. Lemma II.4 relates the characteristic function of the jumps under the two measures.

Lemma II.4 (Jump Size Characteristic Function).
The characteristic function of the sequence of random variables $(Y_i)_{i\in\mathbb{N}}$ *under the probability measure* $\mathbb{P}^*$ *is given by*

$$\phi^*_{Y_1}(\omega) = \frac{\phi_{Y_1}(\omega - \mathrm{i}\beta)}{\phi_{Y_1}(-\mathrm{i}\beta)}.$$

Proof This immediately follows from using the representation

$$\begin{aligned} f^*(Y_i) &= \frac{\lambda}{\lambda^*} f(Y_i)\,\mathrm{e}^{\beta Y_i} \\ &= \frac{1}{\phi_{Y_1}(-\mathrm{i}\beta)} f(Y_i)\,\mathrm{e}^{\beta Y_i} \end{aligned}$$

for the jump size distribution under $\mathbb{P}^*$. □

The discounted asset price process is a $(\mathbb{P}^*, \mathbb{F})$-martingale if $\psi^*_{X_1}(-\mathrm{i}) = r$ or equivalently,

$$g(\beta^*) = \gamma - r + \left(\beta^* + \frac{1}{2}\right)\sigma^2 + \lambda \int_{-\infty}^{+\infty} (\mathrm{e}^x - 1) f(x)\mathrm{e}^{\beta^* x}\mathrm{d}x = 0, \qquad \text{(II.3)}$$

where the integral evaluates to

$$\int_{-\infty}^{+\infty} (\mathrm{e}^x - 1) f(x)\mathrm{e}^{\beta x}\mathrm{d}x = \lambda\left(\phi_{Y_1}(-\mathrm{i}(1+\beta)) - \phi_{Y_1}(-\mathrm{i}\beta)\right).$$

Proposition II.2 (Existence and Uniqueness).
The ETMM exists and is unique. That is, Equation II.3 has a unique solution $\beta^* \in \mathcal{B}$.

Proof The proof is similar to the sketch of the proof of Proposition 9.9 in Cont and Tankov (2004), pp. 310–311. Using the dominated convergence theorem, we can show that $g(\beta)$ is both continuous and differentiable; see for example Theorems 2.24 and 2.27 in Folland (1984), pp. 53, 54. Since $\lim_{\beta\downarrow-\eta_-} g(\beta) = -\infty$, $\lim_{\beta\uparrow\eta_+} g(\beta) = \infty$ and $g'(\beta) > 0$ for all $\beta \in \mathcal{B}$, the claim follows. All details are given in Appendix II.B.2.

Alternatively and less rigorously, we recognize the integral as the difference between the moment generating function $\theta_{Y_1}(x) = \phi_{Y_1}(-\mathrm{i}x)$ evaluated at $x = \beta + 1$ and $x = \beta$. By Theorem 7.1.4 in Lukacs (1970), p. 197, $\theta_{Y_1}(x)$ is strictly convex on $x \in \mathcal{B}$. Thus, $\theta(1+\beta) - \theta(\beta)$ and also $g(\beta)$ is strictly increasing in β. □

Under the Esscher transform, the market price of Wiener risk is given by $-\beta^*\sigma$ with risk premium $-\beta^*\sigma^2$. The jump risk is now priced and the corresponding risk premium is given by

$$\begin{aligned} & \lambda\left(\phi_{Y_1}(-\mathrm{i}) - 1\right) - \lambda^*\left(\phi^*_{Y_1}(-\mathrm{i}) - 1\right) \\ = \; & \lambda\left(\phi_{Y_1}(-\mathrm{i}) - 1\right)\left(1 - \frac{\phi_{Y_1}\left(-\mathrm{i}\left(1+\beta^*\right)\right) - \phi_{Y_1}\left(-\mathrm{i}\beta^*\right)}{\phi_{Y_1}(-\mathrm{i}) - 1}\right); \end{aligned}$$

compare to Section 4 in Cheang and Chiarella (2011), pp. 4–5. The following corollary suggests that we will find $\beta^* < 0$ for assets that bear a positive amount of systematic risk.

Corollary II.1 (Sign of the Transform Parameter).
The sign of β^* is positive (negative) if the excess return $\mu - r$ is negative (positive). When the excess return is zero, then $\beta^* = 0$ and all the parameters under $\mathbb{P}^*$ and $\mathbb{P}$ coincide.

Proof We first substitute

$$\gamma = \mu - \frac{1}{2}\sigma^2 - \lambda\left(\phi_{Y_1}(-\mathrm{i}) - 1\right)$$

in Equation II.3 to obtain a condition in terms the mean return. We then immediately see that a zero excess return implies that $\beta^* = 0$. Thus, $\nu_t\left(\mathbb{P}, \mathbb{P}^*\right) = 1$ for all $t \in [0, T^*]$ and consequently the two probability measures $\mathbb{P}$ and $\mathbb{P}^*$ coincide. As shown in the proof of Proposition II.2, the function $g(\beta)$ is strictly increasing. Consequently, a positive value of the excess return has to be compensated by a negative value of β^* and *vice versa*. □

Corollary II.2 (Comparative Statics for the Transform Parameter).
Compared to the physical probability measure $\mathbb{P}$, positive (negative) values for β

(i) dampen (increase) the lower tail of the jump size distribution,

(ii) increase (dampen) the upper tail,

Table II.2: Example parameters under the physical probability measure and the ETMM, where in addition to the values given the table $\mu = 10\%$, $r = 0\%$, $\sigma = 10\%$, $\kappa_+ = +1.50\%$, $\kappa_- = -2.00\%$ and $\beta^* \simeq -3.2468$.

Parameter	$\mathbb{P}$	$\mathbb{P}^*$
λ	15	15.66
p	40.00%	35.10%
η_+	80.00	83.25
η_-	60.00	56.75

(iii) decrease (increase) the probability p^* of an up-jump,

(iv) increase (decrease) the mean jump return $\mathbb{E}_{\mathbb{P}^*}[Y_1]$ and

(v) might either increase or decrease the intensity λ^*.

Proof By Proposition II.1, we have $\eta_-^* - \eta_- = \beta$ ($\eta_+^* - \eta_+ = -\beta$). Since the length of the lower (upper) tail under $\mathbb{P}^*$ is decreasing in η_-^* (η_+^*), Properties (i) and (ii) follow. Property (iii) holds since $\partial p^*/\partial\beta > 0$. Property (iv) is a direct consequence of Properties (i)–(iii). To prove Property (v), it is sufficient to show that the slope of the moment generating function $\theta_{Y_1}(x) = \phi_{Y_1}(-\mathrm{i}x)$ in $x = 0$ might be both positive and negative, depending on the parameters of the AD-DE distribution. The required computations can be found in Appendix II.B.3. □

We now consider an example for how the risk-neutral parameters relate to the physical ones under this choice of the risk-neutral probability measure. Using the parameters given in Table II.2, Equation II.3 is solved numerically to find $\beta^* \simeq -3.2468$. As postulated by Corollary II.1, the sign of β^* is negative in the presence of a positive excess return. Figure II.6 compares the Lévy measures under the two probability measures. In accordance with Corollary II.2, the risk-neutral jump size density assigns a lower (higher) weight to positive (negative) jumps. To gain some intuition for this, we can consider a simple binomial tree model for the asset price. Compared to the physical probability measure, the probability of an up-move is lower under the risk-neutral probability measure. This is necessary to compensate for discounting the expected payoff at the risk-free interest rate instead of the higher risk-adjusted rate, while keeping the current asset price fixed.

At first, choosing the Esscher transform to obtain the risk-neutral probability measure seems just as ad-hoc as just changing the drift. However, as shown in Section II.4, the

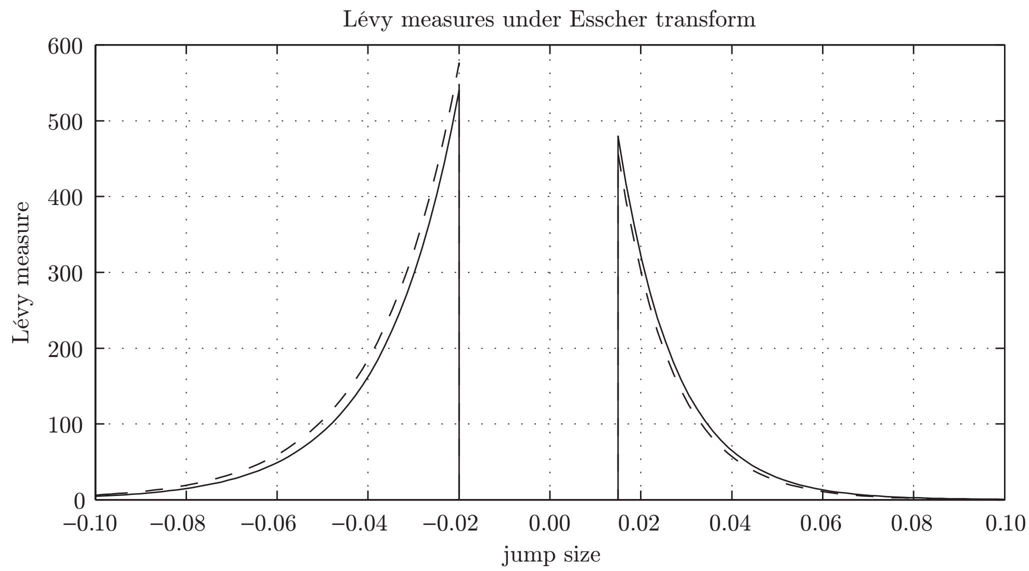

Figure II.6: The solid (dotted) line represents the Lévy measures under $\mathbb{P}$ ($\mathbb{P}^*$). The risk-neutral probability measure is found using the Esscher transform. All parameters are identical to those given in Table II.2.

discounted Esscher transform arises as the pricing kernel in a model economy in which the equilibrium logarithmic stock price follows an AD-DE jump-diffusion process. That is, under the given model assumptions, a representative agent values contingent claims in equilibrium in a way that is consistent with the prices obtained under the ETMM. Furthermore, the ETMM is closely related to the minimal entropy martingale measure (MEMM). The latter is the equivalent martingale measure, which minimizes the Kullback-Leibler divergence to the physical probability measure and is thus closest to it in terms of its statistical information content; see Miyahara (1999, 2004) and Fujiwara and Miyahara (2003). In Miyahara (1999), the choice of the MEMM is motivated economically through its link to utility indifference pricing when the agent has exponential utility; see also Frittelli (2000). Finally, as shown in Section II.5, these results are important when changing the numéraire from the money market account B to the asset price S in order to simplify the option pricing problem.

II.4 General Equilibrium Analysis

The exposition thus far has mainly focused on discussing the stochastic and statistical properties of the proposed model. Once these have been decided upon, a common approach in the mathematical finance literature is to consider the dynamics as exogenously specified. However, from an economic viewpoint, it is desirable to show that there exists a model economy that embeds the postulated asset price dynamics in equilibrium. We consider a continuous time Lucas (1978) type pure exchange economy, which is based on the one proposed by Naik and Lee (1990). While the latter authors focus on the Merton (1973) jump-diffusion model, their setup is sufficiently general to accommodate most exponential Lévy models. Milne and Madan (1991) also use this framework to define the risk-neutral probability measure in the variance gamma model introduced by Madan and Senata (1990).

The stochastic setup is the same as discussed earlier but we now consider an infinite horizon by letting $T^* \to \infty$. This simplifies the portfolio and consumption choice problem by removing the explicit dependence on time and thus rendering it stationary. The following assumptions characterize our economy; see also Naik and Lee (1990).

Assumption II.1 (Consumption Good).
There exists a single perishable physical good. It can be used for either immediate consumption or trade in the financial assets. All prices are expressed in terms of units of this good.

Assumption II.2 (Production).
There exists a single fully equity financed firm with one unit of share outstanding. It engages in costless production and pays a continuous dividend at the stochastic rate $\delta = \{\delta_t, t \in [0, \infty)\}$ *such that the cumulative dividends over the time interval* $[0, t]$ *are given by*

$$D_t = \int_0^t \delta_u \mathrm{d}u.$$

The dividend follows the exponential AD-DE jump-diffusion process in Equation (II.1), that is $X_t = \ln(\delta_t/\delta_0)$ *and*

$$\delta_t = \delta_s \exp\left\{\gamma(t-s) + \sigma(W_t - W_s) + \sum_{i=N_s+1}^{N_t} Y_i\right\}$$

for $0 \le s \le t$ *and with* $\delta_s > 0$.

The exponential form of the solution to the dividend process along with a strictly positive initial value ensures that the aggregate income in the economy stays strictly positive as well. Exogenously specifying the dividends to follow the same type of dynamics that we previously postulated for the stock price turns out to be a crucial assumption. Kou (2002) considers a variation of the Naik and Lee (1990) model economy where the logarithmic endowment of the representative agent follows a jump-diffusion process.

Assumption II.3 (Contingent Claims).
There exists a market for a variety of competitively traded and perfectly divisible contingent claims on the dividend process δ. Each contingent claim is defined through its instantaneous payout process $\zeta = \{\zeta_t, t \in [0,\infty)\}$ such that ζ_t is $\mathfrak{F}_t$-measurable.

Note in particular, that both the stock price $S = \{S_t, t \in [0,\infty)\}$ and zero-coupon bonds $B(\cdot, T) = \{B(t,T), t \in [0,T]\}$ with unit notional and maturities in $T \in [0,\infty)$ can be considered special cases of contingent claims on the dividend process. Consequently, there exists a market for borrowing and lending for all maturities. We thus do not need to explicitly introduce a short-rate to this economy. In what follows, we will determine the equilibrium prices of the stock as well as the zero-coupon bonds and give a general valuation equation for all other contingent claims. All financial assets, except for the stock, are in zero net supply in equilibrium such that any long position by one agent has to be offset by a short position of another. We emphasize that our motivation for introducing the additional assets to this market is not to artificially complete it. This is a common approach in the no-arbitrage literature and would require a continuum of European contingent claims of all maturities and strikes due to the random jump sizes. Instead, all assets are valued endogenously in equilibrium.

Assumption II.4 (Agents).
There exists a fixed number of individuals who are identical with respect to their initial endowment, expectations and preferences. All agents agree on the stochastic dynamics of the dividend process and can observe its current value at any point in time. Each has the same iso-elastic utility of consumption

$$u\left(C_t\right) = \begin{cases} \ln\left(C_t\right) & \textit{if } \alpha = 1 \\ \left(C_t^{1-\alpha} - 1\right) / (1-\alpha) & \textit{otherwise} \end{cases},$$

where $\alpha \in \mathbb{R}_+$ is the coefficient of relative risk aversion. At each point in time, $t \geq 0$, each agent chooses her portfolio allocation process such as to maximize her expected lifetime utility.

$$\mathbb{E}_{\mathbb{P}}\left[\int_t^{\infty} \mathrm{e}^{-\rho v} u\left(C_v\right) \mathrm{d}v \,\middle|\, \mathfrak{F}_t\right]$$

in the von Neumann and Morgenstern (1947) sense, subject to the wealth dynamics $V = \{V_t, t \in [0, \infty)\}$. Here, $\rho \in \mathbb{R}$ is her subjective rate of time preference.

Note that this parametrization of the constant relative risk aversion utility function differs from the one in Naik and Lee (1990) and Kou (2002). However, the two formulations represent the same preferences and are thus equivalent. The assumption of homogeneity of preferences implies that ρ and α are the same for all agents. They further allow for the use of the Rubinstein (1974) aggregation theorem. The equilibrium prices can thus be determined assuming a representative agent facing the same expected utility maximization problem. This significantly simplifies the analysis of the equilibrium since the representative agent has to hold the one unit of the stock outstanding and no pure contingent claims at any point in time since they are in zero net supply.

Assumption II.5 (Transversality Condition).
Let $J(t, V_t)$ be the indirect utility function corresponding to the representative agent's utility maximization problem satisfying

$$\lim_{t \to \infty} \mathbb{E}_{\mathbb{P}}\left[J\left(t, V_t\right)\right] = 0.$$

This transversality condition is the infinite horizon counterpart of a bequest terminal condition and guarantees the convergence of the above integral; see for example Section 6 in Merton (1969), pp. 252–253.

Definition II.1 (Competitive Equilibrium).
A competitive equilibrium in this economy is a set of asset price processes such that at all times the representative agent holds one stock, none of the zero-coupon bonds or other contingent claims and her instantaneous consumption is equal to the dividend $C_t^* = \delta_t$. △

In equilibrium, the representative agent thus engages in an exogenous production such that this yields her optimal consumption. Lemma II.5 gives a general valuation formula that characterizes the equilibrium price of all assets; see also Naik and Lee (1990).

Lemma II.5 (Equilibrium General Valuation Formula).
In a competitive equilibrium, the time $t \geq 0$ price of an asset with instantaneous payout process ζ is given by

$$\pi_t(\zeta) = \frac{1}{\mathrm{e}^{-\rho t} u'(\delta_t)} \mathbb{E}_{\mathbb{P}} \left[\int_t^{\infty} \mathrm{e}^{-\rho v} u'(\delta_v) \zeta_v \mathrm{d}v \middle| \mathfrak{F}_t \right],$$

where π is the valuation operator and assuming that this quantity is finite.

Proof Let $M = \{M_t, t \in [0, \infty)\}$ be the stochastic discount factor process in this economy. We refer to for example Sections 13.5 and 13.6 in Back (2010), pp. 236–241, and Section 12.4 in Pennacchi (2008) for general discussions in the context of continuous time consumption and portfolio choice. Then by definition, the accrued, that is cum dividend or interest, price of any asset deflated with M is a $(\mathbb{P}, \mathbb{F})$-martingale. Setting up the Lagrangian of the representative agent's optimization problem yields the following first-order condition for optimal consumption

$$\mathrm{e}^{-\rho v} u'(\delta_v) = \lambda M_v \qquad \forall v \in [t, \infty),$$

where λ is the Lagrange multiplier. By the properties of the stochastic discount factor, we have

$$\pi_t(\zeta) M_t = \mathbb{E}_{\mathbb{P}} \left[\int_t^{\infty} \zeta_u M_u \mathrm{d}u \middle| \mathfrak{F}_t \right]$$

and Lemma II.5 follows; see Appendix II.C.1 for details. $\square$

We can now use this result to value the assets under consideration and obtain an explicit representation of the pricing kernel. The following assumptions guarantee, that both the risk-free interest rate and the stock price are strictly positive and that the stock price is in addition finite.

Assumption II.6 (Existence Conditions).
The subjective discount rate ρ satisfies

(i) $\rho - \psi_{X_1}(\mathrm{i}\alpha) > 0$

(ii) $\rho - \psi_{X_1}(\mathrm{i}(\alpha - 1)) > 0$

The lower tail parameter of the jump size distribution satisfies $\eta_- > \alpha - 1$.

Note that we could alternatively interpret Assumption II.6 as a constraint on the drift μ, while considering the subjective discount rate ρ as fixed.

Proposition II.3 (Equilibrium Zero-Coupon Bond Price).

The time $t \geq 0$ price of a zero-coupon bond with unit notional and maturity in $T \geq t$ is given by

$$B(t,T) = \exp\left\{(T-t)\left(\psi_{X_1}(\mathrm{i}\alpha) - \rho\right)\right\}.$$

The risk-free interest rate is the same for all maturities and given by

$$r = \rho - \psi_{X_1}(\mathrm{i}\alpha).$$

From Assumption II.6.(i), it follows that $r > 0$.

Proof We use the general valuation formula from Lemma II.5 with the payout process $\zeta_t = \Delta(T-t)$ where $\Delta(x)$ is the Dirac delta function. This yields

$$B(t,T) = \frac{1}{\mathrm{e}^{-\rho t}\delta_t^{-\alpha}} \mathbb{E}_{\mathbb{P}}\left[\mathrm{e}^{-\rho T}\delta_T^{-\alpha}\middle|\,\mathfrak{F}_t\right].$$

This expectation can be computed using the fact that X is a Lévy process with i.i.d. increments and known characteristic exponent. The corresponding yield is then obtained through

$$y(t,T) = -\frac{1}{T-t}\ln B(t,T).$$

We observe that the latter is also constant and independent of time and the bond maturity; see Appendix II.C.2 for details. □

The following Proposition II.4 is the analogue of Proposition 1 in Naik and Lee (1990), p. 499–500, corresponding to our dividend dynamics.

Proposition II.4 (Equilibrium Stock Price).

The time $t \geq 0$ price of the stock is given by

$$S_t = \frac{\delta_t}{\rho - \psi_{X_1}(\mathrm{i}(\alpha-1))}.$$

From Assumptions II.2 and II.6.(ii), it follows that $S_t > 0$ for all $t \geq 0$.

Proof We apply the general valuation formula for $\zeta_t = \delta_t$ to obtain

$$S_t = \frac{1}{\mathrm{e}^{-\rho t}\delta_t^{-\alpha}}\mathbb{E}_{\mathbb{P}}\left[\int_t^{\infty} \mathrm{e}^{-\rho u}\delta_u^{1-\alpha}\mathrm{d}u\middle|\mathfrak{F}_t\right]$$

Again, the expectation can be evaluated using elementary properties of the Lévy process X. Assumption II.6.(ii) is necessary to ensure that the integral converges; see Appendix II.C.3 for details. □

Note, in particular, that the stock price and dividend process are identical up to a scaling factor. Thus, in equilibrium, the logarithmic stock price dynamics also follow an AD-DE jump-diffusion processes. Given the equilibrium zero-coupon bond and stock price processes, we can now define a new equivalent probability measure $\mathbb{P}^*$, such that the prices of all assets are given by the discounted expectation under it. Milne and Madan (1991) and Kou (2002) also use this approach to define a risk-neutral probability measure in similar model economies.

Proposition II.5 (Equilibrium Risk-Neutral Measure).
Define a new probability measure $\mathbb{P}^*$ equivalent to $\mathbb{P}$ through the Radon-Nikodým derivative process

$$\nu_t(\mathbb{P}, \mathbb{P}^*) = \left.\frac{\mathrm{d}\mathbb{P}^*}{\mathrm{d}\mathbb{P}}\right|\mathfrak{F}_t = \mathrm{e}^{rt}\frac{M_t}{M_0} \qquad \mathbb{P}\text{-}a.s.,$$

where M is the stochastic discount factor process in this economy. Then the time $t \geq 0$ price of any asset in this economy with instantaneous payout process ζ is given by

$$\pi_t(\zeta) = \mathbb{E}_{\mathbb{P}^*}\left[\int_t^{\infty} \mathrm{e}^{-r(u-t)}\zeta_u \mathrm{d}u\right].$$

Proof We again only give the outline of the proof; all details can be found in Appendix II.C.4. We first note that the process $\nu(\mathbb{P}, \mathbb{P}^*)$ is a $(\mathbb{P}, \mathbb{F})$-martingale starting at one. Thus, it constitutes a valid Radon-Nikodým derivative process for an equivalent measure change; see for example Chapter III.8 in Protter (2004), pp. 131–143. We then use the general valuation formula from Lemma II.5, substitute M by $\nu(\mathbb{P}, \mathbb{P}^*)$ and change the measure from $\mathbb{P}$ to $\mathbb{P}^*$ to obtain the result. □

Lemma II.6 shows that the measure change implicit in this model economy is given by an Esscher transform of the logarithmic spot price, as discussed in Section II.3.2.

Lemma II.6 (Equilibrium Risk-Neutral Measure as an Esscher Transform). *The risk-neutral probability measure* $\mathbb{P}^*$ *defined in Proposition II.5 corresponds to an Esscher transform of the process* X *with transform parameter* $-\alpha$*, that is*

$$\nu_t\left(\mathbb{P}, \mathbb{P}^*\right) = \exp\left\{-\alpha X_t - t\psi_{X_1}(\mathrm{i}\alpha)\right\}.$$

Proof This follows immediately from substituting for M_t/M_0 in the expression for $\nu_t\left(\mathbb{P}, \mathbb{P}^*\right)$ and using Proposition II.3. □

In accordance with Corollary II.1, the transform parameter $\beta^* = -\alpha$, which defines the ETMM, is strictly negative. Both the market prices of Wiener and jump risk are strictly positive.

II.5 Option Pricing

Probably the main reason for the popularity of the Kou (2002) model is that it explicitly incorporates non-normal higher moments but still features analytical solutions for European plain vanilla options. In Kou and Wang (2003), the authors furthermore obtain solutions for the Laplace transform of the first passage time density and use it in Kou and Wang (2004) to price path-dependent contingent claims such as lookback and barrier options. In this section, we show that analytical solutions for European plain vanilla options can also be attained when the jump sizes follow an AD-DE distribution.

The structure of this section is as follows. In Section II.5.1 we start by deriving a few important auxiliary results regarding the distribution of a sum of random variables following an SD-DE distribution. These results are generalized to the case of asymmetric displacements in Section II.5.2. This two-step approach helps to focus on the main problem associated with symmetric displacement terms first. The asymmetric case then follows from these results by considering a shift of the origin. The corresponding tail probabilities are computed in Section II.5.3. One of the main results of this chapter is the analytical expressions for European plain vanilla options developed in Section II.5.4. Finally, Section II.5.5 provides some comparative static results for the shapes of the implied volatility smiles (IVS), which typical parameter combinations of the model generate.

II.5.1 Auxiliary Results for Symmetric Displacements

The main property of the Kou (2002) model that makes it possible to obtain analytical expressions for the tail probabilities is the memorylessness of the exponential distribution. For $\kappa_+ = \kappa_- = 0$, we have

$$\mathbb{P}\left\{\xi^+ - \xi^- \middle| \xi^+ > \xi^-\right\} \sim \xi^+.$$

This feature is retained in the SD-DE specification with $\kappa_+ = -\kappa_-$ but not in the general model with asymmetric displacements. In this section, we only consider this special case and, for the moment, set $\kappa = \kappa_+ = -\kappa_-$. In Section II.5.2 we show that asymmetric displacements can be regarded as being symmetrically displaced around a different origin. This enables us to generalize the results obtained here to the general model. We choose this two-step approach to focus on the main ideas of the derivation first before stating the quite formidable general results. Lemma II.7 is a direct consequence of the memorylessness property.

Lemma II.7 (Distribution of $\boldsymbol{\xi}^+ - \boldsymbol{\xi}^-$).
The distribution of $\xi^+ - \xi^-$ ($\xi^- - \xi^+$) conditional on $\xi^+ > \xi^-$ ($\xi^- > \xi^+$) is that of an exponential random variable with mean $1/\eta_+$ ($1/\eta_-$). Taking into account the respective probabilities of the two complementary sets that we are conditioning on, we get

$$\xi^+ - \xi^- \sim \begin{cases} \xi^+ - \kappa & \text{with probability } \eta_-/\left(\eta_+ + \eta_-\right) \\ -\xi^- + \kappa & \text{with probability } \eta_+/\left(\eta_+ + \eta_-\right) \end{cases}.$$

Proof This follows from explicitly calculating the respective conditional probabilities; see Appendix II.D.1 for details. □

Now let

$$A(n,m)=\sum_{i=1}^{n}\xi_i^{+}-\sum_{j=1}^{m}\xi_j^{-}$$

for $n,m\geq 1$. Lemma II.8 characterizes the distribution of $A(n,m)$ in terms of a probability-weighted average over the distributions $A(k,0)$ or $A(0,l)$, that is, sums only involving either ξ^{+} or ξ^{-}. This step is important as we can explicitly compute the joint distribution of a normal random variable and either $A(k,0)$ or $A(0,l)$, but in general not $A(n,m)$.

Lemma II.8 (Distribution of $A(n,m)$).
The distribution of $A(n,m)$ admits the following decomposition

$$A(n,m)\sim\begin{cases}A(k,0)+(n-k-m)\kappa & \text{with probability } \tilde{p}(n,m,k)\\ & \text{for } k=1,2,\dots,n\\ A(0,l)+(n-m+l)\kappa & \text{with probability } \tilde{q}(n,m,l)\\ & \text{for } l=1,2,\dots,m\end{cases},$$

where

$$\begin{aligned}\tilde{p}(n,m,k) &= \binom{n-k+m-1}{m-1}\left(\frac{\eta_+}{\eta_++\eta_-}\right)^{n-k}\left(\frac{\eta_-}{\eta_++\eta_-}\right)^{m},\\ \tilde{q}(n,m,l) &= \binom{n-1+m-l}{n-1}\left(\frac{\eta_+}{\eta_++\eta_-}\right)^{n}\left(\frac{\eta_-}{\eta_++\eta_-}\right)^{m-l}.\end{aligned}$$

Proof The proof follows along the same steps as the one given for Lemma B.1 in Kou (2002), pp. 1098–1099, carefully taking the additional displacement term into account. We again only discuss the main idea here and provide all details in Appendix II.D.2. The auxiliary result obtained in Lemma II.7 allows us to express $A(n,m)$ as a probability weighted average of the distribution of $A(n,m-1)-\kappa$ and $A(n-1,m)+\kappa$. This step is iteratively repeated until we are left with an expression of either the form $A(k,0)$ or $A(0,l)$ plus some multiple of κ. $\square$

Let $\tau_n=\inf\{t\geq 0: N_t=n\}$ for $n=1,2,\dots$ be the arrival time of the n-th jump and consider the random variable $X^{j}_{\tau_n}=\sum_{i=1}^{n}Y_i$. We can interpret $X^{j}_{\tau_j}$ as randomly taking the values $A(i,n-i)$ plus some constant for $i=0,1,\dots,n$, following a binomial $\mathcal{B}(n,p)$

distribution. Proposition II.6, which is the analogue of Proposition B.1 in Kou (2002), p. 1098, states this result, which will be central to computing the tail probabilities in Section II.5.3.

Proposition II.6 (Distribution of $X^j_{\tau_n}$).
The distribution of $X^j_{\tau_n}$ admits the following decomposition

$$X^j_{\tau_n} \sim \begin{cases} \sum_{j=1}^k \xi_j^+ + (2i-n-k)\kappa & \textit{with probability } \hat{p}(i,n)\tilde{p}(i,n-i,k) \\ & \textit{for } k=1,2,\dots,n-1; i=k,k+1,\dots,n-1 \\ \sum_{j=1}^n \xi_j^+ & \textit{with probability } \hat{p}(n,n) \\ -\sum_{j=1}^l \xi_j^- + (2i-n+l)\kappa & \textit{with probability } \hat{p}(i,n)\tilde{q}(i,n-i,l) \\ & \textit{for } l=1,2,\dots,n-1; i=1,2,\dots,n-l \\ -\sum_{j=1}^n \xi_j^- & \textit{with probability } \hat{p}(0,n) \end{cases},$$

where

$$\begin{aligned} \hat{p}(i,n) &= \mathbb{P}\left\{X^j_{\tau_n} \sim A(i,n-i)\right\} \\ &= \binom{n}{i} p^i (1-p)^{n-i} \end{aligned}$$

is the binomial probability.

Proof The proof immediately follows from Lemma II.8. We replace $A(n,m)$ by $A(i,n-i)$ and multiply by the probability $\hat{p}(i,n-i)$ of observing i up-jumps when the total number of jumps is n. Note that $A(k,0)$ ($A(0,l)$) appears only in the decompositions of $A(i,n-i)$ for $i=k,k+1,\dots,n-1$ ($i=1,2,\dots,n-l$). □

Due to the additional displacement term κ, we cannot decompose $X^j_{\tau_n}$ into a probability-weighted sum of either the ξ_i^+ or the ξ_i^- alone as in Proposition B.1 in Kou (2002), p. 1098. The reason is that the factor multiplying κ depends on the starting point $A(i,n-i)$.

II.5.2 Auxiliary Results for Asymmetric Displacements

Our approach to solving the pricing problem for the asymmetrically displaced case is to transform it such that our previous results apply. The key idea is to consider asymmetric displacements as being symmetrically displaced with respect to a different y-axis.

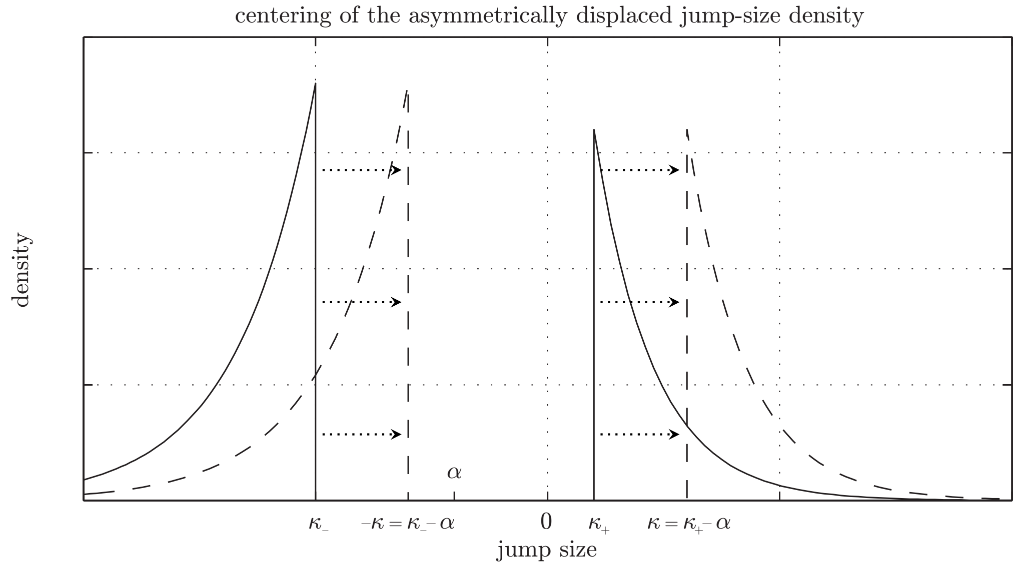

Figure II.7: Centering of the AD-DE jump size density. The point $\alpha = (\kappa_+ - \kappa_-)/2$ is the midpoint of the interval $[\kappa_-, \kappa_+]$. Both tails are shifted by $-\alpha$ to have the origin as the new midpoint.

Define $\alpha = (\kappa_+ + \kappa_-)/2$ to be the midpoint of the interval $[\kappa_-, \kappa_+]$. Next, introduce two auxiliary random variables $\hat{\xi}^+ = \xi^+ - \alpha$ and $\hat{\xi}^- = \xi^- + \alpha$ and let $\kappa = \kappa_+ - \alpha = -(\kappa_- - \alpha)$. Then $\hat{\xi}^+ - \kappa \sim \mathcal{E}(\eta_+)$ and $\hat{\xi}^- - \kappa \sim \mathcal{E}(\eta_-)$ are exponentially distributed. Consequently, the sequence of i.i.d. random variables $(\hat{Y}_i)_{i\in\mathbb{N}}$ given by

$$\hat{Y}_i \sim \begin{cases} \hat{\xi}^+ & \text{with probability } p \in [0,1] \\ -\hat{\xi}^- & \text{with probability } 1-p \end{cases}$$

follows an SD-DE distribution. Figure II.7 illustrates that we obtain $\hat{Y}_i$ by adding the constant term $-\alpha$ to Y_i, thus centering the formerly asymmetric displacement around zero. Note, that when $\kappa_+ = -\kappa_-$, then $\alpha = 0$ and thus the results in this section encompass the previous ones as special cases. The following lemma directly follows from and replaces Lemma II.7.

Lemma II.7* (Distribution of $\boldsymbol{\xi}^+ - \boldsymbol{\xi}^-$).
The distribution of $\hat{\xi}^+ - \hat{\xi}^-$ is given by

$$\hat{\xi}^+ - \hat{\xi}^- \sim \begin{cases} \xi^+ - \alpha - \kappa & \textit{with probability } \eta_-/(\eta_+ + \eta_-) \\ -\xi^- - \alpha + \kappa & \textit{with probability } \eta_+/(\eta_+ + \eta_-) \end{cases}.$$

Proof Apply Lemma II.7 to $\hat{\xi}^+ - \hat{\xi}^-$ and substitute the definitions of the two displaced exponential random variables. $\square$

Next, we need to extend Lemma II.8 to account for the additional term $-\alpha$.

Lemma II.8* (Distribution of $A(n, m)$).

The distribution of $A(n, m)$ admits the following decomposition

$$A(n,m) \sim \begin{cases} A(k,0) + (n-k)(\alpha+\kappa) + m(\alpha-\kappa) & \textit{with probability } \tilde{p}(n,m,k) \\ & \textit{for } k = 1,2,\ldots,n \\ A(0,l) + n(\alpha+\kappa) + (m-l)(\alpha-\kappa) & \textit{with probability } \tilde{q}(n,m,l) \\ & \textit{for } l = 1,2,\ldots,m \end{cases},$$

where the probabilities $\tilde{p}(n, m, k)$ and $\tilde{q}(n, m, l)$ are as given in Lemma II.8.

Proof The steps to this proof are analogous to the original proof to Lemma II.8; see Appendix II.D.3 for details. $\square$

The extension of Proposition II.6 then follows nearly effortlessly.

Proposition II.6* (Distribution of $X^j_{\tau_n}$).

The distribution of $X^j_{\tau_n}$ admits the decomposition

$$X^j_{\tau_n} \sim \begin{cases} \sum_{j=1}^k \xi_j^+ + (n-k)\alpha & \textit{with probability } \hat{p}(i,n)\tilde{p}(i,n-i,k) \\ +(2i-n-k)\kappa & \textit{for } k = 1,2,\ldots,n-1; i = k,k+1,\ldots,n-1 \\ \sum_{j=1}^n \xi_j^+ & \textit{with probability } \hat{p}(n,n) \\ -\sum_{j=1}^l \xi_j^- + (n-l)\alpha & \textit{with probability } \hat{p}(i,n)\tilde{q}(i,n-i,l) \\ +(2i-n+l)\kappa & \textit{for } l = 1,2,\ldots,n-1; i = 1,2,\ldots,n-l \\ -\sum_{j=1}^n \xi_j^- & \textit{with probability } \hat{p}(0,n) \end{cases},$$

where the probabilities $\hat{p}(i, n)$ are as given in Proposition II.6.

Proof The proof is the same as the one given for Proposition II.6. $\square$

II.5.3 Tail Probabilities

We first define

$$Z_t\left(A_1, n\right) = \gamma t + \sigma W_t + \sum_{i=1}^{n} A_i,$$

where $\left(A_i\right)_{i \in \mathbb{N}}$ is a sequence of i.i.d. random variables with the same distribution as the random variable A_1. Thus, $X_t = Z_t\left(Y_1, N_t\right)$ is a jump-diffusion process whose jump size distribution follows an AD-DE law. Throughout this section, we repeatedly need a slight generalization of Proposition B.3 in Kou (2002), p. 1100.

Lemma II.9 (Distribution of $Z_t\left(A_1, n\right)$).
Let ξ_1 be an exponential random variable with arrival rate η. Then for every $n \geq 1$, we have

$$\begin{aligned}\mathbb{P}\left\{Z_t\left(\pm\xi_1, n\right) \in \mathrm{d}x\right\} &= \frac{(\sigma\eta\sqrt{t})^n}{\sigma\sqrt{2\pi t}} \exp\left\{\frac{1}{2}(\sigma\eta)^2 t \mp (x-\gamma t)\eta\right\} \\ &\quad \mathrm{Hh}_{n-1}\left(\mp\frac{x-\gamma t}{\sigma\sqrt{t}} + \sigma\eta\sqrt{t}\right)\mathrm{d}x\end{aligned}$$

and

$$\mathbb{P}\left\{Z_t\left(\pm\xi_1, n\right) \geq x\right\} = \frac{(\sigma\eta\sqrt{t})^n}{\sigma\sqrt{2\pi t}} \exp\left\{\frac{1}{2}(\sigma\eta)^2 t\right\} \mathrm{I}_{n-1}\left(x-\gamma t; \mp\eta, \mp\frac{1}{\sigma\sqrt{t}}, -\sigma\eta\sqrt{t}\right),$$

where

$$\begin{aligned}\mathrm{Hh}_{-1}(x) &= \mathrm{e}^{-x^2/2}, \\ \mathrm{Hh}_0(x) &= \sqrt{2\pi}\Phi(-x), \\ \mathrm{Hh}_n(x) &= \frac{1}{n!}\int_x^{\infty}(t-x)^n \mathrm{e}^{-t^2/2}\mathrm{d}t \qquad n = 1, 2, \ldots, \\ \mathrm{I}_n(c; \alpha, \beta, \delta) &= \int_c^{\infty} \mathrm{e}^{\alpha x}\mathrm{Hh}_n(\beta x - \delta)\mathrm{d}x \qquad n = 0, 1, \ldots.\end{aligned}$$

Proof See the proof of Proposition B.3 in Kou (2002), p. 1100. □

The Hh_n-function is a special function from mathematical physics. Its properties are discussed in detail in Abramowitz and Stegun (1972) and Kou (2002). Section 7.2 in Abramowitz and Stegun (1972), pp. 299-300, establishes the connection between the Hh_n-

function and the error function and gives an iterative recurrence relation for the latter. In the same spirit, Proposition B.2 in Kou (2002), p. 1099, derives a closed-form expression for the I_n-function in terms of finite sums over the Hh_m-function for $m = 1, 2, \dots, n$ evaluated at the same point. It is valid for all parameter combinations that are relevant for our purposes. For practical implementations, we choose these representations as they are both exact and can be implemented efficiently without the need for numerical quadrature.

The following theorem is an extension of Theorem B.1 in Kou (2002), p. 1098, to asymmetrically displaced jumps. It represents our main result.

Theorem II.1 (Tail Probability of X_t).
The upper tail probability of the process $X_t = Z_t\left(Y_1, N_t\right)$ is given by

$$\begin{aligned}
&\mathbb{P}\left\{X_t \geq x\right\} \\
=\;& \mathbb{P}\left\{N_t = 0\right\} \mathbb{P}\left\{Z_t(\cdot, 0) \geq x\right\} \\
&+\sum_{n=1}^{\infty} \mathbb{P}\left\{N_t = n\right\} \Big(\mathbb{P}\left\{Z_t\left(\xi^{+} - \kappa_{+}, n\right) + n\kappa_{+} \geq x\right\} \hat{p}(n, n) \\
&+\mathbb{P}\left\{Z_t\left(-\xi^{-} - \kappa_{-}, n\right) + n\kappa_{-} \geq x\right\} \hat{p}(0, n) \\
&+\sum_{k=1}^{n-1}\sum_{i=k}^{n-1} \Big(\mathbb{P}\left\{Z_t\left(\xi^{+} - \kappa_{+}, k\right) + i\kappa_{+} + (n-i)\kappa_{-} \geq x\right\} \hat{p}(i, n)\tilde{p}(i, n-i, k) \\
&+\mathbb{P}\left\{Z_t\left(-\xi^{-} - \kappa_{-}, k\right) + (n-i)\kappa_{+} + i\kappa_{-} \geq x\right\} \hat{p}(n-i, n)\tilde{q}(n-i, i, k)\Big)\Big),
\end{aligned}$$

where the probabilities on the right-hand side are given in Lemmata II.8, II.9 and Proposition II.6, and

$$\mathbb{P}\left\{N_t = n\right\} = \frac{(\lambda t)^n}{n!} \mathrm{e}^{-\lambda t}$$

is the Poisson probability mass function.

Proof The proof is given in Appendix II.D.4. □

Corollary II.3 (Density of X_t).

The PDF of the process X is given by

$$
\begin{aligned}
& \mathbb{P}\{X_t \in \mathrm{d}x\} \\
= \;& \mathbb{P}\{N_t = 0\}\,\mathbb{P}\{Z_t(\cdot,0) = x\} \\
& + \sum_{n=1}^{\infty} \mathbb{P}\{N_t = n\} \Big(\mathbb{P}\big\{ Z_t\big(\xi^+ - \kappa_+, n\big) + n\kappa_+ = x \big\}\, \hat{p}(n,n) \\
& + \mathbb{P}\big\{ Z_t\big(-\xi^- - \kappa_-, n\big) + n\kappa_- = x \big\}\, \hat{p}(0,n) \\
& + \sum_{k=1}^{n-1} \sum_{i=k}^{n-1} \Big(\mathbb{P}\big\{ Z_t\big(\xi^+ - \kappa_+, k\big) + i\kappa_+ + (n-i)\kappa_- = x \big\}\, \hat{p}(i,n)\tilde{p}(i,n-i,k) \\
& + \mathbb{P}\big\{ Z_t\big(-\xi^- - \kappa_-, k\big) + (n-i)\kappa_+ + i\kappa_- = x \big\}\, \hat{p}(n-i,n)\tilde{q}(n-i,i,k) \Big) \Big) \mathrm{d}x.
\end{aligned}
$$

Proof This immediately follows from Theorem II.1 and the details are omitted for brevity.
□

While these expressions look quite formidable, they are composed entirely of elementary functions. Thus, they can be evaluated readily in standard programming languages. When implementing these formulas, we need to truncate the infinite summation at some level $n_{\max}$ which has to be determined such that the truncation error does not exceed a predefined threshold. As will be shown, the summands quickly converge to zero, thanks to the factorial term in the denominator of the Poisson probability mass function. Lemma II.10 provides the necessary results.

Lemma II.10 (Truncation Error Bound).

The truncation error induced by computing the upper tail probability based on the first $n_{\max}$ terms only is bounded by

$$
\sum_{n_{\max}+1}^{\infty} \mathbb{P}\{N_t = n\}\,\mathbb{P}\{Z_t(Y_1, n) \geq x\} \leq \frac{\gamma(n_{\max}+1, \lambda t)}{n_{\max}!},
$$

where

$$
\gamma(s,x) = \int_0^x t^{s-1} \mathrm{e}^{-t} \mathrm{d}t
$$

is the lower incomplete gamma function.

Proof Since $\mathbb{P}\{Z_t(Y_1, n) \geq x\} \in [0,1]$, we can bound the truncation error by $\mathbb{P}\{N_t > n_{\max}\}$, which yields the given expression; see Appendix II.D.5 for details. □

It should be noted that the error bound in Lemma II.10 is of course not unique and there might exist better bounds. The inverse problem of finding the smallest $n_{\max}$ such that the truncation error is below a fixed absolute threshold can be solved by using the Poisson inverse cumulative distribution function, which is implemented in most statistical computing libraries.

II.5.4 European Plain Vanilla Options

Let $t \geq 0$ be the current point in time and $C = \{C_t : t \in [0,T]\}$ be the price process of a European plain vanilla call option on the spot asset S with maturity in $t \leq T \leq T^*$ and terminal payoff $C_T = (S_T - K)^+$. Denote the time-to-maturity by $\tau = T - t$.

Proposition II.7 (European Plain Vanilla Call Options on Spot Assets).
Let

$$\Lambda(x; t, \gamma, \sigma, \lambda, p, \eta_+, \eta_-, \kappa_+, \kappa_-) = \mathbb{P}\{X_t \geq x\},$$

be the upper tail probability of the jump-diffusion process X with drift γ, diffusion coefficient σ, jump intensity λ and AD-DE jump size distribution with parameters p, η_+, η_-, κ_+ and κ_- as given in Theorem II.1. The price of the European plain vanilla call option is given by

$$C_t = S_t \Lambda_1 - B(t,T) K \Lambda_2,$$

where

$$\begin{aligned}
\Lambda_1 &= \Lambda\left(\ln\left(\frac{K}{S_t}\right); \tau, \gamma^S, \sigma, \lambda^S, p^S, \eta_+^S, \eta_-^S, \kappa_+, \kappa_-\right), \\
\Lambda_2 &= \Lambda\left(\ln\left(\frac{K}{S_t}\right); \tau, \gamma^*, \sigma, \lambda^*, p^*, \eta_+^*, \eta_-^*, \kappa_+, \kappa_-\right)
\end{aligned}$$

and

$$
\begin{aligned}
\gamma^* &= r - \frac{1}{2}\sigma^2 - \lambda^* \left(p^* \frac{\eta_+^*}{\eta_+^* - 1} \mathrm{e}^{\kappa_+} + (1-p^*) \frac{\eta_-^*}{\eta_-^* + 1} \mathrm{e}^{\kappa_-} - 1 \right), \\
\gamma^S &= \gamma^* + \sigma^2, \\
\lambda^S &= \lambda^* \left(p^* \frac{\eta_+^*}{\eta_+^S} \mathrm{e}^{\kappa_+} + (1-p^*) \frac{\eta_-^*}{\eta_-^S} \mathrm{e}^{\kappa_-} \right), \\
f^S(x) &= p^S \eta_+^S \mathrm{e}^{-\eta_+^S (x-\kappa_+)} 1\{x \geq \kappa_+\} + \left(1 - p^S\right) \eta_-^S \mathrm{e}^{\eta_-^S (x-\kappa_-)} 1\{x \leq \kappa_-\}, \\
p^S &= p^* \frac{\lambda^* \eta_+^*}{\lambda^S \eta_+^S} \mathrm{e}^{\kappa_+}, \\
\eta_\pm^S &= \eta_\pm^* \mp 1.
\end{aligned}
$$

All parameters under the risk-neutral probability measure are as determined in Section II.3.

Proof We apply the risk-neutral pricing formula - see for example Proposition 9.1 in Cont and Tankov (2004), p. 298 - and expand the payoff function to express the call price in terms of two expectations under the risk-neutral probability measure. While the second expectation can be readily computed using Theorem II.1, we need to first apply a change of numéraire from the bank account to the asset price to compute the second. It turns out that this measure change is equivalent to an Esscher transform with transform parameter $\beta = 1$ and thus Proposition II.1 can be used to obtain the asset price dynamics under this new measure; see Appendix II.D.6 for all details. □

The resulting formula is similar in structure to the Black and Scholes (1973) formula with two terms representing the expected values of the asset and the strike price payment upon exercise. Heston (1993) obtains a similar expression in a stochastic volatility context. We note that in the special case when $\kappa_+ = \kappa_- = 0$, the European plain vanilla call price formula reduces to the one given in Theorem 2 in Kou (2002), p. 1095. For the dynamic risk-management of derivative books, the availability of analytical solutions for the hedge ratio and other Greeks is just as important as the possibility to rapidly re-evaluate the option positions themselves.

Lemma II.11 (Delta and Gamma of European Plain Vanilla Call Options). *The delta and gamma of the European plain vanilla call option are given by*

$$
\Delta_t^C = \Lambda_1 \qquad \textit{and} \qquad \Gamma_t^C = -\frac{1}{S_t} \Lambda_1',
$$

where

$$\Lambda'\left(x; t, \gamma, \sigma, \lambda, p, \eta_+, \eta_-, \kappa_+, \kappa_-\right)$$

is the PDF of X_t as given in Corollary II.3.

Proof While the expression for delta seems obvious given the call price formula, care has to be taken when taking the partial derivative of C_t with respect to S_t as both probabilities Λ_1 and Λ_2 are functions of the asset price as well. However, we do not need to explicitly apply the chain rule of differentiation but can instead use a homogeneity result. Like all exponential Lévy models, the asset price S exhibits constant returns to scale. By Theorem 9 in Merton (1973), p. 149, it then follows that the European plain vanilla call price is homogeneous of degree one in the spot and the strike price; see also Reiss and Wystup (2001) for related results and generalizations. Thus, by Euler's theorem, it admits the representation

$$C_t = S_t \frac{\partial C_t}{\partial S_t} + K \frac{\partial C_t}{\partial K}.$$

From the model independent pricing formula

$$C_t = B(t,T) \int_K^\infty \left(S_t \mathrm{e}^x - K\right) \mathbb{P}^* \left\{X_\tau \in \mathrm{d}x\right\},$$

we get by differentiating

$$\frac{\partial C_t}{\partial K} = -B(t,T) \mathbb{P}^* \left\{X_\tau \geq x\right\} \mathrm{d}x = -B(t,T)\Lambda_2.$$

Thus,

$$\Delta_t^C = \frac{\partial C_t}{\partial S_t} = \frac{1}{S_t}\left(C_t - B(t,T) K \Lambda_2\right) = \Lambda_1.$$

The formula for gamma follows immediately by differentiating Δ_t^C another time with respect to S_t using the result from Corollary II.3. □

Lemma II.12 (European Plain Vanilla Put Options on Spot Assets). *The price of the corresponding European plain vanilla put option is given by*

$$P_t = B(t,T) K \left(1 - \Lambda_2\right) - S_t \left(1 - \Lambda_1\right)$$

with Greeks

$$\Delta_t^P = \Lambda_1 - 1 \qquad \text{and} \qquad \Gamma_t^P = -\frac{1}{S_t} \Lambda_1'.$$

Proof This follows immediately from the put-call parity relationship,

$$C_t + B(t,T)K = P_t + S_t.$$

$\square$

Corollary II.4 (Sensitivities of European Plain Vanilla Options).
The prices of both European plain vanilla call and put options are ceteris paribus increasing in λ^*.

Proof It immediately follows from the put-call parity relationship, that the sign of the sensitivity with respect to the jump intensity has to be the same for call and put options. By Theorem 8 in Merton (1973), p. 149, it is sufficient to show that the riskiness of the underlying asset's returns is increasing in λ^*. See II.D.7 for details. $\square$

Corollary II.5 (European Plain Vanilla Options on Forwards).
Let $F_S(\cdot,U) = \{F_S(t,U) : t \in [0,T^*]\}$ *be the price process of a forward contract on the asset* S *with maturity in* $U \geq T$. *The prices of the European plain vanilla call and put options on* $F_S(\cdot,U)$ *are given by*

$$\begin{aligned} C_t &= B(t,T)\left(F_S(t,U)\Lambda_1 - K\Lambda_2\right), \\ P_t &= B(t,T)\left(K\left(1-\Lambda_2\right) - F_S(t,U)\left(1-\Lambda_1\right)\right). \end{aligned}$$

where

$$\gamma^* = -\frac{1}{2}\sigma^2 - \lambda^*\left(p^*\frac{\eta_+^*}{\eta_+^*-1}\mathrm{e}^{\kappa_+} + (1-p^*)\frac{\eta_-^*}{\eta_-+1}\mathrm{e}^{\kappa_-} - 1\right)$$

all remaining parameters are as given in Proposition II.7 with $F_S(t,U)$ *replacing* S_t.

Proof We first note that the forward price $F_S(t,U) = S_t/B(t,U)$ is a $(\mathbb{P}^*,\mathbb{F})$-martingale and its logarithm has the drift $\gamma^* - r$. The proof is then fully analogous to that of Proposition II.7; see Appendix II.D.8 for details. $\square$

As usual, European vanilla options on the spot asset can be priced as an option on the forward $F_S(t,T)$, where option and forward maturity are identical.

II.5.5 Comparative Statics for the Implied Volatility Smile

Since the main motivation of adding jumps to the Black and Scholes (1973) diffusion process is to capture the non-zero skewness and excess kurtosis present in most listed options markets, it is interesting to analyze which shapes of the IVS can be generated by the model and what the effect of each of the model parameters is.

Figure II.8 is the analogue of Figure II.5, showing the *ceteris paribus* effect of changes of each individual jump parameter on the shape of the IVS. The solid reference curve is based on our standard sample parameter set and a maturity of three months. We observe that this IVS exhibits a smile pattern that is not symmetric around the at-the-money strike of $K = 100.00$ USD. It is directly linked to the asymmetry in the corresponding distribution of logarithmic returns induced by the larger displacement and slower tail decay of downward jumps. The dashed (dash-dotted) curve corresponds to an up (down) shift of one of the parameters, keeping all others constant. Given the intimate link between the shape of the IVS and the higher moments of the risk-neutral distribution of logarithmic returns, the reasons for the changes in the IVS follow immediately from the discussion of Figure II.8. A higher negative skewness increases the implied volatility of out-of-the-money put options relative to out-of-the-money call options. An increased kurtosis increases the implied volatilities of both out-of-the-money call and put options relative to that of at-the-money options.

II.6 Extension to Displaced Double Gamma Jumps

In this section, we further generalize the results from Section II.5 to the case where each tail of the jump size distribution is given by a AD-DG density with an integer-valued shape parameter. This is possible, because the sum of independent exponential random variables follows a gamma distribution. We choose to only introduce this extension at this stage since its derivation is based on the previously obtained results for the AD-DE model. Considering it right from the start obfuscates the key insights regarding displaced exponential random variables that make it possible to obtain closed-form solutions for European plain vanilla option prices. In this section, we restate the main results of Section II.5 for the AD-DG distribution.

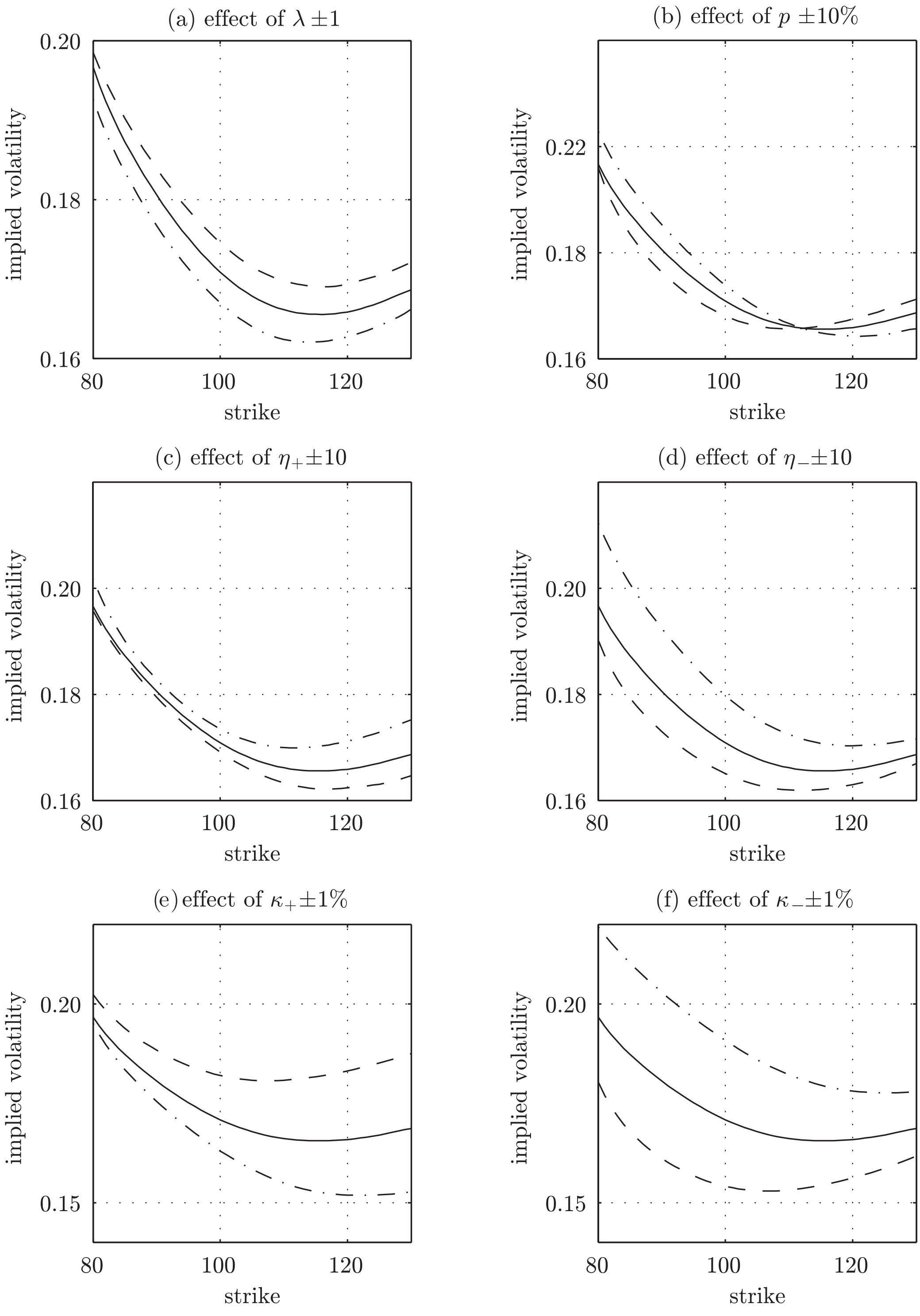

Figure II.8: Effect of changes of the jump parameters on the IVS. The solid reference curve is based on $S_0 = 100.00$ USD, $\tau = 0.25$, $r = 0\%$, $\sigma = 10\%$, $\lambda = 15$, $p = 40\%$, $\eta_+ = 80$, $\eta_- = 60$, $\kappa_+ = +1.50\%$, $\kappa_- = -2.00\%$. The dashed (dash-dot) line corresponds to an up (down) shift of one of the parameters, keeping all others constant.

Formally, the sequence of random variables $(Y_i)_{i\in\mathbb{N}}$ is now defined by

$$Y_i \sim \begin{cases} \zeta^{+} & \text{with probability } p \in [0,1] \\ -\zeta^{-} & \text{with probability } 1-p \end{cases},$$

where $\zeta^{+} - \kappa_{+} \sim \Gamma(\varepsilon_{+}, \delta_{+})$ and $\zeta^{-} - \kappa_{-} \sim \Gamma(\varepsilon_{-}, \delta_{-})$ are gamma random variables with shape parameters $\varepsilon_{+}, \varepsilon_{-} \in \mathbb{N}$ and rate parameters $\delta_{+}, \delta_{-} > 0$. The corresponding jump size density is given by

$$\begin{aligned} f(x) &= p\frac{\delta_{+}^{\varepsilon_{+}}}{\Gamma(\varepsilon_{+}-1)} (x-\kappa_{+})^{\varepsilon_{+}-1} \mathrm{e}^{-\delta_{+}(x-\kappa_{+})} 1\{x \geq \kappa_{+}\} \\ &\quad +(1-p)\frac{\delta_{-}^{\varepsilon_{-}}}{\Gamma(\varepsilon_{-}-1)} (\kappa_{-}-x)^{\varepsilon_{-}-1} \mathrm{e}^{\delta_{-}(x-\kappa_{-})} 1\{x \leq \kappa_{-}\}. \end{aligned}$$

This setup nests the AD-DE model as a special case when $\varepsilon_{\pm} = 1$, $\eta_{+} = \delta_{+}$ and $\eta_{-} = \delta_{-}$.

Lemma II.13 (Characteristic Function of the Jumps).
The characteristic function $\phi_{Y_1}(\omega)$ of the sequence of random variables $(Y_i)_{i\in\mathbb{N}}$ under $\mathbb{P}$ is given by

$$\phi_{Y_1}(\omega) = p\left(\frac{\delta_{+}}{\delta_{+}-\mathrm{i}\omega}\right)^{\varepsilon_{+}} \mathrm{e}^{\mathrm{i}\omega\kappa_{+}} + (1-p)\left(\frac{\delta_{-}}{\delta_{-}+\mathrm{i}\omega}\right)^{\varepsilon_{-}} \mathrm{e}^{\mathrm{i}\omega\kappa_{-}}.$$

Proof This follows either by direct computation or by using the translation property of the Fourier transform in conjunction with the Hermitian property of the characteristic function; see Appendix II.E.1 for details. □

By combining Lemmata II.2 and II.13, we obtain the characteristic exponent $\psi_{X_1}(\omega)$ of the logarithmic return process X. Many previous results then carry over to the model of AD-DG jumps without modifications. The general equilibrium analysis in Section II.4, for example, does not depend on the particular functional form of the jump size distribution. Instead, all processes are expressed in terms of $\psi_{X_1}(\omega)$.

Lemma II.14 (Cumulants of the Logarithmic Return Process).
The n-th cumulant of the logarithmic return process X is given by

$$\begin{aligned} c_n(X_t) &= t\Bigg(\gamma 1\{n=1\} + \sigma^2 1\{n=2\} + \lambda\Bigg(p\sum_{i=0}^{n}\binom{n}{i}\frac{(\varepsilon_{+}+n-i-1)!}{(\varepsilon_{+}-1)!}\frac{\kappa_{+}^{i}}{\delta_{+}^{n-i}} \\ &\quad +(1-p)\sum_{i=0}^{n}\binom{n}{i}\frac{(\varepsilon_{-}+n-i-1)!}{(\varepsilon_{-}-1)!}\frac{\kappa_{-}^{i}}{(-\delta_{-})^{n-i}}\Bigg)\Bigg). \end{aligned}$$

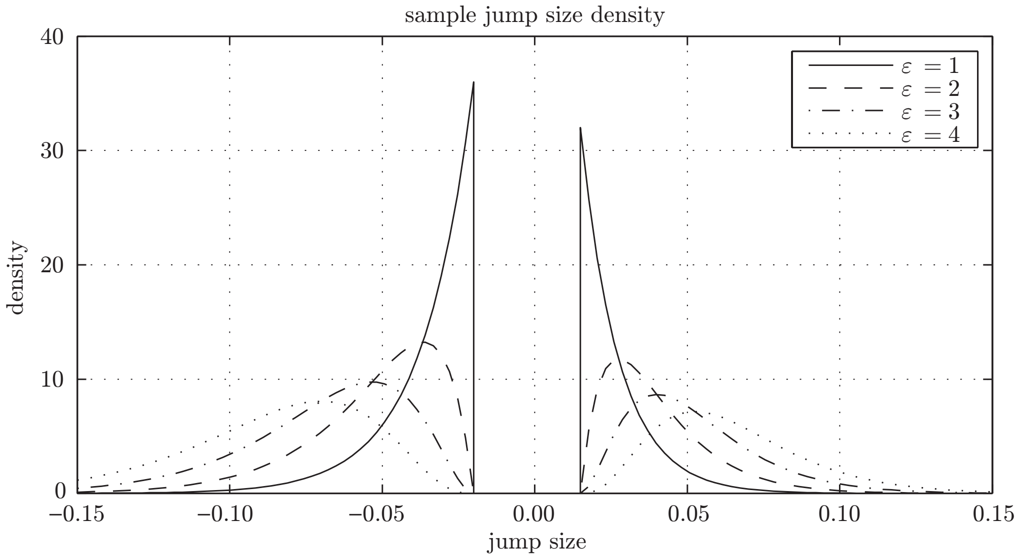

Figure II.9: Sample AD-DG jump size density plot for $\varepsilon_{\pm} \in \{1, 2, 3, 4\}$ $p = 40\%$, $\delta_+ = 80$, $\delta_- = 60$, $\kappa_+ = +1.50\%$ and $\kappa_- = -2.00\%$.

Proof Similar to the proof of Lemma II.3, this follows immediately from computing the n-th derivative of the cumulant generating function $\psi_{X_t}(\omega)$ w.r.t. the transform parameter. $\square$

Figure II.9 shows how the jump size density changes for different values of the shape parameters $\varepsilon_{\pm}$. We observe that the tail decay decreases with increasing values of $\varepsilon_{\pm}$. The peak of the two tails no longer coincides with the displacement terms but is shifted further outward. The AD-DG density introduces an additional degree of asymmetry, since it is possible for ε_+ and ε_- to take on different values.

Up to the particular functional form taken by the characteristic function of the jump size density, all results from Section II.3 continue to hold. Proposition II.8 provides the equivalent result for Proposition II.1.

Proposition II.8 (Esscher Transform Dynamics).
For $\delta \in \mathbb{B} = (-\delta_-, \delta_+)$, the Esscher transform is well-defined. Under the new probability

measure $\mathbb{P}^*$, X is also an AD-DG jump-diffusion process with parameters

$$
\begin{aligned}
\gamma^* &= \gamma + \beta\sigma^2, \\
\lambda^* &= \lambda\left(p\left(\frac{\delta_+}{\delta_+ - \beta}\right)^{\varepsilon_+} \mathrm{e}^{\beta\kappa_+} + (1-p)\left(\frac{\delta_-}{\delta_- + \beta}\right)^{\varepsilon_-} \mathrm{e}^{\beta\kappa_-}\right), \\
f^*(x) &= p^* \frac{\left(\delta_+^*\right)^{\varepsilon_+}}{\Gamma\left(\varepsilon_+ - 1\right)} \left(x - \kappa_+\right)^{\varepsilon_+ - 1} \mathrm{e}^{-\delta_+^*(x-\kappa_+)} 1\left\{x \geq \kappa_+\right\} \\
&\quad + (1-p^*) \frac{\left(\delta_-^*\right)^{\varepsilon_-}}{\Gamma\left(\varepsilon_- - 1\right)} \left(\kappa_- - x\right)^{\varepsilon_- - 1} \mathrm{e}^{\delta_-^*(x-\kappa_-)} 1\left\{x \leq \kappa_-\right\}, \\
p^* &= p\frac{\lambda\delta_+^{\varepsilon_+}}{\lambda^*\left(\delta_+^*\right)^{\varepsilon_+}} \mathrm{e}^{\kappa_+\left(\delta_+ - \delta_+^*\right)}, \\
\delta_\pm^* &= \delta_\pm \mp \beta
\end{aligned}
$$

and characteristic exponent

$$\psi_{X_1}^*(\omega) = \mathrm{i}\omega\left(\gamma + \beta\sigma^2\right) - \frac{1}{2}\omega^2\sigma^2 + \lambda\int_{-\infty}^{+\infty}\left(\mathrm{e}^{\mathrm{i}\omega x} - x\right) f(x)\mathrm{e}^{\beta x}\mathrm{d}x.$$

The diffusion coefficient σ, the two shape parameters ε_+ and ε_- as well as the two displacement terms κ_+ and κ_- are invariant under the measure change.

Proof The proof is fully analogous to that of Proposition II.1 given in Appendix II.B.1 and thus omitted for brevity. □

Again, the jump size distribution under both the physical and the risk-neutral probability measure fall into the same distributional class. This follows from the AD-DG distribution being a natural exponential mixture family in the rate parameters δ_+ and δ_-; see Chapter IV for details. In particular, the shape parameters ε_+ and ε_- are unaffected by the measure transformation. Consequently, their estimates under the physical probability measure can be used for pricing under the ETMM.

Lemma II.15 (Sums of Displaced Exponential Random Variables).
Let $(A_i)_{i\in\mathbb{N}}$ be a sequence of i.i.d. displaced exponential random variables such that $A_i - \kappa/\varepsilon \sim \mathcal{E}(\delta)$. Define

$$B = \sum_{i=1}^{\varepsilon} A_i.$$

Then B follows a displaced gamma distribution, that is $B - \kappa \sim \Gamma(\varepsilon, \delta)$.

Proof This follows immediately from the well-known special case result for zero displacements; see for example Chapter I.3 in Feller (1970), pp. 8–11. □

Now let $\xi_i^+ - \kappa_+/\varepsilon_+ \sim \mathcal{E}(\delta_+)$ and $\xi_i^- + \kappa_-/\varepsilon_- \sim \mathcal{E}(\delta_-)$ be sequences of i.i.d. exponential random variables. Then, by Lemma II.15

$$Y_i \sim \begin{cases} \sum_{i=1}^{\varepsilon_+} \xi_i^+ & \text{with probability } p \in [0,1] \\ -\sum_{i=1}^{\varepsilon_-} \xi_i^- & \text{with probability } 1-p \end{cases}.$$

As in Section II.5.1, define τ_n to be the arrival time of the n-th jump and let $X_{\tau_n}^j = \sum_{i=1}^n Y_i$. We can then interpret $X_{\tau_n}^j$ as randomly taking the values $A(\varepsilon_+ i, \varepsilon_-(n-i))$ plus some constant for $i = 0, 1, \ldots, n$ following a binomial $\mathcal{B}(n,p)$ distribution. The following result then generalizes and replaces Proposition II.6*.

Proposition II.6 (Distribution of $X_{\tau_n}^j$).**
The distribution of $X_{\tau_n}^j$ admits the decomposition

$$X_{\tau_n}^j \sim \begin{cases} \sum_{j=1}^{\varepsilon_+ k} \xi_j^+ + (n-k)\alpha & \textit{with probability } \hat{p}(i,n)\tilde{p}(i,n-i,k) \\ +(2i-n-k)\kappa & \textit{for } k = 1,2,\ldots,n-1; i = k, k+1, \ldots, n-1 \\ \sum_{j=1}^{\varepsilon_+ n} \xi_j^+ & \textit{with probability } \hat{p}(n,n) \\ -\sum_{j=1}^{\varepsilon_- l} \xi_j^- + (n-l)\alpha & \textit{with probability } \hat{p}(i,n)\tilde{q}(i,n-i,l) \\ +(2i-n+l)\kappa & \textit{for } l = 1,2,\ldots,n-1; i = 1,2,\ldots,n-l \\ -\sum_{j=1}^{\varepsilon_- n} \xi_j^- & \textit{with probability } \hat{p}(0,n) \end{cases},$$

where the probabilities $\hat{p}(i,n)$ are as given in Proposition II.6.

Proof The proof is the same as the one given for Proposition II.6. □

Here, α and κ are again the midpoint between the asymmetric displacement terms and the symmetric displacement after shifting the distribution, respectively; see Section II.5.2. We can now re-state our main result in Theorem II.1.

Theorem II.1* (Tail Probability of X_t).
The upper tail probability of the process $X_t = Z_t(Y_1, N_t)$ is given by

$$\begin{aligned}
& \mathbb{P}\{X_t \geq x\} \\
= \; & \mathbb{P}\{N_t = 0\}\,\mathbb{P}\{Z_t(\cdot, 0) \geq x\} \\
& + \sum_{n=1}^{\infty} \mathbb{P}\{N_t = n\} \Big(\mathbb{P}\left\{Z_t\left(\xi^+ - \kappa_+/\varepsilon_+, \varepsilon_+ n\right) + n\kappa_+ \geq x\right\} \hat{p}(n,n) \\
& + \mathbb{P}\left\{Z_t\left(-\xi^- - \kappa_-/\varepsilon_-, \varepsilon_- n\right) + n\kappa_- \geq x\right\} \hat{p}(0,n) \\
& + \sum_{k=1}^{n-1}\sum_{i=k}^{n-1} \left(\mathbb{P}\left\{Z_t\left(\xi^+ - \kappa_+/\varepsilon_+, \varepsilon_+ k\right) + i\kappa_+ + (n-i)\kappa_- \geq x\right\} \hat{p}(i,n)\tilde{p}(i,n-i,k)\right. \\
& \left. + \mathbb{P}\left\{Z_t\left(-\xi^- - \kappa_-/\varepsilon_-, \varepsilon_- k\right) + (n-i)\kappa_+ + i\kappa_- \geq x\right\} \hat{p}(n-i,n)\tilde{q}(n-i,i,k)\right) \Big),
\end{aligned}$$

where the probabilities on the right-hand side are as in the original Theorem II.1.

Proof The proof is fully analogous to that of the original Theorem II.1; see Appendix II.D.4 for details. □

II.7 Parameter Estimation

This section discusses a methodology to estimate the physical parameters of a wide class of model dynamics for the underlying asset based on the time series of logarithmic returns. After introducing our estimation approach based on ML estimation, we briefly discuss alternative estimation methodologies that have been proposed in the literature. We argue that, in addition to its desirable statistical properties, ML requires no ad-hoc decisions about the construction of the moment conditions as do the GMM and the closely related spectral GMM approaches. Furthermore, it can be implemented efficiently through a fractional Fourier transform.

II.7.1 Maximum Likelihood Estimation

The ML estimator is appealing, due to its consistency, asymptotically normal distribution and efficiency. Since its asymptotic variance is given by the inverse of the Fisher information matrix, it achieves the Cramér-Rao lower bound for consistent estimators; see for example Theorem 16.1 in Greene (2008), p. 487. Sørensen (1991) shows that these general properties continue to hold for the inference of jump-diffusion processes under mild regularity conditions. Aït-Sahalia (2002) considers the problem of estimating a general Itō diffusion process based on discrete samples. Aït-Sahalia (2004) establishes that the asymptotic variance of the diffusion coefficient estimator is not deteriorated by the presence of compound Poisson type jumps within the ML framework. He further confirms our intuition that in the limit of infinitely frequent sampling, the jumps and diffusion components can be perfectly disentangled. It is surprising, however, that this result even holds for infinite activity Lévy processes. Bates (2006) adopts the ML approach to the estimation of latent affine processes which allow for both a time-varying volatility and jump intensity. Ramezani and Zeng (1999, 2007) apply ML to estimate the parameters of the original Kou (2002) DE model based on a two year long sample of daily stock returns. Their empirical results support the hypothesis that upward- and downward-jumps exhibit different characteristics. We postpone a more detailed discussion of their results until Section II.8.

We now give a brief overview of the estimator and the corresponding test statistics. Unless explicitly mentioned, Chapter 16 in Greene (2008), pp. 482–572, serves as the main reference for all results in this Section. We consider an equally spaced time series of logarithmic returns $r_{t,\tau} = \ln(S_t/S_{t-\tau})$ for $t = 1, 2, \ldots, T$. When estimating the physical model parameters, the sampling frequency τ should not be too large. Otherwise, as argued in Section II.2.2, the disentanglement of the diffusion and jump components is impeded. The empirical study in Section II.8 is thus based on daily observations. Let

$$\boldsymbol{\Theta} = \{\mu \in \mathbb{R}, \sigma \in \mathbb{R}_+, \lambda \in \mathbb{R}_+, p \in [0,1], \eta_+ \in \mathbb{R}_+, \eta_- \in \mathbb{R}_+, \kappa_+ \in \mathbb{R}_+, \kappa_- \in \mathbb{R}_-\},$$

be the parameter space of the AD-DE model. Since the PDF of logarithmic returns is known in closed-form, we can employ ML estimation. The logarithmic likelihood is given by

$$l(r_{t,\tau}, \boldsymbol{\theta}) = \ln \mathbb{P}\{X_\tau = r_{t,\tau} | \boldsymbol{\theta}\},$$

where the conditional density is as in Corollary II.3. The ML estimator is then defined as the parameter vector $\hat{\boldsymbol{\theta}}_T$, which maximizes the sample likelihood. We have

$$\hat{\boldsymbol{\theta}}_T = \arg\max_{\boldsymbol{\theta} \in \boldsymbol{\Theta}} \mathcal{L}(\boldsymbol{\theta} | \boldsymbol{r}_\tau),$$

where

$$\mathcal{L}\left(\boldsymbol{\theta}|\,\boldsymbol{r}_\tau\right)=\sum_{t=1}^{T} l\left(r_{t,\tau},\boldsymbol{\theta}\right).$$

The asymptotic distribution of the ML estimator is given by

$$\hat{\boldsymbol{\theta}}_T \overset{\text{asym.}}{\sim} \mathcal{N}\left(\boldsymbol{\theta}_0, \boldsymbol{I}^{-1}\left(\boldsymbol{\theta}_0\right)\right),$$

where $\boldsymbol{I}\left(\boldsymbol{\theta}_0\right)$ is the information matrix evaluated at the true parameter vector. Since the latter is not known, we estimate the covariance matrix through the Berndt et al. (1974) estimator

$$\hat{\boldsymbol{I}}^{-1}\left(\hat{\boldsymbol{\theta}}_T\right)=\left(\boldsymbol{G}\left(\hat{\boldsymbol{\theta}}_T\right)'\boldsymbol{G}\left(\hat{\boldsymbol{\theta}}_T\right)\right)^{-1},$$

where $\boldsymbol{G}\left(\boldsymbol{\theta}\right)$ is a $T\times|\boldsymbol{\theta}|$ matrix given by

$$\boldsymbol{G}\left(\boldsymbol{\theta}\right)_{t,i}=\frac{\partial l\left(r_{t,\tau}|\,\boldsymbol{\theta}\right)}{\partial\theta_i}.$$

We employ two different hypothesis and model specification tests. First, restrictions on the estimated model parameters are evaluated using a Wald test. It is based on the asymptotic distribution of a quadratic form of the restrictions being chi-squared distributed. Alternatively, we estimate both the restricted and unrestricted models and compute the corresponding likelihoods. The validity of the restrictions in then evaluated by constructing the likelihood ratio statistic, whose limiting distribution is also chi-squared.

II.7.2 Alternative Estimation Methodologies

A common alternative approach to estimating the physical model parameters of models with a known characteristic function is the Hansen (1982) GMM. The population orthogonality conditions can then be constructed from matching the empirical and model implied central moments and tail probabilities. The model considered in this chapter admits closed-form solutions for both of these types of moment conditions. Furthermore, within any iteration of the corresponding optimization problem, each of these computationally relatively expensive expressions has to be evaluated only once for the full sample. In contrast to this, the conditional likelihood has to be computed for every observation in the sample separately. This suggests that the GMM might be computationally more efficient. However, Section II.7.3 shows that ML estimation can be significantly accelerated by simultaneously computing all conditional likelihoods using the fractional fast Fourier transform (FFT).

There are three main arguments against using the GMM for estimation. First, for the GMM to be asymptotically efficient, a consistent estimator of the covariance matrix of the moment conditions is required. In the presence of serial correlation in the time series of returns, this requires iterated estimations. At each step, an autocorrelation consistent estimator of the covariance matrix has to be computed using, for example, the method suggested by Newey and West (1987). Second, GMM is typically less efficient for finite samples than the ML. Third, the particular choice of the moment conditions and their total number is rather ad-hoc. It is not clear how to optimally choose the central moments and tail values to minimize the variance of the estimator.

Ball and Torous (1983) use a GMM procedure to estimate the Merton (1976) jump-diffusion model. They construct the moment conditions from the first six cumulants of the return process. Ramezani and Zeng (1999) estimate the Kou (2002) DE model using both the cumulant based GMM and ML approaches. In accordance with Press (1968) and Beckers (1981), they find that the cumulant method, unlike ML, sometimes yields economically unreasonable parameter estimates. Furthermore, using higher order moments might be problematic for small samples as the corresponding empirical moment estimates become increasingly noisy.

Singleton (2001) and Chacko and Viceira (2003) suggest a closely related approach based on the empirical characteristic function. They construct the moment conditions from the real and imaginary parts of the characteristic function evaluated at a predefined set of transform parameters. This is particularly appealing when even the cumulants cannot be computed in closed-form. However, their approach suffers from the same shortcomings as the one previously discussed. In particular, it is not clear how to optimally choose the set of transform parameter values.

Finally, we briefly discuss the estimation procedure proposed by Detering et al. (2013), who consider the special case of symmetric displacement terms. The authors start by setting the parameter $\kappa_+ = -\kappa_-$ equal to the average of the absolute logarithmic returns corresponding to the α and $1 - \alpha$ quantiles of the empirical distribution function. They suggest the use of a value of $\alpha = 1\%$ and thus implicitly categorize all absolute logarithmic returns greater than α as jumps. Next, λ is set to be equal to the total number of jumps divided by the total number of observations. However, it is clear that once the level of α has been fixed, the estimate of λ is just equal to the average number of trading days per year times α. The tail parameters η_+ and η_- are chosen such that they fit the mean of the returns classified as jumps. Finally, the diffusive variance is given by the total sample variance minus the variance of the compound Poisson component, whose parameters have already been determined.

While it can be extended to asymmetrically displaced jumps in a straightforward fashion, this approach seems rather ad-hoc. Its parameter estimates fully depend on the discretionary choice of the quantile α. Another important shortcoming is, that it provides no estimate of the covariance matrix of the parameter estimates. Thus, it is not possible to construct confidence intervals or to conduct further hypothesis tests.

II.7.3 Computational Aspects

As indicated in the previous section, the computational bottleneck of ML estimation is the high number of costly evaluations of the conditional likelihood function that it requires. There are two approaches to mitigate this problem and significantly accelerate the estimation. First, it is possible to employ the FFT algorithm to simultaneously obtain the PDF on a fixed grid. These values can then be interpolated to match the observations in the sample. Second, as already indicated in a footnote by Heston (1993), the direct integration can be accelerated through a caching algorithm. This is possible since the values of the characteristic function depend solely on the transform parameter but not on the logarithmic return. Kilin (2011) offers an in-depth discussion of this approach and benchmark results in the context of model calibration.

While caching might prove superior when the total number of function evaluations is rather low, the FFT seems better suited for ML estimation with a large number of observations. It is an efficient algorithm to compute the sums appearing in the discrete Fourier transform through exploiting the orthogonality of the complex exponentials. The FFT reduces the computational effort from $\mathcal{O}\left(N^2\right)$ to $\mathcal{O}\left(N \log_2 N\right)$. The most common FFT algorithm is due to Cooley and Tuckey (1965). Lemma II.16 states the relevant result.

Lemma II.16 (Fast Fourier Transform Approximation).
Given the characteristic function $\phi_{X_t}(\omega)$ of the random variable X_t, its PDF $f_{X_t}(x)$ can be approximated on an equally spaced grid $\boldsymbol{x} = (x_j)_{j=0}^{N-1}$ for $j = 0, 1, \ldots, N$, with N being

a power of two, through

$$
\begin{aligned}
f_{X_t}(x_k) &= \frac{1}{\pi}\mathfrak{Re}\left(\sum_{j=0}^{N-1} \mathrm{e}^{-\mathrm{i}j\Delta\omega k\Delta x} g_j\right) \\
&= \frac{N}{\pi}\mathfrak{Re}\left(\mathfrak{D}^{-1}\{\boldsymbol{g}\}\right)_k,
\end{aligned}
$$

where $\mathfrak{D}^{-1}$ *is the discrete inverse Fourier transform operator and the vector* $\boldsymbol{g} = (g_j)_{j=0}^{N-1}$ *is given by*

$$
g_j = \mathrm{e}^{-\mathrm{i}j\Delta\omega x_0}\phi_X(j\omega).
$$

Here, $\boldsymbol{w} = (w_j)_{j=0}^{N-1}$ *are the integration weights for the* N *sample points* $\boldsymbol{\omega} = (\omega_j)_{j=0}^{N-1}$ *in the frequency domain, which are spaced* $\Delta\omega$ *apart. The corresponding spacing in the spatial domain is given by* $\Delta x = 2\pi/(N\Delta\omega)$*, where the lower endpoint* x_0 *can be freely chosen. When using the Simpson's rule for approximating the integral, the weights are given by*

$$
w_j = \begin{cases} \Delta\omega/3 & \text{if } j \in \{0, N-1\} \\ 4\Delta\omega/3 & \text{if } j/2 \in \mathbb{N} \\ 2\Delta\omega/3 & \text{otherwise} \end{cases}.
$$

Proof This equation is based on the Gil-Pelaez (1951) inversion theorem, which expresses the upper tail probability as a semi-infinite integral over the characteristic function. The corresponding integrand is real-valued and decays at an exponential rate. We thus truncate the upper limit of integration at some point $(N-1)\Delta\omega$ and approximate the resulting integral through Gaussian quadrature. The values of $f_{X_t}(x_k)$ can then efficiently be computed simultaneously by the FFT algorithm; see Appendix II.F.1 for details. □

Remark. Note that the definition of the inverse Fourier transform $\mathfrak{D}^{-1}$ given in Appendix II.F.1 is consistent with the definition of the characteristic function as the forward Fourier transform of the density function. This is the convention typically used in statistics. However, an alternative definition is often employed in the engineering literature, where the signs in the exponents are reversed.

For a fixed number of sample points N, there is a trade-off between the spacing of the x- and the ω-values. A finer spacing of the spatial grid directly leads to a coarser grid for the integration reducing the numerical accuracy of the FFT and *vice versa*.

We construct an example to illustrate this problem. Let's assume that based on the structure of the integrand, we require a spacing of $\Delta\omega = 0.05$ in the frequency domain and truncate the integral at $\bar{\omega} = 200$. The number of points needed is then given by

$$N = \left\{ 2^i : i \in \mathbb{N}, 2^{i-1} < \frac{\bar{\omega}}{\Delta\omega} \leq 2^i \right\}$$

and we get $N = 4,096$ with $\omega_{N-1} = 204.80$. By the above restriction, it follows that $\Delta x = 3.07\%$ and the corresponding spatial grid has the lower endpoint $x_0 = -6,281.65\%$. In the context of ML estimation, $f_{X_t}(x)$ is typically the PDF of at most daily logarithmic returns. It is obvious, that the spatial grid is both much wider than necessary and has too big a spacing. Thus, we are not only computing many unnecessary values in the far tails of the distribution, but more importantly also do not achieve the necessary accuracy in its center. In case of equity indices, for example, a grid with a spacing of $\Delta x = 0.05\%$ and covering the interval $[-20\%, +20\%]$ would be a conservative choice. Fixing $\Delta x = 0.05\%$ then requires $N = 1,024$ points and we get $x_0 = -25.58\%$. The corresponding frequency grid has a spacing of $\Delta\omega = 12.27$ with truncation point $\omega_{N-1} = 12,544.10$. Thus, starting by specifying the spatial grid just shifted the problem to the frequency domain. To achieve the necessary required precision in both domains simultaneously, we fix $\Delta\omega = 0.05$ and search for the smallest $i \in \mathbb{N}$ such that $\Delta x \leq 0.05\%$. We obtain $i = 20$ and get $\Delta x = 0.05\%$, $\omega_{N-1} = 52.428.75$ and $x_0 = -6,283.18\%$. While this yields the necessary precision, it comes at the cost of increasing the number of complex multiplications and additions in the Cooley and Tuckey (1965) radix-2 algorithm by a factor of approximately 427 compared to a grid size of $N = 4,096$.

This link between the two grid spacings can be broken by using the fractional FFT algorithm proposed by Bailey and Swarztrauber (1991, 1994). They show how sums of the form

$$\sum_{j=0}^{N-1} \mathrm{e}^{-2\pi \mathrm{i} jn\alpha} g_j$$

for an arbitrary $\alpha \in \mathbb{R}$ can be computed rapidly by invoking three nested FFT procedures with $2N$ points each. The two grid spacings are now linked through $\Delta x \Delta\omega = 2\pi\alpha$. Lemma II.17 states the main result from Bailey and Swarztrauber (1991) applied to the problem of approximating the likelihood function.

Lemma II.17 (Fractional Fast Fourier Transform Approximation).

Given the characteristic function $\phi_{X_t}(\omega)$ of the random variable X_t, its PDF $f_{X_t}(\omega)$ can *be approximated on an equally spaced grid $\boldsymbol{x} = (x_j)_{j=0}^{N-1}$ for $j = 0, 1, \ldots, N$ with N being a power of two through*

$$f_{X_t}(x_k) = \frac{N}{\pi} \mathfrak{Re} \left(\mathrm{e}^{-\mathrm{i}\pi k^2 \alpha} \left(\mathfrak{D} \left\{ \mathfrak{D}^{-1} \{\boldsymbol{\xi}\} \circ \mathfrak{D}^{-1} \{\boldsymbol{\eta}\} \right\} \right)_k \right),$$

where $\mathfrak{D}$ and $\mathfrak{D}^{-1}$ denote the discrete forward and inverse Fourier transform respectively, $\circ$ is the Hadamard element-wise product and

$$\begin{aligned} \boldsymbol{\xi} &= \left(\left(\mathrm{e}^{-\mathrm{i}\pi j^2 \alpha} g_j \right)_{j=0}^{N-1}, (0)_{j=0}^{N-1} \right) \\ \boldsymbol{\eta} &= \left(\left(\mathrm{e}^{\mathrm{i}\pi j^2 \alpha} \right)_{j=0}^{N-1}, \left(\mathrm{e}^{\mathrm{i}(N-j)^2 \alpha} \right)_{j=0}^{N-1} \right). \end{aligned}$$

The definition of the vector $\boldsymbol{g} = (g_j)_{j=0}^{N-1}$ is identical to Lemma II.16 and $\alpha = \Delta x \Delta \omega / 2\pi$.

Chourdakis (2004) applies the fractional FFT to value European plain vanilla options within the Carr and Madan (1999) framework. The main advantage of this algorithm over the standard FFT is that α does not depend on the number of points N. This allows us to first choose the optimal spatial and frequency grid independent of one another and find α by the above relationship. In the previous example, the optimal discretization of the frequency domain requires a higher number of points and we thus set $N = 4,096$. The corresponding spatial grid then has $\Delta x = 0.01\%$ with lower endpoint $x_0 = -20.00\%$ and we get $\alpha = 7.77 \times 10^{-7}$. While the fractional FFT algorithm requires three FFTs instead of one, the much smaller grid size leads to a reduction in the number of complex multiplications and additions by a factor of approximately 90 compared to the FFT with grid size $N = 1,048,576$. Here, we assume that the exponential factors have been precomputed; see the discussion in Section 2 of Bailey and Swarztrauber (1991), p. 390–392.

When computationally maximizing the sample likelihood function, great care has to be taken in selecting an appropriate optimization routine to ensure convergence to the global maximum. Although the question of how to carry out a specific optimization is of central importance to most estimation problems, this point is usually unmentioned in the literature. Through numerical experiments, we find that the convergence of standard gradient-based algorithms strongly depends upon the set of starting values chosen. This suggests the existence of multiple local maxima, and consequently a non-convex nature of the optimization problem at hand. Kiefer (1978) shows within a similar mixture density setting, that the likelihood function may exhibit local optima when the sample size is finite. We thus turn to the class of heuristic optimization routines that use a stochastic search strategy and are guaranteed to converge to the global optimum in the limit. However, their generality comes at the cost of more function evaluations and consequently slower estimations.

Differential evolution is a population based heuristic optimization algorithm developed by Storn and Price (1997). It is suitable for continuous search spaces and is based on a genetic algorithm, which models the evolutionary process of a population of candidate solutions. The population is updated by a random vector-crossover and mutation scheme that retains the fittest candidate solutions at the end of each iteration step. Like all heuristic optimization routines, and in contrast to gradient based methods, differential evolution does not rely on a set of strong assumptions about the underlying optimization problem. While it converges to the global optimum with probability one as the number of iterations becomes large, this comes at the cost of a high number of objective function evaluations. Ardia et al. (2011) estimate the Merton (1976) jump-diffusion model through ML using differential evolution and find that it outperforms all convex optimization routines considered. Gilli and Schumann (2010, 2012) provide further applications of differential evolution in financial econometrics.

II.8 Empirical Results

This section describes the data set used and discusses the empirical results. All tables can be found in Appendix II.F. We estimate the parameters of the AD-DG, AD-DE, SD-DE and DE models based on the 30 year historical daily logarithmic returns from January 1, 1982 to December 31, 2011. All data is obtained from Bloomberg. The assets fall into three main categories: (i) equity indices, (ii) commodity indices and (iii) foreign exchange (FX) rates and spot precious metals. Table II.4 provides the summary statistics.

Category (i) consists of: DAX 30 (Germany), Dow Jones Industrial (USA), Hang Seng (Hong Kong), MSCI World (global), NASDAQ Composite (USA), Nikkei 225 (Japan), S&P 500 (USA) and TOPIX (Japan). All of these indices are market capitalization weighted and, except for the DAX 30, are calculated as price indices. This refers to them not re-investing the dividends paid by their constituent stocks. On any ex-dividend date, the index thus falls by the net dividend amount times the number of stocks in the portfolio. However, all of these indices are highly diversified and the dividend payment dates are spread throughout the year. The dividend payments can thus be well approximated by a continuous dividend yield. Our objective is to estimate the parameters of the different jump size distribution specifications but not the mean return. Consequently, the non-zero dividend yield is irrelevant for our purposes.

Category (ii) corresponds to the S&P GSCI Excess Return (ER) commodity index and three of its sub-indices. The basic index constituents are commodity futures contracts, weighted by their relative world production. The single futures positions are dynamically rolled forward before the respective first notice date or expiry date. The S&P GSCI ER index itself can be broken down into five sub-indices corresponding to the main classes of commodities: S&P GSCI Energy ER, S&P GSCI Industrial Metals ER, S&P GSCI Precious Metals ER, S&P GSCI Agriculture ER and S&P GSCI Livestock ER. This study excludes the S&P GSCI Energy ER and S&P GSCI Livestock ER indices, since no historical data is available on Bloomberg for the first years of the considered time span. However, the S&P GSCI ER index itself strongly overweights the energy futures and thus serves as a good benchmark for this market segment.

Finally, category (iii) contains the three major spot exchange rate pairs EUR/USD, GBP/USD and USD/JPY as well as the spot prices of silver and gold. We remark that, despite the naming convention adopted, USD is the domestic currency in the quotation of the EUR/USD and GBP/USD exchange rate pairs but the foreign currency in USD/JPY quotation.

Tables II.5 and II.6 show the AD-DE parameter estimates and hypotheses tests for equity indices. For convenience, II.3 summarizes the null hypotheses. The key observation is that, without exception, both positive and negative displacement terms are individually significant at the 1% level. Furthermore, both the null hypothesis $\mathcal{H}_0^{(2)}$ of jointly zero displacements as well as the null hypothesis $\mathcal{H}_0^{(1)}$ of symmetric displacements can also be rejected at the 1% level in all cases. However, for some equity indices, such as the Hang Seng and the S&P 500, one of the two displacement terms is economically insignificant. We conclude that the asymmetric displacements succeed at capturing a statistical property that is consistently present in equity index returns. We can thus reject both the SD-DE and the DE model in favor of the AD-DE dynamics. We further note, that on average only 25.35% of the total historical variance can be attributed to the diffusion component.

Table II.3: Overview of the null hypothesis evaluated for the ML AD-DE parameter estimates.

Null Hypothesis	Description
$\mathcal{H}_0^{(1)} : \kappa_+^{\text{AD-DE}} + \kappa_-^{\text{AD-DE}} = 0$	AD-DE displacements are symmetric.
$\mathcal{H}_0^{(2)} : \kappa_+^{\text{AD-DE}} = \kappa_-^{\text{AD-DE}} = 0$	AD-DE displacements are jointly zero.
$\mathcal{H}_0^{(3)} : \eta_+^{\text{AD-DE}} - \eta_-^{\text{AD-DE}} = 0$	AD-DE tails decay at the same rate.
$\mathcal{H}_0^{(4)} : \sigma^{\text{AD-DE}} - \sigma^{\text{DE}} = 0$	AD-DE and DE volatility coefficients are equal.
$\mathcal{H}_0^{(5)} : p^{\text{AD-DE}} - p^{\text{DE}} = 0$	AD-DE and DE upward jump probabilities are equal.
$\mathcal{H}_0^{(6)} : \lambda^{\text{AD-DE}} - \lambda^{\text{DE}} = 0$	AD-DE and DE jump intensities are equal.
$\mathcal{H}_0^{(7)} : \eta_+^{\text{AD-DE}} - \eta_+^{\text{DE}} = 0$	AD-DE and DE upper tails decay at the same rate.
$\mathcal{H}_0^{(8)} : \eta_-^{\text{AD-DE}} - \eta_-^{\text{DE}} = 0$	AD-DE and DE lower tails decay at the same rate.

Except for the three Asian indices, downward jumps are significantly more frequent. For all equity indices except for the DAX 30 and the NASDAQ Composite, η_- is smaller compared to η_+, thus implying a slower decay of the lower tail the jump size distribution. However, due to the relatively large standard errors of these parameter estimates, the null hypothesis $\mathcal{H}_0^{(3)}$ of equal tail decay can only be rejected at the 10% level for three out of eight indices.

The null hypotheses $\mathcal{H}_0^{(4)}$ through $\mathcal{H}_0^{(8)}$ correspond to the estimates of the AD-DE and the DE parameters being identical. They are thus used to test the empirical Hypotheses II.1 through II.4 formulated in Section II.2.2. For all indices, the diffusion coefficient estimate for the DE model is indeed lower than that for the AD-DE model, thus confirming Hypothesis II.1. However, the differences are so small that the null hypothesis $\mathcal{H}_0^{(4)}$ cannot be rejected at the 10% level. In accordance with Hypothesis II.2, the jump frequency under the AD-DE model is always lower than that under the DE model. This difference is significant for at the 10% level for the NASDAQ Composite and the Nikkei. The conditions in Hypothesis II.3 are satisfied in case of the DAX 30, Dow Jones Industrial, MSCI World, NASDAQ Composite and the S&P 500. In all five cases the signs of the differences between the AD-DE and the DE probability of an upward jump are as predicted. They are significant at the 10% level for three indices. The equality of the tail parameters cannot be rejected at a p-value of 90% in all cases thus providing strong support for Hypothesis II.4.

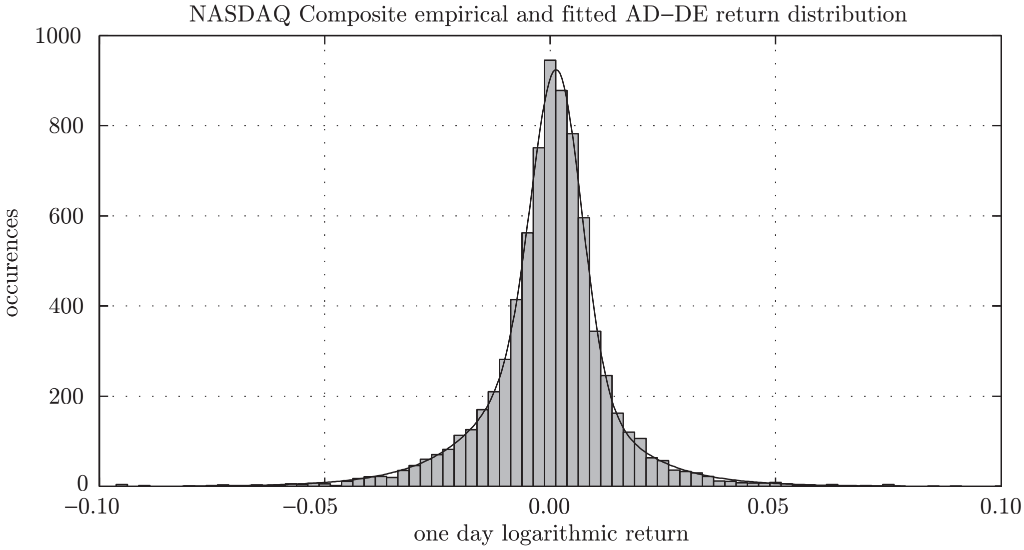

Figure II.10: Fitted AD-DE density for the NASDAQ Composite index based on daily logarithmic returns from January 1, 1982 to December 31, 2011. The parameters are $\sigma = 8.58\%$, $\lambda = 175.55$, $p = 43.74\%$, $\eta_+ = 99.05$, $\eta_- = 104.28$, $\kappa_+ = +0.05\%$ and $\kappa_- = -0.28\%$.

The above results for equity indices also hold for commodity indices, exchange rates and precious metals. For brevity, we thus do not explicitly discuss them. However, all relevant data can be found in Tables II.7 through II.10.

We further estimate the AD-DG model for all assets in the sample. Except for the S&P GSCI Agriculture, we find that the AD-DG and AD-DE parameter estimates coincide, that is the shape parameters of both the positive and negative gamma tails are equal to one. Consequently, the historical return distribution of these assets is consistent with the AD-DE model and the generalization to AD-DG distributed jump sizes provides no further improvement in the fit. As shown in Table II.12, the estimate of the upper tail shape parameter for the S&P GSCI Agriculture is $\delta_+ = 4$. The corresponding displacement term is significant at the 1% level though economically insignificant. A likelihood ratio test for the restriction $\delta_+ = 1$ yields a p-value of 34.29% so that we cannot reject the AD-DE model in favor of the AD-DG model at the 10% level.

In summary, we find very strong empirical support for the AD-DE model dynamics. These results are robust across three different asset classes. For all assets in the sample, both displacement terms are jointly and individually significant at the 1% level. We can reject both the DE as well as the SD-DE model in favor of the AD-DE dynamics. Our results are robust with respect to other estimation horizons. In particular, we obtain the same qualitative results for the 20 year sub-period from January 1, 1992 to December 31, 2011.

Care has to be taken when comparing our results to the studies by Ramezani and Zeng (1999, 2007), which use a slightly different parametrization of the DE model. Instead of estimating the jump frequency and the probability of an up-jump, they estimate the frequency of the independent up- and down-jumps directly. Furthermore, their jump frequency is expressed in number of jumps per trading day instead of per year. When accounting for these difference, then the parameter estimates are of the same order of magnitude. Compared to Detering et al. (2013), we find that the jump frequency for the SD-DE model implied in the time series of logarithmic returns is much higher than the approximately five jumps per year that the authors postulate. Table II.11 contrasts the ML estimates with their approach for the NASDAQ Composite index.

II.9 Conclusion

This chapter extends the Kou (2002) jump-diffusion dynamics by introducing asymmetric displacement terms to the jump size density. The dynamics are supported by an equilibrium economy which also implies a risk-neutral pricing measure. One of our main contributions is to show that the valuation problem for European plain vanilla options still admits a closed-form solution. The model can be further generalized to double gamma jumps without sacrificing analytical tractability. To our knowledge, these are most general jump-diffusion model dynamics yet with this property. Through empirical test, we demonstrate that the extension to asymmetrically displaced jumps is not only academically interesting but also reflects the statistical properties of asset returns. We estimate the model parameters based on a diverse sample of 17 assets across equity indices, commodity indices and foreign exchange. The DE model can be rejected in favor of our AD-DE dynamics for all assets and at the 1% level.

Future research could analyze the ability of the AD-DG model to fit the implied volatility smile or market prices of European plain vanilla options. For reasons discussed in Section II.2.1, different maturities should be analyzed separately instead of jointly. Given the statistically significantly improved fit under the physical probability measure, we expect that the calibration error under the risk-neutral probability measure decreases as well.

Bibliography

Abramowitz, Milton and Irene A. Stegun eds. (1972) *Handbook of Mathematical Functions*, Applied Mathematics Series: National Bureau of Standards, 10th edition.

Aït-Sahalia, Yacine (2002) “Maximum Likelihood Estimation of Discretely Sampled Diffusions: A Closed-Form Approximation Approach,” *Econometrica*, Vol. 70, No. 1, pp. 223–262.

——— (2004) “Disentangling Diffusion from Jumps,” *Journal of Financial Economics*, Vol. 74, No. 3, pp. 487–528.

Albrecher, Hansjörg, Philipp Mayer, Wim Schoutens, and Jurgen Tistaert (2007) “The Little Heston Trap,” *Wilmott Magazine*, pp. 83–92.

Andersen, Leif B. G. and Jesper Andreasen (2002) “Volatile Volatilities,” *Risk*, Vol. 15, No. 12, pp. 163–168.

Andersen, Leif B. G. and Rupert Brotherton-Ratcliffe (1997) “The Equity Option Volatility Smile: An Implicit Finite-Difference Approach,” *Journal of Computational Finance*, Vol. 1, No. 2, pp. 5–37.

Applebaum, David (2004) *Lévy Processes and Stochastic Calculus*: Cambridge University Press.

Ardia, David, Juan David Ospina Arango, and Norman Diego Giraldo Gómez (2011) “Jump-Diffusion Calibration Using Differential Evolution,” *Wilmott Magazine*, No. 55, pp. 76–79.

Attari, Mukarram (2004) “Option Pricing Using Fourier Transforms: A Numerically Efficient Simplification,” Working Paper, Charles River Associates, available at SSRN: http://ssrn.com/abstract=520042.

Back, Kerry E. (2010) *Asset Pricing and Portfolio Choice Theory*, Financial Management Association Survey and Synthesis Series: Oxford University Press.

Bailey, David H. and Paul N. Swarztrauber (1991) “The Fractional Fourier Transform and Applications,” *SIAM Review*, Vol. 33, No. 3, pp. 389–404.

——— (1994) “A Fast Method for the Numerical Evaluation of Continuous Fourier and Laplace Transforms,” *SIAM Journal of Scientific Computing*, Vol. 15, No. 5, pp. 1105–1110.

Bakshi, Gurdip, Charles Cao, and Zhiwu Chen (1997) "Empirical Performance of Alternative Option Pricing Models," *Journal of Finance*, Vol. 52, No. 5, pp. 2003–2049.

Bakshi, Gurdip and Dilip B. Madan (2000) "Spanning and Derivative-Security Valuation," *Journal of Financial Economics*, Vol. 55, pp. 205–238.

Ball, Clifford A. and Walter N. Torous (1983) "A Simplified Jump Process for Common Stock Returns," *Journal of Financial and Quantitative Analysis*, Vol. 18, No. 1, pp. 53–65.

Barndorff-Nielsen, Ole E. (1998) "Processes of Normal Inverse Gaussian Type," *Finance and Stochastics*, Vol. 2, No. 1, pp. 41–68.

Barndorff-Nielsen, Ole E. and Neil G. Shephard (2001a) "Modelling by Lévy Processes for Financial Econometrics," in Ole E. Barndorff-Nielsen, Thomas Mikosch, and Sidney I. Resnick eds. *Lévy Processes - Theory and Applications*: Birkhäuser, pp. 283–318.

——— (2001b) "Non-Gaussian Ornstein-Uhlenbeck-Based Models and Some of Their Uses in Financial Economics," *Journal of the Royal Statistical Society - Series B*, Vol. 63, No. 2, pp. 167–241.

Bates, David S. (1996a) *Statistical Methods in Finance*, Vol. 14 of Handbook of Statistics, Chap. Testing Option Pricing Models, pp. 567–61: North Holland.

——— (1996b) "Jumps and Stochastic Volatility: Exchange Rate Processes Implicit in Deutsche Mark Options," *Review of Financial Studies*, Vol. 9, No. 1, pp. 69–107.

——— (2006) "Maximum Likelihood Estimation of Latent Affine Processes," *Review of Financial Studies*, Vol. 19, No. 3, pp. 909–965.

Beckers, Stan (1981) "A Note on Estimating the Parameters of the Diffusion-Jump Model of Stock Returns," *Journal of Financial and Quantitative Analysis*, Vol. 16, No. 1, pp. 127–140.

Berndt, E. K., B. H. Hall, R. E. Hall, and J. A. Hausman (1974) "Estimation and Inference in Nonlinear Structural Models," *Annals of Economic and Social Measurement*, Vol. 3, No. 4, pp. 653–665.

Black, Fischer and Myron S. Scholes (1973) "The Pricing of Options and Corporate Liabilities," *Journal of Political Economy*, Vol. 3, No. 3, pp. 637–654.

Bühlmann, Hans (1980) "An Economic Premium Principle," *Astin Bulletin*, Vol. 11, No. 1, pp. 52–60.

——— (1984) "The General Economic Premium Principle," *Astin Bulletin*, Vol. 14, No. 1, pp. 13–21.

Carr, Peter P., Hélyette Geman, Dilip B. Madan, and Marc Yor (2003) "Stochastic Volatility for Lévy Processes," *Mathematical Finance*, Vol. 13, No. 3, pp. 345–382.

Carr, Peter P. and Dilip Madan (1999) "Option Valuation Using the Fast Fourier Transform," *Journal of Computational Finance*, Vol. 2, No. 4, pp. 61–73.

Carr, Peter P. and Liuren Wu (2004) "Time-Changed Lévy Processes and Option Pricing," *Journal of Financial Economics*, Vol. 71, No. 1, pp. 113–141.

Chacko, George and Luis M. Viceira (2003) "Spectral GMM Estimation of Continuous-Time Processes," *Journal of Econometrics*, Vol. 116, pp. 259–292.

Cheang, Gerald H. L. and Carl Chiarella (2011) "A Modern View on Merton's Jump-Diffusion Model," Research Paper 287, Quantitative Finance Research Centre, University of Technology Sydney.

Chourdakis, Kyriakos (2004) "Option Pricing Using the Fractional FFT," *Journal of Computational Finance*, Vol. 8, No. 2, pp. 1–18.

Cont, Rama and Peter Tankov (2004) *Financial Modelling with Jump Processes*: Chapman & Hall.

Cooley, James W. and John W. Tuckey (1965) "An Algorithm for the Machine Calculation of Complex Fourier Series," *Mathematics of Computation*, Vol. 19, pp. 297–301.

Cox, John C., Jonathan E. Ingersoll Jr., and Stephen A. Ross (1985) "A Theory of the Term Structure of Interest Rates," *Econometrica*, Vol. 53, No. 2, pp. 385–407.

Cox, John C. and Stephen A. Ross (1976) "The Valuation of Options for Alternative Stochastic Processes," *Journal of Financial Economics*, Vol. 3, pp. 145–166.

Derman, Emanuel, Iraj Kani, and Neil Chriss (1996) "Implied Trinomial Trees of the Volatility Smile," Quantitative Strategies Research Notes, Goldman Sachs.

Derman, Emanuel, Iraj Kani, and Joseph Z. Zou (1995) "The Local Volatility Surface: Unlocking the Information in Index Option Prices," Quantitative Strategies Research Notes, Goldman Sachs.

Detering, Nils, Andreas Weber, and Uwe Wystup (2011) *Statistical Tools for Finance and Insurance*, 2nd edition, Chap. Return Distributions of Equity-Linked Retirement Plans, pp. 393–413: Springer.

——— (2013) "Return Distributions of Equity-Linked Retirement Plans under Jump and Interest Rate Risk," *European Actuarial Journal*, Vol. 3, No. 1, pp. 203–228.

Duffie, Darrell, Jun Pan, and Kenneth Singleton (2000) "Transform Analysis and Asset Pricing for Affine Jump-Diffusions," *Econometrica*, Vol. 68, No. 6, pp. 1343–1376.

Dupire, Bruno (1994) "Pricing with a Smile," *Risk Magazine*, Vol. 7, No. 1, pp. 18–20.

Esscher, Frederik (1932) "On the Probability Function in the Collective Theory of Risk," *Scandinavian Actuarial Journal*, Vol. 15, No. 3, pp. 175–195.

Feller, William (1970) *An Introduction to Probability Theory and Its Applications*, Vol. 2: John Wiley & Sons, 2nd edition.

Folland, Gerald B. (1984) *Real Analysis: Modern Techniques and Their Applications*: John Wiley & Sons.

Frittelli, Marco (2000) "The Minimal Entropy Martingale Measure and the Valuation Problem in Incomplete Markets," *Mathematical Finance*, Vol. 10, No. 1, pp. 39–52.

Fujiwara, Tsukasa and Yoshio Miyahara (2003) "The Minimal Entropy Martingale Measure for Geometric Lévy Processes," *Finance and Stochastics*, Vol. 7, pp. 509–531.

Geman, Hélyette, Dilip B. Madan, and Marc Yor (2001) "Time Changes for Lévy Processes," *Mathematical Finance*, Vol. 11, No. 1, pp. 79–96.

Gerber, Hans U. and Elias S. W. Shiu (1994) "Option Pricing by Esscher Transforms," *Transactions of Society of Actuaries*, Vol. 46, pp. 99–191.

Gil-Pelaez, J. (1951) "Note on the Inversion Theorem," *Biometrica*, Vol. 38, No. 3–4, pp. 481–482.

Gilli, Manfred and Enrico Schumann (2010) "Calibrating the Heston Model with Differential Evolution," in *Applications of Evolutionary Computation*, Vol. 6025 of Lecture Notes in Computer Science: Springer, pp. 242–250.

——— (2012) "Heuristic Optimisation in Financial Modelling," *Annals of Operations Research*, Vol. 193, No. 1, pp. 129–158.

Greene, William H. (2008) *Econometric Analysis*: Pearson Prentice Hall, 6th edition.

Gut, Allan (2005) *Probability: A Graduate Course*: Springer, 1st edition.

Hansen, Lars P. (1982) "Large Sample Properties of Generalized Methods of Moments Estimators," *Econometrica*, Vol. 50, No. 4, pp. 1029–1054.

Harrison, J. Michael and Stanley R. Pliska (1981) "Martingales and Stochastic Integrals in the Theory of Continuous Trading," *Stochastic Processes and Their Applications*, Vol. 11, pp. 215–260.

Heston, Steven L. (1993) "A Closed-Form Solution for Options with Stochastic Volatility with Applications to Bond and Currency Options," *Review of Financial Studies*, Vol. 6, No. 2, pp. 327–343.

Hull, John and Alan White (1987) "The Pricing of Options on Assets with Stochastic Volatilities," *Journal of Finance*, Vol. 42, No. 2, pp. 281–300.

Joshi, Mark and Chao Yang (2011) "Fourier Transform, Option Pricing and Controls," working paper, University of Melbourne, available at http://ssrn.com/abstract=1941464.

Kahl, Christian and Peter Jäckel (2005) "Not-so-Complex Logarithms in the Heston Model," *Wilmott Magazine*, pp. 94–103.

Karatzas, Ioannis and Steven E. Shreve (1991) *Brownian Motion and Stochastic Calculus*: Springer, 2nd edition.

Kiefer, Nicholas M. (1978) "Discrete Parameter Variation: Efficient Estimation of a Switching Regression Model," *Econometrica*, Vol. 46, No. 2, pp. 427–434.

Kilin, Fiodar (2011) "Accelerating the Calibration of Stochastic Volatility Models," *The Journal of Derivatives*, Vol. 18, No. 3, pp. 7–16.

Kou, Steven G. (2002) "A Jump-Diffusion Model for Option Pricing," *Management Science*, Vol. 48, No. 8, pp. 1086–1101.

Kou, Steven G. and Hui Wang (2003) "First Passage Times of a Jump-Diffusion Process," *Advances in Applied Probability*, Vol. 35, pp. 504–531.

——— (2004) "Option Pricing under a Double Exponential Jump-Diffusion Model," *Management Science*, Vol. 50, No. 9, pp. 1178–1192.

Lee, Roger (2004) "Option Pricing by Transform Methods: Extensions, Unification and Error Control," *Journal of Computational Finance*, Vol. 7, No. 3, pp. 51–86.

Lewis, Alan L. (2001) "A Simple Option Formula for General Jump-Diffusion and other Exponential Lévy Processes," Working Paper, Envision Financial Systems and OptionCity.net, available at SSRN: http://ssrn.com/abstract=282110.

Lord, Roger and Christian Kahl (2006) "Why the Rotation Count Algorithm Works," Discussion Paper 2006-065/2, Tinbergen Institute, available at http://ssrn.com/abstract=921335.

——— (2007) "Optimal Fourier Inversion in Semi-Analytical Option Pricing," *Journal of Computational Finance*, Vol. 10, No. 4, pp. 1–30.

——— (2010) "Complex Logarithms in Heston-Like Models," *Mathematical Finance*, Vol. 20, No. 4, pp. 671–694.

Lucas, Robert E., Jr. (1978) "Asset Prices in an Exchange Economy," *Econometrica*, Vol. 46, No. 6, pp. 1429–1445.

Lukacs, Eugene (1970) *Characteristic Functions*: Griffin London, 2nd edition.

Madan, Dilip B., Peter P. Carr, and Eric C. Chang (1998) "The Variance Gamma Process and Option Pricing," *European Finance Review*, Vol. 2, pp. 79–105.

Madan, Dilip B. and Eugene Senata (1990) "The Variance Gamma (V.G.) Model for Share Market Returns," *The Journal of Business*, Vol. 63, No. 4, pp. 511–524.

Merton, Robert C. (1969) "Lifetime Portfolio Selection under Uncertainty: The Continuous-Time Case," *Review of Economics and Statistics*, Vol. 51, No. 3, pp. 247–257.

——— (1973) "Theory of Rational Option Pricing," *The Bell Journal of Economics and Management Science*, Vol. 4, No. 1, pp. 141–183.

——— (1976) "Option Pricing When Underlying Stock Returns Are Discontinuous," *Journal of Financial Economics*, Vol. 3, No. 1-2, pp. 125–144.

Milne, Frank and Dilip B. Madan (1991) "Option Pricing with V.G. Martingale Components," *Mathematical Finance*, Vol. 1, No. 4, pp. 39–55.

Miyahara, Yoshio (1999) "Minimal Entropy Martingale Measure of Jump Type Price Processes in Incomplete Asset Markets," *Asia-Pacific Financial Markets*, Vol. 6, pp. 97–113.

——— (2004) "A Note on Esscher Transformed Martingale Measures for Geometric Lévy Processes," Discussion Paper in Economics 329, Faculty of Economics, Nagoya City University.

Musiela, Marek and Marek Rutkowski (2005) *Martingale Methods in Financial Modelling*: Springer.

Naik, Vasanttilak and Moon Lee (1990) "General Equilibrium Pricing of Options on the Market Portfolio with Discontinuous Returns," *Review of Financial Studies*, Vol. 3, No. 4, pp. 493–521.

von Neumann, John and Oskar Morgenstern (1947) *Theory of Games and Economic Behaviour*: Princeton University Press, 2nd edition.

Newey, Whitney K. and Kenneth D. West (1987) "A Simple, Positive Semi-Definite, Heteroskedasticity and Autocorrelation Consistent Covariance Matrix," *Econometrica*, Vol. 55, No. 3, pp. 703–708.

Pennacchi, George G. (2008) *Theory of Asset Pricing*: Pearson.

Press, S. James (1968) "A Modified Compound Poisson Process with Normal Compounding," *Journal of the American Statistical Association*, Vol. 63, No. 322, pp. 607–613.

Protter, Philip E. (2004) *Stochastic Integration and Differential Equations*: Springer, 2nd edition.

Ramezani, Cyrus A. and Yong Zeng (1999) "Maximum Likelihood Estimation of Asymmetric Jump-Diffusion Processes: Application to Security Prices," Working Paper, Department of Statistics, University of Wisconsin, Madison.

——— (2007) "Maximum Likelihood Estimation of the Double Exponential Jump-Diffusion Process," *Annals of Finance*, Vol. 3, No. 4, pp. 487–507.

Reiss, Oliver and Uwe Wystup (2001) "Efficient Computation of Option Price Sensitivities Using Homogeneity and Other Tricks," *Journal of Derivatives*, Vol. 9, No. 2, pp. 41–53.

Rothschild, Michael and Joseph E. Stiglitz (1970) "Increasing Risk: I. A Definition," *Journal of Economic Theory*, Vol. 2, No. 3, pp. 225–243.

Rubinstein, Mark (1974) "An Aggregation Theorem for Securities Markets," *Journal of Financial Economics*, Vol. 1, No. 3, pp. 225–244.

——— (1985) "Nonparametric Tests of Alternative Option Pricing Models Using All Reported Trades and Quotes on the 30 Most Active CBOE Option Classes from August 23, 1976 through August 31, 1978," *Journal of Finance*, Vol. 40, No. 2, pp. 455–480.

——— (1994) "Implied Binomial Trees," *Journal of Finance*, Vol. 49, No. 3, pp. 771–818.

Schöbel, Rainer and Jianwei Zhu (1999) "Stochastic Volatility with an Ornstein-Uhlenbeck Process: An Extension," *European Finance Review*, Vol. 3, No. 1, pp. 23–46.

Scott, Louis O. (1997) "Pricing Stock Options in a Jump-Diffusion Model with Stochastic Volatility and Interest Rates: Applications of Fourier Inversion Methods," *Mathematical Finance*, Vol. 7, No. 4, pp. 413–424.

Singleton, Kenneth J. (2001) "Estimation of Affine Asset Pricing Models using the Empirical Characteristic Function," *Journal of Econometrics*, Vol. 102, No. 1, pp. 111–141.

Sørensen, Michael (1991) *Statistical Inference in Stochastic Processes*, Chap. Likelihood Methods for Diffusions with Jumps, pp. 67–105: Marcel Dekker.

Stein, Elias M. and Jeremy C. Stein (1991) "Stock Price Distributions with Stochastic Volatility: An Analytic Approach," *Review of Financial Studies*, Vol. 4, No. 4, pp. 727–752.

Storn, Rainer and Kenneth Price (1997) "Differential Evolution - A Simple and Efficient Heuristic for Global Optimization over Continuous Spaces," *Journal of Global Optimization*, Vol. 11, pp. 341–359.

Stuart, Alan and J. Keith Ord (1994) *Kendall's Advanced Theory of Statistics*, Vol. 1: Oxford University Press, 6th edition.

Weber, Andreas and Uwe Wystup (2008) "Riesterrente im Vergleich: Eine Simulationsstudie zur Verteilung der Renditen," working paper 12, Franfurt School of Finance & Management, available at http://www.frankfurt-school.de/clicnetclm/fileDownload.do?goid=000000097900AB4.

Wiggins, James B. (1987) "Option Values under Stochastic Volatility: Theory and Empiricial Estimates," *Journal of Financial Economics*, Vol. 19, No. 2, pp. 351–372.

Yang, Hailiang (2004) *Encyclopedia of Actuarial Science*, Chap. Esscher Transform: Wiley.

II.A Appendix for Section II.2

II.A.1 Characteristic Function of X under $\mathbb{P}$

This appendix contains the detailed proof of Lemma II.2. Let $X = X^c + X^j$, where X^c and X^j are the continuous and pure jump parts of X respectively. Due to the independence of the processes W, N and the sequence of random variables $(Y_i)_{i\in\mathbb{N}}$, the characteristic function factors into the characteristic functions of X^c and X^j. We obtain

$$\begin{aligned}
\phi_{X_t^c}(\omega) &= \mathbb{E}\left[\exp\left\{\mathrm{i}\omega\left(\gamma t + \sigma W_t\right)\right\}\right] \\
&= \exp\left\{\mathrm{i}\omega\gamma t - \frac{1}{2}\omega^2\sigma^2 t\right\}
\end{aligned}$$

and

$$\begin{aligned}
\phi_{X_t^j}(\omega) &= \mathbb{E}\left[\exp\left\{\mathrm{i}\omega\sum_{i=1}^{N_t} Y_i\right\}\right] \\
&= \sum_{n=0}^{\infty}\mathbb{E}\left[\exp\left\{\mathrm{i}\omega\sum_{i=1}^{n} Y_i\right\}\right]\mathbb{P}\left\{N_t = n\right\} \\
&= \sum_{n=0}^{\infty}\left(\mathbb{E}\left[\mathrm{e}^{\mathrm{i}\omega Y_1}\right]\right)^n\mathbb{P}\left\{N_t = n\right\} \\
&= \sum_{n=0}^{\infty}\phi_{Y_1}^n(\omega)\mathrm{e}^{-\lambda t}\frac{(\lambda t)^n}{n!} \\
&= \exp\left\{\lambda t\left(\phi_{Y_1}(\omega) - 1\right)\right\}.
\end{aligned}$$

Here, $\phi_{Y_1}(\omega)$ is the characteristic function of the sequence of random variables $(Y_i)_{i\in\mathbb{N}}$ given by

$$\begin{aligned}
\phi_{Y_1}(\omega) &= p\eta_+\int_{\kappa_+}^{\infty}\mathrm{e}^{x(\mathrm{i}\omega-\eta_+)+\eta_+\kappa_+}\mathrm{d}x + (1-p)\eta_-\int_{-\infty}^{\kappa_-}\mathrm{e}^{x(\mathrm{i}\omega+\eta_-)-\eta_-\kappa_-}\mathrm{d}x \\
&= p\frac{\eta_+}{\mathrm{i}\omega-\eta_+}\mathrm{e}^{x(\mathrm{i}\omega-\eta_+)+\eta_+\kappa_+}\Bigg|_{x=\kappa_+}^{x=\infty} + (1-p)\frac{\eta_-}{\mathrm{i}\omega+\eta_-}\mathrm{e}^{x(\mathrm{i}\omega+\eta_-)-\eta_-\kappa_-}\Bigg|_{x=-\infty}^{x=\kappa_-} \\
&= p\frac{\eta_+}{\eta_+-\mathrm{i}\omega}\mathrm{e}^{\mathrm{i}\omega\kappa_+} + (1-p)\frac{\eta_-}{\eta_-+\mathrm{i}\omega}\mathrm{e}^{\mathrm{i}\omega\kappa_-}.
\end{aligned}$$

Note, that given the characteristic function of the exponential distribution, we could have alternatively used the translation property of the Fourier transform to find the characteristic function of the displaced exponential distribution without further computations; see for example Theorem 4.1.10 in Gut (2005), p. 166. Similarly, the characteristic function of the negative exponential distribution is given by the complex conjugate of the characteristic function of the positive exponential distribution; see for example Theorem 2.1.1 in Lukacs (1970), p. 15. We use this approach to find the characteristic function of the AD-DG distribution in Appendix II.E.1. Putting everything together, we get

$$\phi_{X_t}(\omega) = \phi_{X_t^c}(\omega)\phi_{X_t^j}(\omega) = \exp\left\{\mathrm{i}\omega\gamma t - \frac{1}{2}\omega^2\sigma^2 t + \lambda t\left(\phi_{Y_1}(\omega) - 1\right)\right\}.$$

II.B Appendix for Section II.3

II.B.1 Esscher Transform Logarithmic Return Dynamics

This appendix contains the detailed proof of Proposition II.1. First note that the Radon-Nikodým derivative process can be expressed as

$$\begin{aligned}
\nu_t\left(\mathbb{P},\mathbb{P}^*\right) &= \exp\left\{\beta X_t - t\psi_{X_1}(-\mathrm{i}\beta)\right\} \\
&= \exp\left\{\beta\sigma W_t - \frac{1}{2}\beta^2\sigma^2 t\right\}\exp\left\{\left(\beta\gamma + \frac{1}{2}\beta^2\sigma^2\right)t + \beta\sum_{i=1}^{N_1} Y_i - t\psi_{X_1}(-\mathrm{i}\beta)\right\} \\
&= \exp\left\{\beta\sigma W_t - \frac{1}{2}\beta^2\sigma^2 t\right\}\exp\left\{\beta\sum_{i=1}^{N_t} Y_i - t\psi_{X_1^j}(-\mathrm{i}\beta)\right\}.
\end{aligned}$$

Here, the first factor changes drift of the Brownian motion W and the second term changes the intensity and jump size distribution of the compound Poisson process X^j. By Girsanov's theorem, it follows that W is a drifted Brownian motion under $\mathbb{P}^*$ with drift $\beta\sigma$. Equivalently, the process W^* defined by

$$W_t^* = W_t - \beta\sigma t$$

is a standard Brownian motion under $\mathbb{P}^*$. By Proposition 9.5 in Cont and Tankov (2004), pp. 303–304, in order to define a measure change for a compound Poisson process, the Radon-Nikodým derivative process has to take the form

$$\exp\left\{\beta\sum_{i=1}^{N_t} Y_i - t\psi_{X_1^j}(-\mathrm{i}\beta)\right\} = \exp\left\{\sum_{i=1}^{N_t}\ln\left(\frac{\lambda^* f^*\left(Y_i\right)}{\lambda f\left(Y_i\right)}\right) - \left(\lambda^* - \lambda\right)t\right\}.$$

From this representation, we immediately find that

$$
\begin{aligned}
\lambda^* &= \psi_{X_1^j}(-\mathrm{i}\beta) + \lambda \\
&= \lambda \left(p\frac{\eta_+}{\eta_+ - \beta}\mathrm{e}^{\beta\kappa_+} + (1-p)\frac{\eta_-}{\eta_- + \beta}\mathrm{e}^{\beta\kappa_-} \right) \\
&= \lambda\phi_{Y_1}(-\mathrm{i}\beta).
\end{aligned}
$$

In order for this expression to be well-defined and non-negative, we require that $\eta_+ > \beta$ and $\eta_- > -\beta$. We denote the set of admissible values for the transform parameter β by $\mathcal{B} = (-\eta_-, \eta_+)$. Next,

$$
\begin{aligned}
f^*(x) &= \frac{\lambda}{\lambda^*} f(x)\mathrm{e}^{\beta x} \\
&= \frac{\lambda}{\lambda^*}\left(p\eta_+\mathrm{e}^{-(\eta_+-\beta)x+\eta_+\kappa_+} 1\{x \geq \kappa_+\} + (1-p)\eta_-\mathrm{e}^{(\eta_-+\beta)x-\eta_-\kappa_-} 1\{x \leq \kappa_-\} \right).
\end{aligned}
$$

Now let

$$
\eta_+^* = \eta_+ - \beta, \qquad \eta_-^* = \eta_- + \beta
$$

and group terms to obtain

$$
\begin{aligned}
f^*(x) &= \left(p\frac{\lambda\eta_+}{\lambda^*\eta_+^*}\mathrm{e}^{\kappa_+\left(\eta_+-\eta_+^*\right)} \right) \eta_+^*\mathrm{e}^{-\eta_+^*(x-\kappa_+)} 1\{x \geq \kappa_+\} \\
&\quad + \left((1-p)\frac{\lambda\eta_-}{\lambda^*\eta_-^*}\mathrm{e}^{-\kappa_-\left(\eta_--\eta_-^*\right)} \right) \eta_-^*\mathrm{e}^{\eta_-^*(x-\kappa_-)} 1\{x \leq \kappa_-\} \\
&= p^*\eta_+^*\mathrm{e}^{-\eta_+^*(Y_i-\kappa_+)} 1\{x \geq \kappa_+\} + (1-p^*)\,\eta_-^*\mathrm{e}^{\eta_-^*(x-\kappa_-)} 1\{x \leq \kappa_-\},
\end{aligned}
$$

where the definitions of p^* and $1-p^*$ are implicitly clear. Some tedious algebra shows that these two terms indeed sum to one. Furthermore, $\beta \in \mathcal{B}$ also guarantees that both p^* and $1-p^*$ are non-negative and thus $p^* \in [0,1]$ represents a valid probability. Thus, under $\mathbb{P}^*$, we have

$$
X_t = \gamma^* t + \sigma W_t^* + \sum_{i=1}^{N_t^*} Y_i^*,
$$

where $\gamma^* = \gamma + \beta\sigma^2$, N^* is a Poisson process with intensity λ^* and the Y_i, $i = 1, 2, \ldots$ are i.i.d. random variables with PDF $f^*(x)$. It immediately follows from the results in Appendix II.A.1 that the characteristic exponent of X under $\mathbb{P}^*$ is given by

$$
\begin{aligned}
\psi_X^*(\omega) &= \mathrm{i}\omega\gamma^* - \frac{1}{2}\sigma^2\omega^2 + \lambda^* \int_{-\infty}^{+\infty} \left(\mathrm{e}^{\mathrm{i}\omega x} - 1\right) f^*(x)\mathrm{d}x \\
&= \mathrm{i}\omega\left(\gamma + \beta\sigma^2\right) - \frac{1}{2}\sigma^2\omega^2 + \lambda \int_{-\infty}^{+\infty} \left(\mathrm{e}^{\mathrm{i}\omega x} - 1\right) f(x)\mathrm{e}^{\beta x}\mathrm{d}x,
\end{aligned}
$$

where the integral evaluates to

$$\begin{aligned}
& \lambda \int_{-\infty}^{+\infty} \left(\mathrm{e}^{x}-1\right) f(x) \mathrm{e}^{\beta x} \mathrm{d}x \\
= & \lambda \int_{-\infty}^{+\infty} \mathrm{e}^{x(1+\beta)} f(x) \mathrm{d}x - \lambda^{*} \int_{-\infty}^{+\infty} \frac{\lambda}{\lambda^{*}} \mathrm{e}^{\beta x} f(x) \mathrm{d}x \\
= & \lambda \phi_{Y_1}(-\mathrm{i}(1+\beta)) - \lambda^{*} \\
= & \lambda \left(\phi_{Y_1}(-\mathrm{i}(1+\beta)) - \phi_{Y_1}(-\mathrm{i}\beta)\right).
\end{aligned}$$

II.B.2 Existence and Uniqueness of the Esscher Transform Martingale Measure

This appendix contains the detailed proof of Proposition II.2. Let the function $k : \mathbb{R} \times \mathcal{B} \to \mathbb{R}$ be the integrand in Equation II.3, that is

$$k(x, \beta) = \left(\mathrm{e}^{x} - 1\right) \mathrm{e}^{\beta x} f(x).$$

We need to show that there exists another non-negative function $h : \mathbb{R} \to \mathbb{R}_{+}$ such that for all $\beta \in \mathcal{B}$, $k(x, \beta)$ is bounded by $h(x)$ almost everywhere. Note that

$$\mathrm{e}^{\beta x} f(x) = p\eta_{+} \mathrm{e}^{x(\beta-\eta_{+})+\eta_{+}\kappa_{+}} 1\left\{x \geq \kappa_{+}\right\} + (1-p)\eta_{-} \mathrm{e}^{x(\beta+\eta_{-})-\eta_{-}\kappa_{-}} 1\left\{x \leq \kappa_{-}\right\}.$$

Since $\beta \in (-\eta_{-}, \eta_{+})$, we have that $\lim_{x \to \pm\infty} f(x)\mathrm{e}^{\beta x} = 0$. The function $f(x)\mathrm{e}^{\beta x}$ thus attains its global maximum at either $x = \kappa_{-}$ or $x = \kappa_{+}$. Furthermore since $\mathrm{e}^{\beta x} f(x) \geq 0$ for all $x \in \mathbb{R}$, it follows that

$$|f(x)\mathrm{e}^{\beta x}| \leq \max\left\{p\eta_{+}\mathrm{e}^{\beta\kappa_{+}}, (1-p)\eta_{-}\mathrm{e}^{\beta\kappa_{-}}\right\} \leq \max\left\{p\eta_{+}\mathrm{e}^{\eta_{+}\kappa_{+}}, (1-p)\eta_{-}\mathrm{e}^{-\eta_{-}\kappa_{-}}\right\}$$

and thus

$$|k(x,\beta)| \leq |\mathrm{e}^{x}-1||f(x)\mathrm{e}^{\beta x}| \leq |\mathrm{e}^{x}-1| \max\left\{p\eta_{+}\mathrm{e}^{\eta_{+}\kappa_{+}}, (1-p)\eta_{-}\mathrm{e}^{-\eta_{-}\kappa_{-}}\right\} = l(x).$$

Since in addition $k(x, \beta)$ is continuous in its second argument, it follows by Theorem 2.27.a in Folland (1984), p. 54, that $g(\beta)$ in Equation II.3 is continuous on $\mathcal{B}$. Next, note that the partial derivative

$$\frac{\partial k}{\partial \beta}(x, \beta) = x k(x, \beta)$$

exists for every $x \in \mathbb{R}$ and $\beta \in \mathcal{B}$ and is continuous in its second argument. Furthermore,

$$\left|\frac{\partial k}{\partial \beta}(x, \beta)\right| \leq |x| l(x).$$

It follows by Theorem 2.27.b in Folland (1984), p. 54, that $g(\beta)$ is differentiable on $\mathcal{B}$. The derivative

$$g'(\beta) = \sigma^2 + \lambda \int_{-\infty}^{+\infty} x\left(\mathrm{e}^x - 1\right) f(x) \mathrm{e}^{\beta x} \mathrm{d}x > 0,$$

is strictly positive since the integrand is non-negative. Finally, note that

$$\lim_{\beta \downarrow -\eta_-} g(\beta) = -\infty, \qquad \lim_{\beta \to \eta_+} g(\beta) = \infty.$$

In summary, the function $g(\beta)$ is continuous and strictly increasing on $\mathcal{B}$ with range $\mathbb{R}$. Consequently, the Equation II.3 has a unique solution.

II.B.3 Properties of the Esscher Transform Martingale Measure

This appendix contains the detailed proof of Corollary II.2. As part of the proof of Property (iii) in Corollary II.2, we need to show that $\partial p^*/\partial \beta$ as defined in Proposition II.1 is positive. First, it is convenient to write

$$p^*(\beta) = \left(1 + \frac{(1-p)\eta_-\left(\eta_+ - \beta\right)}{p\left(\eta_- + \beta\right)\eta_+} \mathrm{e}^{\beta(\kappa_- - \kappa_+)}\right)^{-1}.$$

Then

$$\begin{aligned} &\frac{\partial p^*}{\partial \beta}(\beta) \\ = \quad & -\left(p^*(\beta)\right)^2 \left(\frac{(1-p)\eta_-}{p\left(\eta_- + \beta\right)^2 \eta_+} \mathrm{e}^{\beta(\kappa_- - \kappa_+)}\right)\left(\left(\kappa_- - \kappa_+\right)\left(\eta_+ - \beta\right)\left(\eta_- + \beta\right) - \eta_+ - \eta_-\right). \end{aligned}$$

It is obvious that the first two factors are positive. The third one is negative since $\kappa_- \leq \kappa_+$ and both $\eta_- + \beta$ and $\eta_+ - \beta$ are strictly positive due to $\beta \in (-\eta_-, \eta_+)$. It follows that $\partial p^*/\partial \beta > 0$ as claimed.

We next prove Property (v) in Corollary II.2. Since $\lambda^* = \lambda \theta_{Y_1}(\beta)$, where

$$\theta_{Y_1}(x) = \mathbb{E}\left[\mathrm{e}^{x Y_1}\right],$$

it is sufficient to show that there exists two parameter combinations for the AD-DE distribution and a fixed value of β, such that the sign of the moment generating function differs. One possibility to achieve this is to find two parameter combinations such that the slope of the moment generating function at the origin changes. We have

$$\theta_{Y_1}(0) = p\left(\kappa_+ + \frac{1}{\eta_+}\right) + (1-p)\left(\kappa_- - \frac{1}{\eta_-}\right).$$

Now consider $p = 50.00\%$ and $\eta_+ = \eta_-$. Then $\operatorname{sgn}(\theta_{Y_1}(0)) = \operatorname{sgn}(\kappa_+ - \kappa_-)$. Thus, for $\kappa_+ > \kappa_-$, the slope is positive and *vice versa*.

II.C Appendix for Section II.4

II.C.1 Equilibrium Pricing Equation

This appendix contains the detailed proof of Lemma II.5. Let M be a stochastic discount factor process. Then the budget constraint is can be expressed as

$$\mathbb{E}_{\mathbb{P}}\left[\int_t^\infty C_u M_u \mathrm{d}u \middle| \mathfrak{F}_t\right] \leq V_t M_t.$$

To solve the constraint optimization problem, we construct the Lagrangian

$$\mathcal{L}\left(\{C_u, 0 \leq u \leq \infty\}\right) = \mathbb{E}_{\mathbb{P}}\left[\int_t^\infty \left(\mathrm{e}^{-\rho v} u\left(C_v\right) - \lambda M_v\right) \mathrm{d}v \middle| \mathfrak{F}_t\right] + \lambda V_t M_t.$$

The first order condition for optimal consumption is then given by

$$\frac{\partial \mathcal{L}}{\partial C_v}\left(\{C_u, 0 \leq u \leq \infty\}\right) = 0 \qquad \Leftrightarrow \qquad \mathrm{e}^{-\rho v} u'\left(C_v^*\right) = \lambda M_v,$$

which has to hold for all $v \in [t, \infty)$. By the properties of the stochastic discount factor, the time $t \geq 0$ value of the payout stream ζ is given by

$$\begin{aligned} \pi_t(\zeta) &= \frac{1}{M_t}\mathbb{E}_{\mathbb{P}}\left[\int_t^\infty \zeta_u M_u \mathrm{d}u \middle| \mathfrak{F}_t\right] \\ &= \frac{1}{\mathrm{e}^{-\rho t} u'\left(\delta_t\right)}\mathbb{E}_{\mathbb{P}}\left[\int_t^\infty \mathrm{e}^{-\rho v} u'\left(\delta_v\right) \zeta_v \mathrm{d}v \middle| \mathfrak{F}_t\right] \end{aligned}$$

and Lemma II.5 follows.

II.C.2 Equilibrium Risk-Free Rate

This appendix contains the detailed proof of Proposition II.3. A zero-coupon bond with maturity in $T \geq t$ has single payment of one unit of the consumption good at maturity and no intermediate cash-flows. We thus have $\zeta_t = \Delta(T-t)$ where $\Delta(x)$ is the Dirac delta function with the property

$$\int_{-\infty}^{+\infty} f(y)\Delta(x-y)\mathrm{d}y = f(x),$$

for any function $f(x)$. Using the general valuation formula from Lemma II.5 in conjunction with the iso-elastic utility function, we thus get

$$\begin{aligned}
B(t,T) &= \frac{1}{\mathrm{e}^{-\rho t}\delta_t^{-\alpha}}\mathbb{E}_{\mathbb{P}}\left[\int_t^{\infty} \mathrm{e}^{-\rho v}\delta_v^{-\alpha}\Delta(T-v)\mathrm{d}v \middle| \mathfrak{F}_t\right] \\
&= \frac{1}{\mathrm{e}^{-\rho t}\delta_t^{-\alpha}}\mathbb{E}_{\mathbb{P}}\left[\mathrm{e}^{-\rho T}\delta_T^{-\alpha} \middle| \mathfrak{F}_t\right] \\
&= \mathrm{e}^{-\rho(T-t)}\mathbb{E}_{\mathbb{P}}\left[\mathrm{e}^{-\alpha(X_T-X_t)} \middle| \mathfrak{F}_t\right].
\end{aligned}$$

To compute this expectation, we use that the increment $X_T - X_t$ is independent of $\mathfrak{F}_t$ and has the same distribution under $\mathbb{P}$ as X_{T-t}. Thus,

$$\begin{aligned}
B(t,T) &= \mathrm{e}^{-\rho(T-t)}\mathbb{E}_{\mathbb{P}}\left[\mathrm{e}^{-\alpha X_{T-t}}\right] \\
&= \exp\left\{(T-t)\left(\psi_{X_1}(\mathrm{i}\alpha) - \rho\right)\right\}.
\end{aligned}$$

The corresponding yield is then given by

$$\begin{aligned}
y(t,T) &= -\frac{1}{T-t}\ln B(t,T) \\
&= \rho - \psi_{X_1}(\mathrm{i}\alpha).
\end{aligned}$$

We see that Assumption II.6.(i) guarantees that the risk-free interest rate is strictly positive.

II.C.3 Equilibrium Stock Price

This appendix contains the detailed proof of Proposition II.4. Again using the general valuation formula from Lemma II.5 with $\zeta_t = \delta_t$ yields

$$\begin{aligned} S_t &= \frac{1}{\mathrm{e}^{-\rho t}\delta_t^{-\alpha}} \mathbb{E}_{\mathbb{P}}\left[\int_t^\infty \mathrm{e}^{-\rho v}\delta_v^{1-\alpha}\mathrm{d}v \middle| \mathfrak{F}_t\right] \\ &= \delta_t \mathbb{E}_{\mathbb{P}}\left[\int_t^\infty \exp\left\{-\rho(v-t) + (1-\alpha)\left(X_v - X_t\right)\right\}\mathrm{d}v \middle| \mathfrak{F}_t\right] \\ &= \delta_t \mathbb{E}_{\mathbb{P}}\left[\int_t^\infty \exp\left\{-\rho(v-t) + (1-\alpha)X_{v-t}\right\}\mathrm{d}v\right]. \end{aligned}$$

We now need to interchange the integration and expectation. Since,

$$\begin{aligned} \mathbb{E}_{\mathbb{P}}\left[\left|\mathrm{e}^{-\rho(v-t)+(1-\alpha)X_{v-t}}\right|\right] &= \mathbb{E}_{\mathbb{P}}\left[\mathrm{e}^{-\rho(v-t)+(1-\alpha)X_{v-t}}\right] \\ &= \exp\left\{\left(\psi_{X_1}(\mathrm{i}(\alpha-1)) - \rho\right)(v-t)\right\} \\ &\leq 1 \qquad \forall v \in [t,\infty). \end{aligned}$$

this is justified by the stochastic Fubini Theorem; see for example Theorem VI.65 in Protter (2004), p. 207. The inequality follows from Assumption II.6.(ii), which ensures that the exponent is strictly negative for $v > t$. Thus,

$$\begin{aligned} S_t &= \delta_t \int_t^\infty \exp\left\{\left(\psi_{X_1}(\mathrm{i}(\alpha-1)) - \rho\right)(v-t)\right\}\mathrm{d}v \\ &= \frac{\delta_t}{\rho - \psi_{X_1}(\mathrm{i}(\alpha-1))}. \end{aligned}$$

II.C.4 Equilibrium Risk-Neutral Measure

This appendix contains the detailed proof of Proposition II.5. From the proof of Lemma II.5, we have that $M_t \propto \mathrm{e}^{-\rho t}u'\left(\delta_t\right)$. Thus, the Radon-Nikodým derivative process $\nu\left(\mathbb{P},\mathbb{P}^*\right)$ can be expressed as

$$\begin{aligned} \nu_t\left(\mathbb{P},\mathbb{P}^*\right) &= \mathrm{e}^{(r-\rho)t}\frac{u'\left(\delta_t\right)}{u'\left(\delta_0\right)} \\ &= \exp\left\{(r-\rho)t - \alpha X_t\right\} \\ &= \exp\left\{-\alpha X_t - t\psi_{X_1}(\mathrm{i}\alpha)\right\}, \end{aligned}$$

where the last equality uses the expression for the risk-free interest rate obtained in Proposition II.3. By Proposition 2.1.3 in Applebaum (2004), pp. 72–73, $\nu\left(\mathbb{P},\mathbb{P}^*\right)$ is a strictly positive $(\mathbb{P},\mathbb{F})$-martingale with initial value $\nu_0(\mathbb{P},\mathbb{P}^*)=1$. Thus, it constitutes a valid Radon-Nikodým derivative process for an equivalent measure change; see for example Chapter III.8 in Protter (2004), pp. 131–143. Starting from the general valuation formula in Lemma II.5, we then get

$$\begin{aligned}\pi_t(\zeta) &= \frac{1}{M_t}\mathbb{E}_{\mathbb{P}}\left[\int_t^\infty \zeta_u M_u \mathrm{d}u \middle| \mathfrak{F}_t\right] \\ &= \mathbb{E}_{\mathbb{P}}\left[\int_t^\infty \mathrm{e}^{-r(u-t)}\zeta_u \frac{\nu_u(\mathbb{P},\mathbb{P}^*)}{\nu_t(\mathbb{P},\mathbb{P}^*)}\mathrm{d}u \middle| \mathfrak{F}_t\right] \\ &= \mathbb{E}_{\mathbb{P}^*}\left[\int_t^\infty \mathrm{e}^{-r(u-t)}\zeta_u \mathrm{d}u \middle| \mathfrak{F}_t\right].\end{aligned}$$

In the last step, we apply the abstract Bayes rule to change the measure from $\mathbb{P}$ to $\mathbb{P}^*$; see for example Lemma A.1.4 in Musiela and Rutkowski (2005), p. 615.

II.D Appendix for Section II.5

II.D.1 Distribution of $\xi^+ - \xi^-$

This appendix contains the detailed proof of Lemma II.7. First, remember that the random variables ξ^+ and ξ^- are independent and have density functions

$$f_{\xi^+}(x) = \eta_+ \mathrm{e}^{-\eta_+(x-\kappa)}1\{x \geq \kappa\}, \qquad f_{\xi^-}(x) = \eta_- \mathrm{e}^{-\eta_-(x-\kappa)}1\{x \geq \kappa\}.$$

The density function of $\xi^+ - \xi^-$ is thus given by the convolution

$$\begin{aligned}f_{\xi^+-\xi^-}(x) &= \int_{-\infty}^{+\infty} f_{\xi^+}(y) f_{\xi^-}(y-x)\mathrm{d}y \\ &= \int_{\max\{\kappa,x+\kappa\}}^{\infty} \eta_+\eta_- \mathrm{e}^{-(\eta_++\eta_-)(y-\kappa)+\eta_- x}\mathrm{d}y \\ &= \frac{\eta_+\eta_-}{\eta_++\eta_-}\left(\mathrm{e}^{\eta_- x}1\{x<0\} + \mathrm{e}^{-\eta_+ x}1\{x>0\} + 1\{x=0\}\right).\end{aligned}$$

Next,

$$\begin{aligned}\mathbb{P}\left\{\xi^+ \geq \xi^-\right\} &= \int_{-\infty}^{+\infty} f_{\xi^-}(x)\int_x^\infty f_{\xi^+}(y)\mathrm{d}y\mathrm{d}x \\ &= \int_\kappa^\infty \eta_-\mathrm{e}^{-\eta_-(x-\kappa)}\int_x^\infty \eta_+\mathrm{e}^{-\eta_+(y-\kappa)}\mathrm{d}y \\ &= \int_\kappa^\infty \eta_-\mathrm{e}^{-(\eta_++\eta_-)(x-\kappa)}\mathrm{d}y \\ &= \frac{\eta_-}{\eta_++\eta_-}.\end{aligned}$$

This yields the conditional density

$$\begin{aligned} f_{\xi^+-\xi^-|\xi^+\geq\xi^-}(x) &= \eta_+\mathrm{e}^{-\eta_+x}1\{x\geq 0\} \\ &= f_{\xi^+}(x+\kappa). \end{aligned}$$

Similarly, we have

$$\mathbb{P}\left\{\xi^+\leq\xi^-\right\} = 1-\mathbb{P}\left\{\xi^+>\xi^-\right\} = \frac{\eta_+}{\eta_++\eta_-}$$

with corresponding conditional density

$$\begin{aligned} f_{\xi^+-\xi^-|\xi^+\leq\xi^-}(x) &= \eta_-\mathrm{e}^{\eta_-x}1\{x\leq 0\} \\ &= f_{\xi^-}(-x+\kappa))). \end{aligned}$$

In summary, we can decompose the distribution of $\xi^+-\xi^-$ into

$$\xi^+-\xi^-\sim\begin{cases}\xi^+-\kappa & \text{with probability } \eta_-/\left(\eta_++\eta_-\right) \\ -\xi^-+\kappa & \text{with probability } \eta_+/\left(\eta_++\eta_-\right)\end{cases}.$$

II.D.2 Distribution of $A(n,m)$ I

This appendix contains the detailed proof of Lemma II.8. We first apply Lemma II.7 to decompose the distribution of

$$A(n,m)=A(n-1,m-1)+\xi_n^+-\xi_m^-.$$

as

$$\begin{aligned} A(n,m) &\sim \begin{cases} A(n-1,m-1)+\xi_n^+-\kappa & \text{with probability } \eta_-/\left(\eta_++\eta_-\right) \\ A(n-1,m-1)-\xi_m^-+\kappa & \text{with probability } \eta_+/\left(\eta_++\eta_-\right)\end{cases} \\ &\sim \begin{cases} A(n,m-1)-\kappa & \text{with probability } \eta_-/\left(\eta_++\eta_-\right) \\ A(n-1,m)+\kappa & \text{with probability } \eta_+/\left(\eta_++\eta_-\right)\end{cases}. \end{aligned}$$

We can iteratively repeat this step until we are left with an expression of the form $A(k,0)$ or $A(0,l)$ plus a deterministic term which is some multiple of the displacement term κ.

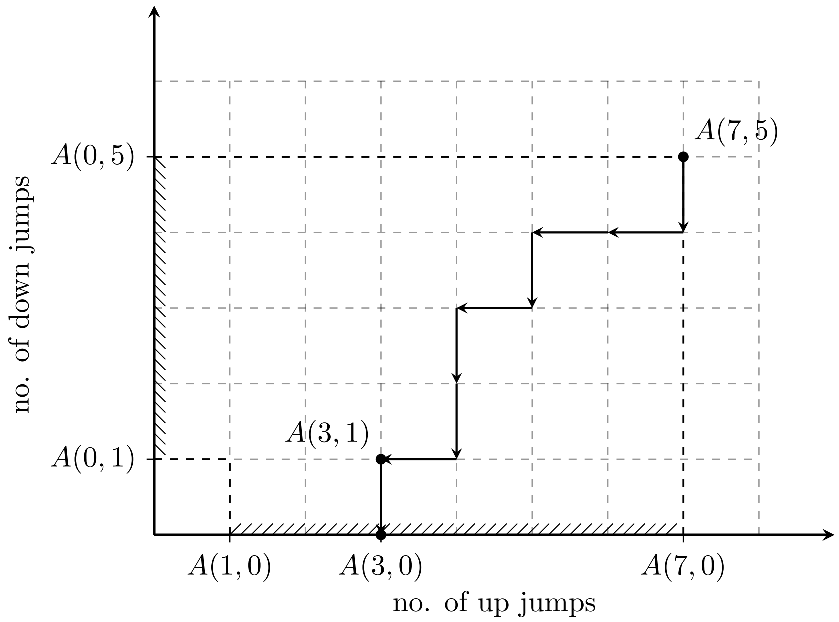

Figure II.11: Sample path of the random walk starting at $A(7,5)$ and moving left four and down five steps to stop at $A(3,0)$. The thick dotted lines represent the boundary of the domain on which the random walk lives. The dashed lines correspond to the parts of the boundary on which the random walk is stopped.

We use the same combinatorial proof as the one given for Lemma B.1 in Kou (2002), pp. 1098–1099. Consider the number of ξ^+ and ξ^- in the sums to be the position of a random walk on an integer lattice starting at $\{n,m\}$ in the first quadrant and stopping once it hits either of the two axes. Each step reduces the number of either ξ^+ or ξ^- in the sums by one and thus corresponds to moving either left or down in the lattice. Consequently, only the nodes $\{k,0\}$ ($\{0,l\}$) for $k=1,2,\ldots,n$ ($l=1,2,\ldots,m$) can be reached on the x-axis (y-axis). In particular, the node $\{0,0\}$ can never be reached. Immediately before hitting the node $\{k,0\}$ ($\{0,l\}$), the random walk has to be at $\{k,1\}$ ($\{1,l\}$) and then take a down (left) step. It has to take a total of $n-k$ ($n-1$) left and $m-1$ ($m-l$) down steps to get from $\{n,m\}$ to $\{k,1\}$ ($\{1,l\}$). There are $\binom{n-k+m-1}{m-1}$ ($\binom{n-1+m-l}{n-1}$) such paths. By the previous result, the probabilities of a left and down step are $\eta_+/\left(\eta_+ + \eta_-\right)$ and $\eta_-/\left(\eta_+ + \eta_-\right)$, respectively. The factor multiplying κ is equal to the difference between the number of left- and down-steps taken. Thus

$$A(n,m) \sim \begin{cases} A(k,0) + (n-k-m)\kappa & \text{with probability } \tilde{p}(n,k) \\ & \quad \text{for } k = 1,2,\ldots,n \\ A(0,l) + (n-m+l)\kappa & \text{with probability } \tilde{q}(n,l) \\ & \quad \text{for } l = 1,2,\ldots,m \end{cases},$$

where

$$\begin{aligned} \tilde{p}(n,k) &= \binom{n-k+m-1}{m-1} \left(\frac{\eta_+}{\eta_+ + \eta_-}\right)^{n-k} \left(\frac{\eta_-}{\eta_+ + \eta_-}\right)^{m}, \\ \tilde{q}(n,l) &= \binom{n-1+m-l}{n-1} \left(\frac{\eta_+}{\eta_+ + \eta_-}\right)^{n} \left(\frac{\eta_-}{\eta_+ + \eta_-}\right)^{m-l}. \end{aligned}$$

Figure II.11 illustrates the domain and a sample path of the random walk starting at $A(7,5)$ and stopping at $A(3,0)$.

II.D.3 Distribution of $A(n,m)$ II

This appendix contains the detailed proof of Lemma II.8*. Using Lemma II.7*, we can decompose the distribution of

$$A(n,m) = A(n-1,m-1) + \hat{\xi}_n^+ - \hat{\xi}_m^- + 2\alpha$$

as

$$A(n,m) \quad \sim \quad \begin{cases} A(n,m-1) + \alpha - \kappa & \text{with probability } \eta_- / (\eta_+ + \eta_-) \\ A(n-1,m) + \alpha + \kappa & \text{with probability } \eta_+ / (\eta_+ + \eta_-) \end{cases}.$$

We again iteratively repeat this step until we are left with an expression of the form $A(k,0)$ or $A(0,l)$. The term multiplying α is equal to the total number of iteration steps taken, which are given by $n-k+m$ and $n+m-l$ respectively.

II.D.4 Jump-Diffusion Upper Tail Probability

This appendix contains the detailed proof of Theorem II.1. We start by expression the upper tail probability of the jump-diffusion process X as a probability weighted sum over the tail probabilities conditional on a fixed total number of jumps, that is

$$\mathbb{P}\left\{Z_t\left(Y,N_t\right)\geq x\right\}=\sum_{n=0}^{\infty}\mathbb{P}\left\{N_t=n\right\}\mathbb{P}\left\{Z_t(Y,n)\geq x\right\}.$$

Using Proposition II.6* and Lemma II.9, we can express the summands in terms of I_n-functions as

$$\begin{aligned}
\ldots \;=\; & \mathbb{P}\left\{N_t=0\right\}\mathbb{P}\left\{Z_t(\cdot,0)\geq x\right\}+\sum_{n=1}^{\infty}\mathbb{P}\left\{N_t=n\right\}\Big(\mathbb{P}\left\{Z_t\left(\xi^+,n\right)\geq x\right\}\hat{p}(n,n)\\
&+\mathbb{P}\left\{Z_t\left(-\xi^-,n\right)\geq x\right\}\hat{p}(0,n)\\
&+\sum_{k=1}^{n-1}\Big(\sum_{i=k}^{n-1}\mathbb{P}\left\{Z_t\left(\xi^+,k\right)+(n-k)\alpha+(2i-n-k)\kappa\geq x\right\}\hat{p}(i,n)\tilde{p}(i,n-i,k)\\
&+\sum_{i=1}^{n-k}\mathbb{P}\left\{Z_t\left(-\xi^-,k\right)+(n-k)\alpha+(2i-n+k)\kappa\geq x\right\}\hat{p}(i,n)\tilde{q}(i,n-i,k)\Big)\Big).
\end{aligned}$$

We can merge the inner two summations by changing the order of summation which corresponds to replacing i by $n-i$ in the second sum and get

$$\begin{aligned}
\ldots \;=\; & \mathbb{P}\left\{N_t=0\right\}\mathbb{P}\left\{Z_t(\cdot,0)\geq x\right\}+\sum_{n=1}^{\infty}\mathbb{P}\left\{N_t=n\right\}\Big(\mathbb{P}\left\{Z_t\left(\xi^+,n\right)\geq x\right\}\hat{p}(n,n)\\
&+\mathbb{P}\left\{Z_t\left(-\xi^-,n\right)\geq x\right\}\hat{p}(0,n)\\
&+\sum_{k=1}^{n-1}\sum_{i=k}^{n-1}\Big(\mathbb{P}\left\{Z_t\left(\xi^+,k\right)+(n-k)\alpha+(2i-n-k)\kappa\geq x\right\}\hat{p}(i,n)\tilde{p}(i,n-i,k)\\
&+\mathbb{P}\left\{Z_t\left(-\xi^-,k\right)+(n-k)\alpha-(2i-n-k)\kappa\geq x\right\}\hat{p}(n-i,n)\tilde{q}(n-i,i,k)\Big)\Big).
\end{aligned}$$

Also, note that the ξ^+ $(-\xi^-)$ are not standard (negative) exponential random variables. To make this explicit such that Lemma II.9 can be directly applied, we write

$$\begin{aligned}
\ldots \;=\; & \mathbb{P}\left\{N_t=0\right\}\mathbb{P}\left\{Z_t(\cdot,0)\geq x\right\}\\
&+\sum_{n=1}^{\infty}\mathbb{P}\left\{N_t=n\right\}\Big(\mathbb{P}\left\{Z_t\left(\xi^+-\kappa_+,n\right)+n\kappa_+\geq x\right\}\hat{p}(n,n)\\
&+\mathbb{P}\left\{Z_t\left(-\xi^--\kappa_-,n\right)+n\kappa_-\geq x\right\}\hat{p}(0,n)\\
&+\sum_{k=1}^{n-1}\sum_{i=k}^{n-1}\Big(\mathbb{P}\left\{Z_t\left(\xi^+-\kappa_+,k\right)+i\kappa_++(n-i)\kappa_-\geq x\right\}\hat{p}(i,n)\tilde{p}(i,n-i,k)\\
&+\mathbb{P}\left\{Z_t\left(-\xi^--\kappa_-,k\right)+(n-i)\kappa_++i\kappa_-\geq x\right\}\hat{p}(n-i,n)\tilde{q}(n-i,i,k)\Big)\Big).
\end{aligned}$$

Here, we also substituted for $\alpha=\left(\kappa_++\kappa_-\right)/2$ and $\kappa=\left(\kappa_+-\kappa_-\right)/2$.

II.D.5 Truncation Error

This appendix contains the detailed proof of Lemma II.10. When truncating the infinite summation at $n_{\max}$, the truncation error is given by

$$\begin{aligned} \sum_{n=n_{\max}+1}^{\infty} \mathbb{P}\left\{N_t = n\right\} \mathbb{P}\left\{Z_t\left(Y_1, n\right) \geq x\right\} &\leq \sum_{n=n_{\max}+1}^{\infty} \mathbb{P}\left\{N_t = n\right\} \\ &= \mathbb{P}\left\{N_t \geq n_{\max} + 1\right\}, \end{aligned}$$

where we use that the second term in the summand takes values in $[0, 1]$. The last expression is equivalent to the probability that the $(n_{max} + 1)$-th jump occurs before time t. Since the time of the n-th jump follows a gamma distribution, see for example Section 2.5 in Cont and Tankov (2004), pp. 44–55, we obtain

$$\begin{aligned} \mathbb{P}\left\{N_t \geq n_{\max} + 1\right\} &= \frac{\lambda}{n_{\max}!} \int_0^t (\lambda u)^{n_{\max}} \mathrm{e}^{-\lambda u} \mathrm{d}u \\ &= \frac{1}{n_{\max}!} \int_0^{\lambda t} v^{n_{\max}} \mathrm{e}^{-v} \mathrm{d}v \\ &= \frac{\gamma\left(n_{\max} + 1, \lambda t\right)}{n_{\max}!}. \end{aligned}$$

II.D.6 European Plain Vanilla Call Options on Spot Assets

This appendix contains the detailed proof of Proposition II.7. By the risk-neutral pricing formula, see for example Proposition 9.1 in Cont and Tankov (2004), we have

$$C_t = B_t \mathbb{E}_{\mathbb{P}^*}\left[\left.\frac{C_T}{B_T}\right| \mathfrak{F}_t\right].$$

Here, we assume that $\mathbb{P}^*$ is a risk-neutral probability measure as defined in Section II.3 such that the discounted asset price S_t/B_t is a $(\mathbb{P}^*, \mathbb{F})$-martingale. Expanding the payoff function yields

$$C_t = B_t \mathbb{E}_{\mathbb{P}^*}\left[\left.\frac{S_T}{B_T} 1\left\{S_T \geq K\right\}\right| \mathfrak{F}_t\right] - B(t, T) K \mathbb{P}^*\left\{S_T \geq K \middle| \mathfrak{F}_t\right\}, \tag{II.4}$$

where $B(t, T) = B_t/B_T$ is the time $t \geq 0$ price of a zero coupon with maturity in $T \geq t$ and a unit notional value. The second expression can be readily computed using Theorem II.1.

We have

$$\begin{aligned}
\mathbb{P}^*\left\{S_T \geq K \middle| \mathfrak{F}_t\right\} &= \mathbb{P}^*\left\{S_t \mathrm{e}^{X_T - X_t} \geq K \middle| \mathfrak{F}_t\right\} \\
&= \mathbb{P}^*\left\{X_\tau \geq \ln\left(K/S_t\right)\right\} \\
&= \Lambda\left(\ln\left(\frac{K}{S_t}\right); \tau, \gamma^*, \sigma, \lambda^*, p^*, \eta_+^*, \eta_-^*, \kappa_+, \kappa_-\right).
\end{aligned}$$

where the second equality is a consequence of the Markov property of X. Here, all parameters are specified under the risk-neutral probability measure. In particular,

$$\gamma^* = r - \frac{1}{2}\sigma^2 - \lambda^*\left(p^* \frac{\eta_+^*}{\eta_+^* - 1}\mathrm{e}^{\kappa_+} + (1 - p^*)\frac{\eta_-^*}{\eta_-^* + 1}\mathrm{e}^{\kappa_-} - 1\right).$$

To compute the first expression, we change the numéraire from B to S. To this end, we define a new probability measure $\mathbb{P}^S$ equivalent to $\mathbb{P}^*$ on $[0, T^*]$ by

$$\begin{aligned}
\frac{\mathrm{d}\mathbb{P}^S}{\mathrm{d}\mathbb{P}^*} &= \frac{S_{T^*} B_0}{S_0 B_{T^*}} \\
&= \exp\left\{(\gamma^* - r)\, T^* + \sigma W_{T^*}^* + \sum_{i=1}^{N_{T^*}} Y_i\right\} \qquad \mathbb{P}^*\text{-a.s..}
\end{aligned}$$

The corresponding the Radon-Nikodým derivative process $\nu\left(\mathbb{P}^*, \mathbb{P}^S\right) = \left\{\nu_t\left(\mathbb{P}^*, \mathbb{P}^S\right) : t \in [0, T^*]\right\}$ is given by

$$\begin{aligned}
\nu_t\left(\mathbb{P}^*, \mathbb{P}^S\right) = \left.\frac{\mathrm{d}\mathbb{P}^S}{\mathrm{d}\mathbb{P}^*}\right| \mathfrak{F}_t &= \frac{S_t B_0}{S_0 B_t} \\
&= \exp\left\{(\gamma^* - r)\, t + \sigma W_t^* + \sum_{i=1}^{N_t} Y_i\right\} \qquad \mathbb{P}^*\text{-a.s.}
\end{aligned}$$

We recognize this expression as an Esscher transform of the risk process X with transform parameter $\beta = 1$ and $\mathbb{P}^*$ taking the role of the prior probability measure. From Proposition II.1, it then immediately follows that X is an AD-DE jump-diffusion process under the new probability measure $\mathbb{P}^S$ with parameters

$$\begin{aligned}
\gamma^S &= \gamma^* + \sigma^2, \\
\lambda^S &= \lambda^*\left(p^* \frac{\eta_+^*}{\eta_+^S}\mathrm{e}^{\kappa_+} + (1 - p^*)\frac{\eta_-^*}{\eta_-^S}\mathrm{e}^{\kappa_-}\right), \\
f^S(x) &= p^S \eta_+^S \mathrm{e}^{-\eta_+^S (x - \kappa_+)} 1\left\{x \geq \kappa_+\right\} + \left(1 - p^S\right) \eta_-^S \mathrm{e}^{\eta_-^S (x - \kappa_-)} 1\left\{x \leq \kappa_-\right\}, \\
p^S &= p^* \frac{\lambda^* \eta_+^*}{\lambda^S \eta_+^S}\mathrm{e}^{\kappa_+}, \\
\eta_\pm^S &= \eta_\pm^* \mp 1.
\end{aligned}$$

Using the abstract Bayes rule, see for example Lemma A.1.4 in Musiela and Rutkowski (2005), p. 615, the first expression in Equation II.4 becomes

$$\begin{aligned}
B_t \mathbb{E}_{\mathbb{P}^*}\left[\frac{S_T}{B_T} 1\{S_T \geq K\} \middle| \mathfrak{F}_t\right] &= S_t \mathbb{E}_{\mathbb{P}^*}\left[\frac{S_T B_t}{S_t B_T} 1\{S_T \geq K\} \middle| \mathfrak{F}_t\right] \\
&= S_t \mathbb{E}_{\mathbb{P}^*}\left[\frac{\nu_T\left(\mathbb{P}^*, \mathbb{P}^S\right)}{\nu_t\left(\mathbb{P}^*, \mathbb{P}^S\right)} 1\{S_T \geq K\} \middle| \mathfrak{F}_t\right] \\
&= S_t \mathbb{P}^S\left\{S_T \geq K \middle| \mathfrak{F}_t\right\}.
\end{aligned}$$

Again using Theorem II.1 yields

$$\mathbb{P}^S\left\{S_T \geq K \middle| \mathfrak{F}_t\right\} = \Lambda\left(\ln\left(\frac{K}{S_t}\right) \tau, \gamma^S, \sigma, \lambda^S, p^S, \eta_+^S, \eta_-^S, \kappa_+, \kappa_-\right).$$

II.D.7 Sensitivities of European Plain Vanilla Options

This appendix contains the detailed proof of Corollary II.4. Similar to Rothschild and Stiglitz (1970), we define the returns of a price process $S^{(2)} = \left\{S_t^{(2)} : t \in [0, T^*]\right\}$ to be riskier under $\mathbb{P}^*$ than those of another asset price process $S^{(1)} = \left\{S_t^{(1)} : t \in [0, T^*]\right\}$ if

$$\frac{S_t^{(2)}}{S_0^{(2)}} \sim_{\mathbb{P}^*} \frac{S_t^{(1)}}{S_0^{(1)}} \varepsilon_t,$$

where ε_t is an non-trivial random variable with $\mathbb{E}_{\mathbb{P}^*}\left[\varepsilon_t \middle| S_t^{(1)}\right] = 1$ for all $S_t^{(1)}$. Assume w.l.o.g. that the jump intensities of these two assets are given by $\lambda^{*,(1)} < \lambda^{*,(2)}$. Then

$$\begin{aligned}
S_t^{(1)} &\sim_{\mathbb{P}^*} S_0^{(1)} \exp\left\{Z_t^{(1)}\right\}, \\
S_t^{(2)} &\sim_{\mathbb{P}^*} S_0^{(2)} \exp\left\{Z_t^{(1)} + Z_t^{(2)}\right\},
\end{aligned}$$

where

$$\begin{aligned}
Z_t^{(1)} &= \left(r - \frac{1}{2}\sigma^2 - \lambda^{*,(1)}\left(\phi^*_{Y_1^{(1)}}(-\mathrm{i}) - 1\right)\right) t + \sum_{i=1}^{N_t^{(1)}} Y_i^{(1)}, \\
Z_t^{(2)} &= -\left(\lambda^{*,(2)} - \lambda^{*,(1)}\right)\left(\phi^*_{Y_1^{(2)}}(-\mathrm{i}) - 1\right) t + \sum_{i=1}^{N_t^{(2)}} Y_i^{(2)}.
\end{aligned}$$

Here, $N^{(1)} = \left\{N_t^{(1)} : t \in [0, T^*]\right\}$ and $N^{(2)} = \left\{N_t^{(2)} : t \in [0, T^*]\right\}$ are independent Poisson processes under $\mathbb{P}^*$ with intensities $\lambda^{*,(1)}$ and $\left(\lambda^{*,(2)} - \lambda^{*,(1)}\right)$ respectively. Similarly,

$\left(Y_i^{(1)}\right)_{i\in\mathbb{N}}$ and $\left(Y_i^{(2)}\right)_{i\in\mathbb{N}}$ are sequences of i.i.d. random variables that are further also independent of each other and the two Poisson processes. This decomposition rests on the additivity of the jump intensity of two independent compound Poisson processes with the same jump size distribution. Now let $\varepsilon_t = \exp\left\{Z_t^{(2)}\right\}$. Then $\mathbb{E}_{\mathbb{P}^*}\left[\left.\varepsilon_t\right| S_t^{(1)}\right] = 1$ due to the independence of $S_t^{(1)}$ and $Z_t^{(2)}$ and the martingale property of the exponential of $Z_t^{(2)}$; see Section II.3.1.

II.D.8 European Plain Vanilla Call Options on Forwards

This appendix contains the detailed proof of Corollary II.5. We first need to compute the dynamics of the forward contract on the asset S. By Lemma 9.6.1 in Musiela and Rutkowski (2005), p. 374, we have

$$F_S(t,U) = \frac{S_t}{B(t,U)} \qquad \forall t \in [0,U]$$

and thus

$$\mathrm{d}F_S(t,U) = F_S(t,U)\left(\frac{\mathrm{d}S_t}{S_t} - r\mathrm{d}t\right).$$

These dynamics imply that $F_S(\cdot,U)$ a $(\mathbb{P}^*,\mathbb{F})$-martingale, such that its logarithm has the drift $\gamma^* - r$. All remaining parameters are identical to those of the process X. We get

$$C_t = \frac{B_t}{B(T,U)}\mathbb{E}_{\mathbb{P}^*}\left[S_T 1\left\{F_S(T,U)\geq K\right\}\middle|\,\mathfrak{F}_t\right] - B(t,T)K\mathbb{P}^*\left\{F_S(T,U)\geq K\middle|\,\mathfrak{F}_t\right\}.$$

All remaining steps are fully analogous to II.D.6. In particular,

$$\mathbb{P}^*\left\{F_S(T,U)\geq K\middle|\,\mathfrak{F}_t\right\} = \Lambda\left(\ln\left(\frac{K}{F_S(t,U)}\right);\tau,\gamma^*-r,\sigma,\lambda^*,p^*,\eta_+^*,\eta_-^*,\kappa_+,\kappa_-\right)$$

and

$$\frac{B_t}{B(T,U)}\mathbb{E}_{\mathbb{P}^*}\left[S_T 1\left\{F_S(T,U)\geq K\right\}\middle|\,\mathfrak{F}_t\right] = B(t,T)F_S(t,U)\mathbb{P}^S\left\{F_S(T,U)\geq K\middle|\,\mathfrak{F}_t\right\},$$

where

$$\mathbb{P}^S\left\{F_S(T,U)\geq K\middle|\,\mathfrak{F}_t\right\} = \Lambda\left(\ln\left(\frac{K}{F_S(t,U)}\right);\tau,\gamma^S-r,\sigma,\lambda^S,p^S,\eta_+^S,\eta_-^S,\kappa_+,\kappa_-\right)$$

II.E Appendix for Section II.6

II.E.1 Characteristic Function of Y_1 under $\mathbb{P}$

This appendix contains the detailed proof of Lemma II.13. The characteristic function $\phi_{Y_1}(\omega)$ of the sequence of random variables Y_i is given by

$$\begin{aligned}
\phi_{Y_1}(\omega) &= p\frac{\delta_+^{\varepsilon_+}}{\Gamma(\varepsilon_+ - 1)}\int_{\kappa_+}^{\infty}(x-\kappa_+)^{\varepsilon_+ - 1}\,\mathrm{e}^{-(\delta_+ - \mathrm{i}\omega)x + \delta_+\kappa_+}\mathrm{d}x \\
&\quad +(1-p)\frac{\delta_-^{\varepsilon_-}}{\Gamma(\varepsilon_- - 1)}\int_{-\infty}^{\kappa_-}(\kappa_- - x)^{\varepsilon_- - 1}\,\mathrm{e}^{(\delta_- + \mathrm{i}\omega)x - \delta_-\kappa_-}\mathrm{d}x \\
&= p\left(\frac{\delta_+}{\delta_+ - \mathrm{i}\omega}\right)^{\varepsilon_+}\mathrm{e}^{\mathrm{i}\omega\kappa_+}\frac{(\delta_+ - \mathrm{i}\omega)^{\varepsilon_+}}{\Gamma(\varepsilon_+ - 1)}\int_{\kappa_+}^{\infty}(x-\kappa_+)^{\varepsilon_+ - 1}\,\mathrm{e}^{-(\delta_+ - \mathrm{i}\omega)(x-\kappa_+)}\mathrm{d}x \\
&\quad +(1-p)\left(\frac{\delta_-}{\delta_- + \mathrm{i}\omega}\right)^{\varepsilon_-}\mathrm{e}^{\mathrm{i}\omega\delta_-}\frac{(\delta_- + \mathrm{i}\omega)^{\varepsilon_-}}{\Gamma(\varepsilon_+ - 1)}\int_{-\infty}^{\kappa_-}(\kappa_- - x)^{\varepsilon_- - 1}\,\mathrm{e}^{(\delta_- + \mathrm{i}\omega)(x-\kappa_-)}\mathrm{d}x.
\end{aligned}$$

Now consider the integral

$$\frac{(\delta_+ - \mathrm{i}\omega)^{\varepsilon_+}}{\Gamma(\varepsilon_+ - 1)}\int_{\kappa_+}^{\infty}(x-\kappa_+)^{\varepsilon_+ - 1}\,\mathrm{e}^{-(\delta_+ - \mathrm{i}\omega)(x-\kappa_+)}\mathrm{d}x.$$

If $\omega \in \mathbb{C}$ was a strictly complex number with $\mathfrak{Re}(\omega) = 0$, then the integrand would be real valued and we would recognize this expression as an integral over the full support of the displaced gamma distribution. It would thus evaluate to one. However, the transform parameter $\omega \in \mathbb{R}$ is a real number and thus this argument cannot be directly employed. Instead, we can make a change of variables by setting $y = x - \kappa_+$ and then expand the complex part of the exponent as a Taylor series around $\omega = 0$ to obtain

$$\begin{aligned}
\dots &= \frac{(\delta_+ - \mathrm{i}\omega)^{\varepsilon_+}}{\Gamma(\varepsilon_+ - 1)}\int_0^{\infty} y^{\varepsilon_+ - 1}\mathrm{e}^{-(\delta_+ - \mathrm{i}\omega)y}\mathrm{d}y \\
&= \frac{(\delta_+ - \mathrm{i}\omega)^{\varepsilon_+}}{\Gamma(\varepsilon_+ - 1)}\int_0^{\infty}\sum_{n=0}^{\infty}\frac{(\mathrm{i}\omega y)^n}{n!}y^{\varepsilon_+ - 1}\mathrm{e}^{-\delta_+ y}\mathrm{d}y \\
&= \frac{(\delta_+ - \mathrm{i}\omega)^{\varepsilon_+}}{\Gamma(\varepsilon_+ - 1)}\sum_{n=0}^{\infty}\frac{(\mathrm{i}\omega)^n}{n!}\int_0^{\infty} y^{\varepsilon_+ - 1 + n}\mathrm{e}^{-\delta_+ y}\mathrm{d}y \\
&= \frac{(\delta_+ - \mathrm{i}\omega)^{\varepsilon_+}}{\Gamma(\varepsilon_+ - 1)}\sum_{n=0}^{\infty}\frac{(\mathrm{i}\omega)^n}{n!}\frac{\Gamma(\varepsilon_+ - 1 + n)}{\delta_+^{\varepsilon_+ + n}} \\
&= \left(\frac{\delta_+ - \mathrm{i}\omega}{\delta_+}\right)^{\varepsilon_+}\sum_{n=0}^{\infty}\frac{(\mathrm{i}\omega/\delta_+)^n}{n!}\prod_{i=0}^{n-1}(\varepsilon_+ - 1 + i) \\
&= 1.
\end{aligned}$$

Here, we used the integrand in the third equality is, after normalization, the PDF of a $\Gamma(\varepsilon_+, \delta_+)$ gamma random variable. The last equality follows from

$$\frac{\partial^n}{\partial\omega^n}\left(\frac{\delta_+}{\delta_+ - \mathrm{i}\omega}\right)^{\varepsilon_+}(0) = \left(\frac{\mathrm{i}}{\delta_+}\right)^n \prod_{i=0}^{n-1}(\varepsilon_+ - 1 + \mathrm{i}),$$

which shows that the sum is a Taylor series expansion of the reciprocal of the first term around $\omega = 0$. Similarly, we can show through analogous computations that the second integral in the equation for $\phi_{Y_1}(\omega)$ evaluates to one as well. Consequently,

$$\phi_{Y_1}(\omega) = p\left(\frac{\delta_+}{\delta_+ - \mathrm{i}\omega}\right)^{\varepsilon_+}\mathrm{e}^{\mathrm{i}\omega\kappa_+} + (1-p)\left(\frac{\delta_-}{\delta_- + \mathrm{i}\omega}\right)^{\varepsilon_-}\mathrm{e}^{\mathrm{i}\omega\delta_-}.$$

The above proof can be substantially simplified by using the known characteristic function of gamma random variables as well as elementary properties of the Fourier transform. First, since the random variable $\zeta^+ - \kappa_+ \sim \Gamma(\varepsilon_+, \delta_+)$ has gamma distribution, its characteristic function $\phi_{\zeta^+ - \kappa_+}(\omega)$ is given by

$$\phi_{\zeta^+ - \kappa_+}(\omega) = \left(\frac{\delta_+}{\delta_+ - \mathrm{i}\omega}\right)^{\varepsilon_+}.$$

Now, by the translation property of the Fourier transform, see for example Theorem 4.1.10 in Gut (2005), the characteristic function $\phi_{\zeta_+}(\omega)$ of ζ_+ is given by

$$\begin{aligned}
\phi_{\zeta_+}(\omega) &= \int_{-\infty}^{+\infty} \mathrm{e}^{\mathrm{i}\omega x} f_{\zeta^+}(x)\mathrm{d}x \\
&= \int_{-\infty}^{+\infty} \mathrm{e}^{\mathrm{i}\omega x} f_{\zeta^+ - \kappa_+}(x - \kappa_+)\,\mathrm{d}x \\
&= \phi_{\zeta^+ - \kappa_+}(\omega)\mathrm{e}^{\mathrm{i}\omega\kappa_+}.
\end{aligned}$$

A similar result holds for the lower tail, where we first find the characteristic function of $\zeta^- + \kappa_-$ and then use that the characteristic function is Hermitian, that is $\phi_{-\zeta^-}(\omega) = \phi_{\zeta^-}(-\omega) = \overline{\phi_{\zeta^-}(\omega)}$; see for example Theorem 2.1.1 in Lukacs (1970), p. 15.

II.F Appendix for Section II.7

II.F.1 Probability Density Approximation

This appendix contains the detailed proof of Lemma II.16. Gil-Pelaez (1951) develops a general inversion theorem for characteristic functions that allows to express the upper tail probability as

$$\mathbb{P}\{X_t \geq x\} = \frac{1}{2} + \frac{1}{2\pi}\int_0^\infty \frac{1}{\mathrm{i}\omega}\left(\mathrm{e}^{-\mathrm{i}\omega x}\phi_{X_t}(\omega) - \mathrm{e}^{\mathrm{i}\omega x}\phi_{X_t}(-\omega)\right)\mathrm{d}\omega.$$

For computational purposes, it is convenient to have a real-valued integrand. By Theorem 2.1.1 in Lukacs (1970), p. 15, the characteristic function is Hermitian, that is $\phi_{X_t}(-\omega) = \overline{\phi_{X_t}(\omega)}$. Thus,

$$\begin{aligned}
\mathbb{P}\{X_t \geq x\} &= \frac{1}{2} + \frac{1}{2\pi}\int_0^\infty \left(\frac{1}{\mathrm{i}\omega}\mathrm{e}^{-\mathrm{i}\omega x}\phi_{X_t}(\omega) + \overline{\frac{1}{\mathrm{i}\omega}\mathrm{e}^{-\mathrm{i}\omega x}\phi_{X_t}(\omega)}\right)\mathrm{d}\omega \\
&= \frac{1}{2} + \frac{1}{\pi}\int_0^\infty \mathfrak{Re}\left(\frac{1}{\mathrm{i}\omega}\mathrm{e}^{-\mathrm{i}\omega x}\phi_{X_t}(\omega)\right)\mathrm{d}\omega \\
&= \frac{1}{2} + \frac{1}{\pi}\int_0^\infty \mathfrak{Im}\left(\frac{1}{\omega}\mathrm{e}^{-\mathrm{i}\omega x}\phi_{X_t}(\omega)\right)\mathrm{d}\omega.
\end{aligned}$$

The former expression can be found in Heston (1993), while the latter one is given in Bates (1996b). Differentiating with respect to x then yields

$$\begin{aligned}
\mathbb{P}\{X_t \in \mathrm{d}x\} &= \frac{1}{\pi}\int_0^\infty \mathfrak{Re}\left(\mathrm{e}^{-\mathrm{i}\omega x}\phi_{X_t}(\omega)\right)\mathrm{d}\omega\mathrm{d}x \\
&= \frac{1}{\pi}\int_0^\infty \mathfrak{Im}\left(\mathrm{i}\mathrm{e}^{-\mathrm{i}\omega x}\phi_{X_t}(\omega)\right)\mathrm{d}\omega\mathrm{d}x.
\end{aligned}$$

Next note that, due to the linearity of the integral,

$$\frac{1}{\pi}\int_0^\infty \mathfrak{Re}\left(\mathrm{e}^{-\mathrm{i}\omega x}\phi_{X_t}(\omega)\right)\mathrm{d}\omega = \frac{1}{\pi}\mathfrak{Re}\left(\int_0^\infty \mathrm{e}^{-\mathrm{i}\omega x}\phi_{X_t}(\omega)\mathrm{d}\omega\right).$$

We now approximate the integral by first truncating its upper limit of integration at some level $\omega_{N-1} = (N-1)\Delta\omega$ and then approximating the resulting definite integral through Gaussian quadrature

$$\begin{aligned}
\int_0^\infty \mathrm{e}^{-\mathrm{i}\omega x}\phi_{X_t}(\omega)\mathrm{d}\omega &= \int_0^{\omega_{N-1}} \mathrm{e}^{-\mathrm{i}\omega x}\phi_{X_t}(\omega)\mathrm{d}\omega + \epsilon(N,\Delta\omega) \\
&\approx \sum_{j=0}^{N-1} w_j \mathrm{e}^{-\mathrm{i}j\omega_j x}\phi_{X_1}(\omega_j).
\end{aligned}$$

Here, $\boldsymbol{w} = (w_j)_{j=0}^{N-1}$ are the integration weights for the N sample points $\boldsymbol{\omega} = (\omega_j)_{j=0}^{N-1}$ in the frequency domain which are spaced $\Delta\omega$ apart. The values of w_j depend on the concrete choice of the numerical integration method used. We implement the Simpson rule and thus have

$$w_j = \begin{cases} \Delta\omega/3 & \text{if } j \in \{0, N-1\} \\ 4\Delta\omega/3 & \text{if } j/2 \in \mathbb{N} \\ 2\Delta\omega/3 & \text{otherwise} \end{cases}.$$

Our aim is now to compute the above approximation simultaneously for a grid $\boldsymbol{x} = (x_j)_{j=0}^{N-1}$ of returns. When choosing N to be a power of two and using the same number of points in the spatial and frequency domain, this can be efficiently accomplished through the FFT. We start by constructing an equidistant grid centered around zero by

$$x_n = x_0 + n\Delta x, \qquad x_0 = -\frac{(N-1)\Delta x}{2}.$$

Substituting back into the discrete approximation and using that $\omega_j = j\Delta\omega$ yields

$$\begin{aligned} f_{X_t}(x_n) &= \frac{1}{\pi}\mathfrak{Re}\left(\sum_{j=0}^{N-1} w_j \mathrm{e}^{-\mathrm{i}j\Delta\omega(x_0 n\Delta x)}\phi_{X_t}(j\Delta\omega)\right) \\ &= \frac{1}{\pi}\mathfrak{Re}\left(\sum_{j=0}^{N-1} \mathrm{e}^{-\mathrm{i}j\Delta\omega n\Delta x} g_j\right), \end{aligned}$$

where

$$g_j = w_j \mathrm{e}^{-\mathrm{i}j\Delta\omega x_0}\phi_{X_t}(j\Delta\omega).$$

Here, the values $\boldsymbol{g} = (g_j)_{j=0}^{N-1}$ have been chosen such that they do not depend on n. Now, the inverse discrete Fourier transform of the vector $\hat{\boldsymbol{f}} = (\hat{f}_j)_{j=0}^{N-1}$ corresponding to the convention used in this chapter is given by

$$f_n = \left(\mathfrak{D}^{-1}\{\hat{\boldsymbol{f}}\}\right)_n = \frac{1}{N}\sum_{j=0}^{N-1} \mathrm{e}^{-2\pi \mathrm{i} jn/N}\hat{f}_j.$$

By comparing the exponents, we obtain

$$\Delta\omega\Delta x = \frac{2\pi}{N} \qquad \Leftrightarrow \qquad \Delta x = \frac{2\pi}{N\Delta\omega}.$$

Consequently,

$$f_{X_t}(x_n) = \frac{N}{\pi}\mathfrak{Re}\left(\mathfrak{D}^{-1}\{\boldsymbol{g}\}\right)_n.$$

II.G Appendix for Section II.8

This appendix hold the detailed estimation results for Section II.8.

Table II.4: Summary statistics for the full data set used in the empirical analysis. Daily logarithmic returns are calculated on a close-to-close basis for the time span from January 1, 1982 to December 31, 2011. Means and standard deviations are annualized assuming 252 trading days per year.

Asset	Bloomberg Ticker	N	Mean	Stand. Dev.	Skew	Excess Kurt.	Min.	Max.
DAX 30	DAX	7,566	8.24%	22.48%	-0.30	6.22	-13.71%	10.80%
Dow Jones Industrial	INDU	7,568	8.75%	18.27%	-1.58	39.48	-25.63%	10.51%
Hang Seng	HSI	7,418	8.81%	28.45%	-2.07	46.35	-40.54%	17.25%
MSCI World	MXWO	7,822	6.73%	14.64%	-0.53	11.29	-10.36%	9.10%
NASDAQ Composite	CCMP	7,569	8.62%	22.30%	-0.24	8.26	-12.05%	13.25%
Nikkei 225	NKY	7,387	0.31%	22.55%	-0.30	8.83	-16.14%	13.23%
S&P 500	SPX	7,569	7.75%	18.61%	-1.21	26.89	-22.90%	10.96%
TOPIX	TPX	7,387	0.82%	20.12%	-0.36	9.94	-15.81%	12.86%
S&P GSCI	SPGSCIP	7,571	2.28%	20.04%	-0.64	9.87	-18.45%	7.53%
S&P GSCI Agriculture	SPGSAGP	7,573	-4.06%	17.26%	-0.11	3.51	-7.48%	7.16%
S&P GSCI Industrial Metals	SPGSINP	7,574	3.85%	23.05%	-0.22	4.02	-12.52%	8.40%
S&P GSCI Precious Metals	SPGSPMP	7,573	0.07%	18.28%	-0.15	5.71	-8.25%	8.76%
EUR/USD	EURUSD	7,689	0.50%	10.40%	0.05	1.96	-3.38%	4.72%
GBP/USD	GBPUSD	7,825	-0.67%	10.03%	-0.07	3.05	-4.13%	4.59%
USD/JPY	USDJPY	7,825	-3.38%	10.75%	-0.36	5.04	-6.95%	5.50%
Silver	XAG	7,707	4.05%	29.90%	-0.68	8.49	-20.39%	13.18%
Gold	XAU	7,693	4.51%	17.32%	-0.11	9.51	-12.90%	10.48%

Table II.5: AD-DE model ML estimation results for equity indices based on daily logarithmic returns over the time span from January 1, 1982 to December 31, 2011. The standard errors are given in parenthesis below the parameter estimates. Black superscripts ***, **, and * denote significance at 1%, 5%, and 10%, respectively, for the displacements terms κ_+ and κ_-. Gray superscript indicate a lack of significance and are used to highlight the parameters that are tested.

Asset	DAX 30	Dow Jones Industrial	Hang Seng	MSCI World	NASDAQ Composite	Nikkei 225	S&P 500	TOPIX
σ	**13.43%**	**9.46%**	**14.95%**	**8.44%**	**8.58%**	**9.46%**	**8.84%**	**9.96%**
	(0.40%)	(0.00%)	(0.01%)	(0.28%)	(0.29%)	(0.35%)	(0.01%)	(0.45%)
λ	**107.70**	**142.46**	**137.18**	**98.45**	**175.55**	**235.41**	**187.33**	**180.89**
	(12.92)	(4.13)	(6.15)	(12.74)	(11.18)	(16.31)	(9.27)	(19.84)
p	**43.17%**	**44.32%**	**52.83%**	**38.66%**	**43.74%**	**56.99%**	**48.34%**	**58.56%**
	(2.16%)	(0.01%)	(0.06%)	(3.76%)	(2.29%)	(2.19%)	(0.07%)	(2.96%)
η_+	**90.20**	**133.71**	**83.36**	**143.31**	**99.05**	**129.92**	**133.35**	**134.80**
	(6.16)	(3.58)	(2.69)	(11.59)	(5.13)	(6.16)	(4.77)	(8.67)
η_-	**92.55**	**115.71**	**67.42**	**129.15**	**104.28**	**123.52**	**119.62**	**120.67**
	(6.00)	(2.73)	(1.96)	(9.29)	(4.54)	(5.89)	(4.15)	(7.15)
κ_+	**+0.10%*****	**+0.24%*****	**+0.00%*****	**+0.28%*****	**+0.05%*****	**+0.08%*****	**+0.03%*****	**+0.08%*****
	(0.01%)	(0.00%)	(0.00%)	(0.05%)	(0.00%)	(0.00%)	(0.00%)	(0.00%)
κ_-	**−0.33%*****	**−0.01%*****	**−0.10%*****	**−0.06%*****	**−0.28%*****	**−0.43%*****	**−0.00%*****	**−0.36%*****
	(0.02%)	(0.00%)	(0.00%)	(0.01%)	(0.02%)	(0.02%)	(0.00%)	(0.02%)
N	7,566	7,568	7,418	7,822	7,569	7,387	7,569	7,387

Table II.6: AD-DE model ML estimation hypothesis tests for equity indices based on daily logarithmic returns over the time span from January 1, 1982 to December 31, 2011. The p-values are given in parenthesis below the parameter estimates. Black superscripts ***, **, and * denote significance at 1%, 5%, and 10%, respectively. Gray superscript indicate a lack of significance and are used to highlight the parameters that are tested. $\mathcal{H}_0^{(1)}: \kappa_+^{\text{AD-DE}} + \kappa_-^{\text{AD-DE}} = 0$, $\mathcal{H}_0^{(2)}: \kappa_+^{\text{AD-DE}} = \kappa_-^{\text{AD-DE}} = 0$ and $\mathcal{H}_0^{(3)}: \eta_+^{\text{AD-DE}} - \eta_-^{\text{AD-DE}} = 0$ are evaluated based on a Wald test. $\mathcal{H}_0^{(4)}: \sigma^{\text{AD-DE}} - \sigma^{\text{DE}} = 0$, $\mathcal{H}_0^{(5)}: p^{\text{AD-DE}} - p^{\text{DE}} = 0$, $\mathcal{H}_0^{(6)}: \lambda^{\text{AD-DE}} - \lambda^{\text{DE}} = 0$, $\mathcal{H}_0^{(7)}: \eta_+^{\text{AD-DE}} - \eta_+^{\text{DE}} = 0$ and $\mathcal{H}_0^{(8)}: \eta_-^{\text{AD-DE}} - \sigma^{\text{DE}} = 0$ are evaluated based on a likelihood ratio test.

Asset	DAX 30	Dow Jones Industrial	Hang Seng	MSCI World	NASDAQ Composite	Nikkei 225	S&P 500	TOPIX
$\mathcal{H}_0^{(1)}$	−0.23%***	+0.23%***	−0.10%***	+0.22%***	−0.23%***	−0.35%***	+0.03%***	−0.29%***
	(0.00%)	(0.00%)	(0.00%)	(0.00%)	(0.00%)	(0.00%)	(0.00%)	(0.00%)
$\mathcal{H}_0^{(2)}$	−***	−***	−***	−***	−***	−***	−***	−***
	(0.00%)	(0.00%)	(0.00%)	(0.00%)	(0.00%)	(0.00%)	(0.00%)	(0.00%)
$\mathcal{H}_0^{(3)}$	−2.35***	+17.99***	+15.95***	+14.16***	−5.23***	+6.39***	+13.72***	+14.13***
	(68.04%)	(0.00%)	(0.00%)	(25.18%)	(38.73%)	(38.13%)	(0.03%)	(11.15%)
$\mathcal{H}_0^{(4)}$	+0.03%***	+0.02%***	+0.00%***	+0.03%***	+0.04%***	+0.19%***	+0.00%***	+0.07%***
	(96.57%)	(95.93%)	(99.42%)	(91.88%)	(88.65%)	(78.17%)	(99.55%)	(90.84%)
$\mathcal{H}_0^{(5)}$	−25.74***	−25.33***	−4.74***	−24.04***	−37.22***	−84.38***	−4.42***	−52.83***
	(15.57%)	(23.30%)	(81.53%)	(11.86%)	(0.63%)	(1.74%)	(85.45%)	(13.40%)
$\mathcal{H}_0^{(6)}$	+5.13%***	−7.70%***	+1.62%***	−7.74%***	+5.67%***	+10.12%***	−0.95%***	+8.00%***
	(27.31%)	(5.30%)	(70.15%)	(6.57%)	(2.54%)	(0.40%)	(79.44%)	(5.57%)
$\mathcal{H}_0^{(7)}$	−0.05***	+0.08***	−0.00***	+0.22***	−0.07***	−0.57***	+0.00***	−0.23***
	(99.59%)	(99.34%)	(100.00%)	(98.42%)	(98.86%)	(94.97%)	(100.00%)	(98.47%)
$\mathcal{H}_0^{(8)}$	+0.06***	−0.06***	−0.00***	−0.13***	0.08***	+0.49***	+0.00***	+0.33***
	(99.31%)	(99.40%)	(100.00%)	(98.90%)	(98.67%)	(94.48%)	(100.00%)	(96.90%)

Table II.7: AD-DE model ML estimation results for commodity indices based on daily logarithmic returns over the time span from January 1, 1982 to December 31, 2011. The standard errors are given in parenthesis below the parameter estimates. Black superscripts ***, **, and * denote significance at 1%, 5%, and 10%, respectively, for the displacements terms κ_+ and κ_-. Gray superscript indicate a lack of significance and are used to highlight the parameters that are tested.

Asset	S&P GSCI	S&P GSCI Agriculture	S&P GSCI Industrial Metals	S&P GSCI Precious Metals
σ	**10.06%**	**11.43%**	**12.72%**	**5.98%**
	(0.26%)	(0.27%)	(0.34%)	(0.23%)
λ	**164.98**	**86.10**	**159.20**	**319.74**
	(11.79)	(9.72)	(15.98)	(16.91)
p	**31.81%**	**26.71%**	**74.25%**	**59.30%**
	(1.16%)	(1.65%)	(2.31%)	(1.71%)
η_+	**163.29**	**153.31**	**117.96**	**184.76**
	(10.63)	(14.46)	(6.86)	(6.99)
η_-	**119.36**	**125.05**	**99.65**	**133.60**
	(5.03)	(7.46)	(6.39)	(5.22)
κ_+	**+0.83%*****	**+1.08%*****	**+0.04%*****	**+0.10%*****
	(0.03%)	(0.06%)	(0.00%)	(0.01%)
κ_-	**−0.01%*****	**−0.06%*****	**−0.89%*****	**−0.04%*****
	(0.00%)	(0.00%)	(0.04%)	(0.00%)
N	7,571	7,573	7,574	7,573

Table II.8: AD-DE model ML estimation hypothesis tests for commodity indices based on daily logarithmic returns over the time span from January 1, 1982 to December 31, 2011. The p-values are given in parenthesis below the parameter estimates. Black superscripts ***, **, and * denote significance at 1%, 5%, and 10%, respectively. Gray superscript indicate a lack of significance and are used to highlight the parameters that are tested. $\mathcal{H}_0^{(1)} : \kappa_+^{\text{AD-DE}} + \kappa_-^{\text{AD-DE}} = 0$, $\mathcal{H}_0^{(2)} : \kappa_+^{\text{AD-DE}} = \kappa_-^{\text{AD-DE}} = 0$ and $\mathcal{H}_0^{(3)} : \eta_+^{\text{AD-DE}} - \eta_-^{\text{AD-DE}} = 0$ are evaluated based on a Wald test. $\mathcal{H}_0^{(4)} : \sigma^{\text{AD-DE}} - \sigma^{\text{DE}} = 0$, $\mathcal{H}_0^{(5)} : p^{\text{AD-DE}} - p^{\text{DE}} = 0$, $\mathcal{H}_0^{(6)} : \lambda^{\text{AD-DE}} - \lambda^{\text{DE}} = 0$, $\mathcal{H}_0^{(7)} : \eta_+^{\text{AD-DE}} - \eta_+^{\text{DE}} = 0$ and $\mathcal{H}_0^{(8)} : \eta_-^{\text{AD-DE}} - \sigma^{\text{DE}} = 0$ are evaluated based on a likelihood ratio test.

Asset	S&P GSCI	S&P GSCI Agriculture	S&P GSCI Industrial Metals	S&P GSCI Precious Metals
$\mathcal{H}_0^{(1)}$	+0.81%***	+1.02%***	−0.85%***	+0.06%***
	(0.00%)	(0.00%)	(0.00%)	(0.00%)
$\mathcal{H}_0^{(2)}$	−***	−***	−***	−***
	(0.01%)	(0.00%)	(0.00%)	(0.00%)
$\mathcal{H}_0^{(3)}$	+43.92***	+28.26***	+18.31***	+51.15***
	(0.00%)	(3.66%)	(2.70%)	(0.00%)
$\mathcal{H}_0^{(4)}$	+0.59%***	+0.63%***	+0.38%***	+0.01%***
	(27.82%)	(9.94%)	(53.36%)	(99.10%)
$\mathcal{H}_0^{(5)}$	−113.50***	−79.79***	−62.27***	−46.28***
	(0.01%)	(0.00%)	(2.73%)	(13.12%)
$\mathcal{H}_0^{(6)}$	−25.24%***	−27.08%***	+16.14%***	−3.21%***
	(0.00%)	(0.00%)	(0.01%)	(20.66%)
$\mathcal{H}_0^{(7)}$	+11.60***	+12.42***	−1.56***	+0.04***
	(25.92%)	(31.39%)	(87.54%)	(99.66%)
$\mathcal{H}_0^{(8)}$	−2.14***	−4.97***	+2.38***	−0.00***
	(79.96%)	(64.82%)	(72.26%)	(100.00%)

Table II.9: AD-DE model ML estimation results for FX and precious metals based on daily logarithmic returns over the time span from January 1, 1982 to December 31, 2011. The standard errors are given in parenthesis below the parameter estimates. Black superscripts ***, **, and * denote significance at 1%, 5%, and 10%, respectively, for the displacements terms κ_+ and κ_-. Gray superscript indicate a lack of significance and are used to highlight the parameters that are tested.

Asset	EUR/USD	GBP/USD	USD/JPY	Silver	Gold
σ	**4.64**%	**4.45**%	**5.72**%	**11.79**%	**5.34**%
	(0.31%)	(0.21%)	(0.22%)	(0.36%)	(0.22%)
λ	**482.98**	**323.15**	**221.74**	**241.71**	**291.37**
	(51.21)	(25.66)	(22.87)	(14.37)	(14.72)
p	**41.74**%	**47.30**%	**51.63**%	**52.46**%	**47.63**%
	(1.95%)	(2.07%)	(2.38%)	(2.05%)	(1.62%)
η_+	**362.27**	**370.14**	**301.27**	**103.93**	**186.44**
	(20.09)	(19.31)	(18.58)	(4.67)	(7.13)
η_-	**387.92**	**305.52**	**230.68**	**76.73**	**157.65**
	(20.93)	(14.49)	(12.39)	(3.18)	(5.77)
κ_+	**+0.09**%***	**+0.16**%***	**+0.11**%***	**+0.29**%***	**+0.24**%***
	(0.01%)	(0.01%)	(0.01%)	(0.02%)	(0.01%)
κ_-	**−0.04**%***	**−0.04**%***	**−0.05**%***	**−0.04**%***	**−0.04**%***
	(0.00%)	(0.00%)	(0.00%)	(0.00%)	(0.00%)
N	7,689	7,825	7,825	7,707	7,693

Table II.10: AD-DE model ML estimation hypothesis tests for FX and precious metals based on daily logarithmic returns over the time span from January 1, 1982 to December 31, 2011. The p-values are given in parenthesis below the parameter estimates. Black superscripts ***, **, and * denote significance at 1%, 5%, and 10%, respectively. Gray superscript indicate a lack of significance and are used to highlight the parameters that are tested. $\mathcal{H}_0^{(1)} : \kappa_+^{\text{AD-DE}} + \kappa_-^{\text{AD-DE}} = 0$, $\mathcal{H}_0^{(2)} : \kappa_+^{\text{AD-DE}} = \kappa_-^{\text{AD-DE}} = 0$ and $\mathcal{H}_0^{(3)} : \eta_+^{\text{AD-DE}} - \eta_-^{\text{AD-DE}} = 0$ are evaluated based on a Wald test. $\mathcal{H}_0^{(4)} : \sigma^{\text{AD-DE}} - \sigma^{\text{DE}} = 0$, $\mathcal{H}_0^{(5)} : p^{\text{AD-DE}} - p^{\text{DE}} = 0$, $\mathcal{H}_0^{(6)} : \lambda^{\text{AD-DE}} - \lambda^{\text{DE}} = 0$, $\mathcal{H}_0^{(7)} : \eta_+^{\text{AD-DE}} - \eta_+^{\text{DE}} = 0$ and $\mathcal{H}_0^{(8)} : \eta_-^{\text{AD-DE}} - \sigma^{\text{DE}} = 0$ are evaluated based on a likelihood ratio test.

Asset	EUR/USD	GBP/USD	USD/JPY	Silver	Gold
$\mathcal{H}_0^{(1)}$	+0.05%***	+0.12%***	+0.06%***	+0.25%***	+0.19%***
	(0.00%)	(0.00%)	(0.00%)	(0.01%)	(0.00%)
$\mathcal{H}_0^{(2)}$	−***	−***	−***	−***	−***
	(0.00%)	(0.00%)	(0.00%)	(0.00%)	(0.00%)
$\mathcal{H}_0^{(3)}$	−25.65***	+64.62***	+70.59***	+27.21***	+28.79***
	(16.27%)	(0.04%)	(0.00%)	(0.00%)	(0.02%)
$\mathcal{H}_0^{(4)}$	+0.02%***	+0.07%***	+0.02%***	+0.05%***	+0.09%***
	(97.74%)	(88.96%)	(97.99%)	(94.02%)	(86.03%)
$\mathcal{H}_0^{(5)}$	−125.99***	−135.74***	−60.07***	−48.75***	−84.54***
	(37.40%)	(8.11%)	(27.88%)	(6.94%)	(1.18%)
$\mathcal{H}_0^{(6)}$	−3.77%***	−11.04%***	−5.42%***	−6.68%***	−8.97%***
	(55.54%)	(1.73%)	(29.08%)	(2.83%)	(0.03%)
$\mathcal{H}_0^{(7)}$	+0.16***	+1.65***	+0.20***	+0.07***	+0.90***
	(99.64%)	(95.53%)	(99.46%)	(99.13%)	(91.82%)
$\mathcal{H}_0^{(8)}$	−0.02***	−0.38***	−0.05***	−0.02***	−0.13***
	(100.00%)	(98.81%)	(99.80%)	(99.63%)	(98.79%)

Table II.11: Detailed Estimation Results for the NASDAQ Composite based on daily logarithmic returns over the time span from January 1, 1982 to December 31, 2011. The parameters for models (1) through (3) are obtained from ML estimation. The parameters of model (4) are fixed using the approach proposed in Detering et al. (2013). When applicable, the standard errors are given in parenthesis below the parameter estimates. Black superscripts ***, **, and * denote significance at 1%, 5%, and 10%, respectively, for the displacements terms κ_+ and κ_-. Gray superscript indicate a lack of significance and are used to highlight the parameters that are tested.

Asset Model	NASDAQ Composite (1) AD-DE	NASDAQ Composite (2) D-DE	NASDAQ Composite (3) DE	NASDAQ Composite (4) DE
σ	**8.58%**	**8.54%**	**8.54%**	**18.10%**
	(0.29%)	(0.25%)	(0.24%)	
λ	**175.55**	**198.18**	**212.77**	**5.04**
	(11.18)	(11.81)	(12.73)	
p	**43.74%**	**38.15%**	**38.07%**	**50.00%**
	(2.29%)	(1.70%)	(1.35%)	
η_+	**99.05**	**99.13**	**99.13**	**62.32**
	(5.13)	(4.36)	(4.12)	
η_-	**104.28**	**104.20**	**104.20**	**64.70**
	(4.54)	(4.22)	(3.94)	
κ_+	**+0.05%*****	**+0.07%*****	–	**+4.01%**
	(0.00%)	(0.00%)		
κ_-	**−0.28%*****	–	–	
	(0.02%)			
$\mathcal{L}$	22,755.20	22,755.20	22,755.20	22,317.54
N	7,569	7,569	7,569	7,569

Table II.12: Detailed Estimation Results for the S&P GSCI Agriculture based on daily logarithmic returns over the time span from January 1, 1982 to December 31, 2011. The parameters for both models (1) through (2) are obtained from ML estimation. When applicable, the standard errors are given in parenthesis below the parameter estimates. Black superscripts ***, **, and * denote significance at 1%, 5%, and 10%, respectively, for the displacements terms κ_+ and κ_-. Gray superscript indicate a lack of significance and are used to highlight the parameters that are tested.

Asset Model	S&P GSCI Agriculture (1) AD-DG	S&P GSCI Agriculture (2) AD-DE
σ	**11.45%**	**11.43%**
	(0.28%)	(0.27%)
λ	**80.08**	**86.10**
	(9.71)	(9.72)
p	**34.33%**	**26.71%**
	(1.37%)	(1.65%)
ε_+	**4**	–
	(–)	
ε_-	**1**	–
	(–)	
δ_+/η_+	**264.04**	**153.31**
	(14.21)	(14.46)
δ_+/η_-	**124.48**	**125.05**
	(8.41)	(7.46)
κ_+	**+0.00%***	**+1.08%***
	(0.00%)	(0.06%)
κ_-	**−0.20%***	**−0.06%***
	(0.00%)	(0.00%)
N	7,573	7,573

II.H Glossary of Notation

$\square$	end of a proof
$\triangle$	end of a definition
$\circ$	Hadamard element-wise product
$1\{A\}$	indicator of the set A
α	Sharpe ratio; midpoint between the displacements $\kappa_\pm$
$\mathbb{P}^A$-a.s.	almost surely under $\mathbb{P}^A$
AD-DE	asymmetric displaced double exponential
AD-DG	asymmetric displaced double gamma
$B(t,T)$	zero-coupon bond value
β	Esscher transform parameter
$c_i(X)$	i-th cumulant of the random variable X
$\mathfrak{D}$	discrete forward Fourier transform
$\mathfrak{D}^{-1}$	discrete inverse Fourier transform
$\delta_\pm^A$	upper/lower tail decay of the double gamma density under $\mathbb{P}^A$
$\Delta(x)$	Dirac delta function
DE	double exponential
$\mathbb{E}_{\mathbb{P}^A}$	expectation under $\mathbb{P}^A$
$\varepsilon_\pm$	upper/lower shape parameter of the double gamma density
$\eta_\pm^A$	upper/lower tail decay of the double exponential density under $\mathbb{P}^A$
ETMM	Esscher transform martingale measure
$\mathbb{F}$	sigma algebra
$\mathfrak{F}_t$	filtration at time t
FFT	fast Fourier transform
GMM	generalized method of moments
i	imaginary unit
i.i.d.	independent and identically distributed
$\mathfrak{Im}(x)$	imaginary part of the complex number x
IVS	implied volatility smile/surface
K	strike price
$\kappa_\pm$	positive/negative displacement of the double exponential/gamma
λ^A	jump intensity under $\mathbb{P}^A$

$\mathcal{L}_X^A$	infinitesimal generator of X under $\mathbb{P}^A$
M	stochastic discount factor process
ML	maximum likelihood
$\mathcal{N}$	$\mathbb{P}$-null sets
N^A	one-dimensional Poisson process under $\mathbb{P}^A$
$\nu_X(\mathrm{d}x)$	Lévy measure of the process X
$\nu\left(\mathbb{P}^A, \mathbb{P}^B\right)$	Radon-Nikodým derivative process between $\mathbb{P}^A$ and $\mathbb{P}^B$
Ω	probability space
p^A	probability of an upwards jump under $\mathbb{P}^A$
$\mathbb{P}$	physical/real-world probability measure
$\mathbb{P}^*$	bank account martingale measure/risk-neutral probability measure
$\mathbb{P}^S$	asset price martingale measure
PDF	probability density function
$\phi_X^A(\omega)$	characteristic function of the random variable X under $\mathbb{P}^A$
$\psi_X^A(\omega)$	cumulant generating function of the random variable X under $\mathbb{P}^A$
r	continuously compounded risk-free interest rate
$\mathfrak{Re}(x)$	real part of the complex number x
ρ	subjective rate of time preference
S	asset price process
SD-DE	symmetric displaced double exponential
σ	diffusion coefficient
T	maturity date
T^*	terminal time
τ	current time-to-maturity
$u\left(C_t\right)$	utility of consumption
V	wealth process
W^A	standard one-dimensional Brownian motion under $\mathbb{P}^A$
w.l.o.g.	without loss of generality
X	logarithmic return process
ζ	instantaneous payout process of a contingent claim

Chapter III

Volatility Smile-Adjusted Closed-Form Pricing and Risk Management of Barrier Options

We propose an approach to valuation and risk management of deferred start barrier options within the Black and Scholes (1973) framework. We provide closed-form solutions which are functions of the implied volatility smile. Our barrier options are contingent claims on two perfectly correlated assets that diffuse with different volatilities. While the terminal payoff is a function of one of the assets, the barrier trigger is determined by the path of the other. To mitigate the dynamic hedging problems associated with large discontinuous sensitivities, we suggest the application of an additional exponential bending of the barrier close to maturity. In contrast to existing approaches we explicitly take the time-dependence of the risk exposure into account. By generalizing the method of images, we obtain closed-form solutions for both deferred start piecewise exponential barrier options and associated rebates.

Keywords: barrier option, volatility smile, two volatility, barrier bending, method of images, closed-form solution

JEL Classification: G13
MS Classification (2010): 35K20, 60G51

III.1 Introduction

Vanilla barrier options belong to the class of first generation exotic options. However, due to their widespread use, they are now mostly regarded as flow derivatives. Besides American plain vanilla options, barrier options are amongst the fundamental types of weakly path-dependent contingent claims. They are also one of the first contract types to be traded in the United States market, even before the Chicago Board Options Exchange (CBOE) opened in 1973; see Chapter 10.1 in Zhang (1998), pp. 232–233. A barrier option has a terminal payoff equal to that of a plain vanilla option in case it expires active. A knock-in (knock-out) barrier option is initially inactive (active) and is activated (deactivated) once the underlying asset price breaches a predefined barrier level for the first time after the contract's inception, the so-called trigger event. Depending on whether the asset price breaches the barrier from below or above, these contracts are referred to as up- or down-barrier options. Both knock-in and knock-out barrier options might have a cash rebate at maturity in case they expire inactive. Knock-out barrier options might alternatively have a cash rebate that is paid immediately upon the trigger event. A further distinction is made between conventional and reverse barrier options. While the barrier of conventional barrier options lies in the out-of-the-money region, reverse barrier options knock-in or -out when in-the-money.

The popularity of barrier options stems from them offering the possibility to take directional positions on more specific market views. Compared to the otherwise identical plain vanilla option, a barrier option is always strictly cheaper. Many structured equity, foreign exchange and commodity products implicitly contain positions in barrier options. These contracts are both held in the portfolios of institutional investors and are actively traded, for example, in the European markets for retail derivatives.

Just like American plain vanilla options, most common types of barrier options exhibit a weak path-dependence and are thus solutions to the Black and Scholes (1973) partial differential equation (PDE) subject to appropriate terminal and boundary conditions. One counterexample are Asian barrier options. Unlike for American options, there is no free boundary, which greatly simplifies the valuation problem.

III.1.1 Literature Review

By solving for the price of a down & out put call option, Merton (1973) obtains the first explicit solutions for barrier options within the Black and Scholes (1973) framework. He transforms the terminal boundary value problem for the Black and Scholes (1973) PDE into a corresponding problem for the heat equation which has a well-known solution. In Chapter 7.4, pp. 408–412, Cox and Rubinstein (1985) give the valuation function for down & out call and put options on non-dividend paying stocks with a rebate paid at maturity. They also mention the possibility to extend these results to barriers and rebates which are exponential and mixed linear-exponential functions of the time-to-maturity respectively. Reiner and Rubinstein (1991b) obtain analytical solutions for all eight types of vanilla barrier options on dividend paying stocks as well as the associated rebates paid at expiry. They explicitly evaluate the corresponding conditional expectations under the risk-neutral probability measure. Rich (1994) details the steps involved in their derivation using the probabilistic approach. The author also derives the first passage time probability density function (PDF) as well as the joint PDF of the terminal underlying asset price and its running minimum or maximum as auxiliary results.

As a result of the Feynman-Kac formula, most contingent claim pricing problems can be equally approached probabilistically or through PDE methods. Buchen (2001b) shows how the method of images for the Black and Scholes (1973) PDE can be used to solve a large class of initial boundary value problems; see also Chapter 12 in Wilmott et al. (1995), pp. 206–232. Similar to Merton (1973), the author implicitly applies a coordinate change and then exploits symmetry relationships of the heat equation. The virtue of his approach is that he defines an image operator that can be directly applied to the solution of a related full-range problem to obtain the valuation function for vanilla barrier options. It is thus not necessary to carry out the change of variables explicitly. The fundamental building blocks in these valuation functions are often (higher-order) binary options; see Ingersoll (2000) and Buchen (2004). Skipper and Buchen (2003) generalize most previous results on binary options by considering a power payoff in a multi-period and multi-asset setting.

A closely related strand of the literature is concerned with the pricing of exotic barrier options. These contracts have been developed to accommodate the demand for payoff structures that fit even more refined market views. The following overview is by no means exhaustive. Cox and Rubinstein (1985) already mention the possibility to price barrier options with exponential boundaries. Omberg (1987) approximates the optimal exercise boundary for American put options through an exponential function of time. He then values them as down & out barrier options with an immediate rebate equal to the intrinsic value upon the trigger event.

Kunitomo and Ikeda (1992) obtain a valuation formula for double barrier options with curved boundaries. For these contracts, the trigger event corresponds to the first hitting time of either the upper or the lower barrier. They compute the PDF for staying between the two boundaries and their solution takes the form of a rapidly converging sum of an infinite series. Hui (1996) also considers double knock-out binary options and solves the corresponding boundary value problem for the heat equation using Fourier series. Geman and Yor (1996) derive the Laplace transform of the option price with respect to its maturity date and then numerically invert this expression. Pelsser (2000) analytically inverts the Laplace transform of the PDFs and prices a wide variety of double barrier options. Buchen and Konstandatos (2009) reproduce the results by Kunitomo and Ikeda (1992) by extending the method of images for the Black and Scholes (1973) PDE to exponentially bent double barriers.

Heynen and Kat (1994a) analyze the valuation of partial barrier options where the monitoring period is restricted to either the start or the end of the option's lifetime. Their results are based on an explicit evaluation of the integrals corresponding to the risk-neutral conditional expectation; see also Carr (1995) and Hui (1997). Buchen (2004) shows that given the valuation function for higher-order binary options, these results follow almost immediately from the method of images in Buchen (2001b). See also Chapter 4.2 in Konstandatos (2003), pp. 85–90, for an extension to multiple barrier windows. Finally, Heynen and Kat (1994b) discuss outside barrier options, where the terminal payoff and the barrier trigger event depend on two different but correlated assets; see also Carr (1995).

While this chapter focuses on expanding the universe of analytical solutions for barrier option prices, a large strand of the literature is concerned with numerical approaches. The motivation for using numerical methods is twofold. First, they make it possible to obtain approximate solutions to exotic valuation problems for which an analytical solution is not known, even within the Black and Scholes (1973) framework. Second, they are usually necessary to price barrier options under alternative underlying dynamics. These include, for example, the stochastic volatility and jump-diffusion models proposed by Heston (1993), Schöbel and Zhu (1999) and Duffie et al. (2000), the local volatility dynamics as in Dupire (1994), Rubinstein (1994) and Derman et al. (1995b), as well as the class of (time-changed) exponential Lévy models, as in Madan et al. (1998), Barndorff-Nielsen and Shephard (2001a,b) and Carr et al. (2003). Since the focus of this chapter is on the Black and Scholes (1973) framework, the numerical approaches used within this setting are briefly reviewed below. In particular, Monte Carlo simulations and finite difference schemes are used to validate our main results.

Boyle (1977) introduces Monte Carlo methods to the area of contingent claim pricing. This approach involves simulating the stochastic differential equation (SDE) defining the underlying asset dynamics or, if available, its solution on a discrete time grid; see also the monograph by Kloeden and Platen (1995). In order to value continuously monitored barrier options through Monte Carlo simulation, one can use the relationship obtained by Broadie and Glasserman (1997) when analyzing the inverse problem. Alternatively, the hitting probability between two samples can be computed analytically using the known conditional distribution of the maximum or minimum over the time interval; see for example Karatzas and Shreve (1991) and Glasserman (2003).

The convergence of tree methods for barrier options is impeded by the inability of the exogenously specified lattice to reflect the contractual terms of the barrier option. Boyle and Lau (1994) optimally determine the number of binomial tree steps to employ with the objective to minimize the difference between the contractual and the effective barriers. Ritchken (1995) constructs a trinomial tree whose nodes pass exactly through the contractual barrier; see also Kamrad and Ritchken (1991). Derman et al. (1995a) propose to improve the convergence in a binomial tree through interpolating between the prices of two auxiliary barrier options that can be accurately priced on the given lattice. Analogous to the approach used in Monte Carlo simulations, Barone-Adesi et al. (2007) adjust the binomial tree backward induction algorithm to account for the probability of a barrier breach between two nodes that both lie within the active domain.

III.1.2 Contribution

This chapter jointly addresses two fundamental problems related to the pricing and risk management of barrier options. First, we discuss how a two-volatility pricing approach succeeds in capturing some of the distributional information embedded in the implied volatility surface while staying within the Black and Scholes (1973) framework and retaining full analytical tractability. As a novel contribution, this chapter formally establishes the equivalence of the two-volatility outside barrier pricing problem and that of valuing an exponential barrier option. Second we introduce a new approach to mitigate the dynamic hedging problems associated with the large in absolute value and discontinuous delta of reverse barrier options. It combines a flat barrier shift with an exponential bending toward the option maturity. We argue that, in contrast to the standard approach of using a constant barrier shift, this functional form provides a better model of the time-dependent risk exposure without sacrificing analytical tractability. One main insight is that valuing a two-volatility option with an exponentially bent barrier is equivalent to pricing a one-volatility option with a continuous and piecewise exponential barrier.

We approach the valuation problem by developing the method of images for exponentially bent barriers. While the result itself is known, we establish its connection to an appropriately chosen coordinate transformation applied to the underlying Black and Scholes (1973) PDE. Furthermore, we provide an alternative derivation using a probabilistic approach that explicitly evaluates the corresponding conditional expectation. The application of the image operator to obtain solutions for deferred start piecewise exponential knock-out barrier options and the associated rebates is novel. We establish additional properties of the image operator in the steps leading to the derivation of these valuation functions. The robustness of the proposed risk management approach is evaluated using Monte Carlo simulations of the delta hedging profit & loss under the Merton (1976) jump-diffusion dynamics. We find that, given the same initial option price, the exponential bending yields significantly lower standard deviation of hedging errors.

This chapter is structured as follows. Section III.2 introduces the two-volatility framework for barrier option pricing. Section III.3.3 proposes an improved risk management approach which involves a piecewise exponential barrier. Section III.4 develops the method of images for exponentially bent barriers. A repeated application of the image operator yields the valuation functions for deferred start piecewise exponential barrier options in Section III.6. The corresponding rebates are dealt with separately in Sections III.7 and III.8. Section III.9 simulates the delta hedging profit & loss distribution for shifted and exponentially bent barrier. Section III.10 concludes by summarizing the main results and proposing potential avenues for future research.

III.2 Two-Volatility Pricing Approach

This section discusses the problem of pricing barrier options within the Black and Scholes (1973) framework when the market implied volatility exhibits a smile or skew pattern. The two-volatility pricing approach proposed in Chapter 14.2 of Brockhaus et al. (2000), pp. 144–146, provides a simple and tractable remedy to this problem. One of the main contributions of this section is to establish that there exists an equivalent and simpler valuation problem in terms of an exponential barrier option.

III.2.1 Background

While the Black and Scholes (1973) and Merton (1973) framework relies on a number of unrealistic assumptions about the underlying dynamics and the market, its most severe shortcoming is to model the logarithmic asset price through a pure diffusion process with independent and stationary Gaussian increments. This misspecification is unveiled in the strong pricing biases first reported by Rubinstein (1985); see also the review by Bates (1996).

Within this framework, all input parameters of the valuation function for European plain vanilla options, except for the diffusion coefficient, are either contract-specific constants or traded quantities in other markets with readily observable prices. Consequently, all deviations from the model assumptions have to be incorporated in the choice of this single degree of freedom. Given the market price of a European plain vanilla option, it is possible to numerically invert the valuation function for the implied volatility. A solution to this problem exists, given that the market prices do not violate the lower and upper static no-arbitrage bounds. It is unique, since the price of European plain vanilla options is a continuous and strictly monotonically increasing function of the underlying asset's volatility. For options whose strike prices are not too far away from the forward price, a good initial guess can be obtained by approximation methods. Corrado and Miller (1996), for example, use a modified second-order Taylor series expansion of the cumulative normal distribution function. By the put-call parity, the implied volatility of an otherwise identical call and put option have to coincide in order for the prices to be free of arbitrage. We refer to, for example, Jäckel (2006) and Li and Lee (2011) for robust algorithms that efficiently handle the task of computing the implied volatility from observed market prices.

The implied volatilities typically exhibit both a strike and time-to-maturity dependence. Tompkins (2001) finds that implied volatilities in many different markets and for near-the-money strikes can be approximated well through a second-order polynomial as a function of a time-to-maturity adjusted logarithmic moneyness measure; see also Chapter 18 in Natenberg (1994), pp. 385–418. The shape of the implied volatility surface is intimately linked to the non-normal higher moments of the risk-neutral distribution of logarithmic yields. *Ceteris paribus*, a positive (negative) skewness as the only deviation from normality, yields a positively (negatively) sloped implied volatility smile (IVS). A positive (negative) excess kurtosis generates a convex (concave) IVS. We refer to the Edgeworth series expansion approach proposed by Rubinstein (1998), which parameterizes the risk-neutral distribution directly in terms of its higher third and fourth moments and thus allows for a convenient analysis; see also Balieiro Filho and Rosenfeld (2004).

Absence of arbitrage within an IVS for any fixed maturity is equivalent to the strict monotonicity and convexity of the corresponding European plain vanilla call or put option prices; see for example Theorem 4 in Merton (1973), p. 146, and Breeden and Litzenberger (1978). Lee (2004) establishes the relationship between the asymptotic behavior of the IVS and the number of finite moments in the underlying asset's distribution. He shows that the arbitrage free implied variance has to be asymptotically linear in the logarithmic strike, unless one assumes that the underlying asset has finite moments of all orders. Fengler (2009) shows that the absence of calendar spread arbitrage requires that the total variance is a strictly increasing function of the time-to-maturity for any constant strike to forward ratio; see also Gatheral (2004, 2006). We refer to the monograph by Fengler (2006) for an extensive overview of approaches to infer the implied volatility surface from listed options quotes. Gatheral (2004) and Gatheral and Jacquier (2012) propose a widely adopted flexible class of IVS parametrizations and discuss their arbitrage-free calibration.

III.2.2 Barrier Valuation Problem

When pricing European plain vanilla options for a strike and maturity combination that is not traded in the market, the aforementioned approaches can be used to construct and interpolate the IVS in an arbitrage-free fashion. This interpolated value is then substituted back into the standard Black and Scholes (1973) valuation function. Despite using a pricing model that is inconsistent with the market as a whole, this approach still yields a market consistent price for the single contract under consideration. However, in

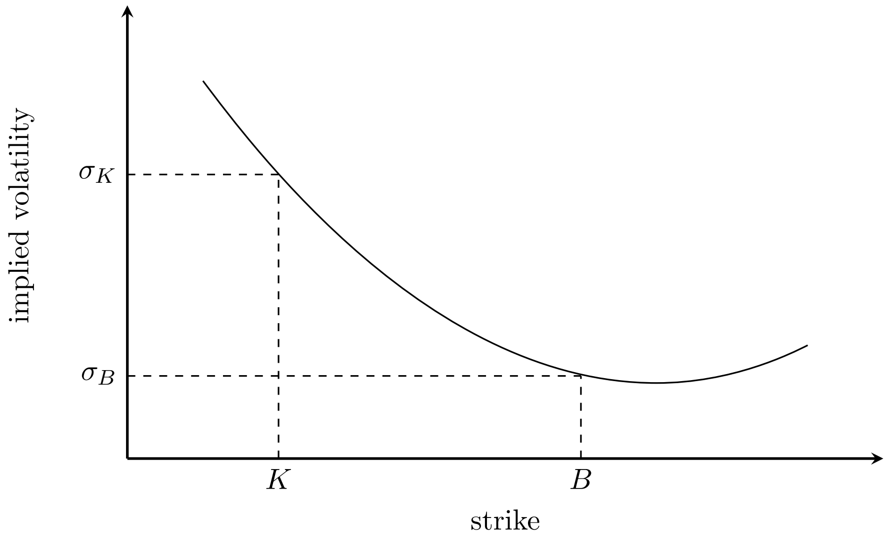

Figure III.1: Illustration of the barrier option pricing problem when the implied volatility exhibits a smile pattern.

the case of barrier options, it is not clear how the value of the underlying asset's diffusion coefficient should be chosen in the presence of a non-flat IVS. Figure III.1 illustrates the associated pricing problem within the Black and Scholes (1973) framework for a typical shape of the IVS. We consider an up & out call option for which the implied volatility at the strike price K is greater than that at the barrier B. Setting the diffusion parameter equal to the implied volatility at either the strike or the barrier seems just as arbitrary as any weighted average of these values. Consider, for example, using the higher strike volatility σ_K as the input to the valuation function obtained by Reiner and Rubinstein (1991b). The decreasing IVS suggests that the asset on average diffuses at a lower rate as the spot price increases. Consequently, the model probability of a knock-out is too high and the corresponding barrier option price is too low. We can make an analogous argument against using the barrier volatility σ_B.

To gain some intuition for how the prices of up & out call options should depend on the shape of the volatility smile, we consider a super-replication strategy. Consider a portfolio that holds (i) a long position in one European vanilla call option with a strike price of K, (ii) a short position in one European plain vanilla call option with a strike price of B and (iii) a short position in $(B - K)$ bond binaries with a strike price B and a unit notional each. All options expire at the same time as the up & out call option. The terminal payoff of this portfolio is equal to that of the barrier option conditional on no prior knock-out. Since its payoff is independent of the path taken by the underlying asset, it is often referred to as a European barrier option. The value of this portfolio thus represents an upper bound for the value of the up & out call option. It is the smallest such upper bound that can be constructed from European options with a single maturity. *Ceteris paribus*, as the barrier (strike) volatility increases, so do the values of the corresponding call and binary options (the corresponding call option) and consequently the portfolio value decreases (increases). Thus, we expect the price of the up & out call to be decreasing in the slope of the IVS.

In a brief discussion of this problem in Chapter 14.2, Brockhaus et al. (2000), pp. 144–146, outline an approach to capture some of the information embedded in the IVS while at the same time staying within the Black and Scholes (1973) framework and thus preserving full analytical tractability. In analogy to the outside barrier options discussed by Heynen and Kat (1994b), they suggest to model two perfectly correlated geometric Brownian motion spot assets, which start at the same initial value but have different diffusion coefficients. While the option payoff is a function of the terminal value of the first asset, the trigger event is determined by the maximum or minimum of the second asset. We adopt this so-called two-volatility approach to attain smile-adjusted barrier option prices.

In the following section, we formally set up the two-volatility model and show that, as a result of the perfect correlation between the two assets, the valuation problem can be reduced to that of pricing a one-volatility barrier option with an exponentially bent barrier. The valuation functions for these types of contracts are well known; see for example Omberg (1987) and the discussion in Cox and Rubinstein (1985), p. 411. First, however, it should be emphasized that this valuation approach is merely a contract-type specific adjustment applied to the Black and Scholes (1973) model in order to capture some of the non-normality of the market implied asset return distributions. In particular, the two-volatility approach is solely based on the IVS corresponding to the time-to-maturity of the option but does not take into account the term-structure information embedded in the full implied volatility surface. Much of the recent literature in option pricing has focused on generalizing and modifying the underlying asset dynamics; see the references provided in Section III.1. These approaches have in common that their parameters are first calibrated to the observable market prices of all plain vanilla options before using them to price path-dependent contingent claims. This usually requires the use of numerical methods such as finite difference lattices or Monte Carlo simulation. A notable exception is the Kou (2002) double exponential jump diffusion model where the joint PDF of the overshoot and the first passage time can be computed analytically; see Kou and Wang (2003) and

Table III.1: Overview of the March 2013 exchange turnover in German retail listed derivatives as reported by Deutscher Derivate Verband (2013).

Product Category	No. of Issues	Volume (1,000 EUR)	No. of Trades
Capital Guaranteed Certificates	3,141	112,647	5,497
Structured Bonds	466	80,573	3,626
Reverse Convertible Bonds	54,383	207,647	11,569
Discount Certificates	177,182	669,801	18,387
Express Certificates	2,153	94,924	4,788
Bonus Certificates	185,018	465,685	17,642
Index & Participation Certificates	5,165	470,736	26,908
Outperformance & Sprint Certificates	2,603	5,466	445
Warrants	341,122	459,912	90,497
Knock-Out Certificates	217,396	901,597	207,624
Total	988,629	3,468,988	386,983

Kou and Wang (2004). However, like all pure exponential Lévy models, it generates IVSs that flatten out with increasing time-to-maturity. It is thus not rich enough to fit the whole term structure of implied volatilities. The two-volatility model is fundamentally different from the aforementioned approaches in that it can neither be fitted to the market prices of all European plain vanilla options, even of a single maturity, nor can it be universally applied to value all contract types. Its main appeal stems from the possibility to obtain analytic solutions for partial barrier options where the barrier follows a piecewise exponential function of time. The motivation for considering these seemingly highly exotic contracts is discussed in this section and the next.

The availability of analytical solutions that capture some of the distributional information embedded in the market prices of plain vanilla options is especially important in a high-frequency environment. While barrier options are usually traded in an on-request basis in the over-the-counter market, there exist exchanges where they are quoted in a continuous fashion. Examples are the European markets for structured limited liability retail derivatives. In Germany, products known as bonus certificates are traded, which can be decomposed into, among others, long positions in (deferred start) down & out put options. As shown in Table III.1, both the number of issues as well as their exchange turnover are significant. Some variants of reverse convertible bonds and discount certificates also implicitly contain positions in (deferred start) barrier options.

The continuous market making of these issues based on purely numerical methods is computationally unfeasible. A common compromise between computational speed and pricing accuracy is to use a valuation model with an analytical solution for the continuous quotation. These prices are then adjusted for the pricing error with respect to a more realistic model that is evaluated numerically on a lower frequency only. The latter should be chosen depending on the risk-sensitivities of the contract under consideration.

III.2.3 Model Setup

In this section, we formally setup the two-volatility model dynamics. Let $W^* = \{W_t^* : t \in [0, T^*]\}$ be a one-dimensional standard Brownian motion on a complete filtered probability space $(\Omega, \mathfrak{F}, \mathbb{F}, \mathbb{P}^*)$. As we are solely interested in pricing, we interpret $\mathbb{P}^*$ to be the risk-neutral probability measure corresponding to the bank account numéraire and consider continuous trading in the interval $[0, T^*]$ for a fixed terminal time $0 < T^* < \infty$. The filtration $\mathbb{F} = (\mathfrak{F}_t)_{t \in [0,T^*]}$ is the $\mathbb{P}^*$-augmentation of the natural filtration induced by the process W^*. The market consists of a bank account $B = \{B_t : t \in [0, T^*]\}$ with non-random dynamics

$$\mathrm{d}B_t = rB_t \mathrm{d}t.$$

It's initial value is $B_0 = 1$ and the risk-free interest rate is constant at $r \in \mathbb{R}$. In addition, there are two perfectly correlated risky spot assets $S^{(1)} = \left\{S_t^{(1)} : t \in [0, T^*]\right\}$ and $S^{(2)} = \left\{S_t^{(2)} : t \in [0, T^*]\right\}$ with dynamics

$$\mathrm{d}S_t^{(1)} = (r - \delta_1)\, S_t^{(1)} \mathrm{d}t + \sigma_1 S_t^{(1)} \mathrm{d}W_t^*$$

and

$$\mathrm{d}S_t^{(2)} = (r - \delta_2)\, S_t^{(2)} \mathrm{d}t + \sigma_2 S_t^{(2)} \mathrm{d}W_t^*,$$

where the diffusion coefficients $\sigma_1, \sigma_2 \in \mathbb{R}_+$ and the dividend yields $\delta_1, \delta_2 \in \mathbb{R}$ are constants. The initial values $S_0^{(1)} = S_0^{(2)}$ agree and are equal to $S_0 \in \mathbb{R}_+$.

We now consider an American knock-out barrier option on these two assets where without loss of generality (w.l.o.g.) we assume that the terminal payoff is that of a plain vanilla option on the first risky asset $S^{(1)}$, conditional on the second risky asset $S^{(2)}$ not having breached the barrier during the lifetime of the option. Here, the term "American" is used to indicate that the barrier is continuously monitored and does not refer to early exercise rights as in the context of plain vanilla options. The value of the otherwise

Table III.2: Knock-out barrier option types corresponding to the different combinations of the indicators ϕ and ψ.

Option Type	ϕ	ψ
Up & Out Call	+1	-1
Down & Out Call	+1	+1
Up & Out Put	-1	-1
Down & Out Put	-1	+1

identical knock-out barrier option then follows from the in-out parity for barrier options; see for example Chapter 4.17 in Haug (2007), pp. 152–167. Let $0 \leq T \leq T^*$ be the option maturity and let ν be the first hitting time of the asset $S^{(2)}$ to the constant barrier $B \in \mathbb{R}_+$ defined as

$$\nu = \inf \left\{ t \geq 0 : \psi S_t^{(2)} \leq \psi B \right\}.$$

Here, $\psi \in \{-1, +1\}$ is the indicator for an up- or down-barrier. Note that the convention employed in the definition of ψ is rather uncommon. It is chosen for consistency with the PDE approach discussed in Section III.4. Throughout this chapter, we follow the convention to set $\nu = \infty$ on the set where the asset price process never breaches the barrier. From Theorem I.4 in Protter (2004), p. 5, for example, it follows that ν is a valid stopping time. The terminal option payoff is then given by

$$V_T = \left(\phi S_T^{(1)} - \phi K \right)^+ 1 \{ \nu \geq T \},$$

where $\phi \in \{-1, +1\}$ is the indicator for a put or call option. Table III.2 provides an overview of the knock-out barrier option types corresponding to the different combinations of the indicators ϕ and ψ. For the moment, we only consider barrier options that do not pay a rebate when knocked-out prior to expiration. This assumption is dropped in Sections III.7 and III.8, which discusses the pricing of fixed rebates that are paid either at the option maturity or immediately upon the trigger event.

We next give a formal definition of an exponential boundary. Throughout this chapter, we follow the convention of denoting the time-to-maturity of an option by $\tau = T - t$. Deterministic functions of the calendar time are denoted in capital Latin letters as, for example $B(t)$, while functions of the time-to-maturity are annotated by a tilde, for example $\tilde{B}(\tau)$. While probably not obvious at first, it is convenient for computational purposes to define a time-varying barrier as a function of the time-to-maturity, where the initial condition corresponds to the barrier level at the expiry of the option.

Definition III.1 (Exponential Boundary).
A function $\tilde{B} : \mathbb{R}_+ \to \mathbb{R}_+$ is an exponential boundary if it can be represented as

$$\tilde{B}(\tau) = \tilde{B}(0)\mathrm{e}^{\xi\tau}$$

with initial value $\tilde{B}(0) \in \mathbb{R}_+$ and shape parameter $\xi \in \mathbb{R}$. The corresponding barrier level as a function of the calendar time is then given by $B(t) = \tilde{B}(T-t)$. $\triangle$

Using this definition, we can now establish an equivalent valuation problem that can be formulated solely in terms of the first risky asset.

Lemma III.1 (Link between Two-Volatility and Exponential Barrier Options).
Define a new random time $\hat{\nu}$ by

$$\hat{\nu} = \inf\left\{t \geq 0, \psi S_t^{(1)} \leq \psi \tilde{B}^*(T-t)\right\},$$

where $\tilde{B}^* : [0, T^*] \to \mathbb{R}_+$ is an exponential boundary given by

$$\tilde{B}^*(\tau) = \tilde{B}^*(0)\mathrm{e}^{\xi^*\tau}$$

with

$$\begin{aligned}
\tilde{B}^*(0) &= S_0 \left(\frac{B}{S_0}\right)^{\sigma_1/\sigma_2} \mathrm{e}^{-\xi^* T}, \\
\xi^* &= r\left(\frac{\sigma_1}{\sigma_2} - 1\right) + \delta_1 - \frac{\sigma_1\delta_2}{\sigma_2} + \frac{1}{2}\sigma_1\left(\sigma_1 - \sigma_2\right).
\end{aligned}$$

Then

$$\nu = \hat{\nu} \qquad \mathbb{P}^*\text{-}a.s..$$

Proof The perfect correlation between the two risky assets suggests that we can also express the first hitting time in terms of the first risky asset $S^{(1)}$. We have

$$\begin{aligned}
& S_t^{(2)} &=& \ B \\
\Leftrightarrow \quad & W_t^* &=& \ \frac{1}{\sigma_2}\left(\ln\left(\frac{B}{S_0}\right) - \left(r - \delta_2 - \frac{1}{2}\sigma_2^2\right)t\right) \\
\Leftrightarrow \quad & S_t^{(1)} &=& \ S_0\left(\frac{B}{S_0}\right)^{\sigma_1/\sigma_2} \exp\left\{\left(r\left(1 - \frac{\sigma_1}{\sigma_2}\right) - \delta_1 + \frac{\sigma_1\delta_2}{\sigma_2} + \frac{1}{2}\sigma_1\left(\sigma_2 - \sigma_1\right)\right)t\right\} \\
& &=:& \ \tilde{B}^*(T-t),
\end{aligned}$$

with $\tilde{B}^* : [0, T^*] \to \mathbb{R}_+$ as given in Lemma III.1. $\square$

Consequently, the problem of pricing a two-volatility barrier option with a constant barrier can be reduced to that of pricing a standard one-volatility barrier option with an exponential barrier. Stated differently, the Lemma establishes that the value of an outside barrier options converges to that of an exponential barrier option in the limit when the correlation between the two assets approaches one. It is thus not necessary to use the outside barrier option valuation functions obtained by Heynen and Kat (1994b).

One peculiarity of the two-volatility approach for reverse knock-out barrier options is that the maximal payoff at the option maturity, which is assigned a strictly positive probability, is in general not equal to the absolute value of the difference between strike and barrier. Consider, for example, a three-month up & out call option with strike $K =$ 100.00 USD and barrier $B = 120.00$ USD. Further assume that the current spot price is $S_0 = 100.00$ USD, the risk-free interest rate and dividend are equal for both assets and given by $r = 5.00\%$ and $\delta = 0.00\%$. Finally, the strike and barrier volatilities are $\sigma_K = 20.00\%$ and $\sigma_B = 15.00\%$ respectively. Using the result from Lemma III.1, we then obtain $\tilde{B}^*(0) = 124.79$ USD. Thus, although we are pricing a contingent claim whose maximal contractual payoff is equal to $B - K = 20.00$ USD, it is valued as if the highest achievable payoff was instead $\tilde{B}^*(0) - K = 24.79$ USD. This effect is due to the perfect correlation between the two assets and the volatility at the barrier being lower than that at the strike. *Ceteris paribus*, if the barrier volatility was instead $\sigma_B = 25.00\%$, then we would obtain $\tilde{B}^*(0) = 117.45$ USD. Note however, that $\tilde{B}^*(0) \to B$ as the spot price approaches the barrier.

Figure III.2 illustrates the dependence of the two-volatility price of an up & out call option on the underlying asset price for different barrier volatilities. *Ceteris paribus*, for higher (lower) barrier volatilities, the probability of a knock-out increases (decreases) and

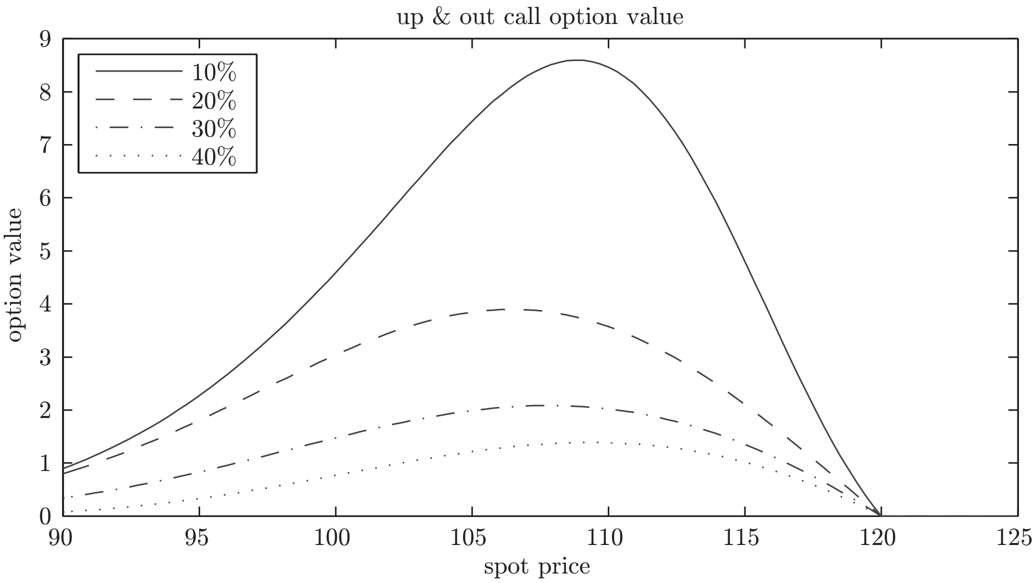

Figure III.2: Price of a three-month two-volatility up & out call option as a function of the underlying asset price and for different barrier volatilities. The fixed contract and market parameters are $K = 100.00$ USD, $B = 120.00$ USD, $\sigma_K = 20.00\%$, $r = 5.00\%$ and $\delta = 0.00\%$.

consequently the barrier option price decreases (increases). This is in accordance with the previously discussed dependence of the super-replicating portfolio value on the slope of the IVS.

There are two more results related to the link between exponential boundaries and dividend yields that will be useful in Section III.8 when pricing fixed rebates that are paid immediately upon the first hitting time of the barrier.

Lemma III.2 (First Hitting Time PDF).
Let $\tilde{B}(\tau)$ be an exponential boundary where $\tau = T - t$ for some time $T \in [0, T^*]$ and let the dynamics of the spot asset $S = \{S_t : t \in [0, T^*]\}$ under the risk-neutral probability measure $\mathbb{P}^*$ be given by

$$\mathrm{d}S_t = (r - \delta)S_t \mathrm{d}t + \sigma S_t \mathrm{d}W_t^*.$$

Then the first hitting time ν of S to the barrier $\tilde{B}(\tau)$ on the interval $[0, T]$ is defined as

$$\nu = \inf\left\{t \in [0, T] : S_t = \tilde{B}(T - t)\right\}.$$

The corresponding first hitting time PDF is given by

$$\mathbb{P}^*\{\nu \in \mathrm{d}t\} = \frac{|\alpha|}{t\sqrt{2\pi t}} \exp\left\{-\frac{(\alpha - \lambda t)^2}{2t}\right\} \mathrm{d}t,$$

where

$$\begin{aligned}\alpha &= \frac{1}{\sigma}\left(\ln\left(\frac{\tilde{B}(0)}{S_0}\right)+\xi T\right),\\ \lambda &= \frac{1}{\sigma}\left(r-\delta+\xi-\frac{1}{2}\sigma^2\right).\end{aligned}$$

Proof It is easy to show that the problem of finding the first hitting time PDF of a geometric Brownian motion asset to an exponential barrier can be reduced to that of finding the first hitting time PDF of a drifted Brownian motion to the constant barrier α. See Appendix III.A.1 for details. □

Corollary III.1 (Link between Exponential Barriers and Dividend Yields). *When considering the barrier as fixed at* $\hat{B} = \tilde{B}(0)\mathrm{e}^{\xi T}$*, then the first hitting time PDF* $\mathbb{P}^*\{\nu \in \mathrm{d}t\}$ *depends on the dividend yield* δ *and the shape parameter* ξ *only through their difference* $\xi - \delta$*.*

Proof This is obvious from the solution for the first hitting time PDF given in Lemma III.2. Alternatively, from Definition III.1 and the solution to the SDE for S, we find that $S_t = \tilde{B}(T-t)$ when

$$W_t^* + \frac{1}{\sigma}\left(r-\delta+\xi-\frac{1}{2}\sigma^2\right)t = \frac{1}{\sigma}\left(\ln\left(\frac{\tilde{B}(0)}{S_0}\right)+\xi T\right)$$

and the claim follows. □

From this corollary, it follows that the problem of pricing contingent claims with exponential barriers, whose payoffs solely depend on the first hitting time but not the corresponding spot price, can be reduced to that of pricing contingent claims with a flat barrier and a modified dividend yield.

III.3 Risk Management

This section analyzes the risks involved in dynamically hedging barrier options in real-world markets and how the valuation can be adjusted to account for them. In particular, it focuses on the potential problems arising from limited market liquidity, non-continuous price paths and discrete trading. While our discussion in general applies to all types of barrier options, the impact of a violation of the model assumptions is most pronounced for reverse barrier options which knock-in or -out when in-the-money. Thus, an up & out call option is used as a consistent example throughout this section.

We focus on the case when a position in the barrier options is dynamically hedged through a self-financing trading strategy by taking positions in the underlying asset and the bank account. Following a static-dynamic hedging strategy as in Derman et al. (1994), where positions in European plain vanilla options are added to match the barrier option value at some points of the boundary and at the maturity, mitigates the problem but does not eliminate it; see also Bowie and Carr (1994) and Carr et al. (1998).

In order not to obscure the actual risk management issues, we first take a step back and analyze the sensitivities of barrier options in the standard Black and Scholes (1973) one-volatility setting. The qualitative insights continue to hold in the two-volatility valuation approach discussed in Section III.2. The synthesis between the separately developed volatility smile and risk adjustments is then performed in Section III.3.4.

The main contribution of this section is to introduce a time-dependent barrier shift that better reflects the risk profile of dynamically hedging reverse barrier options than existing approaches do. By modeling it as a piecewise exponential function, we retain full analytical tractability within the Black and Scholes (1973) framework. Furthermore, it can be easily combined with the two-volatility approach to pricing developed in Section III.2.

III.3.1 Background

Dynamically hedging reverse barrier options is challenging for two reasons. First, the sensitivities are discontinuous at the barrier and, second, the absolute exposure becomes very large near the option maturity when the spot price is close to the barrier. See, for example, Chapter 19 in Taleb (1996), pp. 312–346, or Chapter 10 in de Weert (2008), pp. 57–69, for general discussions.

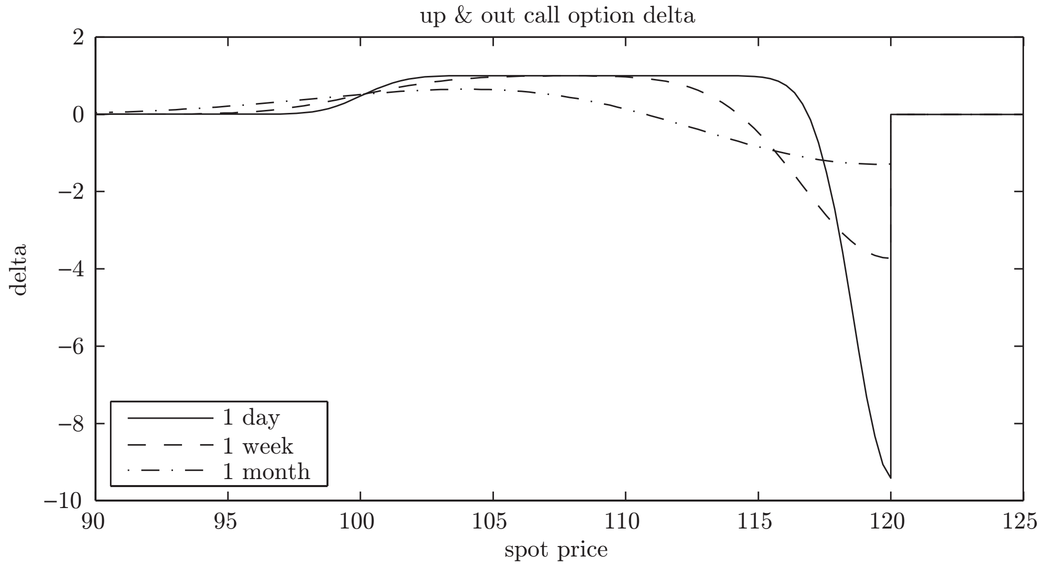

Figure III.3: Delta of an up & out call option as a function of the underlying asset price and for different times-to-maturity. The fixed contract and market parameters are $K = 100.00$ USD, $B = 120.00$ USD, $\sigma = 20.00\%$, $r = 5.00\%$ and $\delta = 0.00\%$.

Figure III.3 depicts the delta of an up & out call option with strike price $K = 100.00$ USD and barrier $B = 120.00$ USD as a function of the spot price and for different times-to-maturity. In contrast to plain vanilla options, the payoff function of reverse barrier options is not monotonic in the underlying asset price and consequently its delta can be both positive and negative. Its sign is the same as that of the otherwise identical plain vanilla option near the strike price and it changes as the spot price approaches the barrier. Once the barrier is breached, the option immediately matures and thus all of its sensitivities vanish. This causes a discontinuity of the delta and other Greeks at the barrier. In the case of the up & out call option and as the holder of a short position in the contingent claim, we hedge by taking a short position in the underlying asset when its spot price is close to the barrier. Figure III.3 also reveals that the absolute size of this position is increasing as the time-to-maturity decreases and is in particular not bounded by one. With one trading day to maturity, the absolute delta takes on values as high as 9.41 units of the underlying asset per barrier option. This hedge position has to be fully unwound upon the barrier trigger event.

Within the Black and Scholes (1973) framework, this presents no difficulty as markets are frictionless, trading is continuous and the underlying asset follows a pure diffusion process. Thus, the valuation is implicitly based upon the assumption that we are always

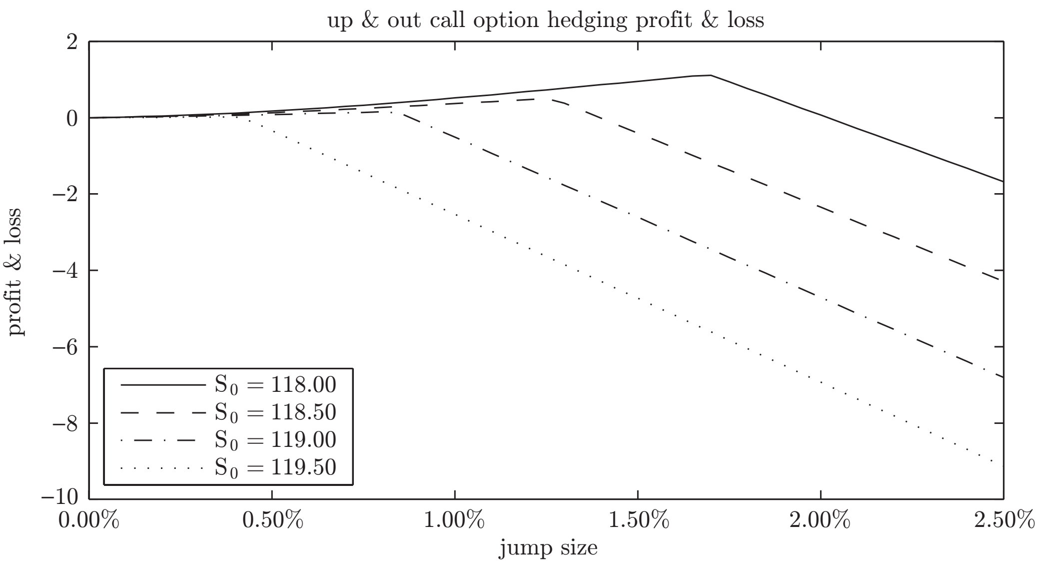

Figure III.4: Profit & loss of a delta hedged short position in a one week up & out call as a function of the instantaneous jump size and for different initial spot prices. All remaining contract and market parameters are as in Figure III.3.

able to close out the complete delta hedge position in the underlying asset exactly on the barrier. However, even when abstracting from the discreteness of the price grid, asset prices in real markets jump during the market opening hours and because of the exogenously imposed overnight period between two trading days. Furthermore, assets are not perfectly elastic, especially during the adjustment process after the arrival of news. The unwinding of a delta hedge position that is large relative to the liquidity of the underlying asset is thus likely to move the spot price further beyond the barrier.

Since the delta is decreasing with increasing prices of the underlying asset, the holder of the short position in the up & out call option has a long gamma position close to the barrier. This is less problematic from a risk management perspective as failing to continuously delta hedge a gamma long position in the worst case forfeits the profit from re-balancing the underlying asset position. However, the discontinuity at the barrier corresponds to a large short gamma singularity. The cost corresponding to an unwinding of the hedge position beyond the barrier is equal to the number of shares held times the difference between the mean transaction price and the barrier.

Figure III.4 shows the overall profit & loss of a delta hedged short position in the one week up & out call as a function of the instantaneous jump size and for different initial spot prices. Here, we ignore w.l.o.g. the price impact of the hedge transactions and assume that the full delta hedge can be closed out at the post jump price. The profit & loss is

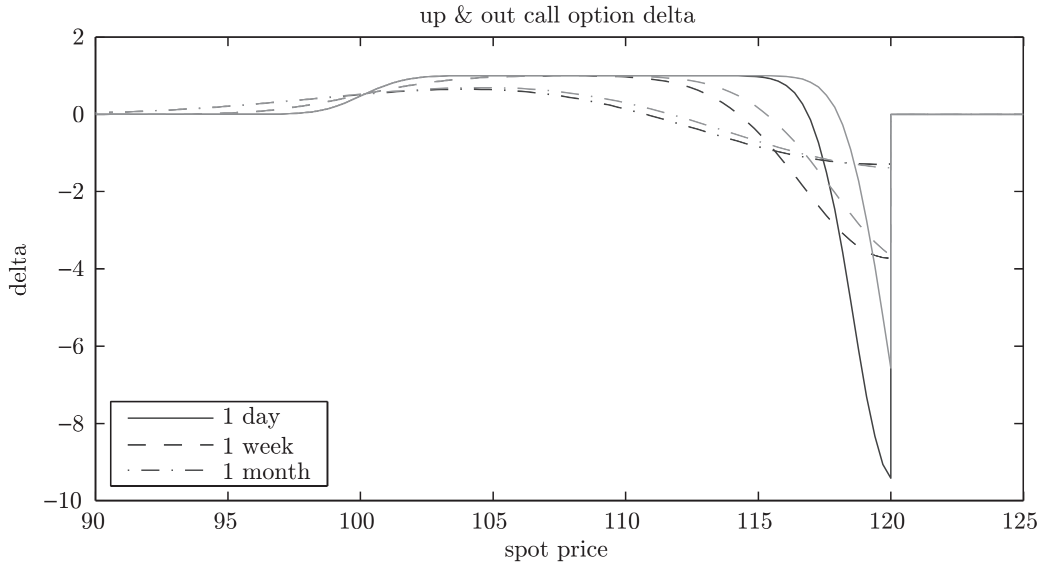

Figure III.5: Delta of an up & out call option as a function of the underlying asset price and for different times-to-maturity. The black curves correspond to the contractual barrier at $B = 120.00$ USD. The dark gray curves correspond to a barrier that is shifted up in parallel by 1.00% to $B = 121.20$ USD. The remaining fixed contract and market parameters are as in Figure III.3.

first increasing and convex in the jump size due to the local concavity of the barrier option price. It is linearly decreasing from the point where the jump results in a spot price that crosses the barrier. Assume for example that we last hedged the up & out call at a spot price of 119.50 USD by taking a short position in 3.67 underlying assets. A subsequent instantaneous up-jump of +1.00% to 120.70 USD then corresponds to an overall loss of 2.54 USD per contract. While the value of the short option position drops by 1.86 USD, the delta hedge position yields a loss of 4.40 USD. In percentage terms, this corresponds to a loss of 136.23% of the last barrier option prior to the trigger event.

III.3.2 Barrier Shifting

A common approach to account for the liquidity and jump risk associated with dynamically hedging reverse barrier options is to apply a barrier shift; see for example Chapter 10.2 in de Weert (2008), pp. 58–60, or Chapter 4.4 in Ekstrand (2011), pp. 69–73. Instead of the contractually agreed upon barrier, the valuation and risk management is based on a shifted barrier level. The sign of the barrier shift is chosen such that the payoff of the priced contract dominates the contractual payoff. Shifting the barrier serves two main purposes. First, it reduces the maximum absolute delta exposure near the barrier and thus yields a more well-behaved hedge. Second, it provides a buffer within which the hedge position can be unwound without incurring a loss. This can be seen as follows. If the official barrier is not breached before the option maturity, then the contractual and hedged payoffs coincide. Otherwise, the value of the hedged claim upon the barrier trigger event is non-negative while the contractual value is zero. The value of the hedged barrier option is strictly positive if the spot price that breaches the contractual barrier does not cross the shifted barrier at the same time. Consequently, the hedger faces a net loss only if the loss of unwinding the delta hedge beyond the barrier exceeds the value of the hedge portfolio immediately prior to the knock-out. The motivation for using a barrier shift is thus very similar to that for super-replicating a European bond binary through an appropriately chosen European plain vanilla call or put spread; see for example Chapter 17 in Taleb (1996), pp. 273–294.

The first effect is visualized in Figure III.5, which compares the delta exposure profile of the up & out call option using the contractual barrier of $B = 120.00$ USD to a barrier that is shifted up in parallel by 1.00% to $B = 121.20$ USD. At one week to maturity for example, this reduces the absolute delta exposure at a spot price of 119.50 USD from 3.67 to 3.37 units of the underlying asset per barrier option. A subsequent instantaneous up-jump of +1.00% now corresponds to an overall windfall profit of 2.45 USD. It can be broken down into a profit of 6.48 USD from the last portfolio value prior to the knock-out and a loss of 4.03 USD from the delta hedge position. The break-even jump size for this scenario is given by 1.61%, which corresponds to a spot price of 121.42 USD.

It remains to be decided how the barrier shift should be determined in practice. Starting from a model that captures both the statistical dynamics of the underlying asset as well as the price impact of an order as a function of the trade size, we can determine the break-even barrier shift. As the above numerical example illustrates, setting the barrier shift equal to the expected average jump size yields a positive windfall profit on expectation.

III.3.3 Barrier Bending

Section III.3.2 discusses how a parallel shift of the barrier can be used to mitigate the risks involved in dynamically hedging reverse barrier options. It is introduced to create a buffer within which the potentially large delta hedge position can be unwound once the barrier is breached. This cushion is mainly needed very close to maturity where

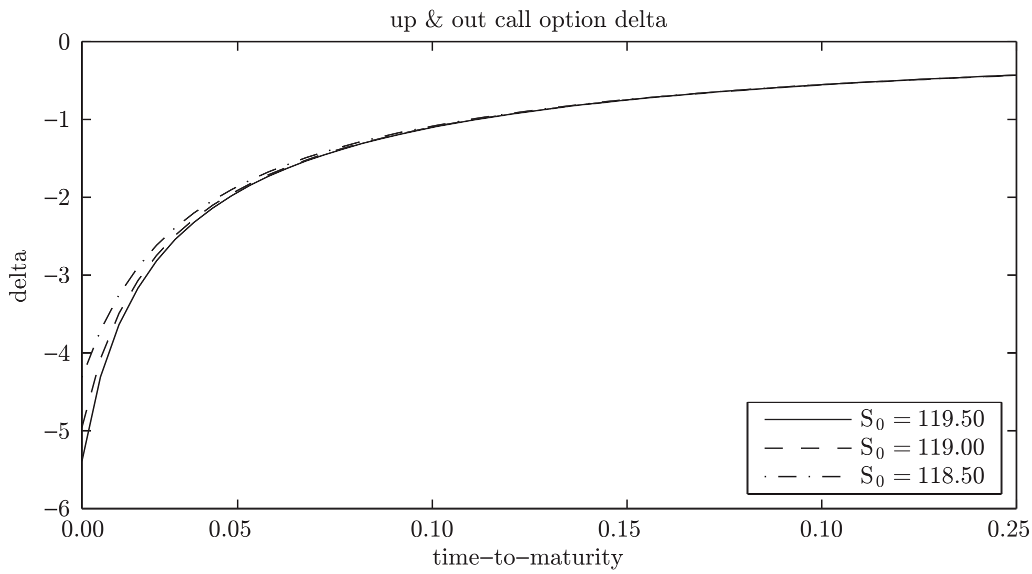

Figure III.6: Delta of an up & out call option as a function of the time-to-maturity in years and for different underlying asset prices. All remaining contract and market parameters are as in Figure III.3.

the absolute hedge ratio becomes large. However, by using a parallel shift we obtain a buffer whose size is independent of the time-to-maturity. Using a break-even analysis as suggested before yields a barrier shift that averages over all knock-out events, irrespective of their time of occurrence. This results in too large (too small) a buffer when the time-to-maturity is large (small).

From a risk management perspective, it is thus preferable to model the barrier shift in such a way that it takes into account the time-dependent nature of the delta hedging risk. Figure III.6 shows the change in the delta of the up & out call option as the time-to-maturity becomes shorter, keeping the underlying asset price unchanged at different levels close to the barrier. This so-called delta bleed is small in magnitude for long times-to-maturity and it increases exponentially as the expiration approaches. In what follows, we propose a parametrization of the barrier shift which reflects this. Let $0 < T_B < T$ be a fixed point of time with corresponding time-to-maturity $\hat{\tau}_B = T - T_B$ and define the percentage barrier shift $b : \mathbb{R}_+ \to \mathbb{R}$ as

$$\tilde{b}(\tau) = \begin{cases} (1+b_1)\exp\left\{\frac{1}{\hat{\tau}_B}\ln\left(\frac{1+b_1}{1+b_2}\right)\tau\right\} - 1 & \text{if } \tau \in [0, \hat{\tau}_B] \\ b_1 & \text{if } \tau > \hat{\tau}_B \end{cases}.$$

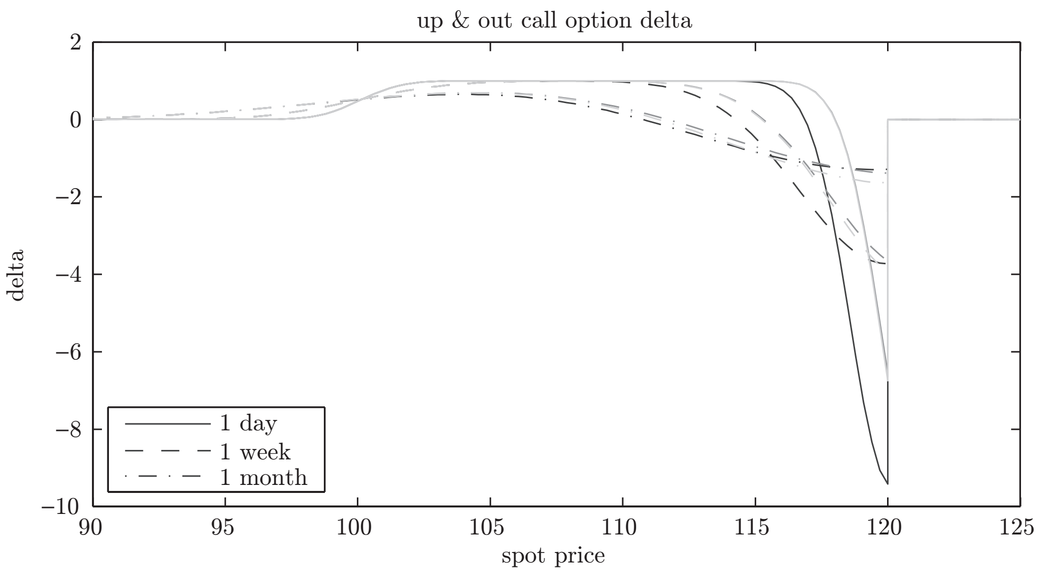

Figure III.7: Delta of an up & out call option as a function of the spot price and for different times-to-maturity. The black and dark gray curves are as in Figure III.5. The light gray curves correspond to an exponential bending of the barrier over the last month from an initial shift of 0.00% to a terminal shift of 1.00%. The remaining fixed contract and market parameters are as in Figure III.3.

where $b_1 \in \mathbb{R}$ is the flat barrier shift before the bending start date T_B and $b_2 \in \{x \in \mathbb{R} : \operatorname{sgn}(x) = \operatorname{sgn}(b_1), |x| \geq |b_1|\}$ is the terminal barrier shift at the option maturity. We then define the absolute barrier level by $\tilde{B}(\tau) = B\big(1 + \tilde{b}(\tau)\big)$ so that

$$\tilde{B}(\tau) = \begin{cases} \tilde{B}(0)\mathrm{e}^{\gamma\tau} & \text{if } \tau \in [0, \hat{\tau}_B] \\ \tilde{B}(0)\mathrm{e}^{\gamma\hat{\tau}_B} & \text{if } \tau > \hat{\tau}_B \end{cases},$$

where

$$\begin{aligned} \tilde{B}(0) &= B\left(1 + b_2\right), \\ \tilde{B}\left(\hat{\tau}_B\right) &= B\left(1 + b_1\right), \\ \gamma &= \frac{1}{\hat{\tau}_B} \ln\left(\frac{\tilde{B}\left(\hat{\tau}_B\right)}{\tilde{B}(0)}\right). \end{aligned}$$

Consequently, as a function of calendar time the absolute barrier is also first constant at $\tilde{B}\left(\hat{\tau}_B\right)$ and then exponentially bends to $\tilde{B}(0)$. The parameters b_1, b_2 and T_B can be again determined from a model of the underlying asset dynamics and its liquidity by minimizing the volatility of delta hedging profits & losses subject to the break-even condition.

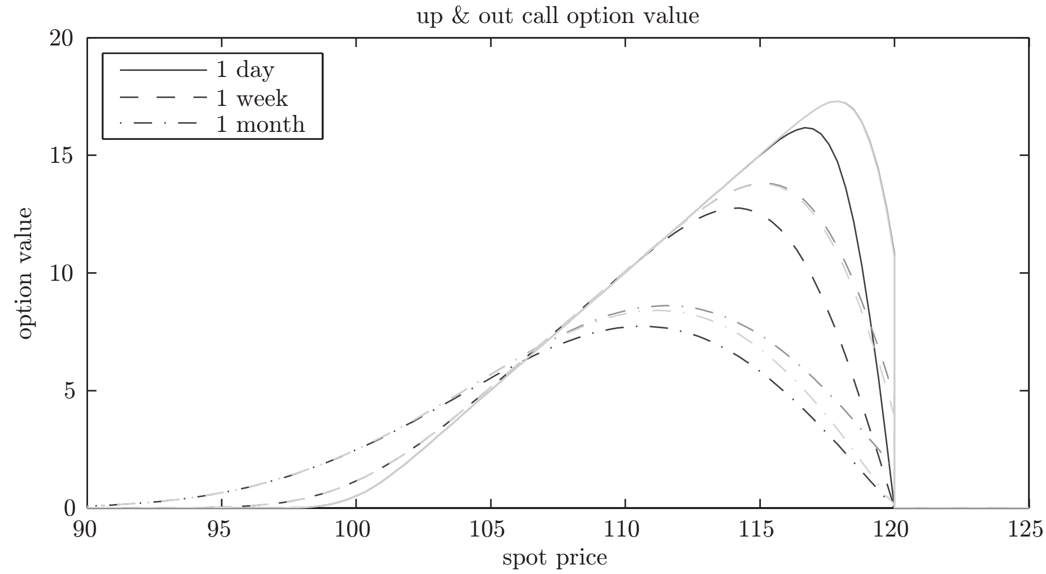

Figure III.8: Price of an up & out call option as a function of the spot price and for different times-to-maturity. See Figure III.7 for details.

Figures III.7 and III.8 compare the delta profile and the prices of an up & out call option with no barrier shift, a parallel barrier shift and an exponential barrier shift over the last month. We observe no significant difference in either graph between the parallel and exponential barrier shifts when the time-to-maturity is one day or one week. In these cases the exponentially bent barrier is already very close to its terminal level. The prices of contracts with one month to maturity, however, clearly differ for high enough spot prices, as the exponentially bent barrier is still equal to the contractual one.

III.3.4 Synthesis: Two-Volatility Bent Barrier Options

In this section, we combine the two-volatility pricing and the exponentially bent barrier risk management approaches. We start by generalizing Definition III.1 to a continuous piecewise exponential function.

Definition III.2 (Piecewise Exponential Boundary).
Let $0 < T_B < T$ be the bending change time and define $\tau_B = T_B - t$ and $\hat{\tau}_B = T - T_B$. A function $\tilde{B} : \mathbb{R}_+ \to \mathbb{R}_+$ is a continuous piecewise exponential boundary if it can be represented as

$$\tilde{B}(\tau) = \begin{cases} \tilde{B}(0)\mathrm{e}^{\gamma\tau} & \text{if } \tau \in [0, \hat{\tau}_B] \\ \tilde{B}(0)\mathrm{e}^{\gamma\hat{\tau}_B + \kappa\tau_B} & \text{if } \tau > \hat{\tau}_B \end{cases}$$

with initial value $\tilde{B}(0) \in \mathbb{R}_+$ and shape parameters $\gamma, \kappa \in \mathbb{R}$. The corresponding barrier level as a function of the calendar time is then given by $B(t) = \tilde{B}(T-t)$. $\triangle$

Note that the bent barrier risk management approach discussed in Section III.3.3 yields a piecewise exponential boundary with $\kappa = 0$. As in Section III.2, we again consider two perfectly correlated assets $S^{(1)}$ and $S^{(2)}$ and start by defining the first hitting time ν of the asset $S^{(2)}$ to the piecewise exponential boundary $\tilde{B}(\tau)$ as

$$\nu = \inf\left\{t \geq 0 : \psi S_t^{(2)} \leq \psi \tilde{B}(T-t)\right\}.$$

The terminal option payoff is then given by

$$V_T = \left(\phi S_T^{(1)} - \phi K\right)^+ 1\{\nu \geq T\}.$$

Next, we establish the analog to Lemma III.1 for piecewise exponential boundaries.

Lemma III.3 (Link between Two-Volatility Bent Barrier and Piecewise Exponential Barrier Options).
Define a new random time $\hat{\nu}$ by

$$\hat{\nu} = \inf\left\{t \geq 0, \psi S_t^{(1)} \leq \psi \tilde{B}^*(T-t)\right\},$$

where $\tilde{B}^* : [0, T^*] \to \mathbb{R}_+$ is a piecewise exponential boundary given by

$$\tilde{B}^*(\tau) = \begin{cases} \tilde{B}^*(0)\mathrm{e}^{\gamma^*\tau} & \text{if } \tau \in [0, \hat{\tau}_B] \\ \tilde{B}^*(0)\mathrm{e}^{\gamma^*\hat{\tau}_B + \kappa^*\tau_B} & \text{if } \tau > \hat{\tau}_B \end{cases},$$

with

$$\begin{aligned} \tilde{B}^*(0) &= S_0 \left(\frac{\tilde{B}(0)}{S_0}\right)^{\sigma_1/\sigma_2} \mathrm{e}^{-\xi^* T}, \\ \gamma^* &= \frac{\sigma_1 \gamma}{\sigma_2} + \xi^*, \\ \kappa^* &= \frac{\sigma_1 \kappa}{\sigma_2} + \xi^*, \\ \xi^* &= r\left(\frac{\sigma_1}{\sigma_2} - 1\right) + \delta_1 - \frac{\sigma_1 \delta_2}{\sigma_2} + \frac{1}{2}\sigma_1(\sigma_1 - \sigma_2). \end{aligned}$$

Then

$$\nu = \hat{\nu} \qquad \mathbb{P}^*\text{-a.s.}.$$

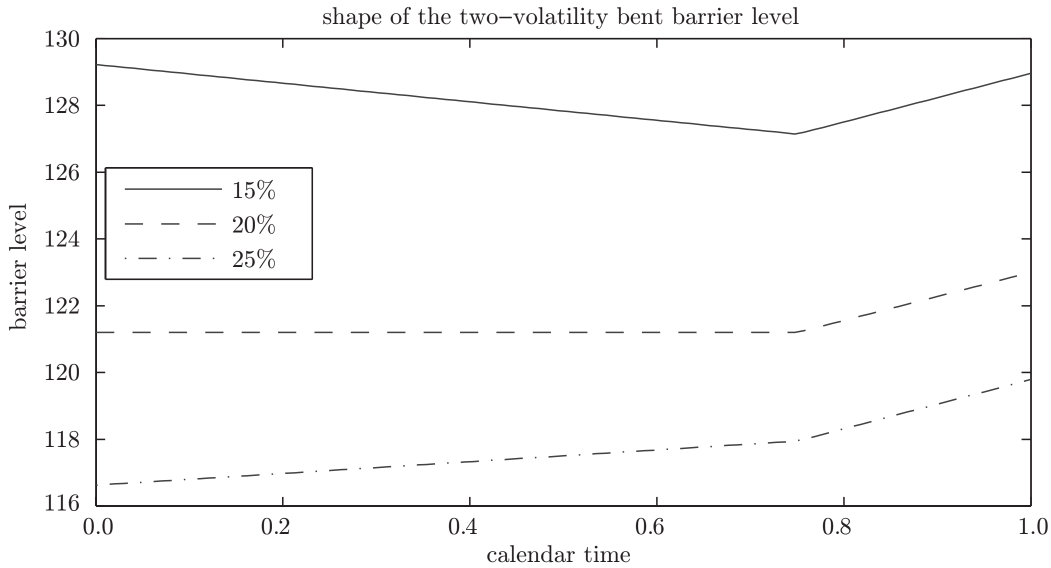

Figure III.9: Sample shapes of the two-volatility bent barrier level for a one-year up & out call option as a function of the calendar time and for different barrier volatilities. The barrier bending is performed over the last three months from $b_1 = 1.00\%$ to $b_2 = 2.50\%$. The spot price is $S_0 = 100.00$ USD and all remaining fixed contract and market parameters are as in Figure III.2.

Proof The proof is nearly fully analogous to that of Lemma III.1 and is thus omitted. □

Consequently, the problem of pricing a two-volatility bent barrier option can be reduced to that of pricing a standard one-volatility barrier option with a piecewise exponential barrier.

Figure III.9 depicts the time-dependent shapes of the barrier level corresponding to the two-volatility bent barrier valuation approach for different barrier volatilities. The barrier is first shifted up in parallel by 1.00% and a bending to the terminal barrier shift of 2.00% is performed over the last three months before expiration. When the barrier volatility is below (above) the strike volatility and no barrier shifts are employed, then the initial barrier level used for pricing is above (below) the official barrier and it is downward (upward) sloping over time. The bending start date can be easily recognized through the kink point in the barrier levels.

III.3.5 Relation to Leverage Constraints

An alternative stream of the literature approaches the dynamic risk-management problem of derivatives with discontinuous payoff by explicitly imposing upper and/or lower bounds for the number of underlying assets held in the replication portfolio at any point in time. Based on earlier work by, among others, Cvitanić and Karatzas (1993), El Karoui and Quenez (1995) and Broadie et al. (1998), Schmock et al. (2001, 2002) analyze the problem of finding the lowest initial capital that permits a super-replication of weakly path-dependent contingent claims with discontinuous payoffs under leverage constraints. In particular, the authors consider the valuation of an up-and-out barrier option when short-selling possibilities are limited. They show that the corresponding dual problem becomes one of singular stochastic control and obtain closed-form solutions for the so-called upper hedging price.

We now briefly discuss the relation of the exponentially bent barrier approach in this chapter to the leverage constraint replication portfolio considered by Schmock et al. (2001, 2002). Both aim at alleviating the dynamic replication problem associated with reverse barrier options and construct a super-replicating portfolio that has the same terminal payoff. They implicitly or explicitly constrain the maximum absolute position held in the underlying asset at any point in time. The trading strategy proposed in this chapter furthermore explicitly accounts for the risk of closing out the delta hedge position at a price beyond the barrier. A windfall profit is realized if it can be unwound at a price better than the then-current shifted barrier level. In contrast to this, the value of the leverage constraint replication portfolio constructed by Schmock et al. (2001, 2002) matches that of the barrier option on the contractual boundary. Their upper hedging price thus does not contain any provisions for potential discontinuities.

As discussed previously, any choice for the parameters of the exponentially bent barrier implies a maximum absolute number of underlying assets held at any point in time. Conversely, and as already suggested by Schmock et al. (2001, 2002), there might exist an equivalent formulation of the leverage constraint valuation problem in terms of a time-dependent shifted barrier function. It is a topic of future research to further investigate the link between these two approaches.

III.4 Method of Images

The method of images for the heat transfer equation provides a simple solution to many initial boundary value problems. Analogously to the reflection principle for the paths of Brownian motions, it exploits symmetry relationships in the Kolmogorov forward equation satisfied by the transition PDF. The central idea is to extend a problem defined on a semi-infinite domain into a related problem on an infinite domain. The latter can then be solved though standard techniques by a convolution of its initial condition with the corresponding Green's function. The infinite domain problem is constructed such as to satisfy the same initial condition on the original domain and for its solution to match the prescribed value on the boundary. It can be further decomposed into two infinite domain auxiliary problems, the first of which has the same initial condition as the original problem on the corresponding semi-infinite domain and zero outside it. The second has a non-zero initial condition on the opposite semi-infinite domain, which is chosen such that the sum of their solutions takes the desired value on the boundary.

The method of images often significantly simplifies the solution of boundary value problems that are hard to handle through probabilistic methods. This is particularly true when dealing with high-dimensional problems such as the multiple barrier windows in this chapter. Wilmott et al. (1995), Buchen (2001b) and Konstandatos (2003) provide an introduction in the context of standard barrier options. Buchen (2001b), Konstandatos (2003) and Buchen and Konstandatos (2005, 2009) apply the method of images to the pricing of various exotic (double) barrier and lookback options. In Chapter 9 of Konstandatos (2003), pp. 187–205, the author further generalizes it to two dimensional asset dynamics.

This section explicitly establishes the link between the image operator for exponentially bent barriers and a change of variables for the Black and Scholes (1973) PDE. It further provides an alternative probabilistic derivation.

III.4.1 Zero Temperature Boundary Value Problem

We start by giving a fundamental motivating example for the method of images; see also the discussion in Chapter 12.2 of Wilmott et al. (1995), pp. 207–209. Consider the problem of finding the temperature distribution on a semi-infinite rod, where a zero temperature boundary is imposed on its left end, that is

$$\begin{aligned}\mathcal{H}\{u\}(x,\tau) &= 0 \qquad \text{for } (x,\tau)\in(b,\infty)\times(0,\infty),\\ u(x,0) &= \hat{f}(x),\\ u(b,\tau) &= 0 \qquad \text{for } \tau\in[0,\infty).\end{aligned}$$

Here, $b \in \mathbb{R}$ is the coordinate of its left end and $\mathcal{H}$ is the one-dimensional heat operator defined by

$$\mathcal{H}\{u\} = -\frac{\partial u}{\partial \tau} + \frac{\partial^2 u}{\partial x^2}.$$

We remark that $\mathcal{H}$ is a second-order differential operator. This formulation of the problem is slightly uncommon, as we would normally impose the boundary to lie at zero. However, when applying the method of images to price barrier options within the Black and Scholes (1973) framework, a coordinate transformation will yield an equivalent initial boundary value problem for the heat equation with a boundary that, in general, does not lie at the origin. We define the corresponding full-range problem $u_b(x,\tau)$ on an infinite rod by removing the boundary condition and multiplying the initial condition by the indicator for the spatial domain of the original problem $u(x,\tau)$, that is

$$\begin{aligned}\mathcal{H}\left\{u_b\right\}(x,\tau) &= 0 \qquad \text{for } (x,\tau)\in\mathbb{R}\times(0,\infty),\\ u_b(x,0) &= \hat{f}(x)1\{x>b\}.\end{aligned}$$

The corresponding image problem $\overset{*}{u}_b\,(x,\tau)$ is obtained by reflecting the initial condition of the full-range problem about the axis passing through the barrier. It satisfies

$$\begin{aligned}\mathcal{H}\{\,\overset{*}{u}_b\,\}(x,\tau) &= 0 \qquad \text{for } (x,\tau)\in\mathbb{R}\times(0,\infty),\\ \overset{*}{u}_b\,(x,0) &= \hat{f}(2b-x)1\{x<b\}.\end{aligned}$$

It then follows from the symmetry property of the heat transfer equation that, on the boundary, the solutions for the full-range problem and its image coincide at all times. Consequently, their difference satisfies the zero temperature boundary condition of the original problem

$$u_b(b,\tau) - \overset{*}{u}_b\,(b,\tau) = u(b,\tau) = 0 \qquad \text{for } \tau\in[0,\infty).$$

In general, if the initial temperature distribution of an infinite rod is an odd function with respect to some point $b \in \mathbb{R}_+$, then the positive and negative temperatures will exactly

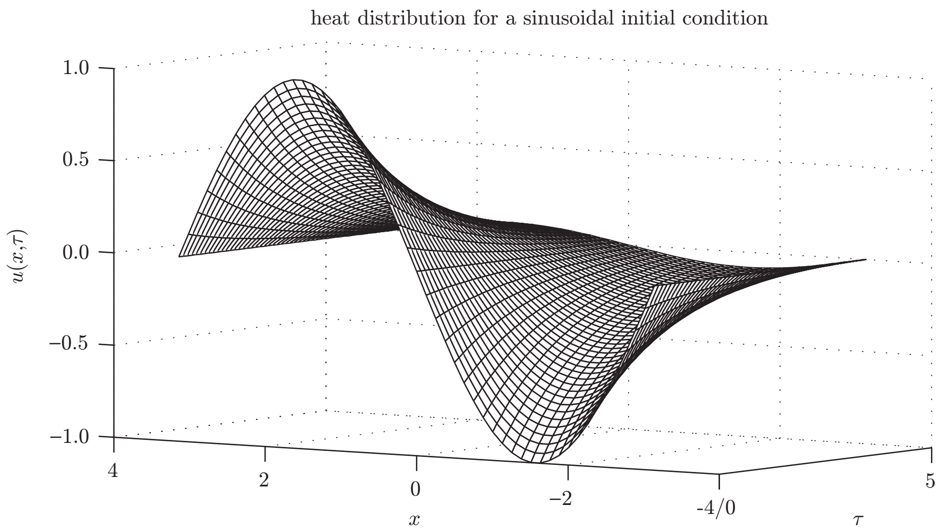

Figure III.10: Evolution of the heat distribution in an infinite rod when the initial condition is given by a sinusoidal function. At the spatial points given by multiples of pi, the temperature is zero at all times.

offset each other in this point at all times. Furthermore, by construction, the difference also satisfies the same initial condition on the semi-infinite rod. By the linearity of the differential operator, it has the same dynamics on the domain of the original problem

$$\mathcal{H}\{u_b - \overset{*}{u}_b\}(x,\tau) = \mathcal{H}\{u\}(x,\tau) = 0 \qquad \text{for } (x,\tau) \in (b,\infty)\times(0,\infty).$$

Consequently, the two solutions coincide on this domain as well

$$u(x,\tau) = u_b(x,\tau) - \overset{*}{u}_b(x,\tau) \qquad \text{for } (x,\tau) \in (b,\infty)\times(0,\infty).$$

Example III.1 (Boundary Value Problem with Sinusoidal Initial Condition). As an example, consider the following problem

$$\begin{aligned} \mathcal{H}\{u\}(x,\tau) &= 0 \qquad \text{for } (x,\tau) \in (0,\infty)\times(0,\infty), \\ u(x,0) &= \sin(x), \\ u(0,\tau) &= 0 \qquad \text{for } \tau \in [0,\infty). \end{aligned}$$

Since the sine is an odd function with respect to the origin, it follows by the method of images that dropping the boundary condition yields the correct solution for $u(x,\tau)$ on the original domain. See Figure III.10 for an illustration that shows the heat distribution in an infinite rod when the initial condition is a sinusoidal function. At all times, the positive and negative temperatures exactly offset each other at all multiples of pi and at zero in particular.

III.4.2 Three Transformations of the Black and Scholes (1973) PDE

This section discuses how a carefully chosen coordinate transformation reduces the Black and Scholes (1973) PDE to the one-dimensional heat transfer equation such that the exponential barrier becomes a constant boundary under the new coordinates. We emphasize that obtaining a constant boundary in the transformed space is necessary for the method of images to be applicable. Note, that, in general, there is no single unique change of variables such that the new function satisfies the heat equation. We will first review the two transformations commonly encountered in the literature and discuss their properties. It then turns out that we need a mixture of these two approaches in order for the transformed barrier to become a constant.

We start by giving two central definitions.

Definition III.3 (Black and Scholes (1973) Forward Operator).
The one-dimensional Black and Scholes (1973) forward operator $\mathcal{L}$ is defined as

$$\mathcal{L}\{\tilde{V}\} = -\frac{\partial \tilde{V}}{\partial \tau} + (r-\delta)S\frac{\partial \tilde{V}}{\partial S} + \frac{1}{2}\sigma^2 S^2 \frac{\partial^2 \tilde{V}}{\partial S^2} - r\tilde{V}. \qquad \triangle$$

Definition III.4 (Black and Scholes (1973) Initial Exponential Boundary Value Problem).
Let $\tilde{B}(\tau)$ be an exponential boundary. The function $\tilde{V}(S,\tau)$ satisfies an initial exponential boundary value problem (IEBVP) if

$$\begin{aligned} \mathcal{L}\big\{\tilde{V}\big\}(S,\tau) &= 0 \qquad \text{for } (S,\tau) \in \mathcal{D}, \\ \tilde{V}(S,0) &= f(S), \\ \tilde{V}\big(\tilde{B}(\tau),\tau\big) &= 0 \qquad \text{for } \tau \in [0,\infty), \end{aligned}$$

where the active domain $\mathcal{D} \subseteq \mathbb{R}^2_+$ is given by

$$\mathcal{D} = \big\{(S,\tau) : \psi S > \psi \tilde{B}(\tau),\, \tau \in (0,\infty)\big\}$$

and $\psi \in \{-1, +1\}$ indicates an upper or lower boundary. $\triangle$

Now let $\tilde{V}(S, \tau)$ be the value of a knock-out barrier option on the spot asset with current price $S \in \mathbb{R}_+$, time-to-maturity $\tau \in \mathbb{R}_+$ and time-dependent exponential barrier $\tilde{B}(\tau) = \tilde{B}(0)\mathrm{e}^{\gamma\tau}$. Then $\tilde{V}(S, \tau)$ satisfies a Black and Scholes (1973) IEBVP with initial condition $f(S) = (\phi S - \phi K)^+$ in the case of a vanilla payoff. Note that in defining the valuation problem, we already implicitly reversed time by setting $\tau = T - t$ and made the change of variables $V(S, t) = \tilde{V}(S, \tau)$ thus transforming the terminal condition into an initial condition.

The first candidate transformation of the Black and Scholes (1973) PDE considered here is the most straight forward one and can often be found in the literature on the pricing of non-path-dependent contingent claims.

Lemma III.4 (Heat Equation I).
Let $\tilde{V}(S, \tau)$ satisfy a Black and Scholes (1973) IEBVP. Define

$$
\begin{aligned}
x &= \ln(S) + \xi\tau, \\
\xi &= r - \delta - \frac{1}{2}\sigma^2, \\
V(S, \tau) &= \mathrm{e}^{-r\tau} u(x, \tau).
\end{aligned}
$$

Then the function $u(x, \tau)$ satisfies the following initial boundary value problem

$$
\begin{aligned}
\mathcal{H}\{u\}(x, \tau) &= 0 \qquad \text{for } (x, \tau) \in \hat{\mathcal{D}}, \\
u(x, 0) &= \hat{f}(x), \\
u\left(b(\tau), \tau\right) &= 0 \qquad \text{for } \tau \in [0, \infty),
\end{aligned}
$$

where

$$
\begin{aligned}
\hat{f}(x) &= f\left(\mathrm{e}^x\right), \\
b(\tau) &= \ln\left(\tilde{B}(\tau)\right) + \xi\tau, \\
\hat{\mathcal{D}} &= \left\{(x, \tau) : \psi x > \psi b(\tau), \tau \in (0, \infty)\right\}.
\end{aligned}
$$

Proof By the chain rule, we obtain

$$\begin{aligned}
\frac{\partial \tilde{V}}{\partial \tau} &= \mathrm{e}^{-r\tau}\left(-ru + \xi\frac{\partial u}{\partial x} + \frac{\partial u}{\partial \tau}\right), \\
\frac{\partial \tilde{V}}{\partial S} &= = \mathrm{e}^{-r\tau}\frac{1}{S}\frac{\partial u}{\partial x}, \\
\frac{\partial^2 V}{\partial S^2} &= \mathrm{e}^{-r\tau}\frac{1}{S^2}\left(\frac{\partial^2 u}{\partial x^2} - \frac{\partial u}{\partial x}\right).
\end{aligned}$$

Substituting back into the forward Black and Scholes (1973) PDE yields

$$0 = -\frac{\partial u}{\partial \tau} + \left(r - q - \frac{1}{2}\sigma^2 - \xi\right)\frac{\partial u}{\partial x} + \frac{1}{2}\sigma^2\frac{\partial u}{\partial x^2}.$$

The parameter ξ as given in Lemma III.4 is determined such that the convection term vanishes. $\square$

Note that an exponential boundary $\tilde{B}(\tau) = \tilde{B}(0)\mathrm{e}^{\gamma\tau}$ in the original coordinates is transformed into a time-dependent linear boundary $b(\tau) = \ln\left(\tilde{B}(0)\right) + (\xi + \gamma)\tau$. Furthermore, the parameter ξ is determined from the objective of eliminating the convection term and can thus not be freely chosen. Consequently, the method of images cannot be directly applied to this valuation problem except for in the unlikely special case when $\gamma = -\xi$. However, non-path-dependent European style option with various terminal payoffs can be easily priced through a convolution of the heat kernel with the corresponding initial condition.

Another approach to transform the Black and Scholes (1973) PDE into the heat equation seems more common in the literature and has some advantages, as discussed later; see for example Chapter 5.4 in Wilmott et al. (1995), pp. 76–81.

Lemma III.5 (Heat Equation II).
Let $\tilde{V}(S, \tau)$ satisfy a Black and Scholes (1973) IEBVP. Define

$$\begin{aligned}
x &= \ln(S), \\
\alpha &= \frac{1}{2} - \frac{r - \delta}{\sigma^2}, \\
\beta &= -\frac{\left(2(r-\delta) + \sigma^2\right)^2}{8\sigma^2}, \\
\tilde{V}(S, \tau) &= \mathrm{e}^{\alpha x + \beta\tau} u(x, \tau).
\end{aligned}$$

Then the function $u(x,\tau)$ satisfies the following initial boundary value problem

$$\begin{aligned}
\mathcal{H}\{u\}(x,\tau) &= 0 \qquad \textit{for } (x,\tau) \in \hat{\mathcal{D}}, \\
u(x,0) &= \hat{f}(x), \\
u\left(b(\tau),\tau\right) &= 0 \qquad \textit{for } \tau \in [0,\infty),
\end{aligned}$$

where

$$\begin{aligned}
\hat{f}(x) &= \mathrm{e}^{-\alpha x} f\left(\mathrm{e}^{x}\right), \\
b(\tau) &= \ln\left(\tilde{B}(\tau)\right), \\
\hat{\mathcal{D}} &= \left\{(x,\tau) : \psi x > \psi b(\tau), \tau \in (0,\infty)\right\}.
\end{aligned}$$

Proof By the chain rule, we obtain

$$\begin{aligned}
\frac{\partial \tilde{V}}{\partial \tau} &= \mathrm{e}^{\alpha x + \beta \tau}\left(\beta u + \frac{\partial u}{\partial \tau}\right), \\
\frac{\partial \tilde{V}}{\partial S} &= \mathrm{e}^{\alpha x + \beta \tau}\frac{1}{S}\left(\alpha u + \frac{\partial u}{\partial x}\right), \\
\frac{\partial^2 \tilde{V}}{\partial S^2} &= \mathrm{e}^{\alpha x + \beta \tau}\frac{1}{S^2}\left(\alpha(\alpha-1)u + (2\alpha-1)\frac{\partial u}{\partial x} + \frac{\partial^2 u}{\partial x^2}\right).
\end{aligned}$$

Substituting back into the Black and Scholes (1973) PDE yields

$$\begin{aligned}
0 &= -\frac{\partial u}{\partial \tau} + \left(r - \delta + \sigma^2\left(\alpha - \frac{1}{2}\right)\right)\frac{\partial u}{\partial x} + \frac{1}{2}\sigma^2\frac{\partial^2 u}{\partial x^2} \\
&\quad -\left(\beta - \alpha\left(r - \delta + \frac{1}{2}\sigma^2(\alpha-1)\right) + r\right)u.
\end{aligned}$$

The parameters α and β as given in Lemma III.5 are determined such that both the reaction and convection terms vanish. □

This approach is the method of choice for standard barrier options since a constant boundary $\tilde{B}(\tau) = \tilde{B}(0)$ in the original coordinates stays constant under the transformation at $b(\tau) = \ln\left(\tilde{B}(0)\right)$. However, an exponential boundary is again transformed into a time-dependent linear function.

Finally, we consider a mixture of the first two approaches which encompasses the second one as a special case. The idea is to be able to freely choose the parameter ξ (in particular to set $\xi = -\gamma$) and then determine the values for the parameters α and β such that the convection and reaction terms cancel out.

Lemma III.6 (Heat Equation III).
Let $\tilde{V}(S,\tau)$ satisfy a Black and Scholes (1973) IEBVP. Define

$$\begin{aligned}
x &= \ln(S) + \xi\tau, \\
\alpha &= \frac{1}{2} - \frac{r-\delta-\xi}{\sigma^2}, \\
\beta &= -\frac{\left(2(r-q-\xi)+\sigma^2\right)^2}{8\sigma^2}, \\
\tilde{V}(S,\tau) &= \mathrm{e}^{\alpha x+\beta\tau} u(x,\tau).
\end{aligned}$$

Then the function $u(x,\tau)$ satisfies the following initial boundary value problem

$$\mathcal{H}\{u\}(x,\tau) = 0 \qquad \text{for } (x,\tau) \in \hat{\mathcal{D}}, \tag{III.1a}$$

$$u(x,0) = \hat{f}(x), \tag{III.1b}$$

$$u\left(b(\tau),\tau\right) = 0 \qquad \text{for } \tau \in [0,\infty), \tag{III.1c}$$

where

$$\begin{aligned}
\hat{f}(x) &= \mathrm{e}^{-\alpha x} f\left(\mathrm{e}^{x}\right), \\
b(\tau) &= \ln\left(\tilde{B}(\tau)\right) + \xi\tau, \\
\hat{\mathcal{D}} &= \left\{(x,\tau) : \psi x > \psi b(\tau), \tau \in (0,\infty)\right\}.
\end{aligned}$$

Proof By the chain rule, we obtain,

$$\begin{aligned}
\frac{\partial \tilde{V}}{\partial t} &= \mathrm{e}^{\alpha x+\beta\tau}\left((\beta+\alpha\xi)u + \xi\frac{\partial u}{\partial x} + \frac{\partial u}{\partial \tau}\right), \\
\frac{\partial \tilde{V}}{\partial S} &= \mathrm{e}^{\alpha x+\beta\tau}\frac{1}{S}\left(\alpha u + \frac{\partial u}{\partial x}\right), \\
\frac{\partial^2 \tilde{V}}{\partial S^2} &= \mathrm{e}^{\alpha x+\beta\tau}\frac{1}{S^2}\left(\alpha(\alpha-1)u + (2\alpha-1)\frac{\partial u}{\partial x} + \frac{\partial^2 u}{\partial x^2}\right).
\end{aligned}$$

Substituting back into the Black and Scholes (1973) PDE yields

$$\begin{aligned} 0 &= -\frac{\partial u}{\partial \tau} + \left(r - \delta + \sigma^2\left(\alpha - \frac{1}{2}\right) - \xi\right)\frac{\partial u}{\partial x} + \frac{1}{2}\sigma^2\frac{\partial^2 u}{\partial x^2} \\ &\quad - \left(\beta - \alpha\left(r - \delta + \frac{1}{2}\sigma^2(\alpha - 1) - \xi\right) + r\right)u. \end{aligned}$$

Given the value of the parameter ξ, the parameters α and β as given in Lemma III.6 are determined such that both the reaction and convection terms vanish. □

III.4.3 Image Operator

The following definition is a generalization of Theorem 1 in Buchen (2001b), p. 128, to dividend paying assets and exponential barriers; see also Section 2 in Buchen and Konstandatos (2009), pp. 502–503.

Definition III.5 (Image Operator).
Let $\tilde{V}(S,\tau)$ be a solution to the Black and Scholes (1973) PDE. The image of $\tilde{V}(S,\tau)$ relative to the exponential barrier $\tilde{B}(\tau) = \tilde{B}(0)\mathrm{e}^{\gamma\tau}$ is given by

$$\overset{\tilde{B}(0),\gamma,\tau}{\mathcal{I}}\left\{\tilde{V}(S,\tau)\right\} = \left(\frac{S}{\tilde{B}(0)\mathrm{e}^{\gamma\tau}}\right)^{2\alpha}\tilde{V}\left(\frac{\tilde{B}^2(0)\mathrm{e}^{2\gamma\tau}}{S},\tau\right),$$

where

$$\alpha = \frac{1}{2} - \frac{r - \delta + \gamma}{\sigma^2}. \qquad \triangle$$

Note that the dependence of the image operator on the parameters defining the exponential barrier and time-to-maturity is made explicit through superscript notation. While this may seem unnecessary at first, it will be essential when dealing with more complex contingent claims where the barrier is either a continuous piecewise exponential function or only partially active or both.

While this definition seems *ad-hoc* at first, it immediately follows from applying the method of images to the heat transfer equation and then reversing the coordinate transformation, as the proof to Proposition III.1 shows.

Proposition III.1 (Method of Images for the Black and Scholes (1973) PDE). *Let $\tilde{V}(S,\tau)$ satisfy a Black and Scholes (1973) IEBVP. Let $\tilde{V}_{\tilde{B}(0),\gamma}(S,\tau)$ be the solution to the corresponding full-range problem*

$$\begin{aligned}\mathcal{L}\{\tilde{V}_{\tilde{B}(0),\gamma}\}(S,\tau) &= 0 \qquad \text{for } (S,\tau) \in \mathbb{R}^2_+,\\ \tilde{V}_{\tilde{B}(0),\gamma}(S,0) &= f(x)1\{\psi S > \psi \tilde{B}(0)\}.\end{aligned}$$

Then $\tilde{V}(S,\tau)$ is given by

$$\tilde{V}(S,\tau) = \tilde{V}_{\tilde{B}(0),\gamma}(S,\tau) - \overset{\tilde{B}(0),\gamma,\tau}{\mathcal{I}}\{\tilde{V}_{\tilde{B}(0),\gamma}(S,\tau)\}.$$

Proof As shown in Section III.4.2, applying the change of variables proposed in Lemma III.6 and setting $\xi = -\gamma$ yields a constant boundary in the transformed coordinates at $b = \ln\big(\tilde{B}(0)\big)$. Consequently, the method of images can be applied. It follows from the results in Section III.4.1 that the initial boundary value problem in Equation (III.1) satisfies

$$u(x,\tau) = u_b(x,\tau) - u_b(2b - x,\tau),$$

where

$$\begin{aligned}\mathcal{H}\{u_b\}(x,\tau) &= 0 \qquad \text{for } (x,\tau) \in \mathbb{R} \times (0,\infty),\\ u_b(x,0) &= \hat{f}(x)1\{\psi x > \psi b\}\end{aligned}$$

is the related full-range problem for the heat transfer equation. Let $\tilde{V}_{\tilde{B}(0),\gamma}(S,\tau)$ be the corresponding full-range problem for the Black and Scholes (1973) PDE as defined in Proposition III.1. The image solution for the Black and Scholes (1973) PDE is then given by

$$\begin{aligned}\overset{\tilde{B}(0),\gamma,\tau}{\mathcal{I}}\{\tilde{V}_{\tilde{B}(0),\gamma}(S,\tau)\} &= \mathrm{e}^{\alpha x + \beta\tau} u(2b - x,\tau)\\ &= \mathrm{e}^{2\alpha(x-b)}\mathrm{e}^{\alpha(2b-x)+\beta\tau} u(2b - x,\tau)\\ &= \left(\frac{S}{\tilde{B}(0)\mathrm{e}^{\gamma\tau}}\right)^{2\alpha} \tilde{V}_{\tilde{B}(0),\gamma}\left(\frac{\tilde{B}^2(0)\mathrm{e}^{2\gamma\tau}}{S},\tau\right)\end{aligned}$$

and Proposition III.1 follows. □

Proposition III.2 provides the most important properties of the image operator.

Proposition III.2 (General Properties of the Image Operator).
Let $\tilde{V}(S,\tau)$ and $\tilde{U}(S,\tau)$ be solutions to the Black and Scholes (1973) PDE. The image operator in Definition III.5 has the following properties.

(i) $\mathcal{I}$ is an involution, that is

$$\overset{\tilde{B}(0),\gamma,\tau}{\mathcal{I}} \left\{ \overset{\tilde{B}(0),\gamma,\tau}{\mathcal{I}} \left\{\tilde{V}(S,\tau)\right\}\right\} = \tilde{V}(S,\tau).$$

(ii) $\mathcal{I}$ is a linear operator, that is for constants $a, b \in \mathbb{R}$

$$\overset{\tilde{B}(0),\gamma,\tau}{\mathcal{I}} \left\{a\tilde{U}(S,\tau) + b\tilde{V}(S,\tau)\right\} = a \overset{\tilde{B}(0),\gamma,\tau}{\mathcal{I}} \left\{\tilde{U}(S,\tau)\right\} + b \overset{\tilde{B}(0),\gamma,\tau}{\mathcal{I}} \left\{\tilde{V}(S,\tau)\right\}.$$

(iii) If

$$\mathcal{L}\left\{\tilde{V}(S,\tau)\right\} = 0 \qquad \textit{for } (S,\tau) \in \mathcal{D}$$

on some domain

$$\mathcal{D} = \left\{(S,\tau) : \psi S > \psi \tilde{B}(0)\mathrm{e}^{\gamma\tau},\ \tau \in (0,\infty)\right\}$$

then

$$\mathcal{L}\left\{ \overset{\tilde{B}(0),\gamma,\tau}{\mathcal{I}} \left\{\tilde{V}(S,\tau)\right\}\right\} = 0 \qquad \textit{for } (S,\tau) \in \mathbb{R}_+^2 \backslash \mathcal{D}.$$

(iv) The values of the original function and the image agree on the boundary

$$\tilde{V}\big(\tilde{B}(\tau),\tau\big) = \overset{\tilde{B}(0),\gamma,\tau}{\mathcal{I}} \left\{\tilde{V}\big(\tilde{B}(\tau),\tau\big)\right\}.$$

Proof For brevity, only the main ideas of the proofs are given here. All details can be found in Appendix III.B.1. Properties (i) and (ii) immediately follow from a (repeated) application of Definition III.5. In order to prove Property (iii), we explicitly compute the partial derivatives of the image of $\tilde{V}(S,\tau)$ and then show that it satisfies the Black and

Scholes (1973) PDE. To see that Property (iv) holds, we apply the change of variables in Lemma III.6 setting $\xi = -\gamma$ so that we obtain a constant boundary problem for the heat transfer equation. By the symmetry property, the solution to any initial value problem and its reflection agree on the boundary. Reversing the change of variables yields the result in the original coordinates and for the exponential boundary. $\square$

It is important to note that Property (i) in Proposition III.2 only holds if the two image operators are with respect to the same exponential barrier, that is they have the same parameters $\tilde{B}(0)$, γ and τ.

For the dynamic hedging and risk management of contingent claims, the availability of closed form solutions for its sensitivities is of utmost importance. The following three Lemmata provide the major greeks for images of valuation functions. These results all follow from a careful differentiation and the proofs are omitted for brevity.

Lemma III.7 (Delta and Gamma of the Image of a Valuation Function).
Let $\tilde{V}(S,\tau)$ be some valuation function. Then the first- and second-order asset price sensitivities of the image of $\tilde{V}(S,\tau)$ are given by

$$\begin{aligned} &\frac{\partial}{\partial S} \overset{\tilde{B}(0),\gamma,\tau}{\mathcal{I}} \{\tilde{V}(S,\tau)\} \\ =& \left(\frac{S}{\tilde{B}(0)\mathrm{e}^{\gamma\tau}}\right)^{2\alpha} \left(\frac{2\alpha}{S}\tilde{V}\left(\frac{\tilde{B}^2(0)\mathrm{e}^{2\gamma\tau}}{S},\tau\right) - \frac{\tilde{B}^2(0)\mathrm{e}^{2\gamma\tau}}{S^2}\frac{\partial\tilde{V}}{\partial S}\left(\frac{\tilde{B}^2(0)\mathrm{e}^{2\gamma\tau}}{S},\tau\right)\right) \end{aligned}$$

and

$$\begin{aligned} &\frac{\partial^2}{\partial S^2} \overset{\tilde{B}(0),\gamma,\tau}{\mathcal{I}} \{\tilde{V}(S,\tau)\} \\ =& \left(\frac{S}{\tilde{B}(0)\mathrm{e}^{\gamma\tau}}\right)^{2\alpha} \left(\frac{2\alpha(2\alpha-1)}{S^2}\tilde{V}\left(\frac{\tilde{B}^2(0)\mathrm{e}^{2\gamma\tau}}{S},\tau\right)\right. \\ &\left.+\frac{2(1-2\alpha)\tilde{B}^2(0)\mathrm{e}^{2\gamma\tau}}{S^3}\frac{\partial\tilde{V}}{\partial S}\left(\frac{\tilde{B}^2(0)\mathrm{e}^{2\gamma\tau}}{S},\tau\right) + \frac{\tilde{B}^4(0)\mathrm{e}^{4\gamma\tau}}{S^4}\frac{\partial^2\tilde{V}}{\partial S^2}\left(\frac{\tilde{B}^2(0)\mathrm{e}^{2\gamma\tau}}{S},\tau\right)\right). \end{aligned}$$

Lemma III.8 (Theta of the Image of a Valuation Function).
Let $\tilde{V}(S,\tau)$ be some valuation function. Then the first-order time-to-maturity sensitivity

of the image of $\tilde{V}(S,\tau)$ is given by

$$
\begin{aligned}
&\frac{\partial}{\partial \tau} \overset{\tilde{B}(0),\gamma,\tau}{\mathcal{I}} \left\{\tilde{V}(S,\tau)\right\} \\
= \; & \left(\frac{S}{\tilde{B}(0)\mathrm{e}^{\gamma\tau}}\right)^{2\alpha} \left(-2\alpha\gamma\tilde{V}\left(\frac{\tilde{B}^2(0)\mathrm{e}^{2\gamma\tau}}{S},\tau\right) + 2\gamma\frac{\tilde{B}^2(0)\mathrm{e}^{2\gamma\tau}}{S}\frac{\partial\tilde{V}}{\partial S}\left(\frac{\tilde{B}^2(0)\mathrm{e}^{2\gamma\tau}}{S},\tau\right)\right. \\
& \left. +\frac{\partial\tilde{V}}{\partial\tau}\left(\frac{\tilde{B}^2(0)\mathrm{e}^{2\gamma\tau}}{S},\tau\right)\right),
\end{aligned}
$$

Lemma III.9 (Vega of the Image of a Valuation Function).
Let $\tilde{V}(S,\tau)$ be some valuation function. Then the first-order volatility sensitivity of the image of $\tilde{V}(S,\tau)$ is given by

$$
\begin{aligned}
&\frac{\partial}{\partial \sigma} \overset{\tilde{B}(0),\gamma,\tau}{\mathcal{I}} \left\{\tilde{V}(S,\tau)\right\} \\
= \; & \left(\frac{S}{\tilde{B}(0)\mathrm{e}^{\gamma\tau}}\right)^{2\alpha} \left(\frac{2(1-2\alpha)}{\sigma}\ln\left(\frac{S}{\tilde{B}(0)\mathrm{e}^{\gamma\tau}}\right) + \frac{\partial\tilde{V}}{\partial\sigma}\left(\frac{\tilde{B}^2(0)\mathrm{e}^{2\gamma\tau}}{S},\tau\right)\right).
\end{aligned}
$$

III.4.4 Probabilistic Derivation of the Image Operator

This section shows how the image operator for exponential boundaries can alternatively be obtained within a probabilistic setting. The Feynman-Kac formula provides a connection between a Cauchy problem and a corresponding conditional expectation; see for example Theorem V.7.6 in Karatzas and Shreve (1991), p. 366. It is thus not surprising that the method of images for the Black and Scholes (1973) PDE can also be derived by exploiting the symmetry properties of the Brownian motion. However, we are not aware of a reference in the literature that explicitly establishes this link, even for the special case of a flat boundary. This approach requires us to first obtain a closed-form solution for the probability distribution of the terminal spot prices conditional on the barrier not having been breached before. The derivation is thus much more involved compared to the one discussed in Section III.4.3, which simply requires an appropriately chosen coordinate transformation for the Black and Scholes (1973) PDE.

The reflection principle, see for example Section II.6.A in Karatzas and Shreve (1991), pp. 79–81, allows us to solve for the joint PDF of the terminal underlying asset price and the indicator of no prior breach of an exponential barrier. The following Lemma provides the precise result. See also Omberg (1987), who approximates the early exercise boundary for American plain vanilla options through an exponential function.

Lemma III.10 (Joint Density of S_t and $\{\tau > t\}$).
Let $\tilde{B}(\tau)$ be an exponential boundary where $\tau = T - t$ for some time $T \in [0, T^*]$ and let the dynamics of the spot asset $S = \{S_t : t \in [0, T^*]\}$ under the risk-neutral probability measure $\mathbb{P}^*$ and the first hitting time ν of S to the barrier $\tilde{B}(\tau)$ be as in Lemma III.2. Then the unconditional joint PDF is given by

$$\mathbb{P}^* \{S_t \in \mathrm{d}x, \nu > t\} = \frac{1}{x\sigma\sqrt{t}} \left(\mathcal{N}' \left(\frac{\alpha(x) - \lambda t}{\sqrt{t}} \right) - \mathrm{e}^{2\lambda\beta} \mathcal{N}' \left(\frac{2\beta - \alpha(x) + \lambda t}{\sqrt{t}} \right) \right) \mathrm{d}x,$$

where

$$\begin{aligned} \alpha(x) &= \frac{1}{\sigma} \left(\ln \left(\frac{x}{S_0} \right) + \gamma t \right), \\ \beta &= \frac{1}{\sigma} \left(\ln \left(\frac{\tilde{B}(0)}{S_0} \right) + \gamma T \right), \\ \lambda &= \frac{1}{\sigma} \left(r - \delta + \gamma - \frac{1}{2}\sigma^2 \right). \end{aligned}$$

Proof The proof can be found in Appendix III.B.2. $\square$

The image operator can now be recovered from the risk-neutral pricing formula.

Proposition III.3 (Probabilistic Method of Images for the Black and Scholes (1973) Model).
Let $V = \{V_t, t \in [0, T]\}$ be the value process of a contingent claim with maturity in $T \in (0, T^*]$ and terminal payoff

$$V_T = f(S_T)\, 1\{\nu > T\},$$

where the dynamics of the spot asset $S = \{S_t : t \in [0, T^*]\}$ and the first hitting time ν to an exponential boundary $\tilde{B}(\tau)$ are as in Lemma III.10. Let $V^{\tilde{B}(0)} = \left\{ V_t^{\tilde{B}(0)} : t \in [0, T] \right\}$ be *the value process of the corresponding full-range problem given by the risk-neutral pricing formula*

$$V_t^{\tilde{B}(0)} = \mathrm{e}^{-r(T-t)} \mathbb{E}_{\mathbb{P}^*} \left[f(S_T) \, 1\{\psi S_T > \psi \tilde{B}(0)\} \middle| \mathfrak{F}_t \right].$$

Then

$$V_t = V_t^{\tilde{B}(0)} + \overset{\tilde{B}(0),\gamma,T-t}{\mathcal{I}} \left\{ V_t^{\tilde{B}(0)} \right\},$$

where the image operator $\mathcal{I}$ is as in Definition III.5.

Proof This follows from applying the risk-neutral pricing formula and expressing the expectation as an integral over the terminal payoff multiplied by the joint PDF obtained in Lemma III.10. All details can be found in Appendix III.B.4. □

III.5 Binary and $\mathcal{Q}$ Options

As shown in Buchen (2001b), the method of images yields a solution for the prices of standard barrier options in terms of a linear combination of cash-or-nothing (bond) and asset-or-nothing (asset) binaries and their respective images. As we will show, this continues to hold when the barrier is a continuous and piecewise exponential function of time. Ingersoll (2000) also shows that a wide variety of exotic payoffs can be priced in terms of elementary digital options. Skipper and Buchen (2003) generalize much of the previous literature on digital option pricing by introducing the so called $\mathbb{M}$-binary. These multi-asset and multi-period exotic binary options can be used to price most rainbow options, whose terminal payoff depends on the asset prices at a discrete set of monitoring points. Examples include fixed and floating strike discrete geometric average Asian options and discretely monitored multi-asset barrier and lookback options. Veiga et al. (2012) independently obtain similar results in a slightly more general setting with time-dependent drift and diffusion functions. Both the Skipper and Buchen (2003) $\mathbb{M}$-binaries and the Veiga et al. (2012) generic contracts allow to value the same types of elementary payoff structures.

The basic building blocks for the prices of the barrier options considered in this chapter are higher-order bond and asset binaries. Our notation is very similar to that used by Skipper and Buchen (2003).

Definition III.6 ($\boldsymbol{n}$-th Order Bond and Asset Binaries).
Let $\boldsymbol{s} = (s_1, s_2, \ldots, s_n)'$ be a n-dimensional column vector of indicators with values $s_i \in \{-1, +1\}$, let $\boldsymbol{T} = (T_1, T_2, \ldots, T_n)' \in \mathbb{R}^n_+$ be a n-dimensional column vector of maturity dates such that $T_i < T_j$ for $i < j$ and let $\boldsymbol{\xi} = (\xi_1, \xi_2, \ldots, \xi_n)' \in \mathbb{R}^n_+$ be a n-dimensional column vector of strike prices. The n-th order bond binary $\mathcal{B}^{\boldsymbol{s}}_{\boldsymbol{\xi}}$ and asset binary $\mathcal{A}^{\boldsymbol{s}}_{\boldsymbol{\xi}}$ have the time T_n payoff

$$
\begin{aligned}
\mathcal{B}^{\boldsymbol{s}}_{\boldsymbol{\xi}}(\boldsymbol{S_T}, T_n) &= 1_n \{\operatorname{diag}(\boldsymbol{s})\boldsymbol{S_T} > \operatorname{diag}(\boldsymbol{s})\boldsymbol{\xi}\}, \\
\mathcal{A}^{\boldsymbol{s}}_{\boldsymbol{\xi}}(\boldsymbol{S_T}, T_n) &= S_{T_n} 1_n \{\operatorname{diag}(\boldsymbol{s})\boldsymbol{S_T} > \operatorname{diag}(\boldsymbol{s})\boldsymbol{\xi}\}.
\end{aligned}
$$

Here, $\boldsymbol{S_T} = (S_{T_2}, S_{T_2}, \ldots, S_{T_n})' \in \mathbb{R}^n$ is the n-dimensional column vector of spot prices at the maturity dates and $\operatorname{diag}(\boldsymbol{s})$ is the $n \times n$ diagonal matrix created from the vector $\boldsymbol{s}$. The n-dimensional indicator function 1_n is defined element-wise as

$$
1_n \{\boldsymbol{x} > \boldsymbol{a}\} = \prod_{i=1}^{n} 1 \{x_i > a_i\}. \qquad \triangle
$$

Thus, an n-th order bond (asset) binary has a payoff of one unit of cash (one asset) at the terminal maturity date T_n, if and only if $s_i S_{T_i} > s_i \xi_i$ for all $i \in \{1, 2, \ldots, n\}$. Again, each $s_i \in \{-1, +1\}$ serves as an indicator for a less-than or greater-than inequality, respectively. Higher-order binary options can also be regarded as compound options. A second-order binary, for example, is a binary option to receive a first-order binary at time T_1 given that $s_1 S_{T_1} > s_1 \xi_1$. In general, for $n > 1$ we have at the first maturity date

$$
\begin{aligned}
\mathcal{B}^{s_1 s_2 \ldots s_n}_{\xi_1 \xi_2 \cdots \xi_n}(S, T_1) &= \mathcal{B}^{s_2 s_3 \ldots s_n}_{\xi_2 \xi_3 \cdots \xi_n}(S, T_1)\, 1 \{s_1 S > s_1 \xi_1\} \\
\mathcal{A}^{s_1 s_2 \ldots s_n}_{\xi_1 \xi_2 \cdots \xi_n}(S, T_1) &= \mathcal{A}^{s_2 s_3 \ldots s_n}_{\xi_2 \xi_3 \cdots \xi_n}(S, T_1)\, 1 \{s_1 S > s_1 \xi_1\}.
\end{aligned}
$$

Proposition III.4 (Valuation of $\boldsymbol{n}$-th Order Bond and Asset Binaries).
The time $0 \le t \le T_1$ values of the n-th order bond and asset binaries are given by

$$
\begin{aligned}
\mathcal{B}^{\boldsymbol{s}}_{\boldsymbol{\xi}}(S, t) &= \mathrm{e}^{-r\tau_n} \mathcal{N}_n(\operatorname{diag}(\boldsymbol{s})\boldsymbol{d}_-; \boldsymbol{C}), \\
\mathcal{A}^{\boldsymbol{s}}_{\boldsymbol{\xi}}(S, t) &= S\mathrm{e}^{-\delta\tau_n} \mathcal{N}_n(\operatorname{diag}(\boldsymbol{s})\boldsymbol{d}_+; \boldsymbol{C}),
\end{aligned}
$$

where $\mathcal{N}_n(\boldsymbol{x}; \boldsymbol{C})$ is the n-variate standard normal cumulative distribution function evaluated at point $\boldsymbol{x}$ and with correlation matrix $\boldsymbol{C}$. The n-dimensional column vectors $\boldsymbol{d}_{\pm} = (d_{\pm,1}, d_{\pm,2}, \ldots, d_{\pm,n})' \in \mathbb{R}^n$ are defined by

$$d_{\pm,i} = \frac{\ln(S/\xi_i) + \left(r - \delta \pm \frac{1}{2}\sigma^2\right)\tau_i}{\sigma\sqrt{\tau_i}},$$

where $\tau_i = T_i - t$ is the i-th time-to-maturity and $\boldsymbol{C} \in \mathbb{R}^n \times \mathbb{R}^n$ is a symmetric positive definite correlation matrix given by

$$\boldsymbol{C}_{i,j} = \begin{cases} 1 & \text{if } i = j \\ s_i s_j \sqrt{\tau_i/\tau_j} & \text{if } i < j \\ s_i s_j \sqrt{\tau_j/\tau_i} & \text{otherwise} \end{cases}.$$

Proof This result is a special case of the generalized $\mathbb{M}$ binary valuation equation given in Theorem 1 in Skipper and Buchen (2003), pp. 10–11, when there is only a single underlying asset. Section 5.2.(b) of their paper, p. 15, gives an example. □

Following Buchen (2004), we define higher-order $\mathcal{Q}$ options (pronounced /kjuː/) to have a payoff equal to that of a European plain vanilla call option with strike price ξ_n at the terminal maturity date T_n conditional on $s_i S_{T_i} > s_i \xi_i$ for all $i \in \{1, 2, \ldots, n\}$; see also the related working paper Buchen (2001a) for the origin of this notation. The concept of a $\mathcal{Q}$ option is thus a natural extension of standard European plain vanilla options to higher orders. Introducing these contracts is not necessary to solve the valuation problem in this chapter since a $\mathcal{Q}$ option corresponds to a special linear combination of higher order asset and bond binary options. However, it often simplifies the notation by reducing the number of terms involved.

Definition III.7 (n-th Order $\mathcal{Q}$ Options).
Let $\boldsymbol{s}$, $\boldsymbol{\xi}$ and $\boldsymbol{T}$ be as in Definition III.6. The n-th order $\mathcal{Q}$ option has the time T_n payoff

$$\mathcal{Q}^{\boldsymbol{s}}_{\boldsymbol{\xi}}(\boldsymbol{S_T}, T_n) = \mathcal{A}^{\boldsymbol{s}}_{\boldsymbol{\xi}}(\boldsymbol{S_T}, T_n) - \xi_n \mathcal{B}^{\boldsymbol{s}}_{\boldsymbol{\xi}}(\boldsymbol{S_T}, T_n). \qquad \triangle$$

By Definition III.7, the value of a standard European plain vanilla call option with strike price K is $\mathcal{Q}_K^+(S,\tau)$ while that of the otherwise identical put option is $-\mathcal{Q}_K^-(S,\tau)$.

Corollary III.2 (Valuation of n-th Order $\mathcal{Q}$ Options).
The time $0 \le t \le T_1$ value of the n-th order $\mathcal{Q}$ option is given by

$$\mathcal{Q}_{\boldsymbol{\xi}}^{\boldsymbol{s}}(S,t) = S\mathrm{e}^{-\delta\tau_n}\mathcal{N}_n\left(\mathrm{diag}(\boldsymbol{s})\boldsymbol{d}_+;\boldsymbol{C}\right) - \xi_n\mathrm{e}^{-r\tau_n}\mathcal{N}_n\left(\mathrm{diag}(\boldsymbol{s})\boldsymbol{d}_-;\boldsymbol{C}\right).$$

Proof This immediately follows from Definition III.7 and Proposition III.4 as well as the linearity of the pricing rule. □

In order to hedge against the random changes in the underlying asset price, we need to be able to compute the first partial derivative of the contingent claim prices with respect to it. Propositions III.5 and III.6 provide the necessary results for binary options. These represent novel contributions.

Proposition III.5 (Delta of n-th Order Bond and Asset Binaries).
Let $\boldsymbol{\alpha}_\pm = \mathrm{diag}(\boldsymbol{s})\boldsymbol{d}_\pm$. Let, $\boldsymbol{\rho}_i$ be the i-th column of the matrix $\boldsymbol{C}$ then

$$\begin{aligned}
\hat{\boldsymbol{V}}_i &= \boldsymbol{C}^{-i} - \boldsymbol{\rho}_i^{-i}\left(\boldsymbol{\rho}_i^{-i}\right)', \\
\hat{\boldsymbol{D}}_i^2 &= \mathrm{diag}\big(\hat{\boldsymbol{V}}_i\big), \\
\hat{\boldsymbol{\alpha}}_{\pm,i} &= \big(\hat{\boldsymbol{D}}_i\big)^{-1}\left(\boldsymbol{\alpha}_\pm^{-i} - \boldsymbol{\rho}_i^{-i}\alpha_{\pm,i}\right), \\
\hat{\boldsymbol{C}}_i &= \big(\hat{\boldsymbol{D}}_i\big)^{-1}\hat{\boldsymbol{V}}_i\big(\hat{\boldsymbol{D}}_i\big)^{-1},
\end{aligned}$$

where we use the notation $\boldsymbol{x}^{-i}$ ($\boldsymbol{X}^{-i}$) to indicate that the i-th element (the i-th row and column) is removed from the vector $\boldsymbol{x}$ (the matrix $\boldsymbol{X}$). The time $0 \le t \le T_1$ first-order asset price sensitivities of the n-th order bond and asset binaries are given by

$$\begin{aligned}
\frac{\partial \mathcal{B}_{\boldsymbol{\xi}}^{\boldsymbol{s}}}{\partial S}(S,t) &= \mathrm{e}^{-r\tau_n}\frac{1}{S}\sum_{i=1}^{n}\frac{s_i}{\sigma\sqrt{\tau_i}}\mathcal{N}'\left(\alpha_{-,i}\right)\mathcal{N}_{n-1}\big(\hat{\boldsymbol{\alpha}}_{-,i};\hat{\boldsymbol{C}}_i\big), \\
\frac{\partial \mathcal{A}_{\boldsymbol{\xi}}^{\boldsymbol{s}}}{\partial S}(S,t) &= \mathrm{e}^{-\delta\tau_n}\left(\mathcal{N}_n\left(\boldsymbol{\alpha}_+;\boldsymbol{C}\right) + \sum_{i=1}^{n}\frac{s_i}{\sigma\sqrt{\tau_i}}\mathcal{N}'\left(\alpha_{+,i}\right)\mathcal{N}_{n-1}\big(\hat{\boldsymbol{\alpha}}_{+,i};\hat{\boldsymbol{C}}_i\big)\right).
\end{aligned}$$

Here, $\mathcal{N}'(x)$ is the univariate standard normal PDF and we define $\mathcal{N}_0(\cdot;\cdot) := 1$.

Proof For brevity, we only outline the derivation of the delta for n-th order bond binaries. The result for the higher-order asset binaries follows analogously. First, we express the n-variate standard normal cumulative distribution function as an integral.

$$\frac{\partial \mathcal{B}_{\boldsymbol{\xi}}^{\boldsymbol{s}}}{\partial S}(S,t) = \mathrm{e}^{-r\tau_n} \frac{\partial}{\partial S} \int_{-\infty}^{\boldsymbol{\alpha}_-} \mathcal{N}_n'(\boldsymbol{x};\boldsymbol{C})\mathrm{d}\boldsymbol{x}.$$

Each of the n upper limits of integration $\alpha_{-,i}$ is a function of S. Thus, by a repeated application of the Leibniz rule we get

$$\frac{\partial \mathcal{B}_{\boldsymbol{\xi}}^{\boldsymbol{s}}}{\partial S}(S,t) = \mathrm{e}^{-r\tau_n} \sum_{i=1}^{n} \frac{\partial \alpha_{-,i}}{\partial S} \mathcal{N}'\left(\alpha_{-,i}\right) \int_{-\infty}^{\boldsymbol{\alpha}_-^{-i}} \mathcal{N}_{n-1}'\big(\boldsymbol{x}^{-i};\hat{\boldsymbol{\mu}}_i,\hat{\boldsymbol{V}}_i\big)\mathrm{d}\boldsymbol{x}^{-i}.$$

We use that conditional on $x_i = \alpha_{-,i}$, the vector $\boldsymbol{x}^{-i}$ has a multivariate normal distribution with mean vector $\hat{\boldsymbol{\mu}}_i = \boldsymbol{\rho}_i^{-i}\alpha_{-,i}$ and covariance matrix $\hat{\boldsymbol{V}}_i$ as given in Proposition III.5; see for example Theorem B.7 in Greene (2008), p. 1013. Consequently, $\big(\hat{\boldsymbol{D}}_i\big)^{-1}\left(\boldsymbol{x}^{-i} - \hat{\boldsymbol{\mu}}_i\right)$ has a multivariate standard normal distribution with correlation matrix $\hat{\boldsymbol{C}}_i$ as given in Proposition III.5. The result follows when substituting for the partial derivatives of $\alpha_{-,i}$ using that

$$\frac{\partial \alpha_{\pm,i}}{\partial S} = \frac{s_i}{S\sigma\sqrt{\tau}_i}.$$

□

Proposition III.6 (Vega of n-th Order Bond and Asset Binaries).
The time $0 \le t \le T_1$ first-order volatility sensitivities of the n-th order bond and asset binaries are given by

$$\begin{aligned}
\frac{\partial \mathcal{B}_{\boldsymbol{\xi}}^{\boldsymbol{s}}}{\partial \sigma}(S,t) &= -\mathrm{e}^{-r\tau_n} \sum_{i=1}^{n} \frac{s_i d_{+,i}}{\sigma} \mathcal{N}'\left(\alpha_{-,i}\right) \mathcal{N}_{n-1}\big(\hat{\boldsymbol{\alpha}}_{-,i};\hat{\boldsymbol{C}}_i\big), \\
\frac{\partial \mathcal{A}_{\boldsymbol{\xi}}^{\boldsymbol{s}}}{\partial \sigma}(S,t) &= -\mathrm{e}^{-\delta\tau_n} S \sum_{i=1}^{n} \frac{s_i d_{-,i}}{\sigma} \mathcal{N}'\left(\alpha_{+,i}\right) \mathcal{N}_{n-1}\big(\hat{\boldsymbol{\alpha}}_{+,i};\hat{\boldsymbol{C}}_i\big).
\end{aligned}$$

Proof The proof is fully analogous to that of Proposition III.5 and thus omitted. We use that

$$\frac{\partial \alpha_{\pm,i}}{\partial \sigma} = -\frac{\alpha_{\mp,i}}{\sigma}.$$

□

III.6 Barrier Option Pricing

In this section, we discuss the pricing of knock-out barrier options. Our final objective is to obtain a valuation function for deferred start barrier options, where the barrier, once active, follows a continuous and piecewise exponential function. As shown in Section III.3.4, although this functional form of the barrier might sound arbitrary at first, it arises from a valuation and risk management perspective when dealing with standard deferred start barrier options like the ones embedded in bonus certificates pro. As intermediate results, we obtain the valuation formulas for standard exponential barriers, deferred start exponential barriers and continuous piecewise exponential barriers.

Throughout this section, we assume that the barrier option does not pay any rebate upon knock-out. The separate valuation of only the rebate as an American binary option with its payout either at maturity or at the first hitting time is postponed until Sections III.7 and III.8. Appendix III.E contains an overview of the main results of this and the following two sections for easier reference.

The following lemma establishes that a separation of the valuation problem is indeed possible; Rich (1994) provides a less formal argument.

Lemma III.11 (Valuation of Barrier Options with Rebates).
The valuation function of a knock-out barrier option that pays a rebate when the barrier is breached before maturity is given by the sum of the valuation functions of the terminal payoff and the rebate alone.

Proof Let $0 < T \leq T^*$ be the maturity date and ν be the first hitting time of the barrier during a monitoring period. Let X be a $\mathfrak{F}_T$-measureable random variable, $Y = \{Y_t : t \in [0,T]\}$ be an $\mathbb{F}$-adapted process and $f : \mathbb{R} \to \mathbb{R}$ and $g : [0,T] \times \mathbb{R} \to \mathbb{R}$ be the payoff and rebate functions respectively. By the risk-neutral pricing formula, the value process $V = \{V_t : t \in [0,T]\}$ is then given by

$$V_t = \mathbb{E}_{\mathbb{P}^*}\left[\mathrm{e}^{-r(T-t)} f(X) 1\{\nu > T\} + \mathrm{e}^{-r(\nu-t)} g\left(\nu, Y_\nu\right) 1\{\nu \leq T\} \middle| \mathfrak{F}_t\right]$$

for all $t \in [0, \nu \wedge T]$. The separability follows immediately from the linearity of the expectation operator. $\square$

Note that by defining X to be $\mathfrak{F}_T$-measureable and Y to be $\mathbb{F}$-adapted, the Lemma holds for general payoff and rebate functions. In this chapter, we only consider the case where

X is $\sigma(S_T)$-measurable (that is a function of the terminal stock price) and Y is a constant such that the rebate is a function of the first hitting time alone.

III.6.1 Exponential Barrier Options

In this section, we compute valuation formulas for knock-out barrier options where the barrier is continuously monitored and given by an exponential function of the time-to-maturity $\tilde{B}(\tau) = \tilde{B}(0)e^{\gamma\tau}$ as in Definition III.1. Let ν be the first hitting time of the asset S to the barrier $\tilde{B}(\tau)$ defined as

$$\nu = \inf\left\{t \geq 0 : \psi S_t \leq \psi\tilde{B}(T-t)\right\}.$$

The terminal option payoff is then given by

$$V_T = (\phi S_T - \phi K)^+ \, 1\{\nu > T\}.$$

The option value $\tilde{V}(S,\tau)$ satisfies a Black and Scholes (1973) IEBVP with a plain vanilla initial condition, that is

$$\begin{aligned}
\mathcal{L}\big\{\tilde{V}\big\}(S,\tau) &= 0 \qquad \text{for } (S,\tau) \in \mathcal{D}, \\
\tilde{V}(S,0) &= (\phi S - \phi K)^+, \\
\tilde{V}\big(\tilde{B}(\tau),\tau\big) &= 0 \qquad \text{for } \tau \in [0,\infty),
\end{aligned}$$

where

$$\mathcal{D} = \big\{(S,\tau) : \psi S > \psi\tilde{B}(\tau),\, \tau \in (0,\infty)\big\}.$$

The corresponding full-range problem is given by

$$\begin{aligned}
\mathcal{L}\big\{\tilde{V}_{\tilde{B}(0),\gamma}\big\}(S,\tau) &= 0 \qquad \text{for } (S,\tau) \in \mathbb{R}^2_+, \\
\tilde{V}_{\tilde{B}(0),\gamma}(S,0) &= (\phi S - \phi K)^+ 1\big\{\psi S > \psi\tilde{B}(0)\big\}.
\end{aligned}$$

In what follows, we will always provide all intermediate steps in the solution for the down & out put price which corresponds to $\phi = -1$ and $\psi = +1$. For brevity, we only state the final results for the three other knock-out barrier option types as they follow along the same steps. Alternatively, we can apply a parity result obtained by Buchen (2001b), which expresses the value of all knock-out barrier options in terms of the valuation functions for plain vanilla options and the full-range problem for the corresponding down & out option as well as their respective images. The initial condition of the full-range problem can be decomposed as

$$\begin{aligned}\tilde{V}_{\tilde{B}(0),\gamma}(S,0) &= (K-S)1\{S<K\}1\{S>\tilde{B}(0)\}\\ &= \begin{cases}(K-S)\big(1\{S<K\}-1\{S<\tilde{B}(0)\}\big) & \text{if } K>\tilde{B}(0)\\ \\ 0 & \text{if } K<\tilde{B}(0)\end{cases}.\end{aligned}$$

We thus obtain the following valuation function for the full-range problem

$$\tilde{V}_{\tilde{B}(0),\gamma}(S,\tau) = \begin{cases}-\mathcal{Q}_K^-(S,\tau)-K\mathcal{B}_{\tilde{B}(0)}^-(S,\tau)+\mathcal{A}_{\tilde{B}(0)}^-(S,\tau) & \text{if } K>\tilde{B}(0)\\ \\ 0 & \text{if } K<\tilde{B}(0)\end{cases}.$$

It follows by the method of images that the value of the down & out put is

$$\tilde{V}_{\text{p,do}}(S,\tau) = \begin{cases}-\mathcal{Q}_K^-(S,\tau)-K\mathcal{B}_{\tilde{B}(0)}^-(S,\tau)+\mathcal{A}_{\tilde{B}(0)}^-(S,\tau)\\ +\overset{\tilde{B}(0),\gamma,\tau}{\mathcal{I}}\left\{\mathcal{Q}_K^-(S,\tau)\right\}+K\overset{\tilde{B}(0),\gamma,\tau}{\mathcal{I}}\left\{\mathcal{B}_{\tilde{B}(0)}^-(S,\tau)\right\}\\ -\overset{\tilde{B}(0),\gamma,\tau}{\mathcal{I}}\left\{\mathcal{A}_{\tilde{B}(0)}^-(S,\tau)\right\} & \text{if } K>\tilde{B}(0)\\ \\ 0 & \text{if } K<\tilde{B}(0)\end{cases}.$$

The values of the other three knock-out barrier options are given by

$$\tilde{V}_{\text{p,uo}}(S,\tau) = \begin{cases}K\mathcal{B}_{\tilde{B}(0)}^-(S,\tau)-\mathcal{A}_{\tilde{B}(0)}^-(S,\tau)\\ -K\overset{\tilde{B}(0),\gamma,\tau}{\mathcal{I}}\left\{\mathcal{B}_{\tilde{B}(0)}^-(S,\tau)\right\}+\overset{\tilde{B}(0),\gamma,\tau}{\mathcal{I}}\left\{\mathcal{A}_{\tilde{B}(0)}^-(S,\tau)\right\} & \text{if } K>\tilde{B}(0)\\ \\ -\mathcal{Q}_K^-(S,\tau)+\overset{\tilde{B}(0),\gamma,\tau}{\mathcal{I}}\left\{\mathcal{Q}_K^-(S,\tau)\right\} & \text{if } K<\tilde{B}(0)\end{cases},$$

$$\tilde{V}_{\text{c,do}}(S,\tau) = \begin{cases}\mathcal{Q}_K^+(S,\tau)-\overset{\tilde{B}(0),\gamma,\tau}{\mathcal{I}}\left\{\mathcal{Q}_K^+(S,\tau)\right\} & \text{if } K>\tilde{B}(0)\\ \\ \mathcal{A}_{\tilde{B}(0)}^+(S,\tau)-K\mathcal{B}_{\tilde{B}(0)}^+(S,\tau)\\ -\overset{\tilde{B}(0),\gamma,\tau}{\mathcal{I}}\left\{\mathcal{A}_{\tilde{B}(0)}^+(S,\tau)\right\}+K\overset{\tilde{B}(0),\gamma,\tau}{\mathcal{I}}\left\{\mathcal{B}_{\tilde{B}(0)}^+(S,\tau)\right\} & \text{if } K<\tilde{B}(0)\end{cases},$$

and

$$
\tilde{V}_{\mathrm{c,uo}}(S,\tau)=\begin{cases}0 & \text{if } K>\tilde{B}(0)\\[2ex] \mathcal{Q}_K^{+}(S,\tau)-\mathcal{A}_{\tilde{B}(0)}^{+}(S,\tau)+K\mathcal{B}_{\tilde{B}(0)}^{+}(S,\tau) & \\ -\overset{\tilde{B}(0),\gamma,\tau}{\mathcal{I}}\left\{\mathcal{Q}_K^{+}(S,\tau)\right\}+\overset{\tilde{B}(0),\gamma,\tau}{\mathcal{I}}\left\{\mathcal{A}_{\tilde{B}(0)}^{+}(S,\tau)\right\} & \\ -K\overset{\tilde{B}(0),\gamma,\tau}{\mathcal{I}}\left\{\mathcal{B}_{\tilde{B}(0)}^{+}(S,\tau)\right\} & \text{if } K<\tilde{B}(0)\end{cases}.
$$

III.6.2 Deferred Start Exponential Barrier Options

In this section, we analyze partial time knock-out barrier options with an exponential barrier. For these contracts, the period in which the barrier can be triggered by the underlying asset price is a subset of the lifetime of the option. We only consider the case of deferred start barrier options, where the barrier is not monitored initially but only after some date $0<T_S<T$.

The barrier again follows the exponential function $\tilde{B}(\tau)=\tilde{B}(0)\mathrm{e}^{\gamma\tau}$. Let ν be the first hitting time of the asset S to the barrier $\tilde{B}(\tau)$ after the monitoring start date defined as

$$
\nu=\inf\left\{t\geq T_S:\psi S_t\leq\psi\tilde{B}(T-t)\right\},
$$

The terminal option payoff is then given by

$$
V_T=(\phi S_T-\phi K)^{+}\,1\{\nu>T\}.
$$

During the monitoring period when $t\in[T_S,T]$, the value of the deferred start barrier option is just equal to that of the standard barrier option from Section III.6.1. Before the barrier start date, it can be regarded as a binary option to receive a standard barrier option at time T_S conditional on $\psi S_{T_S}>\psi\tilde{B}(\hat{\tau}_S)$, where $\hat{\tau}_S=T-T_S$ is the time-to-maturity at the barrier start date. The option value $\tilde{V}^{\mathrm{ds}}(S,\tau)$ of the deferred start barrier option outside the monitoring period then satisfies

$$
\begin{aligned}
\mathcal{L}\{\tilde{V}^{\mathrm{ds}}\}(S,\tau) &= 0 \qquad \text{for } (S,\tau)\in\mathbb{R}^{+}\times(\hat{\tau}_S,\infty),\\
\tilde{V}^{\mathrm{ds}}(S,\hat{\tau}_S) &= \tilde{V}(S,\hat{\tau}_S)\,1\{\psi S>\psi\tilde{B}(\hat{\tau}_S)\}.
\end{aligned}
$$

Using the result from Section III.6.1, we can express the value of the deferred start down & out put at the barrier start date as

$$\tilde{V}^{\mathrm{ds}}_{\mathrm{p,do}}\left(S,\hat{\tau}_S\right)=\begin{cases}\Big(-\mathcal{Q}^{-}_{K}\left(S,\hat{\tau}_S\right)-K\mathcal{B}^{-}_{\tilde{B}(0)}\left(S,\hat{\tau}_S\right)+\mathcal{A}^{-}_{\tilde{B}(0)}\left(S,\hat{\tau}_S\right) & \\ +\overset{\tilde{B}(0),\gamma,\hat{\tau}_S}{\mathcal{I}}\left\{\mathcal{Q}^{-}_{K}\left(S,\hat{\tau}_S\right)\right\}+K\overset{\tilde{B}(0),\gamma,\hat{\tau}_S}{\mathcal{I}}\Big\{\mathcal{B}^{-}_{\tilde{B}(0)}\left(S,\hat{\tau}_S\right)\Big\} & \\ -\overset{\tilde{B}(0),\gamma,\hat{\tau}_S}{\mathcal{I}}\Big\{\mathcal{A}^{-}_{\tilde{B}(0)}\left(S,\hat{\tau}_S\right)\Big\}\Big)1\big\{S>\tilde{B}\left(\hat{\tau}_S\right)\big\} & \text{if } K>\tilde{B}(0) \\ 0 & \text{if } K<\tilde{B}(0)\end{cases}.$$

Our aim is to express the right-hand side (r.h.s.) in terms of second-order binary and $\mathcal{Q}$ options and their respective images. While it is an immediate consequence of the discussion following Definition III.6 that for example

$$\mathcal{B}^{-}_{\tilde{B}(0)}\left(S,\hat{\tau}_S\right)1\big\{S>\tilde{B}\left(\hat{\tau}_S\right)\big\}=\mathcal{B}^{+-}_{\tilde{B}(\hat{\tau}_S)\tilde{B}(0)}\left(S,0,\hat{\tau}_S\right),$$

it is not obvious if and how the indicator can be pulled inside the image operator. Note that the notation $\mathcal{C}^{s_1s_2}_{\xi_1\xi_2}\left(S,\tau_1,\tau_2\right)$ is used to denote the value of a second order binary option where the time remaining to the first and second maturity dates is given by τ_1 and τ_2, respectively.

Lemma III.12 (Product of the Image of a Binary and an Indicator).
Let $\mathcal{C}^{s_2}_{\xi_2}(S,\tau)$ be the value of a first-order bond or asset binary. Then the following relationship holds

$$\overset{\tilde{B}(0),\gamma,\tau}{\mathcal{I}}\Big\{\mathcal{C}^{s_2}_{\xi_2}(S,\tau)\Big\}1\left\{s_1S>s_1\xi_1\right\}=\overset{\tilde{B}(0),\gamma\tau}{\mathcal{I}}\Big\{\mathcal{C}^{-s_1s_2}_{\hat{\xi}_1\xi_2}(S,0,\tau)\Big\},$$

where

$$\hat{\xi}_1=\frac{\tilde{B}^2(0)\mathrm{e}^{2\gamma\tau}}{\xi_1}.$$

The property continues to hold for higher-order binary options.

Proof By Definition III.5, we have

$$
\begin{aligned}
&\overset{\tilde{B}(0),\gamma,\tau}{\mathcal{I}}\left\{\mathcal{C}^{s_2}_{\xi_2}(S,\tau)\right\}1\left\{s_1S>s_1\xi_1\right\}\\
=\;&\Xi\,\mathcal{C}^{s_2}_{\xi_2}\left(\frac{\tilde{B}^2(0)\mathrm{e}^{2\gamma\tau}}{S},\tau\right)1\left\{s_1S>s_1\xi_1\right\}\\
=\;&\Xi\,\mathcal{C}^{s_2}_{\xi_2}\left(\frac{\tilde{B}^2(0)\mathrm{e}^{2\gamma\tau}}{S},\tau\right)1\left\{s_1\frac{\tilde{B}^2(0)\mathrm{e}^{2\gamma\tau}}{S}<s_1\frac{\tilde{B}^2(0)\mathrm{e}^{2\gamma\tau}}{\xi_1}\right\}\\
=\;&\Xi\,\mathcal{C}^{-s_1s_2}_{\hat{\xi}_1\xi_2}\left(\frac{\tilde{B}^2(0)\mathrm{e}^{2\gamma\tau}}{S},0,\tau\right)\\
=\;&\overset{\tilde{B}(0),\gamma,\tau}{\mathcal{I}}\left\{\mathcal{C}^{-s_1s_2}_{\hat{\xi}_1\xi_2}(S,0,\tau)\right\},
\end{aligned}
$$

with $\hat{\xi}_1$ defined as in Lemma III.12 and

$$
\Xi=\left(\frac{S}{\tilde{B}(0)\mathrm{e}^{\gamma\tau}}\right)^{2\alpha}.
$$

The proof for higher-order binaries is identical. $\square$

Corollary III.3 (Product of the Image of a Binary and an Indicator). *Let $\mathcal{C}^{s_2}_{\xi_2}(S,\tau)$ be the value of a first-order bond or asset binary. Then the following relationship holds*

$$
\overset{\tilde{B}(0),\gamma\tau}{\mathcal{I}}\left\{\mathcal{C}^{s_2}_{\xi_2}(S,\tau)\right\}1\left\{s_1S>s_1\tilde{B}(\tau)\right\}=\overset{\tilde{B}(0),\gamma\tau}{\mathcal{I}}\left\{\mathcal{C}^{-s_1s_2}_{\tilde{B}(\tau)\xi_2}(S,0,\tau)\right\}.
$$

Proof This follows immediately from Lemma III.12. $\square$

Returning to the valuation problem of the deferred start down & out put, we notice that Corollary III.3 applies. Consequently,

$$
\tilde{V}^{\mathrm{ds}}_{\mathrm{p,do}}(S,\hat{\tau}_S)=\begin{cases}
-\mathcal{Q}^{+-}_{\tilde{B}(\hat{\tau}_S)K}(S,0,\hat{\tau}_S)-K\mathcal{B}^{+-}_{\tilde{B}(\hat{\tau}_S)\tilde{B}(0)}(S,0,\hat{\tau}_S) & \\
+\mathcal{A}^{+-}_{\tilde{B}(\hat{\tau}_S)\tilde{B}(0)}(S,0,\hat{\tau}_S)+\overset{\tilde{B}(0),\gamma,\hat{\tau}_S}{\mathcal{I}}\left\{\mathcal{Q}^{--}_{\tilde{B}(\hat{\tau}_S)K}(S,0,\hat{\tau}_S)\right\} & \\
+K\overset{\tilde{B}(0),\gamma,\hat{\tau}_S}{\mathcal{I}}\left\{\mathcal{B}^{--}_{\tilde{B}(\hat{\tau}_S)\tilde{B}(0)}(S,0,\hat{\tau}_S)\right\} & \\
-\overset{\tilde{B}(0),\gamma,\hat{\tau}_S}{\mathcal{I}}\left\{\mathcal{A}^{--}_{\tilde{B}(\hat{\tau}_S)\tilde{B}(0)}(S,0,\hat{\tau}_S)\right\} & \text{if } K>\tilde{B}(0)\\
0 & \text{if } K<\tilde{B}(0)
\end{cases}
$$

and consequently letting $\tau_S = T_S - t$ be the time-to-barrier start, we get for $\tau > \hat{\tau}_S$

$$\tilde{V}^{\mathrm{ds}}_{\mathrm{p,do}}(S,\tau) = \begin{cases} -\mathcal{Q}^{+-}_{\tilde{B}(\hat{\tau}_S)K}(S,\tau_S,\tau) - K\mathcal{B}^{+-}_{\tilde{B}(\hat{\tau}_S)\tilde{B}(0)}(S,\tau_S,\tau) \\ +\mathcal{A}^{+-}_{\tilde{B}(\hat{\tau}_S)\tilde{B}(0)}(S,\tau_S,\tau) + \overset{\tilde{B}(0),\gamma,\tau}{\mathcal{I}}\left\{\mathcal{Q}^{--}_{\tilde{B}(\hat{\tau}_S)K}(S,\tau_S,\tau)\right\} \\ +K\overset{\tilde{B}(0),\gamma,\tau}{\mathcal{I}}\left\{\mathcal{B}^{--}_{\tilde{B}(\hat{\tau}_S)\tilde{B}(0)}(S,\tau_S,\tau)\right\} \\ -\overset{\tilde{B}(0),\gamma,\tau}{\mathcal{I}}\left\{\mathcal{A}^{--}_{\tilde{B}(\hat{\tau}_S)\tilde{B}(0)}(S,\tau_S,\tau)\right\} & \text{if } K > \tilde{B}(0) \\ 0 & \text{if } K < \tilde{B}(0) \end{cases}$$

The values of the other three knock-out barrier options are given by

$$\tilde{V}^{\mathrm{ds}}_{\mathrm{p,uo}}(S,\tau) = \begin{cases} K\mathcal{B}^{--}_{\tilde{B}(\hat{\tau}_S)\tilde{B}(0)}(S,\tau_S,\tau) - \mathcal{A}^{--}_{\tilde{B}(\hat{\tau}_S)\tilde{B}(0)}(S,\tau_S,\tau) \\ -K\overset{\tilde{B}(0),\gamma,\tau}{\mathcal{I}}\left\{\mathcal{B}^{+-}_{\tilde{B}(\hat{\tau}_S)\tilde{B}(0)}(S,\tau_S,\tau)\right\} \\ +\overset{\tilde{B}(0),\gamma,\tau}{\mathcal{I}}\left\{\mathcal{A}^{+-}_{\tilde{B}(\hat{\tau}_S)\tilde{B}(0)}(S,\tau_S,\tau)\right\} & \text{if } K > \tilde{B}(0) \\ -\mathcal{Q}^{--}_{\tilde{B}(\hat{\tau}_S)K}(S,\tau_S,\tau) + \overset{\tilde{B}(0),\gamma,\tau}{\mathcal{I}}\left\{\mathcal{Q}^{+-}_{\tilde{B}(\hat{\tau}_S)K}(S,\tau_S,\tau)\right\} & \text{if } K < \tilde{B}(0) \end{cases},$$

$$\tilde{V}^{\mathrm{ds}}_{\mathrm{c,do}}(S,\tau) = \begin{cases} \mathcal{Q}^{++}_{\tilde{B}(\hat{\tau}_S)K}(S,\tau_S,\tau) - \overset{\tilde{B}(0),\gamma,\tau}{\mathcal{I}}\left\{\mathcal{Q}^{-+}_{\tilde{B}(\hat{\tau}_S)K}(S,\tau_S,\tau)\right\} & \text{if } K > \tilde{B}(0) \\ \mathcal{A}^{++}_{\tilde{B}(\hat{\tau}_S)\tilde{B}(0)}(S,\tau_S,\tau) - K\mathcal{B}^{++}_{\tilde{B}(\hat{\tau}_S)\tilde{B}(0)}(S,\tau_S,\tau) \\ -\overset{\tilde{B}(0),\gamma,\tau}{\mathcal{I}}\left\{\mathcal{A}^{-+}_{\tilde{B}(\hat{\tau}_S)\tilde{B}(0)}(S,\tau_S,\tau)\right\} \\ +K\overset{\tilde{B}(0),\gamma,\tau}{\mathcal{I}}\left\{\mathcal{B}^{-+}_{\tilde{B}(\hat{\tau}_S)\tilde{B}(0)}(S,\tau_S,\tau)\right\} & \text{if } K < \tilde{B}(0) \end{cases},$$

and

$$\tilde{V}^{\mathrm{ds}}_{\mathrm{c,uo}}(S,\tau) = \begin{cases} 0 & \text{if } K > \tilde{B}(0) \\ \mathcal{Q}^{-+}_{\tilde{B}(\hat{\tau}_S)K}(S,\tau_S,\tau) - \mathcal{A}^{-+}_{\tilde{B}(\hat{\tau}_S)\tilde{B}(0)}(S,\tau_S,\tau) \\ +K\mathcal{B}^{-+}_{\tilde{B}(\hat{\tau}_S)\tilde{B}(0)}(S,\tau_S,\tau) - \overset{\tilde{B}(0),\gamma,\tau}{\mathcal{I}}\left\{\mathcal{Q}^{++}_{\tilde{B}(\hat{\tau}_S)K}(S,\tau_S,\tau)\right\} \\ +\overset{\tilde{B}(0),\gamma,\tau}{\mathcal{I}}\left\{\mathcal{A}^{++}_{\tilde{B}(\hat{\tau}_S)\tilde{B}(0)}(S,\tau_S,\tau)\right\} \\ -K\overset{\tilde{B}(0),\gamma,\tau}{\mathcal{I}}\left\{\mathcal{B}^{++}_{\tilde{B}(\hat{\tau}_S)\tilde{B}(0)}(S,\tau_S,\tau)\right\} & \text{if } K < \tilde{B}(0) \end{cases}.$$

III.6.3 Piecewise Exponential Barrier Options

We now consider a knock-out barrier option, where the barrier is continuously monitored and given by a continuous piecewise exponential function as in Definition III.2. In the first period, from the inception to some date $0 < T_B < T$, the barrier bends exponentially at the rate κ. In the second period, the bending rate is given by γ. We recall that the barrier is given by the following function of the time-to-maturity

$$\tilde{B}(\tau) = \begin{cases} \tilde{B}(0)\mathrm{e}^{\gamma\tau} & \text{if } \tau \in [0, \hat{\tau}_B] \\ \tilde{B}(0)\mathrm{e}^{\gamma\hat{\tau}_B + \kappa\tau_B} & \text{if } \tau > \hat{\tau}_B \end{cases},$$

where $\tau_B = T_B - t$ and $\hat{\tau}_B = T - T_B$. The terminal payoff of a piecewise exponential barrier option is the same as the one given in Section III.6.1 but using the piecewise exponential instead of a standard exponential barrier. Similarly to the deferred start option, its value after the bending change date when $t \in [T_B, T]$ is just equal to that of a standard barrier option from Section III.6.1. The option value $\tilde{V}^{\mathrm{pe}}(S, \tau)$ of the piecewise exponential barrier option before the bending change date then satisfies

$$\begin{aligned} \mathcal{L}\{\tilde{V}^{\mathrm{pe}}\}(S,\tau) &= 0 \qquad \text{for } (S,\tau) \in \mathcal{D}, \\ \tilde{V}^{\mathrm{pe}}(S, \hat{\tau}_B) &= \tilde{V}(S, \hat{\tau}_B)\, 1\{\psi S > \psi \tilde{B}(\hat{\tau}_B)\} \\ \tilde{V}^{\mathrm{pe}}\big(\tilde{B}(\tau), \tau\big) &= 0 \qquad \text{for } \tau \in [\hat{\tau}_B, \infty), \end{aligned}$$

where

$$\mathcal{D} = \big\{(S,\tau) : \psi S > \psi \tilde{B}(\tau),\, \tau \in (\hat{\tau}_B, \infty)\big\}.$$

The corresponding full-range problem is given by

$$\begin{aligned} \mathcal{L}\{\tilde{V}_{\tilde{B}(\hat{\tau}_B),\kappa}\}(S,\tau) &= 0 \qquad \text{for } (S,\tau) \in \mathbb{R}_+ \times (\hat{\tau}_B, \infty), \\ \tilde{V}_{\tilde{B}(\hat{\tau}_B),\kappa}(S, \hat{\tau}_B) &= \tilde{V}(S, \hat{\tau}_B)\, 1\{\psi S > \psi \tilde{B}(\hat{\tau}_B)\}. \end{aligned}$$

We observe that the full-range problem satisfies the same equation as the deferred start barrier option in Section III.6.2 when the bending change date takes the place of the barrier start date. It follows by the method of images that the value of the down & out put for $\tau > \hat{\tau}_B$ is

$$\tilde{V}^{\text{pe}}_{\text{p, do}}(S,\tau) = \begin{cases} -\mathcal{Q}^{+-}_{\tilde{B}(\hat{\tau}_B)K}(S,\tau_B,\tau) - K\mathcal{B}^{+-}_{\tilde{B}(\hat{\tau}_B)\tilde{B}(0)}(S,\tau_B,\tau) & \\ +\mathcal{A}^{+-}_{\tilde{B}(\hat{\tau}_B)\tilde{B}(0)}(S,\tau_B,\tau) + \overset{\tilde{B}(0),\gamma,\tau}{\mathcal{I}}\left\{\mathcal{Q}^{--}_{\tilde{B}(\hat{\tau}_B)K}(S,\tau_B,\tau)\right\} & \\ +K\overset{\tilde{B}(0),\gamma,\tau}{\mathcal{I}}\left\{\mathcal{B}^{--}_{\tilde{B}(\hat{\tau}_B)\tilde{B}(0)}(S,\tau_B,\tau)\right\} & \\ -\overset{\tilde{B}(0),\gamma,\tau}{\mathcal{I}}\left\{\mathcal{A}^{--}_{\tilde{B}(\hat{\tau}_B)\tilde{B}(0)}(S,\tau_B,\tau)\right\} & \\ +\overset{\tilde{B}(\hat{\tau}_B),\kappa,\tau_B}{\mathcal{I}}\left\{\mathcal{Q}^{+-}_{\tilde{B}(\hat{\tau}_B)K}(S,\tau_B,\tau)\right\} & \\ +K\overset{\tilde{B}(\hat{\tau}_B),\kappa,\tau_B}{\mathcal{I}}\left\{\mathcal{B}^{+-}_{\tilde{B}(\hat{\tau}_B)\tilde{B}(0)}(S,\tau_B,\tau)\right\} & \\ -\overset{\tilde{B}(\hat{\tau}_B),\kappa,\tau_B}{\mathcal{I}}\left\{\mathcal{A}^{+-}_{\tilde{B}(\hat{\tau}_B)\tilde{B}(0)}(S,\tau_B,\tau)\right\} & \\ -\overset{\tilde{B}(\hat{\tau}_B),\kappa,\tau_B}{\mathcal{I}}\left\{\overset{\tilde{B}(0),\gamma,\tau}{\mathcal{I}}\left\{\mathcal{Q}^{--}_{\tilde{B}(\hat{\tau}_B)K}(S,\tau_B,\tau)\right\}\right\} & \\ -K\overset{\tilde{B}(\hat{\tau}_B),\kappa,\tau_B}{\mathcal{I}}\left\{\overset{\tilde{B}(0),\gamma,\tau}{\mathcal{I}}\left\{\mathcal{B}^{--}_{\tilde{B}(\hat{\tau}_B)\tilde{B}(0)}(S,\tau_B,\tau)\right\}\right\} & \\ +\overset{\tilde{B}(\hat{\tau}_B),\kappa,\tau_B}{\mathcal{I}}\left\{\overset{\tilde{B}(0),\gamma,\tau}{\mathcal{I}}\left\{\mathcal{A}^{--}_{\tilde{B}(\hat{\tau}_B)\tilde{B}(0)}(S,\tau_B,\tau)\right\}\right\} & \text{if } K > \tilde{B}(0) \\ 0 & \text{if } K < \tilde{B}(0) \end{cases}.$$

The values of the other three knock-out barrier options are given by

$$\tilde{V}^{\text{pe}}_{\text{p,uo}}(S,\tau) = \begin{cases} K\mathcal{B}^{--}_{\tilde{B}(\hat{\tau}_B)\tilde{B}(0)}(S,\tau_B,\tau) - \mathcal{A}^{--}_{\tilde{B}(\hat{\tau}_B)\tilde{B}(0)}(S,\tau_B,\tau) & \\ -K\overset{\tilde{B}(0),\gamma,\tau}{\mathcal{I}}\left\{\mathcal{B}^{+-}_{\tilde{B}(\hat{\tau}_B)\tilde{B}(0)}(S,\tau_B,\tau)\right\} & \\ +\overset{\tilde{B}(0),\gamma,\tau}{\mathcal{I}}\left\{\mathcal{A}^{+-}_{\tilde{B}(\hat{\tau}_B)\tilde{B}(0)}(S,\tau_B,\tau)\right\} & \\ -K\overset{\tilde{B}(\hat{\tau}_B),\kappa,\tau_B}{\mathcal{I}}\left\{\mathcal{B}^{--}_{\tilde{B}(\hat{\tau}_B)\tilde{B}(0)}(S,\tau_B,\tau)\right\} & \\ +\overset{\tilde{B}(\hat{\tau}_B),\kappa,\tau_B}{\mathcal{I}}\left\{\mathcal{A}^{--}_{\tilde{B}(\hat{\tau}_B)\tilde{B}(0)}(S,\tau_B,\tau)\right\} & \\ +K\overset{\tilde{B}(\hat{\tau}_B),\kappa,\tau_B}{\mathcal{I}}\left\{\overset{\tilde{B}(0),\gamma,\tau}{\mathcal{I}}\left\{\mathcal{B}^{+-}_{\tilde{B}(\hat{\tau}_B)\tilde{B}(0)}(S,\tau_B,\tau)\right\}\right\} & \\ -\overset{\tilde{B}(\hat{\tau}_B),\kappa,\tau_B}{\mathcal{I}}\left\{\overset{\tilde{B}(0),\gamma,\tau}{\mathcal{I}}\left\{\mathcal{A}^{+-}_{\tilde{B}(\hat{\tau}_B)\tilde{B}(0)}(S,\tau_B,\tau)\right\}\right\} & \text{if } K > \tilde{B}(0) \\ -\mathcal{Q}^{--}_{\tilde{B}(\hat{\tau}_B)K}(S,\tau_B,\tau) + \overset{\tilde{B}(0),\gamma,\tau}{\mathcal{I}}\left\{\mathcal{Q}^{+-}_{\tilde{B}(\hat{\tau}_B)K}(S,\tau_B,\tau)\right\} & \\ +\overset{\tilde{B}(\hat{\tau}_B),\kappa,\tau_B}{\mathcal{I}}\left\{\mathcal{Q}^{--}_{\tilde{B}(\hat{\tau}_B)K}(S,\tau_B,\tau)\right\} & \\ -\overset{\tilde{B}(\hat{\tau}_B),\kappa,\tau_B}{\mathcal{I}}\left\{\overset{\tilde{B}(0),\gamma,\tau}{\mathcal{I}}\left\{\mathcal{Q}^{+-}_{\tilde{B}(\hat{\tau}_B)K}(S,\tau_B,\tau)\right\}\right\} & \text{if } K < \tilde{B}(0) \end{cases},$$

$$
\tilde{V}^{\mathrm{pe}}_{\mathrm{c,do}}(S,\tau) = \begin{cases}
\mathcal{Q}^{++}_{\tilde{B}(\hat{\tau}_B)K}(S,\tau_B,\tau) - \overset{\tilde{B}(0),\gamma,\tau}{\mathcal{I}}\left\{\mathcal{Q}^{-+}_{\tilde{B}(\hat{\tau}_B)K}(S,\tau_B,\tau)\right\} \\
-\overset{\tilde{B}(\hat{\tau}_B),\kappa,\tau_B}{\mathcal{I}}\left\{\mathcal{Q}^{++}_{\tilde{B}(\hat{\tau}_B)K}(S,\tau_B,\tau)\right\} \\
+\overset{\tilde{B}(\hat{\tau}_B),\kappa,\tau_B}{\mathcal{I}}\left\{\overset{\tilde{B}(0),\gamma,\tau}{\mathcal{I}}\left\{\mathcal{Q}^{-+}_{\tilde{B}(\hat{\tau}_B)K}(S,\tau_B,\tau)\right\}\right\} & \text{if } K > \tilde{B}(0) \\
\\
\mathcal{A}^{++}_{\tilde{B}(\hat{\tau}_B)\tilde{B}(0)}(S,\tau_B,\tau) - K\mathcal{B}^{++}_{\tilde{B}(\hat{\tau}_B)\tilde{B}(0)}(S,\tau_B,\tau) \\
-\overset{\tilde{B}(0),\gamma,\tau}{\mathcal{I}}\left\{\mathcal{A}^{-+}_{\tilde{B}(\hat{\tau}_B)\tilde{B}(0)}(S,\tau_B,\tau)\right\} \\
+K\overset{\tilde{B}(0),\gamma,\tau}{\mathcal{I}}\left\{\mathcal{B}^{-+}_{\tilde{B}(\hat{\tau}_B)\tilde{B}(0)}(S,\tau_B,\tau)\right\} \\
-\overset{\tilde{B}(\hat{\tau}_B),\kappa,\tau_B}{\mathcal{I}}\left\{\mathcal{A}^{++}_{\tilde{B}(\hat{\tau}_B)\tilde{B}(0)}(S,\tau_B,\tau)\right\} \\
+K\overset{\tilde{B}(\hat{\tau}_B),\kappa,\tau_B}{\mathcal{I}}\left\{\mathcal{B}^{++}_{\tilde{B}(\hat{\tau}_B)\tilde{B}(0)}(S,\tau_B,\tau)\right\} \\
+\overset{\tilde{B}(\hat{\tau}_B),\kappa,\tau_B}{\mathcal{I}}\left\{\overset{\tilde{B}(0),\gamma,\tau}{\mathcal{I}}\left\{\mathcal{A}^{-+}_{\tilde{B}(\hat{\tau}_B)\tilde{B}(0)}(S,\tau_B,\tau)\right\}\right\} \\
-K\overset{\tilde{B}(\hat{\tau}_B),\kappa,\tau_B}{\mathcal{I}}\left\{\overset{\tilde{B}(0),\gamma,\tau}{\mathcal{I}}\left\{\mathcal{B}^{-+}_{\tilde{B}(\hat{\tau}_B)\tilde{B}(0)}(S,\tau_B,\tau)\right\}\right\} & \text{if } K < \tilde{B}(0)
\end{cases},
$$

and

$$
\tilde{V}^{\mathrm{pe}}_{\mathrm{c,uo}}(S,\tau) = \begin{cases}
0 & \text{if } K > \tilde{B}(0) \\
\\
\mathcal{Q}^{-+}_{\tilde{B}(\hat{\tau}_B)K}(S,\tau_B,\tau) - \mathcal{A}^{-+}_{\tilde{B}(\hat{\tau}_B)\tilde{B}(0)}(S,\tau_B,\tau) \\
+K\mathcal{B}^{-+}_{\tilde{B}(\hat{\tau}_B)\tilde{B}(0)}(S,\tau_B,\tau) - \overset{\tilde{B}(0),\gamma,\tau}{\mathcal{I}}\left\{\mathcal{Q}^{++}_{\tilde{B}(\hat{\tau}_B)K}(S,\tau_B,\tau)\right\} \\
+\overset{\tilde{B}(0),\gamma,\tau}{\mathcal{I}}\left\{\mathcal{A}^{++}_{\tilde{B}(\hat{\tau}_B)\tilde{B}(0)}(S,\tau_B,\tau)\right\} \\
-K\overset{\tilde{B}(0),\gamma,\tau}{\mathcal{I}}\left\{\mathcal{B}^{++}_{\tilde{B}(\hat{\tau}_B)\tilde{B}(0)}(S,\tau_B,\tau)\right\} \\
-\overset{\tilde{B}(\hat{\tau}_B),\kappa,\tau_B}{\mathcal{I}}\left\{\mathcal{Q}^{-+}_{\tilde{B}(\hat{\tau}_B)K}(S,\tau_B,\tau)\right\} \\
+\overset{\tilde{B}(\hat{\tau}_B),\kappa,\tau_B}{\mathcal{I}}\left\{\mathcal{A}^{-+}_{\tilde{B}(\hat{\tau}_B)\tilde{B}(0)}(S,\tau_B,\tau)\right\} \\
-K\overset{\tilde{B}(\hat{\tau}_B),\kappa,\tau_B}{\mathcal{I}}\left\{\mathcal{B}^{-+}_{\tilde{B}(\hat{\tau}_B)\tilde{B}(0)}(S,\tau_B,\tau)\right\} \\
+\overset{\tilde{B}(\hat{\tau}_B),\kappa,\tau_B}{\mathcal{I}}\left\{\overset{\tilde{B}(0),\gamma,\tau}{\mathcal{I}}\left\{\mathcal{Q}^{++}_{\tilde{B}(\hat{\tau}_B)K}(S,\tau_B,\tau)\right\}\right\} \\
-\overset{\tilde{B}(\hat{\tau}_B),\kappa,\tau_B}{\mathcal{I}}\left\{\overset{\tilde{B}(0),\gamma,\tau}{\mathcal{I}}\left\{\mathcal{A}^{++}_{\tilde{B}(\hat{\tau}_B)\tilde{B}(0)}(S,\tau_B,\tau)\right\}\right\} \\
+K\overset{\tilde{B}(\hat{\tau}_B),\kappa,\tau_B}{\mathcal{I}}\left\{\overset{\tilde{B}(0),\gamma,\tau}{\mathcal{I}}\left\{\mathcal{B}^{++}_{\tilde{B}(\hat{\tau}_B)\tilde{B}(0)}(S,\tau_B,\tau)\right\}\right\} & \text{if } K < \tilde{B}(0)
\end{cases}.
$$

III.6.4 Deferred Start Piecewise Exponential Barrier Options

The final option type considered here are deferred start barrier options with a continuous piecewise exponential barrier. There are three relevant dates $0 < T_S < T_B < T$.

The barrier is not monitored before the barrier start date T_S. During the monitoring period, the barrier follows the same piecewise exponential function as in Section III.6.3. The option value $\tilde{V}^{\mathrm{ds,pe}}(S,\tau)$ of the deferred start piecewise exponential barrier option outside the monitoring period then satisfies

$$\begin{aligned}\mathcal{L}\{\tilde{V}^{\mathrm{ds,pe}}\}(S,\tau) &= 0 \qquad \text{for } (S,\tau)\in\mathbb{R}_+\times(\hat{\tau}_S,\infty)\,,\\ \tilde{V}^{\mathrm{ds,pe}}(S,\hat{\tau}_S) &= \tilde{V}^{\mathrm{pe}}(S,\hat{\tau}_S)\,1\{\psi S>\psi\tilde{B}(\hat{\tau}_S)\}.\end{aligned}$$

Using the result from Section III.6.3, we can express the value of the deferred start piecewise exponential down & out put at the barrier start date as

$$\tilde{V}^{\mathrm{ds,pe}}_{\mathrm{p,do}}(S,\hat{\tau}_S)=\begin{cases}\Big(-\mathcal{Q}^{+-}_{\tilde{B}(\hat{\tau}_B)K}(S,\tau_B,\hat{\tau}_S)\\ -K\mathcal{B}^{+-}_{\tilde{B}(\hat{\tau}_B)\tilde{B}(0)}(S,\tau_B,\hat{\tau}_S)\\ +\mathcal{A}^{+-}_{\tilde{B}(\hat{\tau}_B)\tilde{B}(0)}(S,\tau_B,\hat{\tau}_S)\\ +\overset{\tilde{B}(0),\gamma,\hat{\tau}_S}{\mathcal{I}}\Big\{\mathcal{Q}^{--}_{\tilde{B}(\hat{\tau}_B)K}(S,\tau_B,\hat{\tau}_S)\Big\}\\ +K\overset{\tilde{B}(0),\gamma,\hat{\tau}_S}{\mathcal{I}}\Big\{\mathcal{B}^{--}_{\tilde{B}(\hat{\tau}_B)\tilde{B}(0)}(S,\tau_B,\hat{\tau}_S)\Big\}\\ -\overset{\tilde{B}(0),\gamma,\hat{\tau}_S}{\mathcal{I}}\Big\{\mathcal{A}^{--}_{\tilde{B}(\hat{\tau}_B)\tilde{B}(0)}(S,\tau_B,\hat{\tau}_S)\Big\}\\ +\overset{\tilde{B}(\hat{\tau}_B),\kappa,\tau_B}{\mathcal{I}}\Big\{\mathcal{Q}^{+-}_{\tilde{B}(\hat{\tau}_B)K}(S,\tau_B,\hat{\tau}_S)\Big\}\\ +K\overset{\tilde{B}(\hat{\tau}_B),\kappa,\tau_B}{\mathcal{I}}\Big\{\mathcal{B}^{+-}_{\tilde{B}(\hat{\tau}_B)\tilde{B}(0)}(S,\tau_B,\hat{\tau}_S)\Big\}\\ -\overset{\tilde{B}(\hat{\tau}_B),\kappa,\tau_B}{\mathcal{I}}\Big\{\mathcal{A}^{+-}_{\tilde{B}(\hat{\tau}_B)\tilde{B}(0)}(S,\tau_B,\hat{\tau}_S)\Big\}\\ -\overset{\tilde{B}(\hat{\tau}_B),\kappa,\tau_B}{\mathcal{I}}\Big\{\overset{\tilde{B}(0),\gamma,\hat{\tau}_S}{\mathcal{I}}\Big\{\mathcal{Q}^{--}_{\tilde{B}(\hat{\tau}_B)K}(S,\tau_B,\hat{\tau}_S)\Big\}\Big\}\\ -K\overset{\tilde{B}(\hat{\tau}_B),\kappa,\tau_B}{\mathcal{I}}\Big\{\overset{\tilde{B}(0),\gamma,\hat{\tau}_S}{\mathcal{I}}\Big\{\mathcal{B}^{--}_{\tilde{B}(\hat{\tau}_B)\tilde{B}(0)}(S,\tau_B,\hat{\tau}_S)\Big\}\Big\}\\ +\overset{\tilde{B}(\hat{\tau}_B),\kappa,\tau_B}{\mathcal{I}}\Big\{\overset{\tilde{B}(0),\gamma,\hat{\tau}_S}{\mathcal{I}}\Big\{\mathcal{A}^{--}_{\tilde{B}(\hat{\tau}_B)\tilde{B}(0)}(S,\tau_B,\hat{\tau}_S)\Big\}\Big\}\Big)\\ 1\{S>\tilde{B}(\hat{\tau}_S)\} & \text{if } K>\tilde{B}(0)\\ 0 & \text{if } K<\tilde{B}(0)\end{cases}.$$

Analogously to Section III.6.2, we aim to express the r.h.s. in terms of third-order binary and $\mathcal{Q}$ options and their respective (composite) images. While Lemma III.12 can be applied when the image of a binary option is multiplied by an indicator, we need an analogous result for composite images.

Lemma III.13 (Product of the Composite Image of a Binary and an Indicator). *Let $\mathcal{C}^{s_2s_3}_{\xi_2\xi_3}(S,\tau_B,\tau)$ be the value of a second-order bond or asset binary and $\tilde{B}(\tau)$ be a* *continuous piecewise exponential barrier function. Then the following relationship holds*

$$
\begin{aligned}
&\overset{\tilde{B}(\hat{\tau}_B),\kappa,\tau_B}{\mathcal{I}}\left\{\overset{\tilde{B}(0),\gamma,\tau}{\mathcal{I}}\left\{\mathcal{C}^{s_2s_3}_{\xi_2\xi_3}\left(S,\tau_B,\tau\right)\right\}\right\}1\left\{s_1S>s_1\xi_1\right\}\\
=\;&\overset{\tilde{B}(\hat{\tau}_B),\kappa,\tau_B}{\mathcal{I}}\left\{\overset{\tilde{B}(0),\gamma,\tau}{\mathcal{I}}\left\{\mathcal{C}^{s_1s_2s_3}_{\hat{\xi}_1\xi_2\xi_3}\left(S,0,\tau_B,\tau\right)\right\}\right\},
\end{aligned}
$$

where

$$\hat{\xi}_1=\mathrm{e}^{2(\gamma-\kappa)\tau_B}\xi_1.$$

The property continues to hold for higher-order binary options.

Proof Repeatedly applying Definition III.5 yields

$$
\begin{aligned}
&\overset{\tilde{B}(\hat{\tau}_B),\kappa,\tau_B}{\mathcal{I}}\left\{\overset{\tilde{B}(0),\gamma,\tau}{\mathcal{I}}\left\{\mathcal{C}^{s_2s_3}_{\xi_2\xi_3}\left(S,\tau_B,\tau\right)\right\}\right\}1\left\{s_1S>s_1\xi_1\right\}\\
=\;&\overset{\tilde{B}(\hat{\tau}_2B),\kappa,\tau_B}{\mathcal{I}}\left\{\Xi_1\,\mathcal{C}^{s_2s_3}_{\xi_2\xi_3}\left(\frac{\tilde{B}^2(0)\mathrm{e}^{2\gamma\tau}}{S},\tau_B,\tau\right)\right\}1\left\{s_1S>s_1\xi_1\right\}\\
=\;&\Xi_2\,\mathcal{C}^{s_2s_3}_{\xi_2\xi_3}\left(\frac{\tilde{B}^2(0)\mathrm{e}^{2\gamma\tau}S}{\tilde{B}^2\left(\hat{\tau}_B\right)\mathrm{e}^{2\kappa\tau_B}},\tau_B,\tau\right)1\left\{s_1S>s_1\xi_1\right\}\\
=\;&\Xi_2\,\mathcal{C}^{s_2s_3}_{\xi_2\xi_3}\left(\mathrm{e}^{2(\gamma-\kappa)\tau_B}S,\tau_B,\tau\right)1\left\{s_1\mathrm{e}^{2(\gamma-\kappa)\tau_B}S>s_1\mathrm{e}^{2(\gamma-\kappa)\tau_B}\xi_1\right\}\\
=\;&\Xi_2\,\mathcal{C}^{s_1s_2s_3}_{\hat{\xi}_1,\xi_2\xi_3}\left(\mathrm{e}^{2(\gamma-\kappa)\tau_B}S,0,\tau_B,\tau\right)\\
=\;&\overset{\tilde{B}(\hat{\tau}_2B),\kappa,\tau_B}{\mathcal{I}}\left\{\Xi_1\,\mathcal{C}^{s_1s_2s_3}_{\hat{\xi}_1\xi_2\xi_3}\left(\frac{\tilde{B}^2(0)\mathrm{e}^{2\gamma\tau}}{S},\tau_B,0,\tau\right)\right\}\\
=\;&\overset{\tilde{B}(\hat{\tau}_B),\kappa,\tau_B}{\mathcal{I}}\left\{\overset{\tilde{B}(0),\gamma,\tau}{\mathcal{I}}\left\{\mathcal{C}^{s_1s_2s_3}_{\hat{\xi}_1\xi_2\xi_3}\left(S,0,\tau_B,\tau\right)\right\}\right\}.
\end{aligned}
$$

where $\hat{\xi}_1$ is as defined in Lemma III.13 and

$$
\begin{aligned}
\Xi_1 &= \left(\frac{S}{\tilde{B}(0)\mathrm{e}^{\gamma\tau}}\right)^{2\alpha(\gamma)},\\
\Xi_2 &= \left(\frac{S}{\tilde{B}\left(\hat{\tau}_B\right)\mathrm{e}^{\kappa\tau_B}}\right)^{2\alpha(\kappa)}\left(\frac{\tilde{B}^2\left(\hat{\tau}_2\right)\mathrm{e}^{2\kappa\tau_B}}{\tilde{B}(0)\mathrm{e}^{\gamma\tau}S}\right)^{2\alpha(\gamma)}.
\end{aligned}
$$

Note that we made the dependence of the transform parameter α on the bending parameters γ and κ explicit. The proof for higher-order binaries is identical. □

Applying Lemmata III.12 and III.13 then yields

$$\tilde{V}^{\mathrm{ds,pe}}_{\mathrm{p,do}}(S,\hat{\tau}_S) = \begin{cases} -\mathcal{Q}^{++-}_{\tilde{B}(\hat{\tau}_S)\tilde{B}(\hat{\tau}_B)K}(S,0,\tau_B,\hat{\tau}_S) \\ -K\mathcal{B}^{++-}_{\tilde{B}(\hat{\tau}_S)\tilde{B}(\hat{\tau}_B)\tilde{B}(0)}(S,0,\tau_B,\hat{\tau}_S) \\ +\mathcal{A}^{++-}_{\tilde{B}(\hat{\tau}_S)\tilde{B}(\hat{\tau}_B)\tilde{B}(0)}(S,0,\tau_B,\hat{\tau}_S) \\ +\overset{\tilde{B}(0),\gamma,\hat{\tau}_S}{\mathcal{I}}\left\{\mathcal{Q}^{---}_{\zeta_1\tilde{B}(\hat{\tau}_B)K}(S,0,\tau_B,\hat{\tau}_S)\right\} \\ +K\overset{\tilde{B}(0),\gamma,\hat{\tau}_S}{\mathcal{I}}\left\{\mathcal{B}^{---}_{\zeta_1\tilde{B}(\hat{\tau}_B)\tilde{B}(0)}(S,0,\tau_B,\hat{\tau}_S)\right\} \\ -\overset{\tilde{B}(0),\gamma,\hat{\tau}_S}{\mathcal{I}}\left\{\mathcal{A}^{---}_{\zeta_1\tilde{B}(\hat{\tau}_B)\tilde{B}(0)}(S,0,\tau_B,\hat{\tau}_S)\right\} \\ +\overset{\tilde{B}(\hat{\tau}_B),\kappa,\tau_B}{\mathcal{I}}\left\{\mathcal{Q}^{-+-}_{\zeta_2\tilde{B}(\hat{\tau}_B)K}(S,0,\tau_B,\hat{\tau}_S)\right\} \\ +K\overset{\tilde{B}(\hat{\tau}_B),\kappa,\tau_B}{\mathcal{I}}\left\{\mathcal{B}^{-+-}_{\zeta_2\tilde{B}(\hat{\tau}_B)\tilde{B}(0)}(S,0,\tau_B,\hat{\tau}_S)\right\} \\ -\overset{\tilde{B}(\hat{\tau}_B),\kappa,\tau_B}{\mathcal{I}}\left\{\mathcal{A}^{-+-}_{\zeta_2\tilde{B}(\hat{\tau}_B)\tilde{B}(0)}(S,0,\tau_B,\hat{\tau}_S)\right\} \\ -\overset{\tilde{B}(\hat{\tau}_B),\kappa,\tau_B}{\mathcal{I}}\left\{\overset{\tilde{B}(0),\gamma,\hat{\tau}_S}{\mathcal{I}}\left\{\mathcal{Q}^{+--}_{\zeta_3\tilde{B}(\hat{\tau}_B)K}(S,0,\tau_B,\hat{\tau}_S)\right\}\right\} \\ -K\overset{\tilde{B}(\hat{\tau}_B),\kappa,\tau_B}{\mathcal{I}}\left\{\overset{\tilde{B}(0),\gamma,\hat{\tau}_S}{\mathcal{I}}\left\{\mathcal{B}^{+--}_{\zeta_3\tilde{B}(\hat{\tau}_B)\tilde{B}(0)}(S,0,\tau_B,\hat{\tau}_S)\right\}\right\} \\ +\overset{\tilde{B}(\hat{\tau}_B),\kappa,\tau_B}{\mathcal{I}}\left\{\overset{\tilde{B}(0),\gamma,\hat{\tau}_S}{\mathcal{I}}\left\{\mathcal{A}^{+--}_{\zeta_3\tilde{B}(\hat{\tau}_B)\tilde{B}(0)}(S,0,\tau_B,\hat{\tau}_S)\right\}\right\} & \text{if } K > \tilde{B}(0) \\ \\ 0 & \text{if } K < \tilde{B}(0) \end{cases},$$

where

$$\begin{aligned} \zeta_1 &= \tilde{B}(\hat{\tau}_S)\,\mathrm{e}^{2(\gamma-\kappa)(\hat{\tau}_S-\hat{\tau}_B)}, \\ \zeta_2 &= \tilde{B}(\hat{\tau}_S), \\ \zeta_3 &= \tilde{B}(\hat{\tau}_S)\,\mathrm{e}^{2(\gamma-\kappa)(\hat{\tau}_S-\hat{\tau}_B)}. \end{aligned}$$

Consequently, we get for $\tau > \hat{\tau}_S$

$$\tilde{V}^{\text{ds,pe}}_{\text{p,do}}(S,\tau) = \begin{cases} -\mathcal{Q}^{++-}_{\tilde{B}(\hat{\tau}_S)\tilde{B}(\hat{\tau}_B)K}\,(S,\tau_S,\tau_B,\tau) & \\ -K\mathcal{B}^{++-}_{\tilde{B}(\hat{\tau}_S)\tilde{B}(\hat{\tau}_B)\tilde{B}(0)}\,(S,\tau_S,\tau_B,\tau) & \\ +\mathcal{A}^{++-}_{\tilde{B}(\hat{\tau}_S)\tilde{B}(\hat{\tau}_B)\tilde{B}(0)}\,(S,\tau_S,\tau_B,\tau) & \\ +\overset{\tilde{B}(0),\gamma,\tau}{\mathcal{I}}\left\{\mathcal{Q}^{---}_{\zeta_1\tilde{B}(\hat{\tau}_B)K}\,(S,\tau_S,\tau_B,\tau)\right\} & \\ +K\overset{\tilde{B}(0),\gamma,\tau}{\mathcal{I}}\left\{\mathcal{B}^{---}_{\zeta_1\tilde{B}(\hat{\tau}_B)\tilde{B}(0)}\,(S,\tau_S,\tau_B,\tau)\right\} & \\ -\overset{\tilde{B}(0),\gamma,\tau}{\mathcal{I}}\left\{\mathcal{A}^{---}_{\zeta_1\tilde{B}(\hat{\tau}_B)\tilde{B}(0)}\,(S,\tau_S,\tau_B,\tau)\right\} & \\ +\overset{\tilde{B}(\hat{\tau}_B),\kappa,\tau_B}{\mathcal{I}}\left\{\mathcal{Q}^{-+-}_{\zeta_2\tilde{B}(\hat{\tau}_B)K}\,(S,\tau_S,\tau_B,\tau)\right\} & \\ +K\overset{\tilde{B}(\hat{\tau}_B),\kappa,\tau_B}{\mathcal{I}}\left\{\mathcal{B}^{-+-}_{\zeta_2\tilde{B}(\hat{\tau}_B)\tilde{B}(0)}\,(S,\tau_S,\tau_B,\tau)\right\} & \\ -\overset{\tilde{B}(\hat{\tau}_B),\kappa,\tau_B}{\mathcal{I}}\left\{\mathcal{A}^{-+-}_{\zeta_2\tilde{B}(\hat{\tau}_B)\tilde{B}(0)}\,(S,\tau_S,\tau_B,\tau)\right\} & \\ -\overset{\tilde{B}(\hat{\tau}_B),\kappa,\tau_B}{\mathcal{I}}\left\{\overset{\tilde{B}(0),\gamma,\tau}{\mathcal{I}}\left\{\mathcal{Q}^{+--}_{\zeta_3\tilde{B}(\hat{\tau}_B)K}\,(S,\tau_S,\tau_B,\tau)\right\}\right\} & \\ -K\overset{\tilde{B}(\hat{\tau}_B),\kappa,\tau_B}{\mathcal{I}}\left\{\overset{\tilde{B}(0),\gamma,\tau}{\mathcal{I}}\left\{\mathcal{B}^{+--}_{\zeta_3\tilde{B}(\hat{\tau}_B)\tilde{B}(0)}\,(S,\tau_S,\tau_B,\tau)\right\}\right\} & \\ +\overset{\tilde{B}(\hat{\tau}_B),\kappa,\tau_B}{\mathcal{I}}\left\{\overset{\tilde{B}(0),\gamma,\tau}{\mathcal{I}}\left\{\mathcal{A}^{+--}_{\zeta_3\tilde{B}(\hat{\tau}_B)\tilde{B}(0)}\,(S,\tau_S,\tau_B,\tau)\right\}\right\} & \text{if } K > \tilde{B}(0) \\ 0 & \text{if } K < \tilde{B}(0) \end{cases}.$$

The values of the other three knock-out barrier options are given by

$$\tilde{V}^{\text{ds,pe}}_{\text{p,uo}}(S,\tau) = \begin{cases} K\mathcal{B}^{---}_{\tilde{B}(\hat{\tau}_S)\tilde{B}(\hat{\tau}_B)\tilde{B}(0)}\,(S,\tau_S,\tau_B,\tau) & \\ -\mathcal{A}^{---}_{\tilde{B}(\hat{\tau}_S)\tilde{B}(\hat{\tau}_B)\tilde{B}(0)}\,(S,\tau_S,\tau_B,\tau) & \\ -K\overset{\tilde{B}(0),\gamma,\tau}{\mathcal{I}}\left\{\mathcal{B}^{++-}_{\zeta_1\tilde{B}(\hat{\tau}_B)\tilde{B}(0)}\,(S,\tau_S,\tau_B,\tau)\right\} & \\ +\overset{\tilde{B}(0),\gamma,\tau}{\mathcal{I}}\left\{\mathcal{A}^{++-}_{\zeta_1\tilde{B}(\hat{\tau}_B)\tilde{B}(0)}\,(S,\tau_S,\tau_B,\tau)\right\} & \\ -K\overset{\tilde{B}(\hat{\tau}_B),\kappa,\tau_B}{\mathcal{I}}\left\{\mathcal{B}^{+--}_{\zeta_2\tilde{B}(\hat{\tau}_B)\tilde{B}(0)}\,(S,\tau_S,\tau_B,\tau)\right\} & \\ +\overset{\tilde{B}(\hat{\tau}_B),\kappa,\tau_B}{\mathcal{I}}\left\{\mathcal{A}^{+--}_{\zeta_2\tilde{B}(\hat{\tau}_B)\tilde{B}(0)}\,(S,\tau_S,\tau_B,\tau)\right\} & \\ +K\overset{\tilde{B}(\hat{\tau}_B),\kappa,\tau_B}{\mathcal{I}}\left\{\overset{\tilde{B}(0),\gamma,\tau}{\mathcal{I}}\left\{\mathcal{B}^{-+-}_{\zeta_3\tilde{B}(\hat{\tau}_B)\tilde{B}(0)}\,(S,\tau_S,\tau_B,\tau)\right\}\right\} & \\ -\overset{\tilde{B}(\hat{\tau}_B),\kappa,\tau_B}{\mathcal{I}}\left\{\overset{\tilde{B}(0),\gamma,\tau}{\mathcal{I}}\left\{\mathcal{A}^{-+-}_{\zeta_3\tilde{B}(\hat{\tau}_B)\tilde{B}(0)}\,(S,\tau_S,\tau_B,\tau)\right\}\right\} & \text{if } K > \tilde{B}(0) \\ -\mathcal{Q}^{---}_{\tilde{B}(\hat{\tau}_S)\tilde{B}(\hat{\tau}_B)K}\,(S,\tau_S,\tau_B,\tau) & \\ +\overset{\tilde{B}(0),\gamma,\tau}{\mathcal{I}}\left\{\mathcal{Q}^{++-}_{\zeta_1\tilde{B}(\hat{\tau}_B)K}\,(S,\tau_S,\tau_B,\tau)\right\} & \\ +\overset{\tilde{B}(\hat{\tau}_B),\kappa,\tau_B}{\mathcal{I}}\left\{\mathcal{Q}^{+--}_{\zeta_2\tilde{B}(\hat{\tau}_B)K}\,(S,\tau_S,\tau_B,\tau)\right\} & \\ -\overset{\tilde{B}(\hat{\tau}_B),\kappa,\tau_B}{\mathcal{I}}\left\{\overset{\tilde{B}(0),\gamma,\tau}{\mathcal{I}}\left\{\mathcal{Q}^{-+-}_{\zeta_3\tilde{B}(\hat{\tau}_B)K}\,(S,\tau_S,\tau_B,\tau)\right\}\right\} & \text{if } K < \tilde{B}(0) \end{cases},$$

$$
\tilde{V}^{\text{ds,pe}}_{\text{c,do}}(S,\tau) = \begin{cases}
\mathcal{Q}^{+++}_{\tilde{B}(\hat{\tau}_S)\tilde{B}(\hat{\tau}_B)K}(S,\tau_S,\tau_B,\tau) \\
- \overset{\tilde{B}(0),\gamma,\tau}{\mathcal{I}} \left\{ \mathcal{Q}^{--+}_{\zeta_1\tilde{B}(\hat{\tau}_B)K}(S,\tau_S,\tau_B,\tau) \right\} \\
- \overset{\tilde{B}(\hat{\tau}_B),\kappa,\tau_B}{\mathcal{I}} \left\{ \mathcal{Q}^{-++}_{\zeta_2\tilde{B}(\hat{\tau}_B)K}(S,\tau_S,\tau_B,\tau) \right\} \\
+ \overset{\tilde{B}(\hat{\tau}_B),\kappa,\tau_B}{\mathcal{I}} \left\{ \overset{\tilde{B}(0),\gamma,\tau}{\mathcal{I}} \left\{ \mathcal{Q}^{+-+}_{\zeta_3\tilde{B}(\hat{\tau}_B)K}(S,\tau_S,\tau_B,\tau) \right\} \right\} & \text{if } K > \tilde{B}(0) \\
\\
\mathcal{A}^{+++}_{\tilde{B}(\hat{\tau}_S)\tilde{B}(\hat{\tau}_B)\tilde{B}(0)}(S,\tau_S,\tau_B,\tau) \\
-K\mathcal{B}^{+++}_{\tilde{B}(\hat{\tau}_S)\tilde{B}(\hat{\tau}_B)\tilde{B}(0)}(S,\tau_S,\tau_B,\tau) \\
- \overset{\tilde{B}(0),\gamma,\tau}{\mathcal{I}} \left\{ \mathcal{A}^{--+}_{\zeta_1\tilde{B}(\hat{\tau}_B)\tilde{B}(0)}(S,\tau_S,\tau_B,\tau) \right\} \\
+K \overset{\tilde{B}(0),\gamma,\tau}{\mathcal{I}} \left\{ \mathcal{B}^{--+}_{\zeta_1\tilde{B}(\hat{\tau}_B)\tilde{B}(0)}(S,\tau_S,\tau_B,\tau) \right\} \\
- \overset{\tilde{B}(\hat{\tau}_B),\kappa,\tau_B}{\mathcal{I}} \left\{ \mathcal{A}^{-++}_{\zeta_2\tilde{B}(\hat{\tau}_B)\tilde{B}(0)}(S,\tau_S,\tau_B,\tau) \right\} \\
+K \overset{\tilde{B}(\hat{\tau}_B),\kappa,\tau_B}{\mathcal{I}} \left\{ \mathcal{B}^{-++}_{\zeta_2\tilde{B}(\hat{\tau}_B)\tilde{B}(0)}(S,\tau_S,\tau_B,\tau) \right\} \\
+ \overset{\tilde{B}(\hat{\tau}_B),\kappa,\tau_B}{\mathcal{I}} \left\{ \overset{\tilde{B}(0),\gamma,\tau}{\mathcal{I}} \left\{ \mathcal{A}^{+-+}_{\zeta_3\tilde{B}(\hat{\tau}_B)\tilde{B}(0)}(S,\tau_S,\tau_B,\tau) \right\} \right\} \\
-K \overset{\tilde{B}(\hat{\tau}_B),\kappa,\tau_B}{\mathcal{I}} \left\{ \overset{\tilde{B}(0),\gamma,\tau}{\mathcal{I}} \left\{ \mathcal{B}^{+-+}_{\zeta_3\tilde{B}(\hat{\tau}_B)\tilde{B}(0)}(S,\tau_S,\tau_B,\tau) \right\} \right\} & \text{if } K < \tilde{B}(0)
\end{cases},
$$

and

$$
\tilde{V}^{\text{ds,pe}}_{\text{c,uo}}(S,\tau) = \begin{cases}
0 & \text{if } K > \tilde{B}(0) \\
\\
\mathcal{Q}^{--+}_{\tilde{B}(\hat{\tau}_S)\tilde{B}(\hat{\tau}_B)K}(S,\tau_S,\tau_B,\tau) \\
-\mathcal{A}^{--+}_{\tilde{B}(\hat{\tau}_S)\tilde{B}(\hat{\tau}_B)\tilde{B}(0)}(S,\tau_S,\tau_B,\tau) \\
+K\mathcal{B}^{--+}_{\tilde{B}(\hat{\tau}_S)\tilde{B}(\hat{\tau}_B)\tilde{B}(0)}(S,\tau_S,\tau_B,\tau) \\
- \overset{\tilde{B}(0),\gamma,\tau}{\mathcal{I}} \left\{ \mathcal{Q}^{+++}_{\zeta_1\tilde{B}(\hat{\tau}_B)K}(S,\tau_S,\tau_B,\tau) \right\} \\
+ \overset{\tilde{B}(0),\gamma,\tau}{\mathcal{I}} \left\{ \mathcal{A}^{+++}_{\zeta_1\tilde{B}(\hat{\tau}_S)\tilde{B}(0)}(S,\tau_S,\tau_B,\tau) \right\} \\
-K \overset{\tilde{B}(0),\gamma,\tau}{\mathcal{I}} \left\{ \mathcal{B}^{+++}_{\zeta_1\tilde{B}(\hat{\tau}_B)\tilde{B}(0)}(S,\tau_S,\tau_B,\tau) \right\} \\
- \overset{\tilde{B}(\hat{\tau}_B),\kappa,\tau_B}{\mathcal{I}} \left\{ \mathcal{Q}^{+-+}_{\zeta_2\tilde{B}(\hat{\tau}_B)K}(S,\tau_S,\tau_B,\tau) \right\} \\
+ \overset{\tilde{B}(\hat{\tau}_B),\kappa,\tau_B}{\mathcal{I}} \left\{ \mathcal{A}^{+-+}_{\zeta_2\tilde{B}(\hat{\tau}_B)\tilde{B}(0)}(S,\tau_S,\tau_B,\tau) \right\} \\
-K \overset{\tilde{B}(\hat{\tau}_B),\kappa,\tau_B}{\mathcal{I}} \left\{ \mathcal{B}^{+-+}_{\zeta_2\tilde{B}(\hat{\tau}_B)\tilde{B}(0)}(S,\tau_S,\tau_B,\tau) \right\} \\
+ \overset{\tilde{B}(\hat{\tau}_B),\kappa,\tau_B}{\mathcal{I}} \left\{ \overset{\tilde{B}(0),\gamma,\tau}{\mathcal{I}} \left\{ \mathcal{Q}^{-++}_{\zeta_3\tilde{B}(\hat{\tau}_B)K}(S,\tau_S,\tau_B,\tau) \right\} \right\} \\
- \overset{\tilde{B}(\hat{\tau}_B),\kappa,\tau_B}{\mathcal{I}} \left\{ \overset{\tilde{B}(0),\gamma,\tau}{\mathcal{I}} \left\{ \mathcal{A}^{-++}_{\zeta_3\tilde{B}(\hat{\tau}_S)\tilde{B}(0)}(S,\tau_S,\tau_B,\tau) \right\} \right\} \\
+K \overset{\tilde{B}(\hat{\tau}_B),\kappa,\tau_B}{\mathcal{I}} \left\{ \overset{\tilde{B}(0),\gamma,\tau}{\mathcal{I}} \left\{ \mathcal{B}^{-++}_{\zeta_3\tilde{B}(\hat{\tau}_B)\tilde{B}(0)}(S,\tau_S,\tau_B,\tau) \right\} \right\} & \text{if } K < \tilde{B}(0)
\end{cases}.
$$

III.7 Rebate Pricing: Payout at Maturity

This section discusses the valuation of fixed rebates that are paid at the maturity of the option if the barrier has been breached before. W.l.o.g., we assume that the rebate at maturity is equal to one currency unit. Again, symmetry relationships of the heat transfer equation yield a simple solution in terms of two bond binaries. Like in Section III.6, we first derive various auxiliary valuation formulas before obtaining the solution for the case of a deferred start piecewise exponential barrier. We repeatedly use that the terminal payoff and the rebate of a barrier option can be valued separately; see Lemma III.11.

III.7.1 Exponential Barrier Rebate

Let ν be again the first hitting time of the asset to the exponential boundary $\tilde{B}(\tau)$ as in Section III.6.1. Since the rebate has a unit payoff at maturity conditional on $\nu \leq T$, it follows that its value at the first hitting time is equal to that of a zero coupon bond with a unit notional, that is

$$V_\nu = \mathrm{e}^{-r(T-\nu)} 1\{\nu \leq T\}.$$

The following well-known parity relationship is essential in constructing a static portfolio that satisfies the initial and boundary conditions of the rebate pricing problem.

Lemma III.14 (Bond Binary Parity).
First-order bond binaries satisfy

$$\mathcal{B}_\xi^+(S,\tau) + \mathcal{B}_\xi^-(S,\tau) = \mathrm{e}^{-r\tau}$$

for all $S \in \mathbb{R}_+$.

Proof This follows immediately from

$$\mathcal{B}_\xi^+(S,0) + \mathcal{B}_\xi^-(S,0) = 1$$

for all $S \in \mathbb{R}_+$. $\square$

By Lemma III.14, a portfolio consisting of a long position in one bond binary call and put matches the value of the rebate on the boundary. However, it does not match the zero initial condition at the option maturity since either of the two binary options always expires in-the-money. Proposition III.7 provides a remedy to this problem by using the image function to change the active domain of one of the two bond binaries while keeping its value on the boundary unchanged.

Proposition III.7 (Pay-at-Maturity Bond Binary Valuation).
Let $\tilde{B}(\tau) = \tilde{B}(0)\mathrm{e}^{\gamma\tau}$ be an exponential boundary and let $\tilde{V}(S,\tau)$ satisfy

$$\begin{aligned} \mathcal{L}\{\tilde{V}\}(S,\tau) &= 0 \qquad \textit{for } (S,\tau) \in \mathcal{D}, \\ \tilde{V}(S,0) &= 0, \\ \tilde{V}\big(\tilde{B}(\tau),\tau\big) &= \mathrm{e}^{-r\tau} \qquad \textit{for } \tau \in [0,\infty), \end{aligned}$$

where the active domain $\mathcal{D} \subseteq \mathbb{R}_+^2$ is given by

$$\mathcal{D} = \big\{(S,\tau) : \psi S > \psi \tilde{B}(\tau),\, \tau \in (0,\infty)\big\}$$

and $\psi \in \{-1,+1\}$ indicates an upper or lower boundary. Then

$$\tilde{V}(S,\tau) = \mathcal{B}^{-\psi}_{\tilde{B}(0)}(S,\tau) + \overset{\tilde{B}(0),\gamma,\tau}{\mathcal{I}} \big\{\mathcal{B}^{\psi}_{\tilde{B}(0)}(S,\tau)\big\}.$$

Proof First, note that by Lemma III.14 the trial solution $\tilde{U}(S,\tau)$ given by

$$\tilde{U}(S,\tau) = \mathcal{B}^{-\psi}_{\tilde{B}(0)}(S,\tau) + \mathcal{B}^{\psi}_{\tilde{B}(0)}(S,\tau)$$

satisfies both the Black and Scholes (1973) PDE and the boundary condition. While the payoff of the first bond binary is zero for $\psi S > \psi\tilde{B}(0)$ and non-zero otherwise, that of the second is non-zero on the active domain of the American bond binary. Thus $\tilde{U}(S,\tau)$ does not satisfy the initial condition and consequently also does not solve the problem in Proposition III.7. However, by Properties (iii) and (iv) of Proposition III.2, it follows that the image of the second bond binary has a zero payoff for $\psi S > \psi\tilde{B}(0)$ and its value on the boundary stays unchanged. Consequently, the function $\tilde{V}(S,\tau)$ as given in the Proposition is a solution to the initial boundary value problem. Appendix III.C.1 presents an alternative derivation. $\square$

Proposition III.10 not only solves the valuation problem in this section but also provides the standard tool used to price more complex pay-at-maturity binary options in the following sections.

III.7.2 Deferred Start Exponential Barrier Rebate

Similarly to Section III.6.2, before the barrier start date the deferred start rebate can be valued as a binary option to receive a pay-at-maturity American bond binary at T_S conditional on $\psi S_{T_S} > \psi \tilde{B}(\hat{\tau}_S)$. The option value $\tilde{V}^{\mathrm{ds}}(S,\tau)$ satisfies

$$
\begin{aligned}
\mathcal{L}\{\tilde{V}^{\mathrm{ds}}\}(S,\tau) &= 0 \qquad \text{for } (S,\tau) \in \mathbb{R}_+ \times (\hat{\tau}_S, \infty)\,, \\
\tilde{V}^{\mathrm{ds}}(S,\hat{\tau}_S) &= \tilde{V}(S,\hat{\tau}_S)\,1\{\psi S > \psi \tilde{B}(\hat{\tau}_S)\} + \mathrm{e}^{-r\hat{\tau}_S} 1\{\psi S < \psi \tilde{B}(\hat{\tau}_S)\}.
\end{aligned}
$$

Note that compared to Section III.6.2, we have one additional term in the initial condition. It accounts for the case when the barrier is violated immediately once it becomes active. Using Corollary III.3 with Proposition III.7, we obtain the valuation function

$$
\begin{aligned}
\tilde{V}^{\mathrm{ds}}(S,\tau) &= \tilde{B}^{\psi-\psi}_{\tilde{B}(\hat{\tau}_S)\tilde{B}(0)}(S,\tau_S,\tau) + \overset{\tilde{B}(0),\gamma,\tau}{\mathcal{I}} \left\{ \tilde{B}^{-\psi\psi}_{\tilde{B}(\hat{\tau}_S),\tilde{B}(0)}(S,\tau_S,\tau) \right\} \\
&\quad + \mathrm{e}^{-r\hat{\tau}_S} \mathcal{B}^{-\psi}_{\tilde{B}(\hat{\tau}_S)}(S,\tau_S)\,.
\end{aligned}
$$

III.7.3 Piecewise Exponential Barrier Rebate

When the barrier is continuously monitored and given by a piecewise exponential function as in Section III.6.3, then the option value $\tilde{V}^{\mathrm{pe}}(S,\tau)$ satisfies

$$
\begin{aligned}
\mathcal{L}\{\tilde{V}^{\mathrm{pe}}\}(S,\tau) &= 0 \qquad \text{for } (S,\tau) \in \mathcal{D}, \\
\tilde{V}^{\mathrm{pe}}(S,\hat{\tau}_B) &= \tilde{V}(S,\hat{\tau}_B)\,, \\
\tilde{V}^{\mathrm{pe}}\big(\tilde{B}(\tau),\tau\big) &= \mathrm{e}^{-r\tau} \qquad \text{for } \tau \in [\hat{\tau}_B, \infty)\,,
\end{aligned}
$$

where

$$
\mathcal{D} = \big\{(S,\tau) : \psi S > \psi \tilde{B}(\tau),\, \tau \in (\hat{\tau}_B, \infty)\big\}.
$$

Using Lemma III.11, we separately value the rebate before and after the bending change date. The valuation problem $\tilde{V}^{\mathrm{pe},1}(S,\tau)$ for the rebate before the bending change date alone is given by

$$
\begin{aligned}
\mathcal{L}\big\{\tilde{V}^{\mathrm{pe},1}\big\}(S,\tau) &= 0 \qquad \text{for } (S,\tau)\in\mathcal{D},\\
\tilde{V}^{\mathrm{pe},1}\left(S,\hat{\tau}_B\right) &= 0,\\
\tilde{V}^{\mathrm{pe},1}\big(\tilde{B}(\tau),\tau\big) &= \mathrm{e}^{-r\tau} \qquad \text{for } \tau\in[\hat{\tau}_B,\infty)\,.
\end{aligned}
$$

By Proposition III.7, it has the solution

$$
\tilde{V}^{\mathrm{pe},1}(S,\tau) = \mathcal{B}^{-\psi}_{\tilde{B}(\hat{\tau}_B)}\left(S,\tau_B\right) + \overset{\tilde{B}(\hat{\tau}_B),\kappa,\tau_B}{\mathcal{I}}\left\{\mathcal{B}^{\psi}_{\tilde{B}(\hat{\tau}_B)}\left(S,\tau_B\right)\right\}.
$$

The rebate after the bending change date can be valued as a knock-out barrier option to receive a standard rebate on T_B. The valuation function $\tilde{V}^{\mathrm{pe},2}(S,\tau)$ satisfies the initial boundary value problem

$$
\begin{aligned}
\mathcal{L}\big\{\tilde{V}^{\mathrm{pe},2}\big\}(S,\tau) &= 0 \qquad \text{for } (S,\tau)\in\mathcal{D},\\
\tilde{V}^{\mathrm{pe},2}\left(S,\hat{\tau}_B\right) &= \tilde{V}\left(S,\hat{\tau}_B\right),\\
\tilde{V}^{\mathrm{pe},2}\big(\tilde{B}(\tau),\tau\big) &= 0.
\end{aligned}
$$

The solution to the full-range problem is the same as the one obtained for the deferred start exponential barrier rebate when ignoring the term which accounts for an immediate knock-out at the barrier start date. We thus have

$$
\begin{aligned}
\tilde{V}^{\mathrm{pe},2}(S,\tau) &= \mathcal{B}^{\psi-\psi}_{\tilde{B}(\hat{\tau}_B)\tilde{B}(0)}\left(S,\tau_B,\tau\right) + \overset{\tilde{B}(0),\gamma,\tau}{\mathcal{I}}\left\{\mathcal{B}^{-\psi\psi}_{\tilde{B}(\hat{\tau}_B)\tilde{B}(0)}\left(S,\tau_B,\tau\right)\right\}\\
&\quad - \overset{\tilde{B}(\hat{\tau}_B),\kappa,\tau_B}{\mathcal{I}}\left\{\mathcal{B}^{\psi-\psi}_{\tilde{B}(\hat{\tau}_B)\tilde{B}(0)}\left(S,\tau_B,\tau\right)\right\}\\
&\quad - \overset{\tilde{B}(\hat{\tau}_B),\kappa,\tau_B}{\mathcal{I}}\left\{\overset{\tilde{B}(0),\gamma,\tau}{\mathcal{I}}\left\{\mathcal{B}^{-\psi\psi}_{\tilde{B}(\hat{\tau}_B)\tilde{B}(0)}\left(S,\tau_B,\tau\right)\right\}\right\}.
\end{aligned}
$$

Combining these two results yields

$$
\begin{aligned}
\tilde{V}^{\mathrm{pe}}(S,\tau) &= \mathcal{B}^{-\psi}_{\tilde{B}(\hat{\tau}_B)}\left(S,\tau_B\right) + \overset{\tilde{B}(\hat{\tau}_B),\kappa,\tau_B}{\mathcal{I}}\left\{\mathcal{B}^{\psi}_{\tilde{B}(\hat{\tau}_B)}\left(S,\tau_B\right)\right\}\\
&\quad + \mathcal{B}^{\psi-\psi}_{\tilde{B}(\hat{\tau}_B)\tilde{B}(0)}\left(S,\tau_B,\tau\right) + \overset{\tilde{B}(0),\gamma,\tau}{\mathcal{I}}\left\{\mathcal{B}^{-\psi\psi}_{\tilde{B}(\hat{\tau}_B)\tilde{B}(0)}\left(S,\tau_B,\tau\right)\right\}\\
&\quad - \overset{\tilde{B}(\hat{\tau}_B),\kappa,\tau_B}{\mathcal{I}}\left\{\mathcal{B}^{\psi-\psi}_{\tilde{B}(\hat{\tau}_B)\tilde{B}(0)}\left(S,\tau_B,\tau\right)\right\}\\
&\quad - \overset{\tilde{B}(\hat{\tau}_B),\kappa,\tau_B}{\mathcal{I}}\left\{\overset{\tilde{B}(0),\gamma,\tau}{\mathcal{I}}\left\{\mathcal{B}^{-\psi\psi}_{\tilde{B}(\hat{\tau}_B)\tilde{B}(0)}\left(S,\tau_B,\tau\right)\right\}\right\}.
\end{aligned}
$$

III.7.4 Deferred Start Piecewise Exponential Barrier Rebate

The auxiliary results from Sections III.7.1 through III.7.3 now allow us to value a deferred start rebate with a continuous piecewise exponential barrier. The valuation function $\tilde{V}^{\text{ds, pe}}(S,\tau)$ satisfies

$$\begin{aligned}
\mathcal{L}\big\{\tilde{V}^{\text{ds,pe}}\big\}(S,\tau) &= 0 \qquad \text{for } (S,\tau) \in \mathbb{R}_+ \times (\hat{\tau}_S,\infty)\,, \\
\tilde{V}^{\text{ds,pe}}(S,\hat{\tau}_S) &= \tilde{V}^{\text{pe}}(S,\hat{\tau}_S)\,1\big\{\psi S > \psi\tilde{B}(\hat{\tau}_S)\big\} + \mathrm{e}^{-r\hat{\tau}_S}1\big\{\psi S < \psi\tilde{B}(\hat{\tau}_S)\big\}.
\end{aligned}$$

Using Lemmata III.12 and III.13, we obtain its solution as

$$\begin{aligned}
\tilde{V}^{\text{ds,pe}}(S,\tau) = \;& \mathcal{B}^{\psi-\psi}_{\tilde{B}(\hat{\tau}_S)\tilde{B}(\hat{\tau}_B)}(S,\tau_S,\tau_B) + \overset{\tilde{B}(\hat{\tau}_B),\kappa,\tau_B}{\mathcal{I}}\big\{\mathcal{B}^{-\psi\psi}_{\zeta_1\tilde{B}(\hat{\tau}_B)}(S,\tau_S,\tau_B)\big\} \\
&+\mathcal{B}^{\psi\psi-\psi}_{\tilde{B}(\hat{\tau}_S)\tilde{B}(\hat{\tau}_B)\tilde{B}(0)}(S,\tau_S,\tau_B,\tau) + \overset{\tilde{B}(0),\gamma,\tau}{\mathcal{I}}\big\{\mathcal{B}^{-\psi-\psi\psi}_{\zeta_2\tilde{B}(\hat{\tau}_B)\tilde{B}(0)}(S,\tau_S,\tau_B,\tau)\big\} \\
&- \overset{\tilde{B}(\hat{\tau}_B),\kappa,\tau_B}{\mathcal{I}}\big\{\mathcal{B}^{-\psi\psi-\psi}_{\zeta_1\tilde{B}(\hat{\tau}_B)\tilde{B}(0)}(S,\tau_S,\tau_B,\tau)\big\} \\
&- \overset{\tilde{B}(\hat{\tau}_B),\kappa,\tau_B}{\mathcal{I}}\Big\{\overset{\tilde{B}(0),\gamma,\tau}{\mathcal{I}}\big\{\mathcal{B}^{\psi-\psi\psi}_{\zeta_3\tilde{B}(\hat{\tau}_B)\tilde{B}(0)}(S,\tau_S,\tau_B,\tau)\big\}\Big\} \\
&+\mathrm{e}^{-r\hat{\tau}_S}\mathcal{B}^{-\psi}_{\tilde{B}(\hat{\tau}_S)}(S,\tau_S)\,,
\end{aligned}$$

where ζ_1, ζ_2 and ζ_3 are as in Section III.6.4.

III.8 Rebate Pricing: Payout at Hit

Finally, we discuss the valuation of fixed rebates that are paid immediately upon the first hitting time of the barrier. We once more assume w.l.o.g. that the rebate is equal to one currency unit.

III.8.1 Exponential Barrier Rebate

Let ν be again the first hitting time of the asset to the exponential boundary $\tilde{B}(\tau)$ as in Section III.6.1. Since the rebate is paid upon the first hitting time, it follows by the risk-neutral pricing formula that its value is equal to the expected discount factor, that is

$$V_0 = \mathbb{E}_{\mathbb{P}^*}\left[\mathrm{e}^{-r\nu}1\{\nu \le T\}\right].$$

The following Lemma uses Corollary III.1 to reduce the valuation problem to the well known case of a constant barrier.

Lemma III.15 (Equivalent Constant Barrier Valuation Problem).
Let $\tilde{B}(\tau)$ be an exponential boundary where $\tau = T - t$ for some time $T \in [0, T^*]$ and let the dynamics of the spot asset $S = \{S_t : t \in [0, T^*]\}$ under the risk-neutral probability measure $\mathbb{P}^*$ and the first hitting time ν of S to the barrier $\tilde{B}(\tau)$ be as in Lemma III.2. Set $\hat{B} = \tilde{B}(T)$ and let the dynamics of a second spot asset $\hat{S} = \left\{\hat{S}_t : t \in [0, T^*]\right\}$ under $\mathbb{P}^*$ be given by

$$\mathrm{d}\hat{S}_t = (r - \delta + \gamma)\,\hat{S}_t \mathrm{d}t + \sigma \hat{S}_t \mathrm{d}W_t^*.$$

with initial value $\hat{S}_0 = S_0$. The first hitting time $\hat{\nu}$ of $\hat{S}$ to the barrier $\hat{B}$ on the interval $[0, T]$ is defined as

$$\hat{\nu} = \inf\left\{t \in [0, T] : \hat{S}_t = \hat{B}\right\},$$

where we set $\hat{\nu} = \infty$ on the set where this event occurs after T or never. Then

$$\nu = \hat{\nu} \qquad \mathbb{P}^*\text{-a.s.}$$

and consequently

$$\mathbb{E}_{\mathbb{P}^*}\left[\mathrm{e}^{-r\nu} 1\{\nu \leq T\}\right] = \mathbb{E}_{\mathbb{P}^*}\left[\mathrm{e}^{-r\hat{\nu}} 1\left\{\hat{\nu} \leq T\right\}\right].$$

Proof From Lemma III.2 and Corollary III.1, it follows immediately that $\nu \sim_{\mathbb{P}^*} \hat{\nu}$, where $\sim_{\mathbb{P}^*}$ denotes equality in distribution under $\mathbb{P}^*$. This is sufficient for the two expectations in the Lemma to be equal. Although not necessary for our purposes, equality almost surely can be shown by expressing $S_t = \tilde{B}(T - t)$ and $\hat{S}_t = \hat{B}$ in terms of the Brownian motion W^* analogous to the proof of Lemma III.2 in Appendix III.A.1. □

Note that since S is a Markov process with time-homogeneous increments, we obtain a similar result when conditioning on the sigma algebra $\mathcal{F}_t$ and defining $\hat{\nu}$ to be the first hitting time of the asset S to the constant the barrier $\hat{B} = \tilde{B}(T - t)$. Lemma III.15 corresponds to the special case where $t = 0$. Next, we formally setup the valuation problem in this section.

Definition III.8 (Pay-at-Hit Bond Binary Valuation Problem).
Let $\tilde{B}(\tau) = \tilde{B}(0)\mathrm{e}^{\gamma\tau}$ be an exponential boundary. $\tilde{V}(S,\tau)$ is an exponential barrier pay-at-hit bond binary valuation problem if it satisfies

$$\begin{aligned} \mathcal{L}\{\tilde{V}\}(S,\tau) &= 0 \qquad \text{for } (S,\tau) \in \mathcal{D}, \\ \tilde{V}(S,0) &= 0, \\ \tilde{V}\big(\tilde{B}(\tau),\tau\big) &= 1 \qquad \text{for } \tau \in [0,\infty), \end{aligned}$$

where the active domain $\mathcal{D} \subseteq \mathbb{R}_+^2$ is given by

$$\mathcal{D} = \big\{(S,\tau) : \psi S > \psi\tilde{B}(\tau),\, \tau \in (0,\infty)\big\}$$

and $\psi \in \{-1,+1\}$ indicates an upper or lower boundary. $\triangle$

As a consequence of Lemma III.15, we can use the well-known formula for perpetual American binary options on dividend paying stocks as a component to value the exponential barrier rebate; see for example Chapter 9 in Wilmott (2006), pp. 151–168. Lemma III.16 provides the corresponding result.

Lemma III.16 (Decomposition of the Valuation Problem).
Let $\tilde{V}(S,\tau)$ satisfy an exponential barrier pay-at-hit bond binary valuation problem. Then its solution can be decomposed as

$$\tilde{V}(S,\tau) = U^{\psi}_{\tilde{B}(\tau)}(S) - \tilde{V}^1(S,\tau).$$

Here, $U^{\psi}_{\xi}(\hat{S})$ is the valuation function of a constant barrier perpetual American bond binary on the asset $\hat{S}$ with dividend yield $\delta - \gamma$ defined in Lemma III.15 and strike price ξ. It is given by

$$U^{\psi}_{\xi}(\hat{S}) = \left(\frac{\hat{S}}{\xi}\right)^{\beta(-\psi)},$$

where

$$\begin{aligned} \beta(\psi) &= \alpha + \psi\sigma^2\sqrt{\lambda + \alpha^2}, \\ \alpha &= \frac{1}{2} - \frac{r-\delta+\gamma}{\sigma^2}, \\ \lambda &= \frac{2r}{\sigma^2}. \end{aligned}$$

In particular, α is the same expression as the one given in Definition III.5 for the image operator. $\tilde{V}^1(\hat{S},\tau)$ is a contingent claim on the asset $\hat{S}$, which satisfies for $\tau^* \in [0,\tau]$

$$\begin{aligned} \mathcal{L}\{\tilde{V}^1\}(\hat{S},\tau^*) &= 0 \qquad \textit{for } (\hat{S},\tau^*) \in \mathcal{D}, \\ \tilde{V}^1(\hat{S},0) &= U^{\psi}_{\tilde{B}(\tau)}(\hat{S}), \\ \tilde{V}^1(\tilde{B}(\tau),\tau^*) &= 0 \qquad \textit{for } \tau^* \in [0,\tau], \end{aligned}$$

where

$$\mathcal{D} = \{(\hat{S},\tau^*) : \psi\hat{S} > \psi\tilde{B}(\tau),\ \tau^* \in (0,\tau]\}.$$

Proof Using Lemma III.15, we first construct the equivalent constant barrier valuation problem. A finite maturity American bond binary then corresponds to initially taking a long position in the otherwise identical perpetual claim and closing it out at the maturity given that the constant barrier $\tilde{B}(\tau)$ has not been breached by any spot price $\hat{S}_{\tau^*}$ over the interval $\tau^* \in [0,\tau]$. See Appendix III.D.1 for details on the decomposition. For completeness, Appendix III.D.2 derives the valuation functions for perpetual American bond binaries. □

Remark. Note that all valuation functions in Section III.8, such as $U^{\psi}_{\xi}(\hat{S})$ and $\tilde{V}^1(\hat{S},\tau)$, correspond to the auxiliary asset $\hat{S}$ with a modified dividend yield. We make this explicit in their definition. When using them to value the pay-at-hit bond binary, we evaluate them at the current price of the asset S since the auxiliary asset $\hat{S}$ is constructed such that their initial values agree; see Lemma III.15 and the discussion following it.

Also note that for consistency with our previous notation, we use the unusual convention that $\psi = +1$ ($\psi = -1$) corresponds to a perpetual American call (put) bond binary. The valuation function $\tilde{V}^1(\hat{S},\tau)$ in Lemma III.16 can be computed using Proposition III.1. As an intermediate step, we need to obtain the solution for the corresponding full-range problem. However, the terminal payoff is neither a standard bond nor an standard asset binary. Instead, it can be regarded as the multiple of a power binary on the asset $\hat{S}$. In Sections III.8.2 through III.8.4, when considering deferred start and/or piecewise exponential barriers, we also need to be able to price higher-order power binaries. Definition III.9 and Proposition III.8 formalize this and provide the corresponding valuation functions. It should be noted that various definitions of power options can be found in the literature. A standard reference is Heynen and Kat (1996), who obtain solutions for first-order power binaries and use them as building blocks for more complex power and parabola options.

Definition III.9 ($\boldsymbol{n}$-th Order Power Binaries).
Let $\boldsymbol{s}$, $\boldsymbol{\xi}$ and $\boldsymbol{T}$ be as in Definition III.6. The n-th power binary $\mathcal{P}$ with exponent η on the asset S has the time T_n payoff

$$^{\eta}\mathcal{P}^{\boldsymbol{s}}_{\boldsymbol{\xi}}\left(\boldsymbol{S_T}, T_n\right) = S^{\eta}_{T_n} 1_n \left\{\operatorname{diag}(\boldsymbol{s})\boldsymbol{S_T} > \operatorname{diag}(\boldsymbol{s})\boldsymbol{\xi}\right\}. \qquad \triangle$$

Proposition III.8 (Valuation of $\boldsymbol{n}$-th Order Power Binaries).
The time $0 \leq t \leq T_1$ value of the n-th order power binary is given by

$$^{\eta}\mathcal{P}^{\boldsymbol{s}}_{\boldsymbol{\xi}}(S, t) = S^{\eta} \exp\left\{\left((\eta - 1)\left(r + \frac{1}{2}\eta\sigma^2\right) - \eta\delta\right)\tau_n\right\}\mathcal{N}_n\left(\operatorname{diag}(\boldsymbol{s})\boldsymbol{d}_{\eta}; \boldsymbol{C}\right).$$

Here, $\boldsymbol{d}_{\eta} = (d_{\eta,1}, d_{\eta,2}, \ldots, d_{\eta,n})' \in \mathbb{R}^n$ is a n-dimensional column vector defined by

$$d_{\eta,i} = \frac{\ln\left(S/\xi_i\right) + \left(r - \delta + \left(\eta - \frac{1}{2}\right)\sigma^2\right)\tau_i}{\sigma\sqrt{\tau_i}},$$

where $\tau_i = T_i - t$ is the i-th time-to-maturity and the correlation matrix $\boldsymbol{C}$ is as in Proposition III.4.

Proof Just like Proposition III.4, this result is a special case of the generalized $\mathbb{M}$ binary valuation equation given in Theorem 1 in Skipper and Buchen (2003), pp. 10–12, when there is only a single underlying asset. $\square$

Note that the bond and asset binaries in Definition III.6 can be considered special cases of power binaries when $\eta = 0$ and $\eta = 1$ respectively, that is $\mathcal{B}^{\boldsymbol{s}}_{\boldsymbol{\xi}}(S, \tau) = {}^{0}\mathcal{P}^{\boldsymbol{s}}_{\boldsymbol{\xi}}(S, \tau)$ and $\mathcal{A}^{\boldsymbol{s}}_{\boldsymbol{\xi}}(S, \tau) = {}^{1}\mathcal{P}^{\boldsymbol{s}}_{\boldsymbol{\xi}}(S, \tau)$. We choose to only introduce power binaries at this point, since they are less common in the literature and only required in their full generality to value pay-at-hit rebates.

Proposition III.9 (Delta of n-th Order Power Binaries).
Let $\boldsymbol{\alpha}_\eta = \operatorname{diag}(\boldsymbol{s})\boldsymbol{d}_\eta$. The time $0 \leq t \leq T_1$ first-order asset price sensitivity of the n-th order power binary is given by

$$\begin{aligned}\frac{\partial^\eta \mathcal{P}^{\boldsymbol{s}}_{\boldsymbol{\xi}}}{\partial S}(S,t) &= S^{\eta-1}\exp\left\{\left((\eta-1)\left(r+\frac{1}{2}\eta\sigma^2\right)-\eta\delta\right)\tau\right\}\Bigg(\mathcal{N}_n\left(\boldsymbol{\alpha}_\eta;\boldsymbol{C}\right)\\ &\quad+\sum_{i=1}^{n}\frac{s_i}{\sigma\sqrt{\tau_i}}\mathcal{N}'\left(\alpha_{\eta,i}\right)\mathcal{N}_{n-1}\big(\hat{\boldsymbol{\alpha}}_{\eta,i};\hat{\boldsymbol{C}}_i\big)\Bigg),\end{aligned}$$

where $\hat{\boldsymbol{\alpha}}_{\eta,i}$ and $\hat{\boldsymbol{C}}_i$ are defined analogous to Proposition III.5.

Proof The proof is fully analogous to that of Proposition III.5 and thus omitted. □

After laying the groundwork, we can now state the main result of this section.

Proposition III.10 (Pay-at-Hit Bond Binary Valuation).
Let $\tilde{V}(S,\tau)$ satisfy an exponential barrier pay-at-hit bond binary valuation problem. Then its solution is given by

$$\begin{aligned}\tilde{V}(S,\tau) &= U^{\psi}_{\tilde{B}(\tau)}(S) - \tilde{B}^{-\beta(-\psi)}(\tau)\Big({}^{\beta(-\psi)}\mathcal{P}^{\psi}_{\tilde{B}(\tau)}(S,\tau) - \overset{\tilde{B}(\tau),0,\tau}{\mathcal{I}}\left\{{}^{\beta(-\psi)}\mathcal{P}^{\psi}_{\tilde{B}(\tau)}(S,\tau)\right\}\Big)\\ &= \left(\frac{S}{\tilde{B}(\tau)}\right)^{\beta(-\psi)}\mathcal{N}\left(-\psi d_{\beta(-\psi)}\right)+\left(\frac{S}{\tilde{B}(\tau)}\right)^{\beta(\psi)}\mathcal{N}\left(-\psi d_{\beta(\psi)}\right),\end{aligned}$$

where all contingent claims are on the asset $\hat{S}$ with dividend yield $\delta-\gamma$ defined in Lemma III.15, $\beta(\psi)$, α and λ are as in Lemma III.16 and

$$d_{\beta(\psi)} = \frac{\ln\big(S/\tilde{B}(\tau)\big)+\psi\sigma^2\sqrt{\lambda+\alpha^2}\tau}{\sigma\sqrt{\tau}}.$$

Proof We use Definition III.9 to express the valuation function for the full-range problem $V^1_{\tilde{B}(\tau)}\big(\hat{S},\tau\big)$ corresponding to $V^1\big(\hat{S},\tau\big)$ in Lemma III.16 in terms of a power binary whose value is given by Proposition III.8. The valuation function for $V^1\big(\hat{S},\tau\big)$ then follows by the method of images; see Proposition III.1. Finally, the value of the exponential barrier pay-at-hit bond binary follows from Lemma III.16. To obtain the second expression, we substitute for the option values and combine terms. All details are given in Appendix III.D.3. □

The constant barrier pay-at-hit bond binary valuation function in Proposition III.10 is well-known; see for example Reiner and Rubinstein (1991a). Thus, if our sole interest lies in pricing exponential barrier pay-at-hit bond binaries, then we could resort to these results after establishing the equivalent constant barrier valuation problem in Lemma III.15. However, they are usually obtained by an explicit integration over the first hitting time PDF in Lemma III.2. While this approach has to yield the same final solution, it does not immediately reveal the underlying structure in terms of perpetual American and power binaries and their respective images. Yet it is this decomposition that, together with the valuation formula for higher-order power binaries in Proposition III.8, allows us to solve the deferred start and/or piecewise exponential barrier valuation problems in the following sections.

III.8.2 Deferred Start Exponential Barrier Rebate

The option value $\tilde{V}^{\mathrm{ds}}(S,\tau)$ satisfies

$$\begin{aligned}
\mathcal{L}\{\tilde{V}^{\mathrm{ds}}\}(S,\tau) &= 0 \qquad \text{for } (S,\tau) \in \mathbb{R}_+ \times (\hat{\tau}_S, \infty)\,, \\
\tilde{V}^{\mathrm{ds}}(S,\hat{\tau}_S) &= \tilde{V}(S,\hat{\tau}_S)\, 1\{\psi S > \psi \tilde{B}(\hat{\tau}_S)\} + 1\{\psi S < \psi \tilde{B}(\hat{\tau}_S)\}.
\end{aligned}$$

Compared to Section III.7.1, a violation of the barrier at the beginning of the monitoring period now leads to an immediate unit payoff. Using Corollary III.3 together with Proposition III.10 yields

$$\begin{aligned}
\tilde{V}^{\mathrm{ds}}(S,\tau) = {} & \tilde{B}^{-\beta(-\psi)}(\hat{\tau}_S) \Big({}^{\beta(-\psi)}\mathcal{P}^{\psi}_{\tilde{B}(\hat{\tau}_S)}\left(S\mathrm{e}^{-\gamma\tau_S}, \tau_S\right) \\
& - {}^{\beta(-\psi)}\mathcal{P}^{\psi\psi}_{\tilde{B}(\hat{\tau}_S)\tilde{B}(\hat{\tau}_S)}\left(S\mathrm{e}^{-\gamma\tau_S}, \tau_S, \tau\right) \\
& + \overset{\tilde{B}(\hat{\tau}_S),0,\tau}{\mathcal{I}} \left\{ {}^{\beta(-\psi)}\mathcal{P}^{-\psi\psi}_{\tilde{B}(\hat{\tau}_S)\tilde{B}(\hat{\tau}_S)}\left(S\mathrm{e}^{-\gamma\tau_S}, \tau_S, \tau\right) \right\} \Big) + \mathcal{B}^{-\psi}_{\tilde{B}(\hat{\tau}_S)}\left(S\mathrm{e}^{-\gamma\tau_S}, \tau_S\right),
\end{aligned}$$

where again all contingent claims are on the asset $\hat{S}$ with dividend yield $\delta - \gamma$ defined in Lemma III.15. Adjusting the initial spot price is necessary to obtain the correct underlying asset prices at the barrier start date. While the logarithmic returns of the actual underlying S have a risk-neutral drift of $r - \delta - \frac{1}{2}\sigma^2$, those of the asset $\hat{S}$ that we use for pricing have a risk-neutral drift of $r - \delta + \gamma - \frac{1}{2}\sigma^2$; that is for a positive (negative) value of the bending coefficient γ, the drift of $\hat{S}$ is too high (low) and we compensate by adjusting the initial value downwards (upwards).

III.8.3 Piecewise Exponential Barrier Rebate

When the barrier is continuously monitored and given by a piecewise exponential function as in Section III.6.3, then the option value $\tilde{V}^{\mathrm{pe}}(S,\tau)$ satisfies

$$\begin{aligned}
\mathcal{L}\big\{\tilde{V}^{\mathrm{pe}}\big\}(S,\tau) &= 0 \qquad \text{for } (S,\tau)\in\mathcal{D},\\
\tilde{V}^{\mathrm{pe}}\left(S,\hat{\tau}_B\right) &= \tilde{V}\left(S,\hat{\tau}_B\right),\\
\tilde{V}^{\mathrm{pe}}\big(\tilde{B}(\tau),\tau\big) &= 1 \qquad \text{for } \tau\in[\hat{\tau}_B,\infty)\,,
\end{aligned}$$

where

$$\mathcal{D}=\big\{(S,\tau):\psi S>\psi\tilde{B}(\tau),\,\tau\in(\hat{\tau}_B,\infty)\,\big\}.$$

Analogously to Section III.7.3, we use Lemma III.11 to separately value the rebate before and after the bending change date. The valuation problem $\tilde{V}^{\mathrm{pe},1}(S,\tau)$ for the rebate before the bending change date alone is given by

$$\begin{aligned}
\mathcal{L}\big\{\tilde{V}^{\mathrm{pe},1}\big\}(S,\tau) &= 0 \qquad \text{for } (S,\tau)\in\mathcal{D},\\
\tilde{V}^{\mathrm{pe},1}\left(S,\hat{\tau}_B\right) &= 0,\\
\tilde{V}^{\mathrm{pe},1}\big(\tilde{B}(\tau),\tau\big) &= 1 \qquad \text{for } \tau\in[\hat{\tau}_B,\infty)\,.
\end{aligned}$$

By Proposition III.10 it has the solution

$$\begin{aligned}
\tilde{V}^{\mathrm{pe},1}(S,\tau) &= U^{\psi}_{\tilde{B}(\tau)}(S;\kappa)-\tilde{B}^{-\beta(-\psi;\kappa)}(\tau)\Big({}^{\beta(-\psi;\kappa)}\mathcal{P}^{\psi}_{\tilde{B}(\tau)}\left(S,\tau_B;\kappa\right)\\
&\quad-\overset{\tilde{B}(\tau),0,\tau_B}{\mathcal{I}}\left\{{}^{\beta(-\psi;\kappa)}\mathcal{P}^{\psi}_{\tilde{B}(\tau)}\left(S,\tau_B;\kappa\right)\right\}\Big).
\end{aligned}$$

Here, we augmented the notation to make it explicit that the bending parameter κ is used in the computation of the perpetual American bond binary $U^{\psi}_{\xi}(S;\kappa)$, the function $\beta(\psi;\kappa)$ and the power binaries ${}^{\eta}\mathcal{P}^{\boldsymbol{s}}_{\boldsymbol{\xi}}(S,\tau;\kappa)$. That is, the drift of the underlying asset $\hat{S}$ is given by $\delta-\kappa$. This distinction was not necessary in Sections III.8.1 and III.8.2. We choose to only introduce it at this point to not distract from the main problems when deriving the key result in Proposition III.10. The valuation function $\tilde{V}^{\mathrm{pe},2}$ for the rebate after the bending change date satisfies the initial boundary value problem

$$\begin{aligned}
\mathcal{L}\big\{\tilde{V}^{\mathrm{pe},2}\big\}(S,\tau) &= 0 \qquad \text{for } (S,\tau)\in\mathcal{D},\\
\tilde{V}^{\mathrm{pe},2}\left(S,\hat{\tau}_B\right) &= \tilde{V}\left(S,\hat{\tau}_B\right),\\
\tilde{V}^{\mathrm{pe},2}\big(\tilde{B}(\tau),\tau\big) &= 0.
\end{aligned}$$

Analogous to Section III.7.3, the solution to the corresponding full-range problem $\tilde{V}^{\mathrm{pe},2}_{\tilde{B}(\hat{\tau}_B),\kappa}(S,\tau)$ was obtained as an auxiliary result when valuing the deferred start exponential rebate in Section III.8.2. Using Proposition III.1, we thus obtain

$$
\begin{aligned}
\tilde{V}^{\mathrm{pe},2}(S,\tau) \;=\;& \tilde{B}^{-\beta(-\psi;\gamma)}(\hat{\tau}_B)\Big({}^{\beta(-\psi;\gamma)}\mathcal{P}^{\psi}_{\tilde{B}(\hat{\tau}_B)}\left(S\mathrm{e}^{-\gamma\tau_B},\tau_B;\gamma\right) \\
& -{}^{\beta(-\psi;\gamma)}\mathcal{P}^{\psi\psi}_{\tilde{B}(\hat{\tau}_B)\tilde{B}(\hat{\tau}_B)}\left(S\mathrm{e}^{-\gamma\tau_B},\tau_B,\tau;\gamma\right) \\
& + \overset{\tilde{B}(\hat{\tau}_B),0,\tau}{\mathcal{I}}\left\{{}^{\beta(-\psi;\gamma)}\mathcal{P}^{-\psi\psi}_{\tilde{B}(\hat{\tau}_B)\tilde{B}(\hat{\tau}_B)}\left(S\mathrm{e}^{-\gamma\tau_B},\tau_B,\tau;\gamma\right)\right\} \\
& - \overset{\tilde{B}(\hat{\tau}_B),\kappa,\tau_B}{\mathcal{I}}\left\{{}^{\beta(-\psi;\gamma)}\mathcal{P}^{\psi}_{\tilde{B}(\hat{\tau}_B)}\left(S\mathrm{e}^{-\gamma\tau_B},\tau_B;\gamma\right)\right\} \\
& + \overset{\tilde{B}(\hat{\tau}_B),\kappa,\tau_B}{\mathcal{I}}\left\{{}^{\beta(-\psi;\gamma)}\mathcal{P}^{\psi\psi}_{\tilde{B}(\hat{\tau}_B)\tilde{B}(\hat{\tau}_B)}\left(S\mathrm{e}^{-\gamma\tau_B},\tau_B,\tau;\gamma\right)\right\} \\
& - \overset{\tilde{B}(\hat{\tau}_B),\kappa,\tau_B}{\mathcal{I}}\left\{\overset{\tilde{B}(\hat{\tau}_B),0,\tau}{\mathcal{I}}\left\{{}^{\beta(-\psi;\gamma)}\mathcal{P}^{-\psi\psi}_{\tilde{B}(\hat{\tau}_B)\tilde{B}(\hat{\tau}_B)}\left(S\mathrm{e}^{-\gamma\tau_B},\tau_B,\tau;\gamma\right)\right\}\right\}\Big).
\end{aligned}
$$

Combining these two results yields

$$
\begin{aligned}
\tilde{V}^{\mathrm{pe}}(S,\tau) \;=\;& U^{\psi}_{\tilde{B}(\tau)}(S;\kappa) - \tilde{B}^{-\beta(-\psi;\kappa)}(\tau)\Big({}^{\beta(-\psi;\kappa)}\mathcal{P}^{\psi}_{\tilde{B}(\tau)}\left(S,\tau_B;\kappa\right) \\
& - \overset{\tilde{B}(\tau),0,\tau_B}{\mathcal{I}}\left\{{}^{\beta(-\psi;\kappa)}\mathcal{P}^{\psi}_{\tilde{B}(\tau)}\left(S,\tau_B;\kappa\right)\right\}\Big) \\
& +\tilde{B}^{-\beta(-\psi;\gamma)}(\hat{\tau}_B)\Big({}^{\beta(-\psi;\gamma)}\mathcal{P}^{\psi}_{\tilde{B}(\hat{\tau}_B)}\left(S\mathrm{e}^{-\gamma\tau_B},\tau_B;\gamma\right) \\
& -{}^{\beta(-\psi;\gamma)}\mathcal{P}^{\psi\psi}_{\tilde{B}(\hat{\tau}_B)\tilde{B}(\hat{\tau}_B)}\left(S\mathrm{e}^{-\gamma\tau_B},\tau_B,\tau;\gamma\right) \\
& + \overset{\tilde{B}(\hat{\tau}_B),0,\tau}{\mathcal{I}}\left\{{}^{\beta(-\psi;\gamma)}\mathcal{P}^{-\psi\psi}_{\tilde{B}(\hat{\tau}_B)\tilde{B}(\hat{\tau}_B)}\left(S\mathrm{e}^{-\gamma\tau_B},\tau_B,\tau;\gamma\right)\right\} \\
& - \overset{\tilde{B}(\hat{\tau}_B),\kappa,\tau_B}{\mathcal{I}}\left\{{}^{\beta(-\psi;\gamma)}\mathcal{P}^{\psi}_{\tilde{B}(\hat{\tau}_B)}\left(S\mathrm{e}^{-\gamma\tau_B},\tau_B;\gamma\right)\right\} \\
& + \overset{\tilde{B}(\hat{\tau}_B),\kappa,\tau_B}{\mathcal{I}}\left\{{}^{\beta(-\psi;\gamma)}\mathcal{P}^{\psi\psi}_{\tilde{B}(\hat{\tau}_B)\tilde{B}(\hat{\tau}_B)}\left(S\mathrm{e}^{-\gamma\tau_B},\tau_B,\tau;\gamma\right)\right\} \\
& - \overset{\tilde{B}(\hat{\tau}_B),\kappa,\tau_B}{\mathcal{I}}\left\{\overset{\tilde{B}(\hat{\tau}_B),0,\tau}{\mathcal{I}}\left\{{}^{\beta(-\psi;\gamma)}\mathcal{P}^{-\psi\psi}_{\tilde{B}(\hat{\tau}_B)\tilde{B}(\hat{\tau}_B)}\left(S\mathrm{e}^{-\gamma\tau_B},\tau_B,\tau;\gamma\right)\right\}\right\}\Big).
\end{aligned}
$$

III.8.4 Deferred Start Piecewise Exponential Barrier Rebate

Finally, we consider the valuation of the pay-at-hit rebate linked to a deferred start piecewise exponential barrier option. Its valuation function $\tilde{V}^{\mathrm{ds,pe}}(S,\tau)$ satisfies

$$
\begin{aligned}
\mathcal{L}\big\{\tilde{V}^{\mathrm{ds,pe}}\big\}(S,\tau) &= 0 \qquad \text{for } (S,\tau)\in\mathbb{R}_+\times(\hat{\tau}_S,\infty)\,, \\
\tilde{V}^{\mathrm{ds,pe}}(S,\hat{\tau}_S) &= \tilde{V}^{\mathrm{pe}}(S,\hat{\tau}_S)\,1\big\{\psi S>\psi\tilde{B}(\hat{\tau}_S)\big\}+1\big\{\psi S<\psi\tilde{B}(\hat{\tau}_S)\big\}.
\end{aligned}
$$

Using the results from Sections III.8.1 through III.8.3 in combination with Lemma III.13, we obtain

$$
\begin{aligned}
\tilde{V}^{\mathrm{ds,pe}}(S,\tau) \quad = \quad & \tilde{B}^{-\beta(-\psi;\kappa)}\left(\hat{\tau}_S\right)\Big({}^{\beta(-\psi;\kappa)}\mathcal{P}^{\psi}_{\tilde{B}(\hat{\tau}_S)}\left(S\mathrm{e}^{-\kappa\tau_S},\tau_S;\kappa\right) \\
& -{}^{\beta(-\psi;\kappa)}\mathcal{P}^{\psi\psi}_{\tilde{B}(\hat{\tau}_S)\tilde{B}(\hat{\tau}_S)}\left(S\mathrm{e}^{-\kappa\tau_S},\tau_S,\tau_B;\kappa\right) \\
& + \overset{\tilde{B}(\hat{\tau}_S),0,\tau_B}{\mathcal{I}}\left\{{}^{\beta(-\psi;\kappa)}\mathcal{P}^{-\psi\psi}_{\tilde{B}(\hat{\tau}_S)\tilde{B}(\hat{\tau}_S)}\left(S\mathrm{e}^{-\kappa\tau_S},\tau_S,\tau_B;\kappa\right)\right\}\Big) \\
& +\tilde{B}^{-\beta(-\psi;\gamma)}\left(\hat{\tau}_B\right)\Big({}^{\beta(-\psi;\gamma)}\mathcal{P}^{\psi\psi}_{\zeta_1\tilde{B}(\hat{\tau}_B)}\left(S\mathrm{e}^{-\gamma\tau_B},\tau_S,\tau_B;\gamma\right) \\
& -{}^{\beta(-\psi;\gamma)}\mathcal{P}^{\psi\psi\psi}_{\zeta_1\tilde{B}(\hat{\tau}_B)\tilde{B}(\hat{\tau}_B)}\left(S^{-\gamma\tau_B},\tau_S,\tau_B,\tau;\gamma\right) \\
& + \overset{\tilde{B}(\hat{\tau}_B),0,\tau}{\mathcal{I}}\left\{{}^{\beta(-\psi;\gamma)}\mathcal{P}^{-\psi-\psi\psi}_{\zeta_2\tilde{B}(\hat{\tau}_B)\tilde{B}(\hat{\tau}_B)}\left(S\mathrm{e}^{-\gamma\tau_B},\tau_S,\tau_B,\tau;\gamma\right)\right\} \\
& - \overset{\tilde{B}(\hat{\tau}_B),\kappa,\tau_B}{\mathcal{I}}\left\{{}^{\beta(-\psi;\gamma)}\mathcal{P}^{-\psi\psi}_{\zeta_1\tilde{B}(\hat{\tau}_B)}\left(S\mathrm{e}^{-\gamma\tau_B},\tau_S,\tau_B;\gamma\right)\right\} \\
& + \overset{\tilde{B}(\hat{\tau}_B),\kappa,\tau_B}{\mathcal{I}}\left\{{}^{\beta(-\psi;\gamma)}\mathcal{P}^{-\psi\psi\psi}_{\zeta_1\tilde{B}(\hat{\tau}_B)\tilde{B}(\hat{\tau}_B)}\left(S\mathrm{e}^{-\gamma\tau_B},\tau_S,\tau;\gamma\right)\right\} \\
& - \overset{\tilde{B}(\hat{\tau}_B),\kappa,\tau_B}{\mathcal{I}}\left\{\overset{\tilde{B}(\hat{\tau}_B),0,\tau}{\mathcal{I}}\left\{{}^{\beta(-\psi;\gamma)}\mathcal{P}^{\psi-\psi\psi}_{\zeta_3\tilde{B}(\hat{\tau}_B)\tilde{B}(\hat{\tau}_B)}\left(S\mathrm{e}^{-\gamma\tau_B},\tau_S,\tau_B,\tau;\gamma\right)\right\}\right\} \\
& +\tilde{B}^{-\psi}_{\tilde{B}(\hat{\tau}_S)}\left(S,\tau_S;0\right),
\end{aligned}
$$

where

$$
\begin{aligned}
\zeta_1 &= \tilde{B}\left(\hat{\tau}_S\right)\mathrm{e}^{\gamma(\hat{\tau}_B-\hat{\tau}_S)}, \\
\zeta_2 &= \tilde{B}\left(\hat{\tau}_B\right)\mathrm{e}^{(\kappa-\gamma)(\hat{\tau}_B-\hat{\tau}_S)}, \\
\zeta_3 &= \tilde{B}\left(\hat{\tau}_B\right)\mathrm{e}^{(\kappa-\gamma)(\hat{\tau}_B-\hat{\tau}_S)}.
\end{aligned}
$$

Here, we have carefully adjusted the newly added barrier level $\tilde{B}\left(\hat{\tau}_S\right)$ to account for the shifted initial stock prices as well as the image functions; see Appendix III.D.4 for details.

III.9 Numerical Examples

This section analyzes the distribution of the delta hedging error for short positions knock-out barrier options when the actual underlying dynamics follow a Merton (1976) jump-diffusion process. We show through Monte Carlo simulations that for a fixed initial option price, an exponential bending of the barrier towards the option maturity yields a more robust hedge as opposed to a constant barrier shift. This manifests in lower values for the standard deviation, absolute skewness and excess kurtosis of the hedging error. The mean does not depend on the chosen functional form of the barrier shift.

Following Merton (1976), we assume that the logarithmic returns $X = \{X_t : t \in [0, T^*]\}$ follow a jump-diffusion process with normally distributed jumps. The $\mathbb{P}^*$-dynamics of X are given by

$$X_t = \left(r - \delta - \frac{1}{2}\sigma^2 - \lambda\left(\phi_Y^*(-\mathrm{i}) - 1\right)\right) t + \sigma W_t + \sum_{i=1}^{N_t} Y_i,$$

where $N = \{N_t : t \in [0, T^*]\}$ is a one-dimensional Poisson process with constant intensity $\lambda \in \mathbb{R}_+$ and $(Y_i)_{i \in \mathbb{N}}$ is a sequence of independent identically distributed $\mathcal{N}\left(\alpha, \beta^2\right)$ normal random variables. The characteristic function $\phi_Y^*(\omega)$ of the jump size distribution under $\mathbb{P}^*$ is given by

$$\phi_Y^*(\omega) = \exp\left\{\mathrm{i}\omega\alpha - \frac{1}{2}\omega^2\beta^2\right\}.$$

The compound Poisson process introduces non-normal higher moments to the logarithmic return process. In particular, a non-zero mean jump size α induces a skewness with the same sign and a non-zero jump volatility β induces positive excess kurtosis. These deviations vanish asymptotically as the time horizon becomes large due to the Lindeberg-Lévy central limit theorem. As discussed in Section III.2.1, a non-normal logarithmic return distribution generates a strike dependent IVS. Figure III.11 shows a set of sample IVSs induced by Merton (1976) for a parameter vector that is typical for well-diversified stock indices. The x-axis denotes the scaled moneyness $\ln\left(K/S_0\right)/\sqrt{T}$ in order to facilitate the comparison of different maturities. In accordance with the term-structure of the higher moments, the IVS is strongly convex for short maturities and flattens out for longer times-to-expiration.

In Section III.3, we argue that an exponential bending of the barrier close to the option maturity reflects the time-dependent nature of the jump risk exposure that the hedger of a short position in a knock-out barrier option is exposed to. This hypothesis is evaluated through a Monte Carlo simulation study. Let $\Pi = \{t_0, t_1, t_2, \ldots\}$ be an equally spaced time grid with $t_0 = 0$, $t_i - t_{i-1} = \Delta t$ for all $i \in \mathbb{N}$ and $\Delta t = 1/252$. The same set of model parameters as in Figure III.11 is used to generate 100,000 sample paths of the risky asset on Π. We refer to for example Section 6.1 in Cont and Tankov (2004), pp. 172–178, and Section 3.5.1 in Glasserman (2003), pp. 134–142, for a discussion on efficient simulation approaches. For each knock-out barrier option and sample path, we compute the profit & loss from a self-financing pure delta hedging strategy that is re-adjusted once daily. Let

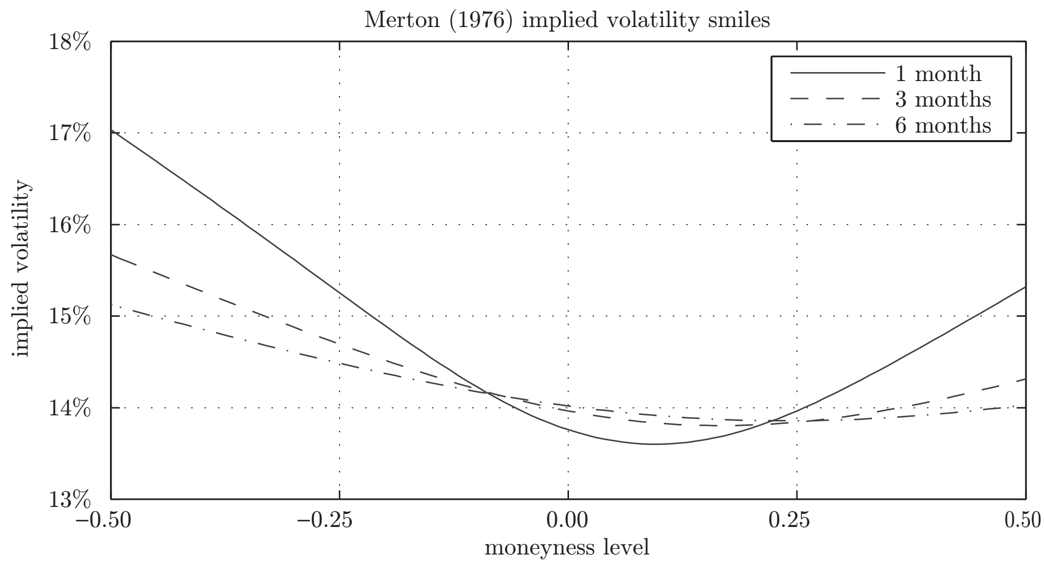

Figure III.11: Sample IVS in the Merton (1976) jump-diffusion model. The model parameters are $S_0 = 100.00$ USD, $r = 5.00\%$, $\delta = 0.00\%$, $\sigma = 10.00\%$, $\lambda = 15.00$, $\alpha = -0.50\%$ and $\beta = 2.50\%$.

$\theta^B = \left\{\theta_t^B : t \in [0, T^*]\right\}$ and $\theta^S = \left\{\theta_t^S : t \in [0, T^*]\right\}$ be the positions in the money market account and the risky asset, respectively. The value process $P = \{P_t : t \in [0, T^*]\}$ of the hedge portfolio is then given by

$$P_t = \theta_t^B B_t + \theta_t^S S_t,$$

where $P_0 = V(S_0, 0)$ is the initial value of the contingent claim. The portfolio weights satisfy

$$\begin{aligned} \theta_t^S &= \begin{cases} \partial V / \partial S \left(S_{t_i}, t_i\right) & \text{if } \nu > t_i \\ 0 & \text{otherwise} \end{cases} \qquad \forall t \in [t_i, t_{i+1}), \\ \theta_t^B &= \frac{P_{t_i} - \theta_{t_i}^S S_{t_i}}{B_{t_i}} \qquad \forall t \in [t_i, t_{i+1}), \end{aligned}$$

where the first hitting time ν of the asset S to the constant barrier B on the grid Π is defined as

$$\nu = \min\left\{i \in \mathbb{N}_0 : \psi S_{t_i} \leq \psi B\right\}.$$

Finally, the hedging error is given by

$$\mathcal{E} = P_T - V(S_T, T).$$

Note that the portfolio process is constructed such that the delta hedge position in unwound upon the knock-out event. The money market account position also stays unchanged until the contractual option maturity while the portfolio values are compounded at the risk-free interest rate. This ensures that the hedging error always corresponds to a value as of the contractual maturity date and can thus be compared across different sample paths.

Figure III.12 shows the first four simulated moments of the hedging error for a down & out put option with a maturity of one year and a barrier equal to 85% of the initial spot price. We compare the profit & loss of using a constant barrier shift between -0.50% and -2.00% to that of a barrier which is first constant at -0.50% and then exponentially bends to levels between -0.50% and -3.00% over the last three months before maturity. We consider one functional form of the barrier shift to yield more stable hedges than another one, if the absolute higher moments of its hedging errors are lower conditional on the same initial option price. To facilitate the comparison between the constant barrier shift and the exponential bending approaches, we thus plot the simulated moments as a function of the corresponding fair values. To account for the noise in the observations, we fit second order polynomials through each set of data points.

Figure III.12.a demonstrates that for any fixed initial option price, the mean hedging error does not depend on the functional form of the barrier. This is not surprising since our simulation is carried out under the risk-neutral probability measure, where the expected return using any admissible trading strategy is the same and equal to the risk-free interest rate.

Figures III.12.b through III.12.d provide strong support for our hypothesis that an exponential bending of the barrier close to maturity yields most robust hedges. As shown in Figure III.12.b shows that the volatility of the hedging error is consistently lower, with the difference being more pronounced for higher initial option prices. The reason is that large parallel barrier shifts yield a high expected windfall profit when the barrier option is knocked-out relatively early after inception. This in accordance with our reasoning in Section III.3. It also explains the large positive skewness of parallel barrier shift in Figure III.12.c. Finally, Figure III.12.d shows that the excess kurtosis is consistently lower under the exponentially bent barrier. This can be explained by fewer large and positive (negative) hedging errors for long (short) times-to-maturity. That is, the number of both

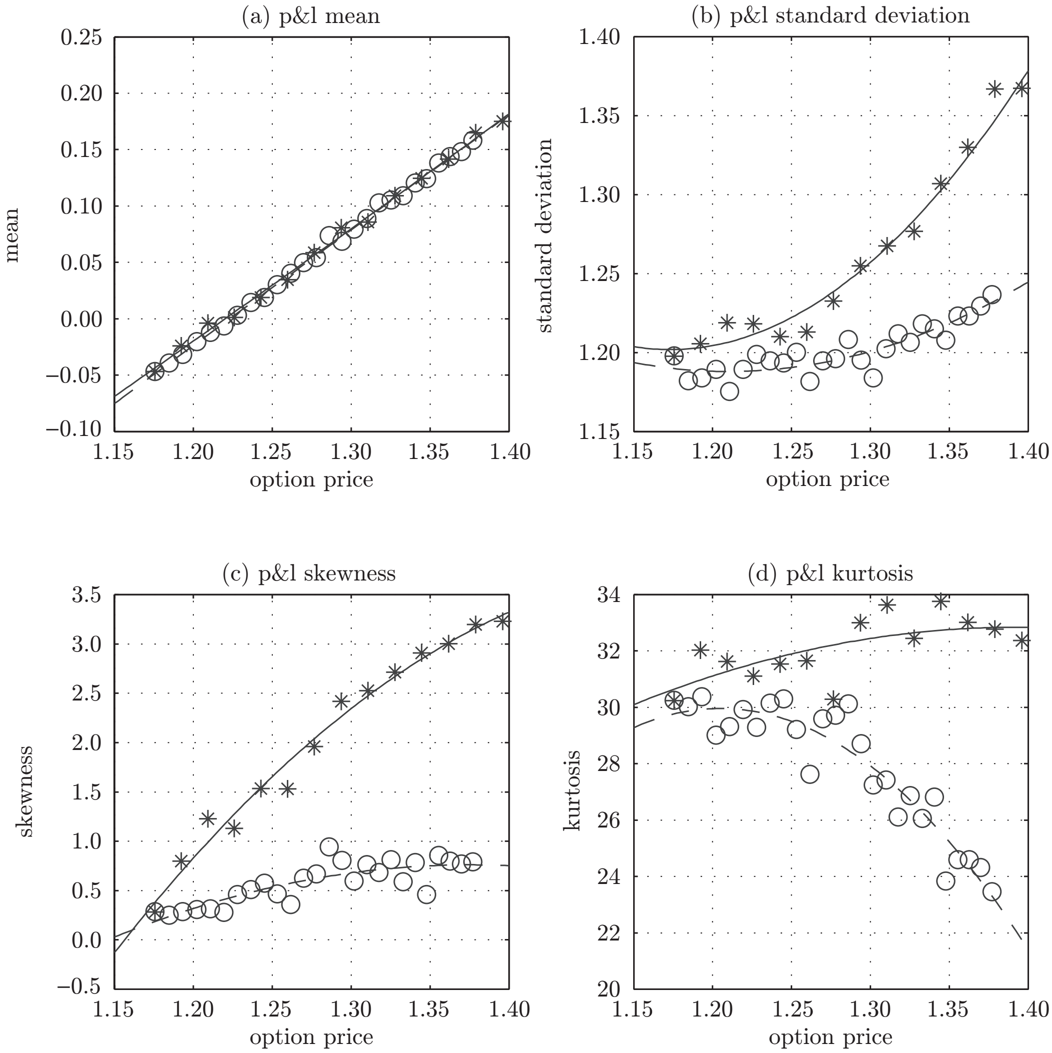

Figure III.12: Simulated moments of the delta hedging error for a down & out put when the actual spot price dynamics follow a Merton (1976) jump-diffusion process. The stars correspond to a constant barrier shift between -0.50% and -2.00%. The circles correspond to a barrier which is first constant at -0.50% and then exponentially bends to levels between -0.50% and -3.00% over the last three months before maturity. The simulation is based on 100,000 paths and daily re-balancing. The common contract and market parameters are $T = 1.00$, $K = 100.00$ USD, $B = 85.00$ USD and $S_0 = 100.00$ USD. The parameters of the jump-diffusion process are as in Figure III.11.

large windfall profits and large losses induced through jumps that breach the barrier is reduced.

We emphasize that the parameters of the exponential bending function used in this example are not optimally chosen. In Section III.3.3, we characterize the optimal parameter vector as the one that minimizes the variance of the hedging error conditional on a fixed mean profit & loss. In Figure III.12 however, we fix the initial barrier shift as well as the bending start time and only vary the final barrier shift. Consequently, an optimal choice of the full parameter vector would further improve the robustness of the delta hedges. Finding a computationally feasible solution to this problem is a topic of future research.

III.10 Conclusion

We develop a unified approach to a volatility smile adjusted pricing and more robust risk management of barrier options within the Black and Scholes (1973) framework. Closed-form solutions for deferred start barrier options and the corresponding rebates are obtained. In the first part of this chapter, we propose to model the barrier shift through a functional form that mimics the time-dependent risk exposure faced by the hedger of a short position in a knock-out barrier option. The option price is further adjusted to account for the distributional information embedded in the market implied volatilities. This yields a valuation problem in terms of a piecewise exponential barrier. The second part of this chapter derives closed-form solutions for these contingent claims using the method of images. The corresponding valuation equations can be expressed in terms of higher-order power binaries. Their computational implementation is straightforward and numerically stable. Finally, we confirm through hedging simulations that our proposed piecewise exponential barrier shift indeed reduces the absolute higher moments of the profit & loss distribution thus yielding more robust hedges.

Future research could further investigate the link between the exponentially bent barrier approach proposed in this chapter and the leverage constraint replication portfolio analyzed by Schmock et al. (2001, 2002), as briefly discussed in Section III.3.5. Furthermore, this chapter characterizes the problem of optimally choosing the parameters of the exponentially bent barriers in Section III.3.3 and gives examples in Section III.9.

However, it remains a topic of future research to find a computationally feasible solution to the optimization problem and analyze its properties.

Bibliography

Balieiro Filho, Ruy Gabriel and Rogerio Rosenfeld (2004) "Testing Option Pricing with the Edgeworth Expansion," *Physica A: Statistical Mechanics and Its Applications*, Vol. 344, No. 3–4, pp. 484–490.

Barndorff-Nielsen, Ole E. and Neil G. Shephard (2001a) "Modelling by Lévy Processes for Financial Econometrics," in Ole E. Barndorff-Nielsen, Thomas Mikosch, and Sidney I. Resnick eds. *Lévy Processes - Theory and Applications*: Birkhäuser, pp. 283–318.

——— (2001b) "Non-Gaussian Ornstein-Uhlenbeck-Based Models and Some of Their Uses in Financial Economics," *Journal of the Royal Statistical Society - Series B*, Vol. 63, No. 2, pp. 167–241.

Barone-Adesi, Giovanni, Nicola Fusari, and John Theal (2007) "Barrier Option Pricing Using Adjusted Transition Probabilities," Research Paper 07-02, Swiss Finance Institute.

Bates, David S. (1996) *Statistical Methods in Finance*, Vol. 14 of Handbook of Statistics, Chap. Testing Option Pricing Models, pp. 567–61: North Holland.

Black, Fischer and Myron S. Scholes (1973) "The Pricing of Options and Corporate Liabilities," *Journal of Political Economy*, Vol. 3, No. 3, pp. 637–654.

Bowie, Jonathan and Peter P. Carr (1994) "Static Simplicity," *Risk*, pp. 44–50.

Boyle, Phelim P. (1977) "Options: A Monte Carlo Approach," *Journal of Financial Economics*, Vol. 4, pp. 323–338.

Boyle, Phelim P. and Sok Hoon Lau (1994) "Bumping up against the Barrier with the Binomial Method," *Journal of Derivatives*, Vol. 1, No. 4, pp. 6–14.

Breeden, Douglas T. and Robert H. Litzenberger (1978) "Prices of State-Contingent Claims Implicit in Option Prices," *Journal of Business*, Vol. 51, No. 4, pp. 621–651.

Broadie, Mark, Jaksa Cvitanić, and H. Mete Soner (1998) "Optimal Replication of Contingent Claims under Portfolio Constraints," *Review of Financial Studies*, Vol. 11, No. 1, pp. 59–79.

Broadie, Mark and Paul Glasserman (1997) "A Continuity Correction for Discrete Barrier Options," *Mathematical Finance*, Vol. 7, No. 4, pp. 325–348.

Brockhaus, Oliver, Michael Farkas, Andrew Ferraris, Douglas Long, and Marcus Overhaus (2000) *Equity Derivatives and Market Risk Models*: Risk Books.

Buchen, Peter W. (2001a) "Q-Options and Dual-Expiry Exotics," working paper, School of Mathematics and Statistics, University of Sydney.

——— (2001b) "Image Options and the Road to Barriers," *Risk Magazine*, Vol. 14, No. 9, pp. 127–130.

——— (2004) "The Pricing of Dual-Expiry Exotics," *Quantitative Finance*, Vol. 4, No. 1, pp. 101–108.

Buchen, Peter W. and Otto Konstandatos (2005) "A New Method of Pricing Lookback Options," *Mathematical Finance*, Vol. 15, No. 2, pp. 245–259.

——— (2009) "A New Approach to Pricing Double-Barrier Options with Arbitrary Payoffs and Exponential Boundaries," *Applied Mathematical Finance*, Vol. 16, No. 6, pp. 497–515.

Carr, Peter P. (1995) "Two Extensions to Barrier Option Valuation," *Applied Mathematical Finance*, Vol. 2, pp. 173–209.

Carr, Peter P., Katrina Ellis, and Vishal Gupta (1998) "Static Hedging of Exotic Options," *Journal of Finance*, Vol. 53, No. 3, pp. 1165–1190.

Carr, Peter P., Hélyette Geman, Dilip B. Madan, and Marc Yor (2003) "Stochastic Volatility for Lévy Processes," *Mathematical Finance*, Vol. 13, No. 3, pp. 345–382.

Cont, Rama and Peter Tankov (2004) *Financial Modelling with Jump Processes*: Chapman & Hall.

Corrado, Charles J. and Thomas W. Jr. Miller (1996) "A Note on a Simple Accurate Formula to Compute Implied Standard Deviations," *Journal of Banking & Finance*, Vol. 20, No. 3, pp. 595–603.

Cox, John C. and Mark Rubinstein (1985) *Options Markets*: Prentice-Hall.

Cvitanić, Jaksa and Ioannis Karatzas (1993) "Hedging Contingent Claims with Constrained Portfolios," *The Annals of Applied Probability*, Vol. 3, No. 3, pp. 652–581.

Derman, Emanuel, Deniz Ergener, and Iraj Kani (1994) "Static Options Replication," Quantitative Strategies Research Notes, Goldman Sachs.

Derman, Emanuel, Iraj Kani, Deniz Ergener, and Indrajit Bardhan (1995a) "Enhanced Numerical Methods for Options with Barriers," Quantitative Strategies Research Notes, Goldman Sachs.

Derman, Emanuel, Iraj Kani, and Joseph Z. Zou (1995b) "The Local Volatility Surface: Unlocking the Information in Index Option Prices," Quantitative Strategies Research Notes, Goldman Sachs.

Deutscher Derivate Verband (2013) "Marktvolumen von Derivativen Wertpapieren," Mar. available at http://www.deutscherderivateverband.de.

Duffie, Darrell, Jun Pan, and Kenneth Singleton (2000) "Transform Analysis and Asset Pricing for Affine Jump-Diffusions," *Econometrica*, Vol. 68, No. 6, pp. 1343–1376.

Dupire, Bruno (1994) "Pricing with a Smile," *Risk Magazine*, Vol. 7, No. 1, pp. 18–20.

Ekstrand, Christian (2011) *Financial Derivatives Modeling*: Springer.

El Karoui, Nicole and Marie-Claire Quenez (1995) "Dynamic Programming and Pricing of Contingent Claims in an Incomplete Market," *SIAM Journal of Control and Optimization*, Vol. 33, No. 1, pp. 29–66.

Fengler, Matthias R. (2006) *Semiparametric Modelling of Implied Volatility*, Springer Finance: Springer.

——— (2009) "Arbitrage-Free Smoothing of the Implied Volatility Surface," *Quantitative Finance*, Vol. 9, No. 4, pp. 417–428.

Gatheral, Jim (2004) "A Parsimonious Arbitrage-Free Implied Volatility Parametrization with Application to the Valuation of Volatility Derivatives," Conference Presentation, Global Derivatives & Risk Management Conference, Madrid.

——— (2006) *The Volatility Surface: A Practitioner's Guide*: Wiley Finance.

Gatheral, Jim and Antoine Jacquier (2012) "Arbitrage-Free SVI Volatility Surfaces," Preprint available at http://arxiv.org/abs/1204.0646.

Geman, Hélyette and Marc Yor (1996) "Pricing and Hedging Double Barrier Options: A Probabilistic Approach," *Mathematical Finance*, Vol. 6, No. 4, pp. 365–378.

Glasserman, Paul (2003) *Monte Carlo Methods in Financial Engineering*, Vol. 53 of Stochastic Modelling and Applied Probability: Springer.

Greene, William H. (2008) *Econometric Analysis*: Pearson Prentice Hall, 6th edition.

Haug, Espen Gaarder (2007) *The Complete Guide to Option Pricing Formulas*: McGraw-Hill, 2nd edition.

Heston, Steven L. (1993) "A Closed-Form Solution for Options with Stochastic Volatility with Applications to Bond and Currency Options," *Review of Financial Studies*, Vol. 6, No. 2, pp. 327–343.

Heynen, Ronald C. and Harry M. Kat (1994a) "Partial Barrier Options," *Journal of Financial Engineering*, Vol. 3, No. 3/4, pp. 253–274.

——— (1994b) "Crossing Barriers," *Risk Magazine*, Vol. 7, No. 6, pp. 46–51.

——— (1996) "Pricing and Hedging Power Options," *Financial Engineering and the Japanese Markets*, Vol. 3, No. 3, pp. 253–261.

Hui, Cho H. (1996) "One-Touch Double Barrier Binary Option Values," *Applied Financial Economics*, Vol. 6, No. 4, pp. 343–346.

——— (1997) "Time-Dependent Barrier Option Values," *Journal of Futures Markets*, Vol. 17, No. 6, pp. 667–688.

Ingersoll, Jonathan E. Jr. (2000) "Digital Contracts: Simple Tools for Pricing Complex Derivatives," *Journal of Business*, Vol. 73, No. 1, pp. 67–88.

Jäckel, Peter (2006) "By Implication," *Wilmott Magazine*, pp. 60–66.

Kamrad, Barida and Peter Ritchken (1991) "Multinomial Approximating Models for Options with k State Variables," *Management Science*, Vol. 37, No. 12, pp. 1640–1652.

Karatzas, Ioannis and Steven E. Shreve (1991) *Brownian Motion and Stochastic Calculus*: Springer, 2nd edition.

Kloeden, Peter E. and Eckhard Platen (1995) *Numerical Solution of Stochastic Differential Equations*: Springer.

Konstandatos, Otto (2003) "A New Framework for Pricing Barrier and Lookback Options," PhD Thesis, University of Sydney.

Kou, Steven G. (2002) "A Jump-Diffusion Model for Option Pricing," *Management Science*, Vol. 48, No. 8, pp. 1086–1101.

Kou, Steven G. and Hui Wang (2003) "First Passage Times of a Jump-Diffusion Process," *Advances in Applied Probability*, Vol. 35, pp. 504–531.

——— (2004) "Option Pricing under a Double Exponential Jump-Diffusion Model," *Management Science*, Vol. 50, No. 9, pp. 1178–1192.

Kunitomo, Naoto and Masayuki Ikeda (1992) "Pricing Options with Curved Boundaries," *Mathematical Finance*, Vol. 2, No. 4, pp. 275–298.

Lee, Roger (2004) "The Moment Formula for Implied Volatility at Extreme Strikes," *Mathematical Finance*, Vol. 14, No. 3, pp. 469–480.

Li, Minqiang and Kyuseok Lee (2011) "An Adaptive Successive Over-Relaxation Method for Computing the Black-Scholes Implied Volatility," *Quanti*, Vol. 11, pp. 1245–1269.

Madan, Dilip B., Peter P. Carr, and Eric C. Chang (1998) "The Variance Gamma Process and Option Pricing," *European Finance Review*, Vol. 2, pp. 79–105.

Merton, Robert C. (1973) "Theory of Rational Option Pricing," *The Bell Journal of Economics and Management Science*, Vol. 4, No. 1, pp. 141–183.

——— (1976) "Option Pricing When Underlying Stock Returns Are Discontinuous," *Journal of Financial Economics*, Vol. 3, No. 1-2, pp. 125–144.

Musiela, Marek and Marek Rutkowski (2005) *Martingale Methods in Financial Modelling*: Springer.

Natenberg, Sheldon (1994) *Option Volatility and Pricing*: McGraw-Hill.

Omberg, Edward (1987) "The Valuation of American Put Options with Exponential Exercise Policies," *Advances in Futures and Options Research*, Vol. 2, pp. 117–142.

Pelsser, Antoon (2000) "Pricing Double Barrier Options Using Laplace Transforms," *Finance and Stochastics*, Vol. 4, No. 1, pp. 95–104.

Protter, Philip E. (2004) *Stochastic Integration and Differential Equations*: Springer, 2nd edition.

Reiner, Eric and Mark Rubinstein (1991a) "Unscrambling the Binary Code," *Risk Magazine*, Vol. 4, pp. 75–83.

——— (1991b) "Breaking down the Barriers," *Risk Magazine*, Vol. 4, No. 8, pp. 28–35.

Rich, Don R. (1994) "The Mathematical Foundations of Barrier Options-Pricing Theory," *Advances in Futures and Options Research*, Vol. 7, pp. 267–311.

Ritchken, Peter (1995) "On Pricing Barrier Options," *Journal of Derivatives*, Vol. 3, No. 2, pp. 19–28.

Rubinstein, Mark (1985) "Nonparametric Tests of Alternative Option Pricing Models Using All Reported Trades and Quotes on the 30 Most Active CBOE Option Classes from August 23, 1976 through August 31, 1978," *Journal of Finance*, Vol. 40, No. 2, pp. 455–480.

——— (1994) "Implied Binomial Trees," *Journal of Finance*, Vol. 49, No. 3, pp. 771–818.

——— (1998) "Edgeworth Binomial Trees," *Journal of Derivatives*, Vol. 5, No. 3, pp. 20–27.

Schmock, Uwe, Steven E. Shreve, and Uwe Wystup (2001) *Foreign Exchange Risk*, Chap. Dealing with Dangerous Digitals: Risk Books.

——— (2002) "Valuation of Exotic Options Under Shortselling Constraints," *Finance and Stochastics*, Vol. 6, No. 2, pp. 143–172.

Schöbel, Rainer and Jianwei Zhu (1999) "Stochastic Volatility with an Ornstein-Uhlenbeck Process: An Extension," *European Finance Review*, Vol. 3, No. 1, pp. 23–46.

Skipper, Max and Peter W. Buchen (2003) "The Quintessential Option Pricing Formula," Working Paper, School of Mathematics and Statistics, University of Sydney.

Taleb, Nassim N. (1996) *Dynamic Hedging: Managing Vanilla and Exotic Options*: John Wiley & Sons.

Tompkins, Robert G. (2001) "Implied Volatility Surfaces: Uncovering Regularities for Options on Financial Futures," *European Journal of Finance*, Vol. 7, No. 3, pp. 198–230.

Veiga, Carlos M. A., Uwe Wystup, and Manuel L. Esquível (2012) "Unifying Exotic Option Closed Formulas," *Review of Derivatives Research*, Vol. 15, No. 2, pp. 99–128.

de Weert, Frans (2008) *Exotic Options Trading*, Wiley Finance: John Wiley & Sons.

Wilmott, Paul (2006) *Paul Wilmott on Quantitative Finance*, Vol. 1: Wiley, 2nd edition.

Wilmott, Paul, Sam Howison, and Jeff Dewynne (1995) *The Mathematics of Financial Derivatives*: Cambridge University Press.

Zhang, Peter G. (1998) *Exotic Options*: World Scientific, 2nd edition.

III.A Appendix for Section III.2

III.A.1 First Hitting Time PDF

This appendix contains the detailed proof of Lemma III.2. First, from Definition III.1 and the solution to the SDE for S, it immediately follows that $S_t = \tilde{B}(T-t)$ when

$$W_t^* + \frac{1}{\sigma}\left(r - \delta + \xi - \frac{1}{2}\sigma^2\right)t = \frac{1}{\sigma}\left(\ln\left(\frac{\tilde{B}(0)}{S_0}\right) + \xi T\right)$$

Now let

$$\lambda = \frac{1}{\sigma}\left(r - \delta + \xi - \frac{1}{2}\sigma^2\right)$$

and define a new probability measure $\hat{\mathbb{P}}$ equivalent to $\mathbb{P}^*$ on $[0, T^*]$ by

$$\frac{\mathrm{d}\hat{\mathbb{P}}}{\mathrm{d}\mathbb{P}^*} = \mathcal{E}_{T^*}\left(-\int_0^{\cdot} \lambda \mathrm{d}W_u^*\right) \qquad \mathbb{P}^*\text{-a.s.,}$$

where $\mathcal{E}$ is the Doléans-Dade exponential martingale. The corresponding Radon-Nikodým derivative process $\xi(\mathbb{P}^*, \hat{\mathbb{P}}) = \{\xi_t(\mathbb{P}^*, \hat{\mathbb{P}}) : t \in [0, T^*]\}$ is given by

$$\xi_t(\mathbb{P}^*, \hat{\mathbb{P}}) = \frac{\mathrm{d}\hat{\mathbb{P}}}{\mathrm{d}\mathbb{P}^*}\bigg|\mathfrak{F}_t = \mathcal{E}_t\left(-\int_0^{\cdot} \lambda \mathrm{d}W_u^*\right) \qquad \mathbb{P}^*\text{-a.s..}$$

It follows by Girsanov's theorem that the process $\hat{W} = \{\hat{W}_t : t \in [0, T^*]\}$ defined by

$$\hat{W}_t = W_t^* + \lambda t \qquad \forall t \in [0, T^*]$$

is a one-dimensional standard Brownian motion under $\hat{\mathbb{P}}$; see for example Theorem III.5.1 in Karatzas and Shreve (1991), p. 191. Next, by the reflection principle for Brownian motion, the first passage time PDF of $\hat{W}$ to a level α is given by

$$\hat{\mathbb{P}}\{\nu \in \mathrm{d}t\} = \frac{|\alpha|}{t\sqrt{2\pi t}} \exp\left\{-\frac{\alpha^2}{2t}\right\} \mathrm{d}t;$$

see for example Equation (II.6.3) in Karatzas and Shreve (1991), p. 80. The corresponding probability under $\mathbb{P}^*$ can then be computed through a change of measure. Using the abstract Bayes rule, see for example Lemma A.1.4 in Musiela and Rutkowski (2005), p.

615, we get

$$\begin{aligned}
\mathbb{P}^*\{\nu \in \mathrm{d}t\} &= \mathbb{E}_{\mathbb{P}^*}\left[1\{\nu \in \mathrm{d}t\}\right] \\
&= \mathbb{E}_{\hat{\mathbb{P}}}\left[\xi_t^{-1}(\mathbb{P}^*, \hat{\mathbb{P}})1\{\nu \in \mathrm{d}t\}\right] \\
&= \mathbb{E}_{\hat{\mathbb{P}}}\left[\exp\left\{\lambda \hat{W}_t - \frac{1}{2}\lambda^2 t\right\} 1\{\nu \in \mathrm{d}t\}\right].
\end{aligned}$$

Now, when $\nu = t$, then $\hat{W}_t = \alpha$ and thus

$$\begin{aligned}
\mathbb{P}^*\{\nu \in \mathrm{d}t\} &= \exp\left\{\lambda\alpha - \frac{1}{2}\lambda^2 t\right\} \hat{\mathbb{P}}\{\tau \in \mathrm{d}t\}. \\
&= \frac{|\alpha|}{t\sqrt{2\pi t}} \exp\left\{-\frac{(\alpha - \lambda t)^2}{2t}\right\} \mathrm{d}t.
\end{aligned}$$

III.B Appendix for Section III.4

III.B.1 General Properties of the Image Operator

This appendix contains the detailed proof of Proposition III.2.

(i) We have

$$\begin{aligned}
& \overset{\tilde{B}(0),\gamma,\tau}{\mathcal{I}} \left\{ \overset{\tilde{B}(0),\gamma,\tau}{\mathcal{I}} \left\{\tilde{V}(S,\tau)\right\}\right\} \\
=\ & \overset{\tilde{B}(0),\gamma,\tau}{\mathcal{I}} \left\{ \left(\frac{S}{\tilde{B}(0)\mathrm{e}^{\gamma\tau}}\right)^{2\alpha} \tilde{V}\left(\frac{\tilde{B}^2(0)\mathrm{e}^{2\gamma\tau}}{S}, \tau\right) \right\} \\
=\ & \left(\frac{S}{\tilde{B}(0)\mathrm{e}^{\gamma\tau}}\right)^{2\alpha} \left(\frac{\tilde{B}(0)\mathrm{e}^{\gamma\tau}}{S}\right)^{2\alpha} \tilde{V}(S,\tau) \\
=\ & \tilde{V}(S,\tau).
\end{aligned}$$

(ii) We have

$$\begin{aligned}
& \overset{\tilde{B}(0),\gamma,\tau}{\mathcal{I}} \left\{a\tilde{U}(S,\tau) + b\tilde{V}(S,\tau)\right\} \\
=\ & \left(\frac{S}{\tilde{B}(0)\mathrm{e}^{\gamma\tau}}\right)^{2\alpha} \left(a\tilde{U}\left(\frac{\tilde{B}^2(0)\mathrm{e}^{2\gamma\tau}}{S}, \tau\right) + b\tilde{V}\left(\frac{\tilde{B}^2(0)\mathrm{e}^{2\gamma\tau}}{S}, \tau\right)\right) \\
=\ & a\left(\frac{S}{\tilde{B}(0)\mathrm{e}^{\gamma\tau}}\right)^{2\alpha} \tilde{U}\left(\frac{\tilde{B}^2(0)\mathrm{e}^{2\gamma\tau}}{S}, \tau\right) + b\left(\frac{S}{\tilde{B}(0)\mathrm{e}^{\gamma\tau}}\right)^{2\alpha} \tilde{V}\left(\frac{\tilde{B}^2(0)\mathrm{e}^{2\gamma\tau}}{S}, \tau\right) \\
=\ & a \overset{\tilde{B}(0),\gamma,\tau}{\mathcal{I}} \left\{\tilde{U}(S,\tau)\right\} + b \overset{\tilde{B}(0),\gamma,\tau}{\mathcal{I}} \left\{\tilde{V}(S,\tau)\right\}.
\end{aligned}$$

(iii) The partial derivatives of the image of $\tilde{V}(S,\tau)$ are given by

$$
\begin{aligned}
&\frac{\partial}{\partial\tau}\overset{\tilde{B}(0),\gamma,\tau}{\mathcal{I}}\left\{\tilde{V}(S,\tau)\right\}\\
= \ &\left(\frac{S}{\tilde{B}(0)\mathrm{e}^{\gamma\tau}}\right)^{2\alpha}\left(-2\alpha\gamma\tilde{V}\left(\frac{\tilde{B}^2(0)\mathrm{e}^{2\gamma\tau}}{S},\tau\right)+2\gamma\frac{\tilde{B}^2(0)\mathrm{e}^{2\gamma\tau}}{S}\frac{\partial\tilde{V}}{\partial S}\left(\frac{\tilde{B}^2(0)\mathrm{e}^{2\gamma\tau}}{S},\tau\right)\right.\\
&\left.+\frac{\partial\tilde{V}}{\partial\tau}\left(\frac{\tilde{B}^2(0)\mathrm{e}^{2\gamma\tau}}{S},\tau\right)\right),
\end{aligned}
$$

$$
\begin{aligned}
&\frac{\partial}{\partial S}\overset{\tilde{B}(0),\gamma,\tau}{\mathcal{I}}\left\{\tilde{V}(S,\tau)\right\}\\
= \ &\left(\frac{S}{\tilde{B}(0)\mathrm{e}^{\gamma\tau}}\right)^{2\alpha}\left(\frac{2\alpha}{S}\tilde{V}\left(\frac{\tilde{B}^2(0)\mathrm{e}^{2\gamma\tau}}{S},\tau\right)-\frac{\tilde{B}^2(0)\mathrm{e}^{2\gamma\tau}}{S^2}\frac{\partial\tilde{V}}{\partial S}\left(\frac{\tilde{B}^2(0)\mathrm{e}^{2\gamma\tau}}{S}\tau\right)\right).
\end{aligned}
$$

and

$$
\begin{aligned}
&\frac{\partial^2}{\partial S^2}\overset{\tilde{B}(0),\gamma,\tau}{\mathcal{I}}\left\{\tilde{V}(S,\tau)\right\}\\
= \ &\left(\frac{S}{\tilde{B}(0)\mathrm{e}^{\gamma\tau}}\right)^{2\alpha}\left(\frac{2\alpha(2\alpha-1)}{S^2}\tilde{V}\left(\frac{\tilde{B}^2(0)\mathrm{e}^{2\gamma\tau}}{S},\tau\right)\right.\\
&\left.+\frac{2(1-2\alpha)\tilde{B}^2(0)\mathrm{e}^{2\gamma\tau}}{S^3}\frac{\partial\tilde{V}}{\partial S}\left(\frac{\tilde{B}^2(0)\mathrm{e}^{2\gamma\tau}}{S},\tau\right)+\frac{\tilde{B}^4(0)\mathrm{e}^{4\gamma\tau}}{S^4}\frac{\partial^2\tilde{V}}{\partial S^2}\left(\frac{\tilde{B}^2(0)\mathrm{e}^{2\gamma\tau}}{S},\tau\right)\right).
\end{aligned}
$$

We have after some simplifications

$$
\begin{aligned}
&-\frac{\partial}{\partial\tau}\overset{\tilde{B}(0),\gamma,\tau}{\mathcal{I}}\left\{\tilde{V}(S,\tau)\right\}+(r-\delta)S\frac{\partial}{\partial S}\overset{\tilde{B}(0),\gamma,\tau}{\mathcal{I}}\left\{\tilde{V}(S,\tau)\right\}\\
&+\frac{1}{2}\sigma^2\frac{\partial^2}{\partial S^2}\overset{\tilde{B}(0),\gamma,\tau}{\mathcal{I}}\left\{\tilde{V}(S,\tau)\right\}-r\overset{\tilde{B}(0),\gamma,\tau}{\mathcal{I}}\left\{\tilde{V}(S,\tau)\right\}\\
= \ &\left(\frac{S}{\tilde{B}(0)\mathrm{e}^{\gamma\tau}}\right)^{2\alpha}\left\{-\frac{\partial\tilde{V}}{\partial\tau}\left(\frac{\tilde{B}^2(0)\mathrm{e}^{2\gamma\tau}}{S},\tau\right)+(r-\delta)\frac{\tilde{B}^2(0)\mathrm{e}^{2\gamma\tau}}{S}\frac{\partial\tilde{V}}{\partial S}\left(\frac{\tilde{B}^2(0)\mathrm{e}^{2\gamma\tau}}{S},\tau\right)\right.\\
&\left.+\frac{1}{2}\sigma^2\frac{\tilde{B}^4(0)\mathrm{e}^{4\gamma\tau}}{S^2}\frac{\partial^2\tilde{V}}{\partial S^2}\left(\frac{\tilde{B}^2(0)\mathrm{e}^{2\gamma\tau}}{S},\tau\right)-r\tilde{V}\left(\frac{\tilde{B}^2(0)\mathrm{e}^{2\gamma\tau}}{S},\tau\right)\right\}
\end{aligned}
$$

and the claim follows.

(iv) Applying the change of variables in Lemma III.6 with $\xi=-\gamma$ yields the initial boundary value problem

$$
\begin{aligned}
\mathcal{H}\{u\}(x,\tau) &= 0 \qquad \text{for } (x,\tau)\in\hat{\mathcal{D}},\\
u(x,0) &= \hat{f}(x),\\
u(b,\tau) &= 0 \qquad \text{for } \tau\in[0,\infty),
\end{aligned}
$$

where $\hat{f}(x)$ is as in Lemma III.6 and

$$\begin{aligned} b &= \ln\left(\tilde{B}(0)\right), \\ \hat{D} &= \{(x,\tau) : \psi x > \psi b, \tau \in (0,\infty)\}. \end{aligned}$$

By the symmetry property of the heat transfer equation, the solution of any initial boundary value problem and its reflection agree on the boundary. Reversing the change of variables yields the result in the original coordinates and for the exponential boundary.

III.B.2 Joint Density of S_t and $\{\tau > t\}$ Part I

This appendix contains the detailed proof of Lemma III.10. To keep the notation simple, we only explicitly discuss the case of an upper barrier. The steps for a lower barrier are fully analogous. We first start by computing $\mathbb{P}^*\{S_t \le x, \nu \le t\}$ as this allows for the application of the reflection principle for Brownian motion. Similar to the proof of Lemma III.2 in Appendix III.A.1, we express the condition $\nu \le t$ in terms of the Brownian motion W^* as

$$\max_{u\in[0,t]}\left\{W_u^* + \frac{1}{\sigma}\left(r - \delta + \gamma - \frac{1}{2}\sigma^2\right)u\right\} \ge \frac{1}{\sigma}\left(\ln\left(\frac{\tilde{B}(0)}{S_0}\right) + \gamma T\right).$$

We define the equivalent probability measure $\hat{\mathbb{P}}$ just like in Appendix III.A.1 with corresponding Brownian motion process $\hat{W} = \left\{\hat{W}_t : t \in [0,T^*]\right\}$. Let

$$\hat{M}_t = \max_{u\in[0,t]}\{\hat{W}_u\}$$

be the maximum value that the Brownian motion path $\hat{W}$ attains over the interval $[0,t]$. Then $\nu \le t$ corresponds to

$$\hat{M}_t \ge \frac{1}{\sigma}\left(\ln\left(\frac{\tilde{B}(0)}{S_0}\right) + \gamma T\right) =: \beta.$$

Similarly, we can express the condition $S_t \le x$ in terms of the Brownian motion W^* as

$$W_t^* + \frac{1}{\sigma}\left(r - \delta - \frac{1}{2}\sigma^2\right)t \le \frac{1}{\sigma}\ln\left(\frac{x}{S_0}\right).$$

Equivalently, in terms of the Brownian motion $\hat{W}$, we get

$$\hat{W}_t \leq \frac{1}{\sigma}\left(\ln\left(\frac{x}{S_0}\right)+\gamma t\right) =: \alpha(x).$$

Then

$$\begin{aligned}
\mathbb{P}^*\left\{S_t \leq x, \nu \leq t\right\} &= \mathbb{E}_{\mathbb{P}^*}\left[1\left\{\hat{W}_t \leq \alpha(x), \hat{M}_t \geq \beta\right\}\right] \\
&= \mathbb{E}_{\hat{\mathbb{P}}}\left[\xi_t^{-1}\big(\mathbb{P}^*, \hat{\mathbb{P}}\big) 1\left\{\hat{W}_t \leq \alpha(x), \hat{M}_t \geq \beta\right\}\right] \\
&= \mathbb{E}_{\hat{\mathbb{P}}}\left[\exp\left\{\lambda \hat{W}_t - \frac{1}{2}\lambda^2 t\right\} 1\left\{\hat{W}_t \leq \alpha(x), \hat{M}_t \geq \beta\right\}\right].
\end{aligned}$$

To explicitly see the next step, we express this expectation as a double integral over the joint PDF and get

$$\begin{aligned}
\ldots &= \int_{-\infty}^{\alpha(x)} \exp\left\{\lambda y - \frac{1}{2}\lambda^2 t\right\} \hat{\mathbb{P}}\left\{\hat{W}_t \in \mathrm{d}y, \hat{M}_t \geq \beta\right\} \\
&= \int_{-\infty}^{\alpha(x)} \exp\left\{\lambda y - \frac{1}{2}\lambda^2 t\right\} \hat{\mathbb{P}}\left\{\hat{W}_t \in 2\beta - \mathrm{d}y, \hat{M}_t \geq \beta\right\} \\
&= \int_{-\infty}^{\alpha(x)} \exp\left\{\lambda y - \frac{1}{2}\lambda^2 t\right\} \hat{\mathbb{P}}\left\{\hat{W}_t \in 2\beta - \mathrm{d}y\right\}.
\end{aligned}$$

Here, we used the reflection principle for Brownian motion in the second step. We now make a change of variables by defining $z = 2\beta - y$ to obtain

$$\begin{aligned}
\ldots &= \int_{2\beta-\alpha(x)}^{\infty} \exp\left\{\lambda(2\beta - z) - \frac{1}{2}\lambda^2 t\right\} \hat{\mathbb{P}}\left\{\hat{W}_t \in \mathrm{d}z\right\} \\
&= \mathbb{E}_{\hat{\mathbb{P}}}\left[\exp\left\{\lambda\left(2\beta - \hat{W}_t\right) - \frac{1}{2}\lambda^2 t\right\} 1\left\{\hat{W}_t \geq 2\beta - \alpha(x)\right\}\right].
\end{aligned}$$

We now define a new probability measure $\tilde{\mathbb{P}}$ equivalent to $\hat{\mathbb{P}}$ on $[0, T^*]$ by

$$\frac{\mathrm{d}\tilde{\mathbb{P}}}{\mathrm{d}\hat{\mathbb{P}}} = \mathcal{E}_{T^*}\left(-\int_0^{\cdot} \lambda \mathrm{d}\hat{W}_u\right) \qquad \hat{\mathbb{P}}\text{-a.s..}$$

The corresponding Radon-Nikodým derivative process $\xi\big(\tilde{\mathbb{P}}, \hat{\mathbb{P}}\big) = \left\{\xi_t\big(\tilde{\mathbb{P}}, \hat{\mathbb{P}}\big) : t \in [0, T^*]\right\}$ is given by

$$\xi_t\big(\tilde{\mathbb{P}}, \hat{\mathbb{P}}\big) = \left.\frac{\mathrm{d}\tilde{\mathbb{P}}}{\mathrm{d}\hat{\mathbb{P}}}\right| \mathfrak{F}_t = \mathcal{E}_t\left(-\int_0^{\cdot} \lambda \mathrm{d}\hat{W}_u\right) \qquad \hat{\mathbb{P}}\text{-a.s..}$$

By Girsanov's theorem, it follows that the process $\tilde{W} = \left\{\tilde{W}_t : t \in [0, T^*]\right\}$ defined by

$$\tilde{W}_t = \hat{W}_t + \lambda t \qquad \forall t \in [0, T^*]$$

is a one-dimensional standard Brownian motion under $\tilde{\mathbb{P}}$. Thus, applying the abstract Bayes rule yields

$$\begin{aligned}
\ldots &= \mathrm{e}^{2\lambda\beta}\mathbb{E}_{\hat{\mathbb{P}}}\left[\xi_t(\tilde{\mathbb{P}},\hat{\mathbb{P}})1\left\{\hat{W}_t \geq 2\beta-\alpha(x)\right\}\right] \\
&= \mathrm{e}^{2\lambda\beta}\tilde{\mathbb{P}}\left\{\tilde{W}_t \geq 2\beta-\alpha(x)+\lambda t\right\} \\
&= \mathrm{e}^{2\lambda\beta}\mathcal{N}\left(-\frac{2\beta-\alpha(x)+\lambda t}{\sqrt{t}}\right).
\end{aligned}$$

Thus,

$$\begin{aligned}
\mathbb{P}^*\left\{\hat{W}_t \leq \alpha(x), \hat{M}_t < \beta\right\} &= \mathbb{P}^*\left\{\hat{W}_t \leq \alpha(x)\right\} - \mathbb{P}^*\left\{\hat{W}_t \leq \alpha(x), \hat{M}_t \geq \beta\right\} \\
&= \mathcal{N}\left(\frac{\alpha(x)-\lambda t}{\sqrt{t}}\right) - \mathrm{e}^{2\lambda\beta}\mathcal{N}\left(-\frac{2\beta-\alpha(x)+\lambda t}{\sqrt{t}}\right).
\end{aligned}$$

Next, note that by the Leibniz rule we have

$$\frac{\partial}{\partial x}\mathbb{P}^*\left\{S_t \leq x, \nu > t\right\}\mathrm{d}x = \mathbb{P}^*\left\{S_t \in \mathrm{d}x, \nu > t\right\}.$$

Consequently,

$$\begin{aligned}
&\mathbb{P}^*\left\{S_t \in \mathrm{d}x, \nu > t\right\} \\
=\ &\frac{\partial}{\partial x}\mathbb{P}^*\left\{\hat{W}_t \leq \alpha(x), \hat{M}_t < \beta\right\}\mathrm{d}x \\
=\ &\frac{\partial}{\partial x}\left\{\mathcal{N}\left(\frac{\alpha(x)-\lambda t}{\sqrt{t}}\right) - \mathrm{e}^{2\lambda\beta}\mathcal{N}\left(-\frac{2\beta-\alpha(x)+\lambda t}{\sqrt{t}}\right)\right\}\mathrm{d}x \\
=\ &\frac{\alpha'(x)}{\sqrt{t}}\left(\mathcal{N}'\left(\frac{\alpha(x)-\lambda t}{\sqrt{t}}\right) - \mathrm{e}^{2\lambda\beta}\mathcal{N}'\left(-\frac{2\beta-\alpha(x)+\lambda t}{\sqrt{t}}\right)\right)\mathrm{d}x \\
=\ &\frac{1}{x\sigma\sqrt{t}}\left(\mathcal{N}'\left(\frac{\alpha(x)-\lambda t}{\sqrt{t}}\right) - \mathrm{e}^{2\lambda\beta}\mathcal{N}'\left(\frac{2\beta-\alpha(x)+\lambda t}{\sqrt{t}}\right)\right)\mathrm{d}x.
\end{aligned}$$

The last step uses the symmetry of the standard normal PDF. We obtain exactly the same result in case of a lower barrier. In this case, we start by computing $\mathbb{P}^*\left\{S_t \geq x, \nu \leq t\right\}$ and follow the same steps.

III.B.3 Joint Density of S_t and $\{\tau > t\}$ Part II

This appendix presents an alternative and significantly simpler derivation of Lemma III.10 based on the method of images. This approach uses results from Section III.5 on bond binaries. We consider a contingent claim that has a unit payoff at its maturity $T \in [0, T^*]$ if the terminal spot price is above some level $x \in \mathbb{R}_+$ such that $\psi x \geq \psi\tilde{B}(0)$

and conditional on no prior breach of the exponential barrier $\tilde{B}(\tau)$. Here, we assume that the barrier is constructed such that at the maturity of the contingent claim its level is given by $\tilde{B}(0)$. This comes at no loss of generality, since an exponential barrier can be equivalently defined with respect to any reference time point. The option value $\tilde{V}(S,\tau)$ then satisfies the Black and Scholes (1973) IEBVP

$$\begin{aligned}
\mathcal{L}\{\tilde{V}\}(S,\tau) &= 0 \qquad \text{for } (S,\tau) \in \mathcal{D}, , \\
\tilde{V}(S,0) &= 1\{\psi S > \psi x\}, \\
\tilde{V}\big(\tilde{B}(\tau),\tau\big) &= 0 \qquad \text{for } \tau \in [0,\infty),
\end{aligned}$$

where

$$\mathcal{D} = \big\{(S,\tau) : \psi S > \psi \tilde{B}(\tau), \tau \in (0,\infty)\big\}.$$

The corresponding full-range problem $\tilde{V}_{\tilde{B}(0),\gamma}(S,\tau)$ is given by

$$\begin{aligned}
\mathcal{L}\{\tilde{V}_{\tilde{B}(0),\gamma}\}(S,\tau) &= 0 \qquad \text{for } (S,\tau) \in \mathbb{R}_+^2, \\
\tilde{V}(S,0) &= 1\{\psi S > \psi x\}.
\end{aligned}$$

However, this is just the value of a bond binary with strike price x. By Proposition III.1, we thus have

$$\tilde{V}(S,\tau) = \tilde{B}_x^{\psi}(S,\tau) - \overset{\tilde{B}(0),\gamma,\tau}{\mathcal{I}} \left\{\tilde{B}_x^{\psi}(S,\tau)\right\}.$$

Since the contingent claim value is just the discounted probability of obtaining the unit payoff at maturity, we have

$$\mathbb{P}^* \left\{\psi S_T \geq \psi x, \nu > T\right\} = \mathrm{e}^{rT}\tilde{V}(S,T).$$

Consequently, we obtain the joint PDF by differentiating this expression with respect to x. We again only explicitly compute the result for $\psi = +1$. The steps for $\psi = -1$ are however nearly identical. We have

$$\begin{aligned}
\mathbb{P}^* \left\{S_T \in \mathrm{d}x, \nu > T\right\} &= -\mathrm{e}^{rT}\frac{\partial}{\partial x}\left(\tilde{B}_x^{\psi}\left(S_0,T\right) - \overset{\tilde{B}(0),\gamma,T}{\mathcal{I}} \left\{\tilde{B}_x^{\psi}\left(S_0,T\right)\right\}\right)\mathrm{d}x \\
&= -\mathrm{e}^{rT}\left(\frac{\partial \tilde{B}_x^{\psi}}{\partial K}\left(S_0,T\right) - \overset{\tilde{B}(0),\gamma,T}{\mathcal{I}} \left\{\frac{\partial \tilde{B}_x^{\psi}}{\partial K}\left(S_0,T\right)\right\}\right)\mathrm{d}x,
\end{aligned}$$

where we used that the image operator does not depend on the strike price K. The partial derivative of the bond binary price with respect to the strike price is given by

$$\frac{\partial B_x^{\psi}}{\partial K}(S_0, T) = -\mathrm{e}^{-rT}\frac{1}{x\sigma T}\mathcal{N}'(\psi d_-(S_0, T)),$$

where

$$d_-(S_0, T) = \frac{\ln(S_0/x) + \left(r - \delta - \frac{1}{2}\sigma^2\right)T}{\sigma\sqrt{T}}.$$

Putting everything together, we obtain

$$\begin{aligned}\mathbb{P}^*\{S_T \in \mathrm{d}x, \nu > T\} &= \frac{1}{x\sigma T}\Bigg(\mathcal{N}'(d_-(S_0, T)) \\ &\quad - \left(\frac{S_0}{\tilde{B}(0)\mathrm{e}^{\gamma T}}\right)^{2\alpha}\mathcal{N}'\left(d_-\left(\frac{\tilde{B}^2(0)\mathrm{e}^{2\gamma T}}{S_0}, T\right)\right)\Bigg)\mathrm{d}x.\end{aligned}$$

It is easy to check that this expression is indeed equivalent to the one previously obtained in Appendix III.B.2.

III.B.4 Probabilistic Method of Images

This appendix contains the detailed proof of Proposition III.3. We again only explicitly prove the case of an upper barrier. By the risk-neutral pricing formula, we have

$$V_t = \mathrm{e}^{-r\tau}\mathbb{E}_{\mathbb{P}^*}\left[f(S_T)1\{\nu > T\}|\,\mathfrak{F}_t\right].$$

Using the result from Lemma III.10, we can express this expectation as an integral

$$\begin{aligned}V_t &= \mathrm{e}^{-r\tau}\int_0^{\infty} f(x)\mathbb{P}^*\{S_T \in \mathrm{d}x, \nu > T|\,\mathfrak{F}_t\} \\ &= \mathrm{e}^{-r\tau}\int_0^{\tilde{B}(0)}\frac{f(x)}{x\sigma\sqrt{\tau}}\left(\mathcal{N}'\left(\frac{\alpha(x) - \lambda\tau}{\sqrt{\tau}}\right) - \mathrm{e}^{2\lambda\beta}\mathcal{N}'\left(\frac{2\beta - \alpha(x) + \lambda\tau}{\sqrt{\tau}}\right)\right)\mathrm{d}x.\end{aligned}$$

We split this integral in two parts. Substituting for $\alpha(x)$ and λ from Lemma III.10, the first part $V_t^{(1)}$ can be expressed as

$$\begin{aligned}V_t^{(1)} &= \mathrm{e}^{-r\tau}\int_0^{\tilde{B}(0)}\frac{f(x)}{x\sigma\sqrt{\tau}}\mathcal{N}'\left(\frac{\alpha(x) - \lambda\tau}{\sqrt{\tau}}\right)\mathrm{d}x \\ &= \mathrm{e}^{-r\tau}\int_0^{\infty}\frac{f(x)1\{x < \tilde{B}(0)\}}{x\sigma\sqrt{\tau}}\mathcal{N}'\left(\frac{\ln(x/S_t) - \left(r - \delta - \frac{1}{2}\sigma^2\right)\tau}{\sigma\sqrt{\tau}}\right)\mathrm{d}x.\end{aligned}$$

We recognize the integrand as the product of the payoff of the full-range value process $V^{\tilde{B}(0)}$ as defined in Proposition III.3 times the log-normal conditional PDF of the terminal spot prices S_T under the risk-neutral probability measure $\mathbb{P}^*$. Consequently, $V_t^{(1)} = V_t^{\tilde{B}(0)}$. Next,

$$\begin{aligned}
e^{2\lambda\beta} &= \exp\left\{\frac{2}{\sigma^2}\left(r-\delta+\gamma-\frac{1}{2}\sigma^2\right)\left(\ln\left(\frac{\tilde{B}(0)}{S_t}\right)+\gamma\tau\right)\right\} \\
&= \left(\frac{S_t}{\tilde{B}(\tau)}\right)^{2\alpha},
\end{aligned}$$

where α is as in Definition III.5. The second part $V_t^{(2)}$ then becomes

$$\begin{aligned}
V_t^{(2)} &= e^{2\lambda\beta}e^{-r\tau}\int_0^{\tilde{B}(0)}\frac{f(x)}{x\sigma\sqrt{\tau}}\mathcal{N}'\left(\frac{2\beta-\alpha(x)+\lambda\tau}{\sqrt{\tau}}\right)\mathrm{d}x \\
&= \left(\frac{S_t}{\tilde{B}(\tau)}\right)^{2\alpha} e^{-r\tau}\int_0^{\infty}\frac{f(x)1\{x<\tilde{B}(0)\}}{x\sigma\sqrt{\tau}} \\
&\quad \mathcal{N}'\left(\frac{\ln\left(xS_t/\tilde{B}^2(\tau)\right)-\left(r-\delta-\frac{1}{2}\sigma^2\right)\tau}{\sigma\sqrt{\tau}}\right)\mathrm{d}x \\
&= \overset{\tilde{B}(0),\gamma,\tau}{\mathcal{I}}\left\{V_t^{\tilde{B}(0)}\right\}.
\end{aligned}$$

Consequently,

$$V_t = V_t^{\tilde{B}(0)} - \overset{\tilde{B}(0),\gamma,\tau}{\mathcal{I}}\left\{V_t^{\tilde{B}(0)}\right\},$$

which completes the proof for this case. As the joint PDF of the terminal spot price and $\nu > T$ is the same for an upper and lower barrier, we simply need to adjust the limits of integration and indicator functions when dealing with a lower barrier.

III.C Appendix for Section III.7

III.C.1 Pay-at-Hit Bond Binary Valuation

This appendix contains an alternative proof of Proposition III.7. Let $\tilde{U}(S,\tau)$ follow the IEBVP

$$\begin{aligned}
\mathcal{L}\{\tilde{U}\} &= 0 \qquad \text{for } (S,\tau)\in\mathcal{D}, \\
\tilde{U}(S,0) &= 1, \\
\tilde{U}(S,1) &= 0 \qquad \text{for } \tau\in[0,\infty),
\end{aligned}$$

where the active domain $\mathcal{D}$ is as in Proposition III.7. Then $\tilde{U}(S,\tau)$ is the valuation function of a contingent claim that has a unit payoff at maturity conditional on no prior crossing of the exponential barrier $\tilde{B}(\tau)$. It follows by Proposition III.1 that

$$\tilde{U}(S,\tau) = \mathcal{B}^{\psi}_{\tilde{B}(0)}(S,\tau) - \overset{\tilde{B}(0),\gamma,\tau}{\mathcal{I}} \left\{\mathcal{B}^{\psi}_{\tilde{B}(0)}(S,\tau)\right\}.$$

Since $\tilde{V}(S,0) + \tilde{U}(S,0) = 1$ and thus $\tilde{V}(S,\tau) + \tilde{U}(S,\tau) = \mathrm{e}^{-r\tau}$, we obtain

$$\tilde{V}(S,\tau) = \mathcal{B}^{-\psi}_{\tilde{B}(0)}(S,\tau) + \overset{\tilde{B}(0),\gamma,\tau}{\mathcal{I}} \left\{\mathcal{B}^{\psi}_{\tilde{B}(0)}(S,\tau)\right\},$$

where we used that $\tilde{B}^{+}_{\xi}(S,\tau) + \tilde{B}^{-}_{\xi}(S,\tau) = \mathrm{e}^{-r\tau}$.

III.D Appendix for Section III.8

III.D.1 Decomposition of the Pay-at-Hit Valuation Problem

This appendix contains the detailed proof of Lemma III.16. Fix some initial $\tau \in [0,\infty)$. As shown in Lemma III.15, it is sufficient to solve the equivalent constant barrier valuation problem for $\tau^* \in [0,\tau]$

$$\begin{aligned}
\mathcal{L}\{\tilde{V}\}\big(\hat{S},\tau^*\big) &= 0 \qquad \text{for } \big(\hat{S},\tau^*\big) \in \mathcal{D}, \\
\tilde{V}\big(\hat{S},0\big) &= 0, \\
\tilde{V}\big(\tilde{B}(\tau),\tau^*\big) &= 1 \qquad \text{for } \tau^* \in [0,\tau],
\end{aligned}$$

where

$$\mathcal{D} = \left\{\big(\hat{S},\tau^*\big) : \psi\hat{S} > \psi\tilde{B}(\tau),\ \tau^* \in (0,\tau]\right\}$$

and the asset $\hat{S}$ has a dividend yield of $\hat{\delta} = \delta - \gamma$. Now define the stationary Black and Scholes (1973) operator $\hat{\mathcal{J}}$ for the asset $\hat{S}$ as

$$\hat{\mathcal{J}}\{U\} = (r - \delta + \gamma)\hat{S}\frac{\mathrm{d}U}{\mathrm{d}\hat{S}} + \frac{1}{2}\sigma^2\hat{S}^2\frac{\mathrm{d}^2 U}{\mathrm{d}\hat{S}^2} - rU$$

and let $U_\xi^\psi\big(\hat{S}\big)$ satisfy the stationary valuation problem

$$\begin{aligned}
\hat{\mathcal{J}}\big\{U_\xi^\psi\big\}\big(\hat{S}\big) &= 0 \qquad \text{for } \psi\hat{S} > \psi\xi, \\
U_\xi^\psi(\xi) &= 1, \\
\lim_{\hat{S}\to\zeta} U_\xi^\psi\big(\hat{S}\big) &= 0 \qquad \text{where } \zeta = \begin{cases} \infty & \text{if } \psi = +1 \\ 0 & \text{if } \psi = -1 \end{cases}.
\end{aligned}$$

$U_\xi^\psi\big(\hat{S}\big)$ is the valuation function of a constant barrier perpetual American bond binary on the asset $\hat{S}$ with strike price ξ. The finite maturity American bond binary $\tilde{V}(S,\tau)$ corresponds to initially taking a long position in the claim $U^\psi_{\tilde{B}(\tau)}(S)$ and closing it out at the maturity given that the constant barrier $\tilde{B}(\tau)$ has not been breached by any spot price $\hat{S}_{\tau^*}$ over the interval $\tau^* \in [0,\tau]$. We thus set

$$\tilde{V}\big(S,\tau\big) = U^\psi_{\tilde{B}(\tau)}(S) - \tilde{V}^1(S,\tau),$$

where $\tilde{V}^1\big(\hat{S},\tau\big)$ satisfies the initial boundary value problem for $\tau^* \in [0,\tau]$

$$\begin{aligned}
\mathcal{L}\big\{\tilde{V}^1\big\}\big(\hat{S},\tau^*\big) &= 0 \qquad \text{for } \big(\hat{S},\tau^*\big) \in \mathcal{D}, \\
\tilde{V}^1\big(\hat{S},0\big) &= U^\psi_{\tilde{B}(\tau)}\big(\hat{S}\big), \\
\tilde{V}^1\big(\tilde{B}(\tau),\tau^*\big) &= 0 \qquad \text{for } \tau^* \in [0,\tau]
\end{aligned}$$

the solution of which can be obtained using Proposition III.1.

III.D.2 Derivation of the Perpetual American Bond Binary Valuation Functions

This appendix provides a detailed derivation of the valuation function for perpetual American bond binaries used in Lemma III.16. This problem is well-known and we refer to for example Chapter 9 in Wilmott (2006), pp. 151–168. We note that the valuation equation in the active domain is a homogeneous linear second-order ordinary differential equation (ODE) with constant coefficients since it can be rearranged to

$$\hat{S}^2 \frac{\mathrm{d}^2 U_\xi^\psi}{\mathrm{d}\hat{S}^2} + \kappa\hat{S}\frac{\mathrm{d}U_\xi^\psi}{\mathrm{d}\hat{S}} - \lambda U_\xi^\psi = 0,$$

where

$$\begin{aligned}
\kappa &= \frac{2(r-\delta+\gamma)}{\sigma^2}, \\
\lambda &= \frac{2r}{\sigma^2}.
\end{aligned}$$

This equation is of the Euler-Cauchy type and we thus try the solution

$$U_\xi^\psi(\hat{S}) = \hat{S}^\beta$$

and get

$$\beta(\beta-1)\hat{S}^\beta + \beta\kappa\hat{S}^\beta - \lambda\hat{S}^\beta = 0.$$

This equation holds for all values of $\hat{S}$ if

$$\beta^2 + \beta(\kappa - 1) - \lambda = 0$$

or

$$\beta_\pm = \pm\sqrt{\lambda + \left(\frac{\kappa-1}{2}\right)^2} - \frac{\kappa-1}{2}.$$

The expression for $\beta_\pm$ can be expanded to

$$\beta(\pm) = \frac{1}{\sigma^2}\left(-\left(r - \delta + \gamma - \frac{1}{2}\sigma^2\right) \pm \sqrt{2r\sigma^2 + \left(r - \delta + \gamma - \frac{1}{2}\sigma^2\right)^2}\right)$$

and we note that $\beta_- < 0$ and $\beta_+ > 0$. Furthermore, for $\delta = \gamma$, we have $\kappa = \lambda$ and thus $\beta_+ = 1$ and $\beta_- = -\gamma$. The general solution to the ODE is given by

$$U_\xi^\psi(\hat{S}) = c_-\hat{S}^{\beta_-} + c_+\hat{S}^{\beta_+},$$

where $c_\pm$ are the constants of integration and have to be determined using the boundary conditions of the particular contract to be priced. In the case of a perpetual American bond binary put, when $\psi = +1$, the upper boundary condition $\lim_{\hat{S}\to\infty} U_\xi^+(\hat{S}) = 0$ implies that $c_+ = 0$. Next, the value matching condition at the lower boundary is

$$U_\xi^+(\xi) = 1 \qquad \Leftrightarrow \qquad c_- = \xi^{-\beta_-}.$$

Consequently,

$$U_\xi^+(\hat{S}) = \left(\frac{\hat{S}}{\xi}\right)^{\beta_-}.$$

Similarly, in case of a perpetual American bond binary call when $\psi = -1$ the lower boundary condition $\lim_{\hat{S}\to 0} U_\xi^-(\hat{S}) = 0$ implies that $c_- = 0$. The value matching condition at the upper boundary is

$$U_\xi^-(\xi) = 1 \qquad \Leftrightarrow \qquad c_+ = \xi^{-\beta_+}.$$

Thus,
$$U_\xi^-\big(\hat{S}\big) = \left(\frac{\hat{S}}{\xi}\right)^{\beta_+}.$$

III.D.3 Pay-at-Hit Bond Binary Valuation

This appendix contains the detailed proof of Proposition III.10. By Lemma III.16, it remains to find the valuation function $\tilde{V}^1\big(\hat{S},\tau\big)$ which satisfies an initial boundary value problem. The corresponding full-range problem for $\tau^* \in [0,\tau]$ is given by

$$\begin{aligned}
\mathcal{L}\big\{\tilde{V}^1_{\tilde{B}(\tau)}\big\}\big(\hat{S},\tau^*\big) &= 0 \qquad \text{for } \big(\hat{S},\tau^*\big) \in \mathbb{R}_+ \times (0,\tau], \\
\tilde{V}_{\tilde{B}(\tau)}\big(\hat{S},0\big) &= U^{\psi}_{\tilde{B}(\tau)}\big(\hat{S}\big)1\big\{\psi\hat{S} > \psi\tilde{B}(\tau)\big\}.
\end{aligned}$$

We recognize the initial condition as the scaled payoff of a power binary as in Definition III.9, that is

$$\tilde{V}_{\tilde{B}(\tau)}(S,0) = \left(\frac{\hat{S}}{\tilde{B}(\tau)}\right)^{\beta(-\psi)} 1\big\{\psi\hat{S} > \psi\tilde{B}(\tau)\big\}.$$

Using Proposition III.8 with $\eta = \beta(-\psi)$, we thus have

$$\begin{aligned}
&\tilde{V}^1_{\tilde{B}(\tau)}\big(\hat{S},\tau\big) \\
=\ &\left(\frac{\hat{S}}{\tilde{B}(\tau)}\right)^{\beta(-\psi)} \exp\left\{\left((\beta(-\psi)-1)\left(r+\frac{1}{2}\beta(-\psi)\sigma^2\right) - \beta(-\psi)\delta\right)\tau\right\}\mathcal{N}\left(\psi d_{\beta(-\psi)}\right) \\
=\ &\left(\frac{\hat{S}}{\tilde{B}(\tau)}\right)^{\beta(-\psi)} \mathcal{N}\left(\psi d_{\beta(-\psi)}\right).
\end{aligned}$$

It is straight forward to check that the terms in the exponential cancel out for both $\psi = \pm 1$. Similarly, term $d_{\beta(-\psi)}$ simplifies to

$$\begin{aligned}
d_{\beta(-\psi)} &= \frac{\ln\big(\hat{S}/\tilde{B}(\tau)\big) + \big(r - \delta + \big(\beta(-\psi) - \frac{1}{2}\big)\sigma^2\big)\tau}{\sigma\sqrt{\tau}} \\
&= \frac{\ln\big(\hat{S}/\tilde{B}(\tau)\big) - \psi\sqrt{\lambda + \alpha^2}\tau}{\sigma\sqrt{\tau}},
\end{aligned}$$

where α and λ are as in Lemma III.16. By the method of images, see Proposition III.1, we thus get

$$\tilde{V}^1\big(\hat{S},\tau\big) = \tilde{V}^1_{\tilde{B}(\tau)}\big(\hat{S},\tau\big) - \overset{\tilde{B}(\tau),0,\tau}{\mathcal{I}}\big\{\tilde{V}^1_{\tilde{B}(\tau)}\big(\hat{S},\tau\big)\big\}.$$

Using Definition III.5 the image term can be simplified to

$$\overset{\tilde{B}(\tau),0,\tau}{\mathcal{I}} \left\{\tilde{V}^1_{\tilde{B}(\tau)}\left(\hat{S},\tau\right)\right\} = \left(\frac{\hat{S}}{\tilde{B}(\tau)}\right)^{\beta(\psi)} \mathcal{N}\left(-\psi d_{\beta(\psi)}\right).$$

III.D.4 Adjusted Strike Levels

This appendix provides details on how the adjusted strike levels in Section III.8.4 are determined. To find ζ_1, we first note that under the correct specification the drift and the initial underlying asset price, the probability of $\psi S_{\tau_S} > \psi \tilde{B}\left(\hat{\tau}_S\right)$ is

$$\mathbb{P}^* \left\{\psi S_0 \exp\left\{\left(r-\delta-\frac{1}{2}\sigma^2\right)\tau_S + \sigma W^*_{\tau_S}\right\} \geq \psi \tilde{B}\left(\hat{\tau}_S\right)\right\}.$$

However, we are instead using the adjusted initial value $S_0 \mathrm{e}^{-\gamma\tau_B}$ and the dividend yield $\delta-\gamma$ in the pricing of the power bond binary. We thus search for an adjusted strike level ζ_1 such that the probability

$$\mathbb{P}\left\{\psi S_0 \exp\left\{-\gamma\tau_B + \left(r-\delta+\gamma-\frac{1}{2}\sigma^2\right)\tau_S + \sigma W_{\tau_S}\right\} \geq \psi\zeta_1\right\}$$

is identical to the aforementioned one. This is clearly the case when

$$\zeta_1 = \tilde{B}\left(\hat{\tau}_S\right)\mathrm{e}^{\gamma(\hat{\tau}_B-\hat{\tau}_S)}.$$

To find ζ_2, we apply an approach very similar to that used in the proof of Lemma III.12. We have for $\tau = \hat{\tau}_S$

$$\begin{aligned}
&\overset{\tilde{B}(\hat{\tau}_B),0,\tau}{\mathcal{I}} \left\{{}^{\beta(-\psi;\gamma)}\mathcal{P}^{-\psi\psi}_{\tilde{B}(\hat{\tau}_B)\tilde{B}(\hat{\tau}_B)}\left(S\mathrm{e}^{-\gamma\tau_B},\tau_B,\tau;\gamma\right)\right\} 1\left\{\psi S > \psi\tilde{B}\left(\hat{\tau}_S\right)\right\} \\
= \quad & \Xi\,{}^{\beta(-\psi;\gamma)}\mathcal{P}^{-\psi\psi}_{\tilde{B}(\hat{\tau}_B)\tilde{B}(\hat{\tau}_B)}\left(\frac{\tilde{B}^2\left(\hat{\tau}_B\right)}{S\mathrm{e}^{-\gamma\tau_B}},\tau_B,\tau;\gamma\right) 1\left\{\psi S > \psi\tilde{B}\left(\hat{\tau}_S\right)\right\} \\
= \quad & \Xi\,{}^{\beta(-\psi;\gamma)}\mathcal{P}^{-\psi\psi}_{\tilde{B}(\hat{\tau}_B)\tilde{B}(\hat{\tau}_B)}\left(\frac{\tilde{B}^2\left(\hat{\tau}_B\right)}{S\mathrm{e}^{-\gamma\tau_B}},\tau_B,\tau;\gamma\right) 1\left\{\psi\frac{\tilde{B}^2\left(\hat{\tau}_B\right)}{S\mathrm{e}^{-\gamma\tau_B}} < \psi\frac{\tilde{B}^2\left(\hat{\tau}_B\right)}{\tilde{B}\left(\hat{\tau}_S\right)\mathrm{e}^{-\gamma\tau_B}}\right\}
\end{aligned}$$

Here,

$$\Xi = \left(\frac{S\mathrm{e}^{-\gamma\tau_B}}{\tilde{B}\left(\hat{\tau}_B\right)}\right)^{2\alpha(\gamma)}.$$

We thus set ζ_2 equal to the r.h.s. expression in the indicator and obtain

$$\zeta_2 = \tilde{B}\left(\hat{\tau}_B\right)\mathrm{e}^{(\kappa-\gamma)(\hat{\tau}_B-\hat{\tau}_S)}.$$

Similarly, to find ζ_3, we follow the same main steps as in the proof of Lemma III.13. We have for $\tau = \hat{\tau}_S$

$$
\begin{aligned}
& \overset{\tilde{B}(\hat{\tau}_B),\kappa,\tau_B}{\mathcal{I}} \left\{ \overset{\tilde{B}(\hat{\tau}_B),0,\tau}{\mathcal{I}} \left\{ {}^{\beta(-\psi;\gamma)}\mathcal{P}^{-\psi\psi}_{\tilde{B}(\hat{\tau}_B)\tilde{B}(\hat{\tau}_B)} \left(S\mathrm{e}^{-\gamma\tau_B}, \tau_B, \tau; \gamma \right) \right\} \right\} 1\left\{ \psi S > \psi \tilde{B}\left(\hat{\tau}_S\right) \right\} \\
= \; & \overset{\tilde{B}(\hat{\tau}_B),\kappa,\tau_B}{\mathcal{I}} \left\{ \Xi_1 \, {}^{\beta(-\psi;\gamma)}\mathcal{P}^{-\psi\psi}_{\tilde{B}(\hat{\tau}_B)\tilde{B}(\hat{\tau}_B)} \left(\frac{\tilde{B}^2\left(\hat{\tau}_B\right)}{S\mathrm{e}^{-\gamma\tau_B}}, \tau_B, \tau; \gamma \right) \right\} 1\left\{ \psi S > \psi \tilde{B}\left(\hat{\tau}_S\right) \right\} \\
= \; & \Xi_2 \, {}^{\beta(-\psi;\gamma)}\mathcal{P}^{-\psi\psi}_{\tilde{B}(\hat{\tau}_B)\tilde{B}(\hat{\tau}_B)} \left(\frac{\tilde{B}^2\left(\hat{\tau}_B\right) S}{\tilde{B}^2\left(\hat{\tau}_B\right) \mathrm{e}^{(2\kappa-\gamma)\tau_B}}, \tau_B, \tau; \gamma \right) 1\left\{ \psi S > \psi \tilde{B}\left(\hat{\tau}_S\right) \right\} \\
= \; & \Xi_2 \, {}^{\beta(-\psi;\gamma)}\mathcal{P}^{-\psi\psi}_{\tilde{B}(\hat{\tau}_B)\tilde{B}(\hat{\tau}_B)} \left(\mathrm{e}^{(\gamma-2\kappa)\tau_B} S, \tau_B, \tau; \gamma \right) 1\left\{ \psi \mathrm{e}^{(\gamma-2\kappa)\tau_B} S > \psi \mathrm{e}^{(\gamma-2\kappa)\tau_B} \tilde{B}\left(\hat{\tau}_S\right) \right\}.
\end{aligned}
$$

Here,

$$
\begin{aligned}
\Xi_1 &= \left(\frac{S\mathrm{e}^{-\gamma\tau_B}}{\tilde{B}\left(\hat{\tau}_B\right)} \right)^{2\alpha(\gamma)}, \\
\Xi_2 &= \left(\frac{S}{\tilde{B}\left(\hat{\tau}_B\right) \mathrm{e}^{\kappa\tau_B}} \right)^{2\alpha(\kappa)} \left(\frac{\tilde{B}\left(\hat{\tau}_B\right) \mathrm{e}^{2\kappa\tau_B}}{S} \right)^{2\alpha(\gamma)}.
\end{aligned}
$$

From the r.h.s. expression in the indicator we thus immediately obtain

$$
\zeta_3 = \tilde{B}\left(\hat{\tau}_B\right) \mathrm{e}^{(\kappa-\gamma)(\hat{\tau}_B - \hat{\tau}_S)}.
$$

III.E Overview of the Main Results

Figures III.13 through III.15 provide a schematic overview of the valuation formulas obtained in this chapter and their inter-relation, and illustrate which auxiliary results were used in their derivation.

III.F MATLAB Code

In this appendix, we provide the MATLAB Code for the valuation of the deferred start piecewise exponential barrier options and rebates in Sections III.6.4, III.7.4 and III.8.4. There is significant potential for errors when implementing the final pricing formulas. This is particularly true for the valuation of the pay-at-hit rebate where one has to be careful,

Figure III.13: Schematic overview of the main results on barrier option valuation. The middle column contains references to the main results and indicates their inter-dependencies. The left (right) column contains references to specific (general) auxiliary results and definitions used in their derivation.

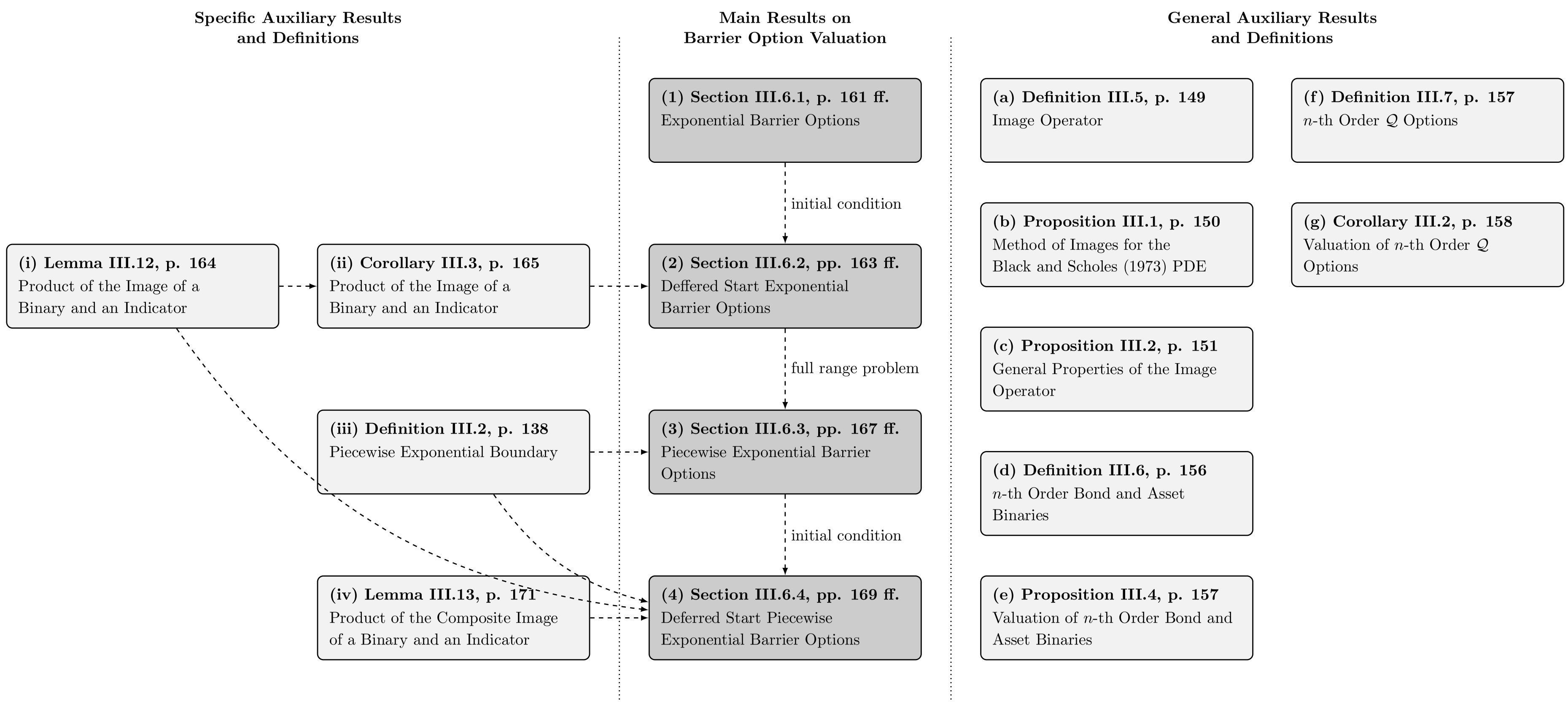

Figure III.14: Schematic overview of the main results on rebate at-maturity valuation. The middle column contains references to the main results and indicates their inter-dependencies. The left (right) column contains references to specific (general) auxiliary results and definitions used in their derivation.

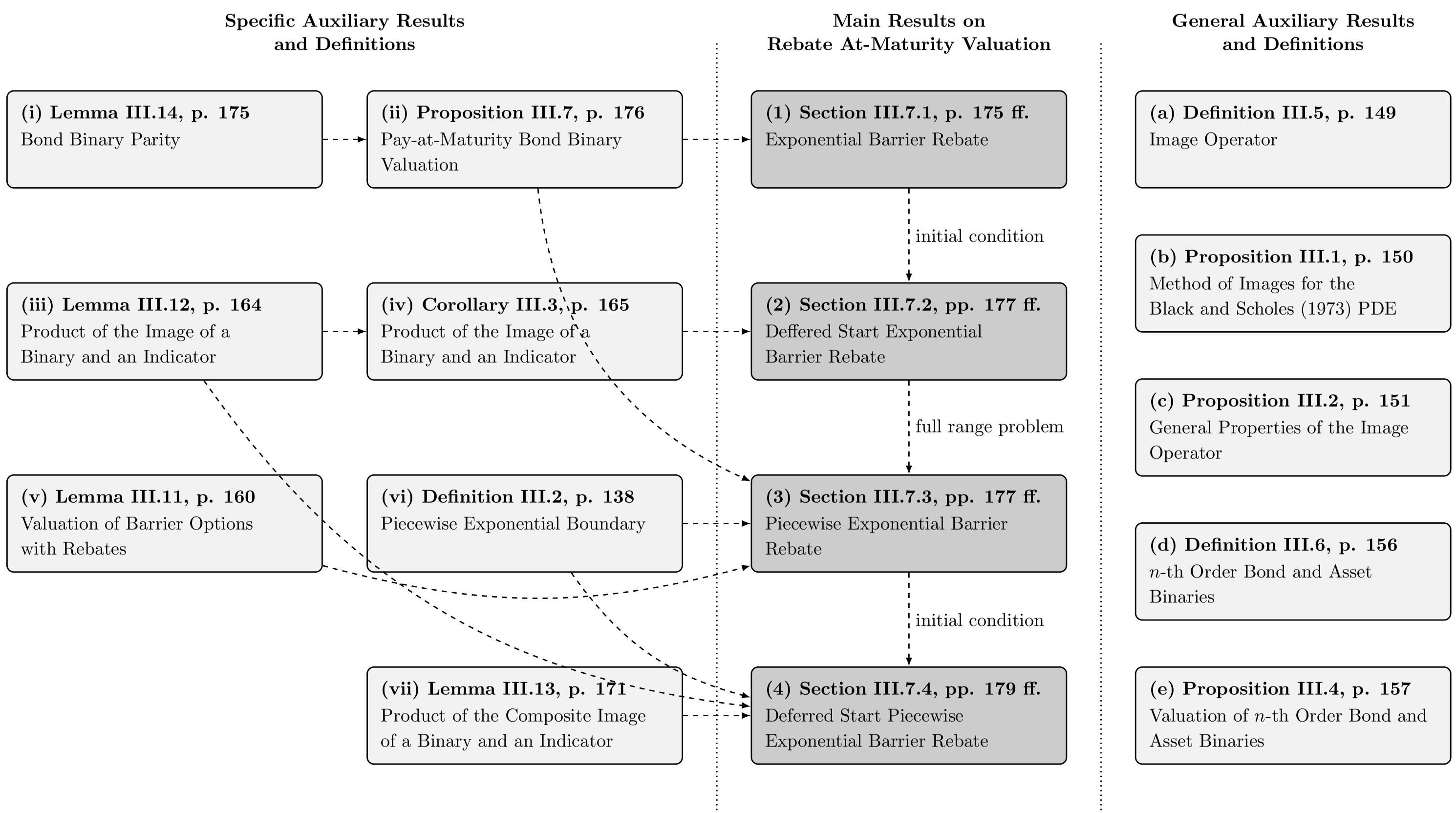

Figure III.15: Schematic overview of the main results on rebate at-hit valuation. The middle column contains references to the main results and indicates their inter-dependencies. The left (right) column contains references to specific (general) auxiliary results and definitions used in their derivation.

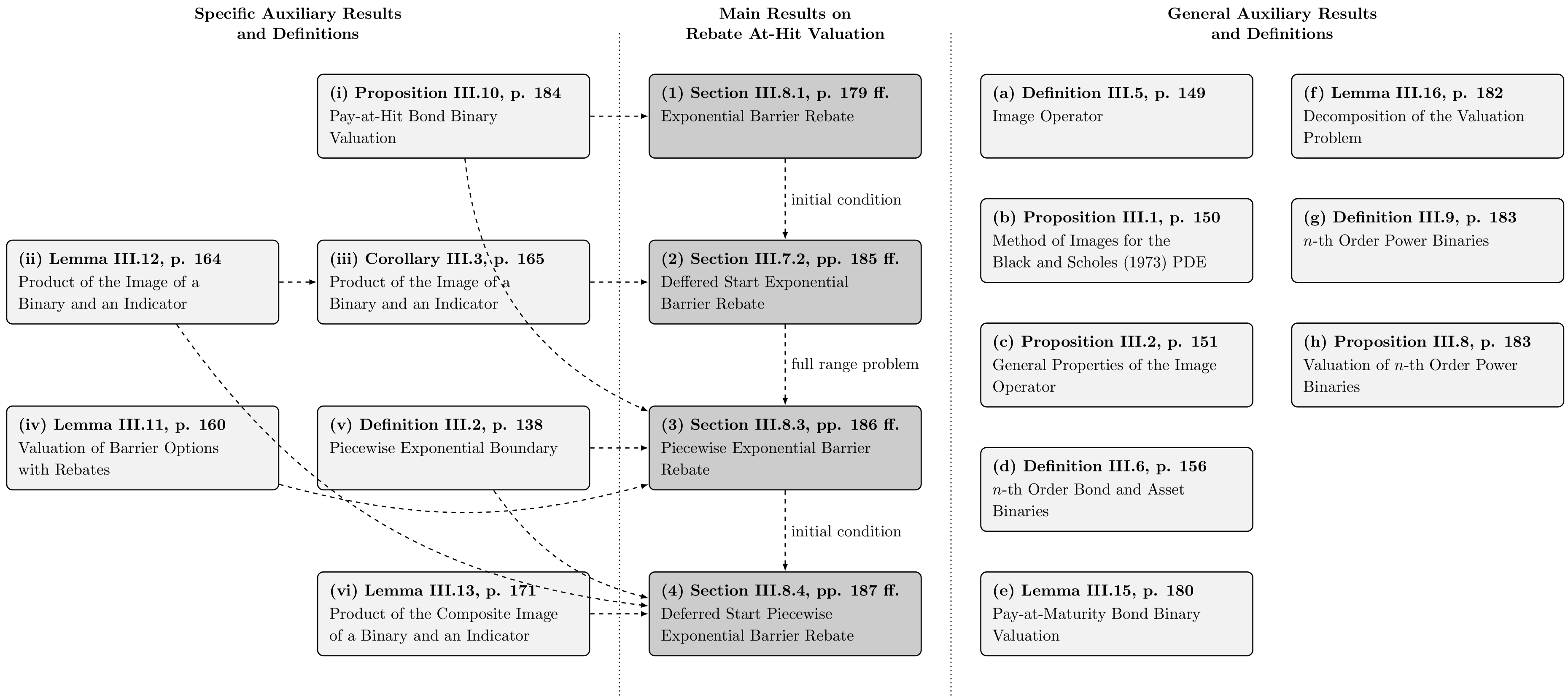

whether the spot price adjustment has to performed at the level of the binary option directly or when taking its image. The sample code fragments provided here should facilitate the implementation in any programming language. For brevity, we often only provide the core functionality and omit the otherwise highly recommended validation of a function's parameters, the handling of other errors and use of extensive code comments. The implementations presented here are also not optimized for performance but instead for ease of readability.

III.F.1 Auxiliary Functions

We repeatedly call the following auxiliary functions that perform the image operation and value general power binaries.

```
function [result] = IIf(condition, valueTrue, valueFalse)
% IIF - inline if function

if (condition)
    result = valueTrue;
else
    result = valueFalse;
end

end
```

```
function [value] = ImageFunction(ValueFunction, barrierFinal, barrierBending, spot, ...
    maturity, rate, dividend, volatility)
% IMAGEFUNCTION - applies the image operator to a valuation function

barrierLevel = barrierFinal * exp(barrierBending * maturity);
alpha = 0.5 - (rate - dividend + barrierBending) / (volatility^2);
value = (spot / barrierLevel)^(2 * alpha) * ValueFunction(barrierLevel^2 / spot);

end
```

```
function [value] = PowerBinary(eta, strikes, flags, spot, maturities, rate, ...
    dividend, volatility)
% POWERBINARY - values a general power binary

order = length(strikes);
CorrelationCoefficient = @(i, j) flags(i) * flags(j) * sqrt(maturities(i) / ...
    maturities(j));
correlationMatrix = eye(order);
```

```
for i = 1:(order - 1)
    for j = (i + 1):order
        correlationMatrix(i, j) = CorrelationCoefficient(i, j);
        correlationMatrix(j, i) = correlationMatrix(i, j);
    end
end
dValues = (log(spot ./ strikes) + (rate - dividend + (eta - 0.5) * volatility^2) * ...
    maturities) ./ (volatility * sqrt(maturity));
value = spot^eta * exp(((eta - 1) * (rate + 0.5 * eta * volatility^2) - eta * ...
    dividend) * maturities(order)) * mvncdf(flags .* dValues, zeros(order, 1), ...
    correlationMatrix);

end
```

III.F.2 Barrier Option Valuation

```
function [value] = KnockOutBarrierOption(spot, rate, dividend, volatility, phi, psi, ...
    strike, barrierFinal, barrierBending, barrierStart, bendingChange, maturity)
% KNOCKOUTBARRIEROPTION - values a deferred start piecewise exponential
% knock-out barrier option without rebate

% compute common expressions
maturities = [barrierStart, bendingChange, maturity];
barrierMiddle = barrierFinal * exp(barrierBending(2) * (maturity - bendingChange));
barrierInitial = barrierMiddle * exp(barrierBending(1) * (bendingChange - ...
    barrierStart));
zeta1 = barrierInitial * exp(2 * (barrierBending(2) - barrierBending(1)) * ...
    (bendingChange - barrierStart));
zeta2 = barrierInitial;
zeta3 = barrierInitial * exp(2 * (barrierBending(2) - barrierBending(1)) * ...
    (bendingChange - barrierStart));

% setup utility functions
BondBinary = @(strikes, flags, spot) PowerBinary(0, strikes, flags, spot, ...
    maturities, rate, dividend, volatility);
AssetBinary = @(strikes, flags, spot) PowerBinary(1, strikes, flags, spot, ...
    maturities, rate, dividend, volatility);
QOption = @(strikes, flags, spot) AssetBinary(strikes, flags, spot) - strikes(end) * ...
    BondBinary(strikes, flags, spot);
ImageOperatorA = @(ValueFunction, spot) ImageFunction(ValueFunction, barrierFinal, ...
    barrierBending(2), spot, maturity, rate, dividend, volatility);
ImageOperatorB = @(ValueFunction, spot) ImageFunction(ValueFunction, barrierMiddle, ...
    barrierBending(1), spot, bendingChange, rate, dividend, volatility);

% compute the option prices
if ((phi == 1) && (psi == 1))
```

```
    % down & out call

    if (strike > barrierFinal)
        value = QOption([barrierInitial, barrierMiddle, strike], [1, 1, 1], spot);
        value = value - ImageOperatorA(@(spot) QOption([zeta1, barrierMiddle, ...
            strike], [-1, -1, 1], spot), spot);
        value = value - ImageOperatorB(@(spot) QOption([zeta2, barrierMiddle, ...
            strike], [-1, 1, 1], spot), spot);
        value = value + ImageOperatorB(@(spot) ImageOperatorA(@(spot) Option([zeta3, ...
            barrierMiddle, strike], [1, -1, 1], spot), spot), spot);
    else
        value = AssetBinary([barrierInitial, barrierMiddle, barrierFinal], [1, 1, ...
            1], spot);
        value = value - strike * BinaryOption([barrierInitial, barrierMiddle, ...
            barrierFinal], [1, 1, 1], spot);
        value = value - ImageOperatorA(@(spot) AssetBinary([zeta1, barrierMiddle, ...
            barrierFinal], [-1, -1, 1], spot), spot);
        value = value + strike * ImageOperatorA(@(spot) BondBinary([zeta1, ...
            barrierMiddle, barrierFinal], [-1, -1, 1], spot), spot);
        value = value - ImageOperatorB(@(spot) AssetBinary([zeta2, barrierMiddle, ...
            barrierFinal], [-1, 1, 1], spot), spot);
        value = value + strike * ImageOperatorB(@(spot) BondBinary([setz2, ...
            barrierMiddle, barrierFinal], [-1, 1, 1], spot), spot);
        value = value + ImageOperatorB(@(spot) ImageOperatorA(@(spot) ...
            AssetBinary([zeta3, barrierMiddle, barrierFinal], [1, -1, 1], spot), ...
            spot), spot);
        value = value - strike * ImageOperatorB(@(spot) ImageOperatorA(@(spot) ...
            BondBinary([zeta3, barrierMiddle, barrierFinal], [1, -1, 1], spot), ...
            spot), spot);
    end
elseif ((phi == 1) && (psi == -1))
    % up & out call

    if (strike > barrierFinal)
        value = 0;
    else
        value = QOption([barrierInitial, barrierMiddle, strike], [-1, -1, 1], spot);
        value = value - AssetBinary([barrierInitial, barrierMiddle, barrierFinal], ...
            [-1, -1, 1], spot);
        value = value + strike * BondBinary([barrierInitial, barrierMiddle, ...
            barrierFinal], [-1, -1, 1], spot);
        value = value - ImageOperatorA(@(spot) QOption([zeta1, barrierMiddle, ...
            strike], [1, 1, 1], spot), spot);
        value = value + ImageOperatorA(@(spot) AssetBinary([zeta1, barrierMiddle, ...
            barrierFinal], [1, 1, 1], spot), spot);
        value = value - strike * ImageOperatorA(@(spot) BondBinary([zeta1, ...
            barrierMiddle, barrierFinal], [1, 1, 1], spot), spot);
        value = value - ImageOperatorB(@(spot) QOption([zeta2, barrierMiddle, ...
            strike], [1, -1, 1], spot), spot);
```

```
        value = value + ImageOperatorB(@(spot) AssetBinary([zeta2, barrierMiddle, ...
            barrierFinal], [1, -1, 1], spot), spot);
        value = value - strike * ImageOperatorB(@(spot) BondBinary([zeta2, ...
            barrierMiddle, barrierFinal], [1, -1, 1], spot), spot);
        value = value + ImageOperatorB(@(spot) ImageOperatorA(@(spot) ...
            QOption([zeta3, barrierMiddle, strike], [-1, 1, 1], spot), spot), spot);
        value = value - ImageOperatorB(@(spot) ImageOperatorA(@(spot) ...
            AssetBinary([zeta3, barrierMiddle, barrierFinal], [-1, 1, 1], spot), ...
            spot), spot);
        value = value + strike * ImageOperatorB(@(spot) ImageOperatorA(@(spot) ...
            BondBinary([zeta3, barrierMiddle, barrierFinal], [-1, 1, 1], spot), ...
            spot), spot);
    end
elseif ((phi == -1) && (psi == 1))
    % down & out put

    if (strike > barrierFinal)
        value = -QOption([barrierInitial, barrierMiddle, strike], [1, 1, -1], spot);
        value = value - strike * BondBinary([barrierInitial, barrierMiddle, ...
            barrierFinal], [1, 1, -1], spot);
        value = value + AssetBinary([barrierInitial, barrierMiddle, barrierFinal], ...
            [1, 1, -1], spot);
        value = value + ImageOperatorA(@(spot) QOption([zeta1, barrierMiddle, ...
            strike], [-1, -1, -1], spot), spot);
        value = value + strike * ImageOperatorA(@(spot) BondBinary([zeta1, ...
            barrierMiddle, barrierFinal], [-1, -1, -1], spot), spot);
        value = value - ImageOperatorA(@(spot) AssetBinary([zeta1, barrierMiddle, ...
            barrierFinal], [-1, -1, -1], spot), spot);
        value = value + ImageOperatorB(@(spot) QOption([zeta2, barrierMiddle, ...
            strike], [-1, 1, -1], spot), spot);
        value = value + strike * ImageOperatorB(@(spot) BondBinary([zeta2, ...
            barrierMiddle, barrierFinal], [-1, 1, -1], spot), spot);
        value = value - ImageOperatorB(@(spot) AssetBinary([zeta2, barrierMiddle, ...
            barrierFinal], [-1, 1, -1], spot), spot);
        value = value - ImageOperatorB(@(spot) ImageOperatorA(@(spot) ...
            QOption([zeta3, barrierMiddle, strike], [1, -1, -1], spot), spot), spot);
        value = value - strike * ImageOperatorB(@(spot) ImageOperatorA(@(spot) ...
            BondBinary([zeta3, barrierMiddle, barrierFinal], [1, -1, -1], spot), ...
            spot), spot);
        value = value + ImageOperatorB(@(spot) ImageOperatorA(@(spot) ...
            AssetBinary([zeta3, barrierMiddle, barrierFinal], [1, -1, -1], spot), ...
            spot), spot);
    else
        value = 0;
    end
else
    % up & out put

    if (strike > barrierFinal)
```

```
        value = strike * BondBinary([barrierInitial, barrierMiddle, barrierFinal], ...
            [-1, -1, -1], spot);
        value = value - AssetBinary([barrierInitial, barrierMiddle, barrierFinal], ...
            [-1, -1, -1], spot);
        value = value - strike * ImageOperatorA(@(spot) BondBinary([zeta1, ...
            barrierMiddle, barrierFinal], [1, 1, -1], spot), spot);
        value = value + ImageOperatorA(@(spot) AssetBinary([zeta1, barrierMiddle, ...
            barrierFinal], [1, 1, -1], spot), spot);
        value = value - strike * ImageOperatorB(@(spot) BondBinary([zeta2, ...
            barrierMiddle, barrierFinal], [1, -1, -1], spot), spot);
        value = value + ImageOperatorB(@(spot) AssetBinary([zeta2, barrierMiddle, ...
            barrierFinal], [1, -1, -1], spot), spot);
        value = value + strike * ImageOperatorB(@(spot) ImageOperatorA(@(spot) ...
            BondBinary([zeta3, barrierMiddle, barrierFinal], [-1, 1, -1], spot), ...
            spot), spot);
        value = value - ImageOperatorB(@(spot) ImageOperatorA(@(spot) ...
            AssetBinary([zeta3, barrierMiddle, barrierFinal], [-1, 1, -1], spot), ...
            spot), spot);
    else
        value = -QOption([barrierInitial, barrierMiddle, strike], [-1, -1, -1], spot);
        value = value + ImageOperatorA(@(spot) QOption([zeta1, barrierMiddle, ...
            strike], [1, 1, -1], spot), spot);
        value = value + ImageOperatorB(@(spot) QOption([zeta2, barrierMiddle, ...
            strike], [1, -1, -1], spot), spot);
        value = value - ImageOperatorB(@(spot) ImageOperatorA(@(spot) ...
            QOption([zeta3, barrierMiddle, strike], [-1, 1, -1], spot), spot), spot);
    end
end

end
```

III.F.3 Rebate Valuation: Payout at Maturity

```
function [value] = RebatePayAtMaturity(spot, rate, dividend, volatility, psi, ...
    barrierFinal, barrierBending, barrierStart, bendingChange, maturity)
% REBATEPAYATMATURITY - values a deferred start piecewise exponential
% barrier pay-at-maturitys rebate

% compute common expressions
maturities2 = [barrierStart, bendingChange];
maturities3 = [barrierStart, bendingChange, maturity];
barrierMiddle = barrierFinal * exp(barrierBending(2) * (maturity - bendingChange));
barrierInitial = barrierMiddle * exp(barrierBending(1) * (bendingChange - ...
    barrierStart));
zeta1 = barrierInitial * exp(2 * (barrierBending(2) - barrierBending(1)) * ...
    (bendingChange - barrierStart));
```

```
zeta2 = barrierInitial;
zeta3 = barrierInitial * exp(2 * (barrierBending(2) - barrierBending(1)) * ...
    (bendingChange - barrierStart));

% setup utility functions
BondBinary = @(strikes, flags, spot, maturities) PowerBinary(0, strikes, flags, ...
    spot, maturities, rate, dividend, volatility);
AssetBinary = @(strikes, flags, spot, maturities) PowerBinary(1, strikes, flags, ...
    spot, maturities, rate, dividend, volatility);
ImageOperatorA = @(ValueFunction, spot) ImageFunction(ValueFunction, barrierFinal, ...
    barrierBending(2), spot, maturity, rate, dividend, volatility);
ImageOperatorB = @(ValueFunction, spot) ImageFunction(ValueFunction, barrierMiddle, ...
    barrierBending(1), spot, bendingChange, rate, dividend, volatility);

% compute the rebate value
value = BondBinary([barrierInitial, barrierMiddle], [psi, -psi], spot, maturities2);
value = value + ImageOperatorB(@(spot) BondBinary([zeta, barrierMiddle], [-psi, ...
    psi], spot, maturities2), spot);
value = value + BondBinary([barrierInitial, barrierMiddle, barrierFinal], [psi, psi, ...
    -psi], spot, maturities3);
value = value + ImageOperatorA(@(spot) BondBinary([zeta2, barrierMiddle, ...
    barrierFinal], [-psi, -psi, -psi], spot, maturities3), spot);
value = value - ImageOperatorB(@(spot) BondBinary([zeta1, barrierMiddle, ...
    barrierFinal], [-psi, psi, -psi], spot, maturities3), spot);
value = value - ImageOperatorB(@(spot) ImageOperatorA(@(spot) BondBinary([zeta3, ...
    barrierMiddle, barrierInitial], [psi, -psi, -psi], spot, maturities3), spot), spot);
value = value + exp(-(maturity - barrierStart) * BondBinary(barrierInitial, -psi, ...
    spot, barrierStart);

end
```

III.F.4 Rebate Valuation: Payout at Hit

```
function [value] = RebatePayAtHit(spot, rate, dividend, volatility, psi, ...
    barrierFinal, barrierBending, barrierStart, bendingChange, maturity)
% REBATEPAYATHIT - values a deferred start piecewise exponential barrier
% pay-at-hit rebate

% compute common expressions
maturities2 = [barrierStart, bendingChange];
maturities3 = [barrierStart, bendingChange, maturity];
alpha = 0.5 - (rate - dividend + barrierBending) / volatility^2;
lambda = 2 * rate / volatility^2;
betaPlus = alpha + sqrt(lambda + alpha.^2);
betaMinus = 2 * alpha - betaPlus;
BetaValue = @(flag, index) IIf(flag == 1, betaPlus(index), betaMinus(index));
```

```
barrierMiddle = barrierFinal * exp(barrierBending(2) * (maturity - bendingChange));
barrierInitial = barrierMiddle * exp(barrierBending(1) * (bendingChange - ...
    barrierStart));
zeta1 = barrierInitial * exp(barrierBending(2) * (barrierStart - bendingChange));
zeta2 = barrierMiddle * exp((barrierBending(1) - barrierBending(2)) * (barrierStart ...
    - bendingChange));
zeta3 = barrierMiddle * exp((barrierBending(1) - barrierBending(2)) * (barrierStart ...
    - bendingChange));
spotAdjustment1 = exp(-barrierBending(1) * barrierStart);
spotAdjustment2 = exp(-barrierBending(2) * bendingChange);

% setup utility functions
ImageOperatorA = @(ValueFunction, spot) ImageFunction(ValueFunction, barrierInitial, ...
    0, spot, bendingChange, rate, dividend - barrierBending(1), volatility);
ImageOperatorB = @(ValueFunction, spot) ImageFunction(ValueFunction, barrierMiddle, ...
    0, spot, maturity, rate, dividend - barrierBending(2), volatility);
ImageOperatorC = @(ValueFunction, spot) ImageFunction(ValueFunction, barrierMiddle, ...
    barrierBending(1), spot, bendingChange, rate, dividend, volatility);

% compute the rebate value
temp = PowerBinary(BetaValue(-psi, 1), barrierInitial, psi, spot * spotAdjustment1, ...
    barrierStart, rate, dividend - barrierBending(1), volatility);
temp = temp - PowerBinary(BetaValue(-psi, 1), [barrierInitial, barrierInitial], [1, ...
    1], spot * spotAdjustment1, maturities2, rate, dividend - barrierBending(1), ...
    volatility);
temp = temp + ImageOperatorA(@(spot) PowerBinary(BetaValue(-psi, 1), ...
    [barrierInitial, barrierInitial], [-1, 1], spot, maturities2, rate, dividend - ...
    barrierBending(1), volatility), spot * spotAdjustment1);
value = temp / barrierInitial^BetaValue(-psi, 1);
temp = PowerBinary(BetaValue(-psi, 2), [zeta1, barrierMiddle], [1, 1], spot * ...
    spotAdjustment2, maturities2, rate, dividend - barrierBending(2), volatility);
temp = temp - PowerBinary(BetaValue(-psi, 2), [zeta1, barrierMiddle, barrierMiddle], ...
    [1, 1, 1], spot * spotAdjustment2, maturities3, rate, dividend - ...
    barrierBending(2), volatility);
temp = temp + ImageOperatorB(@(spot) PowerBinary(BetaValue(-psi, 2), [zeta2, ...
    barrierMiddle, barrierMiddle], [-1, -1, 1], spot, maturities3, rate, dividend - ...
    barrierBending(2), volatility), spot * spotAdjustment2);
temp = temp - ImageOperatorC(@(spot) PowerBinary(BetaValue(-psi, 2), [zeta1, ...
    barrierMiddle], [-1, 1], spot * spotAdjustment2, maturities2, rate, dividend - ...
    barrierBending(2), volatility), spot);
temp = temp + ImageOperatorC(@(spot) PowerBinary(BetaValue(-psi, 2), [zeta1, ...
    barrierMiddle, barrierMiddle], [-1, 1, 1], spot * spotAdjustment2, maturities3, ...
    rate, dividend - barrierBending(2), volatility), spot);
temp = temp - ImageOperatorC(@(spot) ImageOperatorB(@(spot) ...
    PowerBinary(BetaValue(-psi, 2), [zeta3, barrierMiddle, barrierMiddle], [1, -1, ...
    1], spot, maturities3, rate, dividend - barrierBending(2), volatility), spot * ...
    spotAdjustment2), spot);
value = value + temp / barrierMiddle^BetaValue(-psi, 2);
```

```
value = value + PowerBinary(0, barrierInitial, -1, spot, barrierStart, rate, ...
    dividend, volatility);

end
```

III.G Glossary of Notation

$\square$	end of a proof
$\blacksquare$	end of an example
$\triangle$	end of a definition
$1\{A\}$	indicator of the set A
$\mathcal{A}^{\boldsymbol{s}}_{\boldsymbol{\xi}}$	higher-order asset binary
$\mathbb{P}^A$-a.s.	almost surely under $\mathbb{P}^A$
$\mathcal{B}^{\boldsymbol{s}}_{\boldsymbol{\xi}}$	higher-order bond binary
B	constant barrier level
$\tilde{b}(\tau)$	percentage barrier shift
$\tilde{B}(\tau)$	(piecewise) exponential boundary
$\mathcal{D}$	active domain of a PDE
δ	continuously compounded dividend yield
$\mathcal{E}_t\,(X.)$	Doléans-Dade exponential of the process X
$\mathbb{E}_{\mathbb{P}^A}$	expectation under $\mathbb{P}^A$
$\mathbb{F}$	sigma algebra
$\mathfrak{F}_t$	filtration at time t
$\mathcal{H}$	heat operator
$\overset{\tilde{B}(0),\gamma,\tau}{\mathcal{I}}$	exponential barrier image operator
IEBVP	initial exponential boundary value problem
IVS	implied volatility smile
$\mathcal{J}$	stationary Black and Scholes (1973) operator
K	strike price
$\mathcal{L}$	Black and Scholes (1973) operator
ν	first hitting time of a barrier
ODE	ordinary differential equation
Ω	probability space
$\mathbb{P}^*$	bank account martingale measure/risk-neutral measure
${}^{\eta}\mathcal{P}^{\boldsymbol{s}}_{\boldsymbol{\xi}}$	higher-order power binary
PDE	partial differential equation
PDF	probability density function

ϕ	indicator for a put or call option
ψ	indicator for a down- or up-barrier
$\mathcal{Q}_{\boldsymbol{\xi}}^{\boldsymbol{s}}$	higher-order $\mathcal{Q}$ option
r	continuously compounded risk-free interest rate
r.h.s.	right-hand side
S	asset price process
SDE	stochastic differential equation
σ	diffusion coefficient
T	maturity date
T^*	terminal time
T_B	bending change date
T_S	barrier start date
τ	current time-to-maturity
τ_A	current time to the date T_A
$\hat{\tau}_A$	time-to-maturity at the date T_A
$\tilde{V}(S, \tau)$	contingent claim valuation function
W^A	standard one-dimensional Brownian motion under $\mathbb{P}^A$
w.l.o.g	without loss of generality
$\xi\left(\mathbb{P}^A, \mathbb{P}^B\right)$	Radon-Nikodým derivative process between $\mathbb{P}^A$ and $\mathbb{P}^B$

Chapter IV

Jump Size Distributions of Additive Compound Poisson Processes That Are Closed under the Esscher Transform

We model logarithmic asset price dynamics under the physical probability measure as additive jump-diffusion processes, which exhibit a time-dependent jump intensity and jump size distribution. The corresponding risk-neutral probability measure is defined through an Esscher transform. We are interested in the conditions under which the jump size distributions under the two probability measures fall into the same parametric class. We show that it is necessary and sufficient for the jump size distribution to follow a natural exponential mixture family at all points in time. Immediate applications of these results in financial engineering are discussed.

Keywords: Esscher transform, additive processes, compound Poisson, jump-size distribution, natural exponential family

JEL Classification: G13
MS Classification (2010): 60G51, 62E10

IV.1 Introduction

This chapter models asset dynamics as exponential additive jump-diffusion (AJD) processes. In contrast to standard time-homogeneous jump-diffusion (THJD) processes, as considered by for example Merton (1976) and Kou (2002), these allow for a time-dependence of all parameters and, in particular, the jump intensity and the jump size distribution. In general, the corresponding markets are incomplete in the Harrison and Pliska (1981) sense and, consequently, the risk-neutral probability measure is not unique if it exists.

In the mathematical finance literature that solely focuses on the valuation of contingent claims, the problem of selecting a martingale measure is often bypassed by directly specifying the stochastic dynamics under the risk-neutral probability measure; see for example Cai and Kou (2011). The model parameters are then calibrated to the market prices of plain vanilla options. Criteria for model selection are the in- and out-of-sample goodness of fit to the Black and Scholes (1973) implied volatility surface and the empirical robustness of the corresponding hedging and replication strategies; see for example Bakshi et al. (1997).

However, the econometric literature approaches the model selection problem from a different angle by focusing on the physical asset dynamics. The parameters are estimated from the time series of historical returns through maximum likelihood or the generalized method of moments; see for example Ball and Torous (1983), Sørensen (1991), Aït-Sahalia (2002, 2004), Bates (2006) and Ramezani and Zeng (1999, 2007). Models are selected based on their ability to reflect the stylized empirical facts of a particular asset class. Typical test statistics to evaluate the relative fit of two models to the same data set are the likelihood ratio and the Bayesian information criterion. To be able to price contingent claims, one then has to specify the change of measure process that defines the corresponding risk-neutral asset price dynamics.

Often, ad-hoc assumptions about the market price of jump risk are made to obtain a risk-neutral probability measure that differs from the physical probability measure only by the average expected return; see for example Merton (1976). Instead, Gerber and Shiu (1994b) propose to define the Radon-Nikodým derivative process through an Esscher transform of the logarithmic return process. They show that this choice arises as the equilibrium change of measure process in certain economies where the representative agent has iso-elastic utility of consumption. Naik and Lee (1990) obtain a similar result in a Lucas (1978) type pure exchange economy where asset prices follow a Merton (1976) jump-diffusion process. Again, the assumption of iso-elastic utility is key, because it leads to an exponential form of the stochastic discount factor; see Milne and Madan (1991) and Kou (2002) for further applications. In general, the Esscher transform induces a non-zero market price of jump risk. Consequently, the dynamics of the jump components under the physical and risk-neutral probability measures differ. Moreover, the jump size distributions may fall into different parametric classes. However, this is undesirable from a modeling perspective because the two distributions cannot be compared directly to each other based on their respective parameter vectors.

It is beneficial to specify the jump size distribution of logarithmic returns to follow a parametric class that is closed under a measure change defined through an Esscher transform, even when the dynamics under the physical probability measure are irrelevant. As noted by Gerber and Shiu (1994b), the Radon-Nikodým derivative process corresponding to the change of numéraire from the bank account to the spot asset can be represented as an Esscher transform of the logarithmic return process with a unit transform parameter. This application is central because it often simplifies the contingent claim valuation problem significantly. As shown by Geman et al. (1995), it allows to express the value of European plain vanilla options in terms of two probabilities under the risk-neutral and asset price probability measures, respectively. Consequently, if the jump size distribution is closed under an Esscher transform measure change, then being able to evaluate the cumulative distribution function of the logarithmic returns under the risk-neutral probability measure is sufficient to price European plain vanilla options; see for example Kou (2002) for an application.

The literature mostly focuses on asset prices that are driven by THJD processes, and our AJD models nest these as special cases. We show that a time-dependent instantaneous risk-free interest rate, and thus non-constant market prices of risk, renders a THJD processes under the physical probability measure into a strictly AJD process under the Esscher transform martingale measure (ETMM). Similarly, a non-constant jump frequency under the physical probability measure induces a time-dependence of the jump size distribution under the ETMM.

This chapter analyzes conditions under which a class of AJD processes is closed under an Esscher transform measure change. We show that it is both necessary and sufficient for the jump size distribution at each point in time to follow a natural exponential mixture (NEM) family. This result is important as it allows us to narrow down the set of candidate dynamics for a given modeling problem. Further, we fully characterize the parameter vector under the Esscher transform probability measure (ETPM) in terms of the original parameter vector and the transform parameter. Immediate applications of this result to, among others, the THJD models proposed by Merton (1976), Kou (2002) and Cai and Kou (2011) are provided. Finally, we discuss how our result relates to conjugate prior distributions in Bayesian statistics and what its implications for the minimal entropy martingale measure (MEMM) are.

The remainder of this chapter is structured as follows. Section IV.2 introduces the stochastic setup and formally defines AJD processes. We discuss their main properties and derive several auxiliary results. Section IV.3 generalizes the Esscher transform to AJD processes. Section IV.4 discusses AJD processes whose jump size distribution at each point in time follows an NEM family. We show that this class of processes is closed under the Esscher transform and characterize its dynamics under the new probability measure. Applications in financial engineering are also discussed. Section IV.5 concludes the chapter and proposes directions for future research.

IV.2 Stochastic Setup

Let $(\Omega, \mathfrak{F}, \mathbb{F}, \mathbb{P})$ be a complete filtered probability space. We interpret $\mathbb{P}$ to be the physical or real-world probability measure. All considered stochastic processes are defined on the interval $[0, T^*]$ for a fixed terminal time $0 < T^* < \infty$. The filtration $\mathbb{F} = (\mathfrak{F}_t)_{t\in[0,T^*]}$ is the $\mathbb{P}$-augmentation of the natural filtration induced by the process $X = \{X_t : t \in [0, T^*]\}$, defined below. That is

$$\mathfrak{F}_t = \sigma\left(X_u : u \in [0, t]\right) \vee \mathcal{N},$$

where $\mathcal{N}$ are the corresponding $\mathbb{P}$-null sets. By Proposition II.7.7 in Karatzas and Shreve (1991), p. 90, this ensures the right-continuity of $\mathbb{F}$.

Throughout this chapter, the dynamics of X follow an AJD process, as defined in Section IV.2.3. It can be uniquely decomposed into the independent sum of a continuous component $X^c = \{X_t^c : t \in [0, T^*]\}$ and a pure jump component $X^j = \left\{X_t^j : t \in [0, T^*]\right\}$. While X^c follows a drifted Brownian motion with time-dependent drift and diffusion coefficients, which is extensively studied in the literature, the dynamics of X^j are novel. The pure jump component follows an additive compound Poisson (ACP) process, where not only the jump intensity but also the jump size distribution is allowed to be time-dependent, though non-random. In Section IV.2.1, we formally define X^j, show that it is an additive process, and discuss its properties in detail. We then generalize these results to AJD processes in Section IV.2.3.

We consider a frictionless market in which two primary assets can be traded continuously in the interval $[0, T^*]$. $S = \{S_t : t \in [0, T^*]\}$ is the price process of a risky, limited liability spot asset given by

$$S_t = S_0 \mathrm{e}^{X_t},$$

with initial value $S_0 \in \mathbb{R}_+$. $B = \{B_t : t \in [0, T^*]\}$ is the value of a money market account with non-random dynamics

$$\mathrm{d}B_t = r(t) B_t \mathrm{d}t$$

and initial value $B_0 = 1$. Here, $r : [0, T^*] \to \mathbb{R}$ is the deterministic instantaneous risk-free interest rate satisfying

$$\int_0^{T^*} |r(u)| \mathrm{d}u < \infty.$$

Since X follows an ACP process with random jump sizes, this market is generally incomplete in the Harrison and Pliska (1981) sense. Consequently, the risk-neutral probability measure is not unique, if it exists.

Following Jacod and Shiryaev (2003), we start by introducing a stochastic integration operator $\circ$ before defining the dynamics of X because this simplifies the notation in many cases.

Definition IV.1 (Stochastic Integration Operator).
Let $\alpha = \{\alpha_t : t \in [0, T^*]\}$ and $X = \{X_t : t \in [0, T^*]\}$ be two stochastic processes. Then for any $0 \leq s \leq t \leq T^*$, the notation

$$(\alpha \circ X)_{[s,t]} = \int_s^t \alpha_u \mathrm{d}X_u$$

is used to denote the stochastic integral of α with respect to X over the interval $[s, t]$, given that this expression is well-defined. $\triangle$

IV.2.1 Additive Compound Poisson Processes

In the following sections, we use the concept of a Poisson random measure repeatedly. For convenience, we start by providing its definition; see also Definition 19.1 in Sato (1999), p. 119 and Definition 2.18 in Cont and Tankov (2004), p. 57.

Definition IV.2 (Poisson Random Measure).
Let $(\Omega, \mathfrak{F}, \mathbb{P})$ be a probability space and μ be a positive Radon measure on $(E, \mathcal{E})$, where $E \subseteq \mathbb{R}^n$ and $\mathcal{E} := \mathfrak{B}(E)$ is the Borel σ-algebra on the Euclidian subspace E. A Poisson random measure $M : \Omega \times \mathcal{E} \to \mathbb{N}_0$ on E with intensity measure μ is an integer valued random measure such that

(i) for any bounded measurable set $A \in \mathcal{E}$, $M(\cdot, A) < \infty$ is an integer valued random variable,

(ii) for each measurable set $A \in \mathcal{E}$, $M(\cdot, A)$ is a Poisson random variable with mean $\mu(A)$, and

(iii) for disjoint measurable sets $A_1, A_2, \ldots, A_n \in \mathcal{E}$, the random variables $M(\cdot, A_1), M(\cdot, A_2), \ldots, M(\cdot, A_n)$ are independent. $\triangle$

We recall, that a Radon measure on $(E, \mathcal{E})$ assigns a finite measure to every compact measurable set $A \in \mathcal{E}$; see for example Section 7.1 in Folland (1984), pp. 204–209, or Definition 2.2 in Cont and Tankov (2004), p. 23. Note that Definition IV.2 is not in its most general form but is instead chosen to suit our purposes. According to Proposition 19.4 in Sato (1999), p. 122, given any Radon measure μ on $(E, \mathcal{E})$ defined as above, there exists a Poisson random measure M with intensity measure μ; see also Proposition 2.14 in Cont and Tankov (2004), pp. 57–58. Thus, it is sufficient to characterize the intensity measure. Using the concept of Poisson random measures, we can now define an ACP process that allows for a time-dependence in both its jump intensity and its jump size distribution.

Definition IV.3 (Additive Compound Poisson Process).
An ACP process $X^j = \left\{X_t^j : t \in [0, T^*]\right\}$ is defined as

$$X_t^j = \int_0^t \int_{-\infty}^{+\infty} x J_X(\mathrm{d}u \times \mathrm{d}x),$$

where J_X is a Poisson random measure on $(E, \mathcal{E})$ with $E = [0, T^*] \times \mathbb{R}$. Its intensity measure can be decomposed as $\mu(\mathrm{d}t \times \mathrm{d}x) = \lambda(t) f(t,x)\mathrm{d}t\mathrm{d}x$. Here, the jump intensity $\lambda : [0, T^*] \to \mathbb{R}_+$ is a deterministic function satisfying

$$\int_0^{T^*} \lambda(u)\mathrm{d}u < \infty$$

and for each time $0 \leq t \leq T^*$, $f(t, \cdot) : \mathbb{R} \to \mathbb{R}_+$ is a probability density function (PDF). $\triangle$

Note that the above definition, in particular, implies that μ is a finite measure on $\mathbb{R}$ for each $0 \leq t \leq T^*$, that is,

$$\int_0^{T^*} \int_{-\infty}^{+\infty} \mu(\mathrm{d}u \times \mathrm{d}x) < \infty.$$

Thus, X^j has piecewise constant trajectories; see for example Proposition 3.8 in Cont and Tankov (2004), p. 85. Like time-homogeneous compound Poisson processes, X^j is a right-continuous pure jump process. The expected number of jumps over any time interval $[s, t]$ for $0 \leq s \leq t \leq T^*$ is given by

$$\zeta(t) - \zeta(s) = \int_s^t \lambda(u)\mathrm{d}u.$$

Conditional on observing a jump at time $0 \leq t \leq T^*$, its jump size follows the PDF $f(t, x)$. This process no longer has stationary increments because of the time-dependence of the jump intensity and the jump size distribution and, thus, it is generally not a Lévy process. However, as already implied by the chosen nomenclature, X^j is an additive process. The following lemma formally establishes this.

Lemma IV.1 (X^j Is an Additive Process).
The ACP process $X^j = \left\{X_t^j : t \in [0, T^*]\right\}$ *in Definition IV.3 is an additive process. Following Definition 1.6 in Sato (1999), p. 3, this entails that it*

(i) starts at $X_0 = 0$,

(ii) has independent increments, and

(iii) is stochastically continuous;

see also Definition 14.1 in Cont and Tankov (2004), p. 454.

Proof Property (i) is obvious from the definition as an integral. The independence of increments follows immediately from the independence of the Poisson random measure over disjoint sets; see Definition IV.2.(iii). Stochastic continuity requires that

$$\lim_{h\downarrow 0}\mathbb{P}\left\{\left|X^j_{t+h}-X^j_t\right|>\epsilon\right\}=0$$

for all $\epsilon>0$. This can be shown to hold by dominated convergence, since the probability on the left-hand side is bounded from above by the probability of observing one or more jumps over the interval $[t,t+h]$, which converges to zero in the limit. See Appendix IV.A.2 for details. □

Note that some definitions of additive processes also include the extra condition of right-continuous sample paths. However, this is not necessary because every additive process, as defined above, admits a unique right-continuous modification; see Theorem 11.5 in Sato (1999), p. 63. In the following sections, we will always assume implicitly that the process under consideration is this right-continuous modification.

Only a few papers in the mathematical finance literature consider risky asset prices driven by additive processes explicitly. One example is Fujiwara (2009), who characterizes the MEMM under these dynamics. In contrast to this chapter, he allows for more general jump dynamics and does not impose the decomposition of the intensity measure in Definition IV.3.

The result in Proposition IV.1 below is repeatedly applied in what follows to find characteristic functions and construct exponential martingales.

Proposition IV.1 (Exponential Form of X^j).
Let $X^j=\left\{X^j_t:t\in[0,T^*]\right\}$ be an ACP process and let $\alpha:[0,T^*]\to\mathbb{R}$ be a deterministic function. Then for any $0\le t\le T^*$

$$\begin{aligned}\mathbb{E}_{\mathbb{P}}\left[\exp\left\{\mathrm{i}\left(\alpha\circ X^j\right)_{[0,t]}\right\}\right]&=\exp\left\{\int_0^t\int_{-\infty}^{+\infty}\left(\mathrm{e}^{\mathrm{i}\alpha(u)x}-1\right)\lambda(u)f(u,x)\mathrm{d}x\mathrm{d}u\right\}\\&=\exp\left\{\int_0^t\lambda(u)\left(\phi_Y\left(u,\alpha(u)\right)-1\right)\mathrm{d}u\right\},\end{aligned}$$

where

$$\phi_Y(t,\omega)=\int_{-\infty}^{+\infty}\mathrm{e}^{\mathrm{i}\omega x}f(t,x)\mathrm{d}x$$

is the characteristic function of the PDF $f(t,x)$ under $\mathbb{P}$.

Proof This is a special case of the more general Proposition 19.5 in Sato (1999), pp. 123–124, adapted to the ACP process in Definition IV.3; see also Proposition 3.6 in Cont and Tankov (2004), p. 78. □

Corollary IV.1 (Characteristic Function of X^j).
Let $X^j = \left\{X_t^j : t \in [0, T^*]\right\}$ be an ACP process. Then, for any $0 \leq t \leq T^*$, the characteristic function $\phi_{X_t^j}(\omega)$ of X_t^j under $\mathbb{P}$ is given by

$$\begin{aligned}
\phi_{X_t^j}(\omega) &= \exp\left\{\int_0^t \int_{-\infty}^{+\infty} \left(\mathrm{e}^{\mathrm{i}\omega x} - 1\right) \lambda(u) f(u,x) \mathrm{d}x \mathrm{d}u\right\} \\
&= \exp\left\{\int_0^t \lambda(u) \left(\phi_Y(u,\omega) - 1\right) \mathrm{d}u\right\}.
\end{aligned}$$

Proof This immediately follows from applying Proposition IV.1 with $\alpha(u) = \omega$. □

Lemma IV.2 below shows that, as for standard time-homogeneous compound Poisson processes, the distribution of the process at any point in time can be decomposed into the sum of independent processes with the same jump size distribution but a scaled down jump intensity.

Lemma IV.2 (Infinite Divisibility).
Let $X^j = \left\{X_t^j : t \in [0, T^*]\right\}$ be an ACP process. For every $0 \leq t \leq T^*$, the distribution of X_t^j is infinitely divisible. For any $n = 2, 3, \ldots$, there exist n independent and identically distributed (i.i.d.) random variables $Y_t^{1,j}, Y_t^{2,j}, \ldots, Y_t^{n,j}$ such that

$$X_t^j \sim_{\mathbb{P}} \sum_{i=1}^n Y_t^{i,j}.$$

In particular, each $Y^{i,j} = \left\{Y_t^{i,j} : t \in [0, T^*]\right\}$ is an ACP process with jump intensity $\hat{\lambda}(t) = \lambda(t)/n$ and the same time-dependent jump size distribution as X^j.

Proof The infinite divisibility of the distribution of X_t^j for every $0 \leq t \leq T^*$ follows from X^j being an additive process as shown in Lemma IV.1; see Theorem 9.1 in Sato (1999), p. 47. It is straightforward to check that the n-th power of the characteristic function of $Y_t^{1,j}$ is equal to $\phi_{X_t^j}(\omega)$. □

Similar to Lévy processes, the distribution of an additive process at each point in time can be fully characterized through a generating triplet. However, we in general need to define these triplets for each point in time separately because of their non-stationarity.

Lemma IV.3 (System of Generating Triplets).
Let $X^j = \left\{X_t^j : t \in [0, T^*]\right\}$ be an ACP process. Then its system of generating triplets with respect to the truncation function $g(x) = 0$ is given by $\left(\sigma^2, \nu, \gamma\right) = \left\{\left(\sigma^2(t), \nu(t,\cdot), \gamma(t)\right) : t \in [0, T^*]\right\}$, where

$$\begin{aligned} \sigma^2(t) &= 0 \\ \nu(t,x) &= \int_0^t \lambda(u) f(u,x) \mathrm{d}u \\ \gamma(t) &= 0. \end{aligned}$$

Proof This immediately follows from Corollary IV.1, Lemma IV.2 and the Lévy-Khintchine representation; see for example Theorems 8.1 and 9.8 in Sato (1999), pp. 37–38 and p. 52. □

When defining the Esscher transform in Section IV.3, we need to construct exponential martingales from AJD processes. Lemma IV.4 lays the foundation for this.

Lemma IV.4 (Complex Exponential Martingale of X^j).
Let $X^j = \left\{X_t^j : t \in [0, T^*]\right\}$ be an ACP process adapted to the filtration $\mathbb{F}$. Let $\alpha : [0, T^*] \to \mathbb{R}$ be a deterministic function and define the process $Z^j = \left\{Z_t^j : t \in [0, T^*]\right\}$ by

$$Z_t^j = \exp\left\{\mathrm{i}\left(\alpha \circ X^j\right)_{[0,t]}\right\}\left(\mathbb{E}_{\mathbb{P}}\left[\exp\left\{\mathrm{i}\left(\alpha \circ X^j\right)_{[0,t]}\right\}\right]\right)^{-1}.$$

Then Z is a complex valued $(\mathbb{P}, \mathbb{F})$-martingale.

Proof This follows from X^j having independent increments in conjunction with Proposition IV.1. See Appendix IV.A.1 for details. □

IV.2.2 Time-Changed Compound Poisson Processes

In the following sections, we will often consider the special case when the jump size distribution does not depend on time. This yields a standard compound Poisson process with time-dependent intensity and allows for a more well-known representation in terms of a Poisson sum over i.i.d. random variables. The following definitions and lemmata make this precise.

Definition IV.4 (Time-Changed Compound Poisson Process).
A time-changed compound Poisson (TCCP) process is an ACP process whose intensity measure can be decomposed as $\mu(\mathrm{d}t \times \mathrm{d}x) = \lambda(t) f(x) \mathrm{d}t\mathrm{d}x$, where $f : \mathbb{R} \to \mathbb{R}_+$ is a PDF. $\triangle$

Cox (1955) considers a more general class of time-inhomogeneous Poisson processes, where the instantaneous jump intensity is itself stochastic.

Lemma IV.5 (Time-Changed Compound Poisson Representation I).
Let $X^j = \left\{X_t^j : t \in [0, T^*]\right\}$ be a TCCP process with deterministic jump intensity. Then it can be represented as

$$X_t^j = \sum_{i=1}^{N_t} Y_i,$$

where $N = \{N_t : t \in [0, T^*]\}$ is a one-dimensional Poisson process and $(Y_i)_{i\in\mathbb{N}}$ is a sequence of i.i.d. scalar random variables with PDF $f : \mathbb{R} \to \mathbb{R}_+$ on $(\Omega, \mathfrak{F}, \mathbb{F}, \mathbb{P})$. The Poisson process has a deterministic intensity $\lambda : [0, T^*] \to \mathbb{R}_+$ and is independent of the sequence of random variables $(Y_i)_{i\in\mathbb{N}}$.

Proof We compute the characteristic function of the proposed representation of X^j and show that it is equal to the one in Corollary IV.1 when the jump size distribution is time-homogeneous. See Appendix IV.A.3 for details. $\square$

The following lemma justifies the choice of the nomenclature for the class of processes in Definition IV.4.

Lemma IV.6 (Time-Changed Compound Poisson Representation II).
Let $X^j = \left\{X_t^j : t \in [0, T^*]\right\}$ be a TCCP process and let $\tilde{X}^j = \left\{\tilde{X}_t^j : t \in [0, T^*]\right\}$ be defined by

$$\tilde{X}_t^j = \sum_{i=1}^{\tilde{N}_t} Y_i^j,$$

where $\tilde{N} = \left\{ \tilde{N}_t : t \in [0, T^*] \right\}$ *is another one-dimensional Poisson process on* $(\Omega, \mathfrak{F}, \mathbb{F}, \mathbb{P})$*. We assume that* $\tilde{N}$ *has a constant intensity of one and is independent of the sequence of i.i.d. random variables* $\left(Y_i^j\right)_{i \in \mathbb{N}}$*. Then* $X_t^j \sim_{\mathbb{P}} \tilde{X}_{\zeta(t)}^j$ *for all* $0 \leq t \leq \zeta^{-1}(T^*)$*, where* $\sim_{\mathbb{P}}$ *denotes equality in distribution under the measure* $\mathbb{P}$*.*

Proof By construction, N_t and $\hat{N}_{\zeta(t)}$ have the same distribution under $\mathbb{P}$. $\square$

The intuition behind this result is that only the distribution of the total number of jumps is relevant because the jump size distribution is independent of the jump time. Thus, we can define a Poisson process with constant intensity and speed up or slow down calendar time by a deterministic function such that at all times the distribution of the original Poisson process and the time-changed one are identical.

Finally, it is useful to distinguish clearly between ACP processes that are also TCCP processes and the ones that are not. Definition IV.5 makes this precise.

Definition IV.5 (Strictly Additive Compound Poisson Processes).
Let $X^j = \left\{ X_t^j : t \in [0, T^*] \right\}$ be an ACP process. It is a strictly ACP process, if it is not a TCCP process. $\triangle$

IV.2.3 Additive Jump-Diffusion Processes

This section extends the ACP dynamics to include a continuous drift and martingale component. This extension is straightforward but treated separately from the definition of the pure jump component for clarity of exposition. For brevity, we only discuss the results that are central to the following applications.

Definition IV.6 (Additive Jump-Diffusion Process).
An AJD process $X = \{X_t : t \in [0, T^*]\}$ is defined as

$$X_t = X_t^c + X_t^j.$$

Here, the process $X^c = \{X_t^c : t \in [0, T^*]\}$ is the continuous part of X given by

$$X_t^c = \int_0^t \gamma(u) \mathrm{d}u + \int_0^t \sigma(u) \mathrm{d}W_u,$$

where $\gamma : [0,T^*] \to \mathbb{R}$ and $\sigma : [0,T^*] \to \mathbb{R}_+$ are deterministic functions satisfying

$$\int_0^{T^*} \left(|\gamma(u)| + \sigma^2(u)\right) \mathrm{d}u < \infty,$$

$W = \{W_t : t \in [0,T^*]\}$ is a one-dimensional Brownian motion under $\mathbb{P}$, and $X^j = \left\{X_t^j : t \in [0,T^*]\right\}$ is an ACP process independent of W. $\triangle$

Proposition IV.2 provides the exponential form for AJD processes, thus, generalizing Proposition IV.1.

Proposition IV.2 (Exponential Form of X).
Let $X = \{X_t : t \in [0,T^*]\}$ be an AJD process and let $\alpha : [0,T^*] \to \mathbb{R}$ be a deterministic function satisfying

$$\int_0^{T^*} \left(|\alpha(u)\gamma(u)| + \alpha^2(u)\sigma^2(u)\right) \mathrm{d}u < \infty.$$

Then

$$\begin{aligned}\mathbb{E}_{\mathbb{P}}\left[\exp\left\{\mathrm{i}\,(\alpha \circ X)_{[0,t]}\right\}\right] \quad = \quad & \exp\left\{\mathrm{i}\int_0^t \alpha(u)\gamma(u)\mathrm{d}u - \frac{1}{2}\int_0^t \alpha^2(u)\sigma^2(u)\mathrm{d}u\right. \\ & \left. + \int_0^t \int_{-\infty}^{+\infty} \left(\mathrm{e}^{\mathrm{i}\alpha(u)x} - 1\right) \lambda(u) f(u,x)\mathrm{d}x\mathrm{d}u\right\}.\end{aligned}$$

Proof The expectation factors and, thus, the exponential form of X can be expressed as a product of the exponential forms of the continuous and pure jump components because of the independence of X^c and X^j. Using that

$$\int_0^t \alpha(u)\sigma(u)\mathrm{d}W_u \sim \mathcal{N}\left(0, \int_0^t \alpha^2(u)\sigma^2(u)\mathrm{d}u\right),$$

we find that

$$\mathbb{E}_{\mathbb{P}}\left[\exp\left\{\mathrm{i}\,(\alpha \circ X^c)_{[0,t]}\right\}\right] = \exp\left\{\mathrm{i}\int_0^t \alpha(u)\gamma(u)\mathrm{d}u - \frac{1}{2}\int_0^t \alpha^2(u)\sigma^2(u)\mathrm{d}u\right\}$$

and the claim follows. $\square$

Similar to Proposition IV.1, this result yields the characteristic function of X as a special case. Analogous to Lemma IV.4, we can construct a complex exponential martingale from X. We omit the details for brevity.

IV.3 Esscher Transform Probability Measures

This section defines an equivalent probability measure through the Esscher transform when the risk process is given by an AJD process. We show that the ETPM constructed from a time-inhomogeneous jump-diffusion process generally induces a time-dependence of the jump size distribution. The ETMM is a special case of the ETPM, where the transform process is chosen such that the stock price is a martingale under the bank account numéraire. Our analysis unveils an, at the outset surprising, connection between the short-rate process and the jump dynamics under the ETMM.

Following Esscher (1932), we start by giving the definition of an Esscher transform of a random variable.

Definition IV.7 (Esscher Transform).
Let Z be a random variable whose law under $\mathbb{P}$ is given by some distribution function $F_Z(x)$ with corresponding characteristic function $\phi_Z(\omega)$. For a transform parameter $\beta \in \mathbb{R}$, the Esscher transform distribution function $\hat{F}_Z(x)$ of $F_Z(x)$ is given by

$$\mathrm{d}\hat{F}_Z(x) = \frac{\mathrm{e}^{\beta x}\mathrm{d}F_Z(x)}{\phi_Z(-\mathrm{i}\beta)},$$

conditional on

$$\phi_Z(-\mathrm{i}\beta) = \int_{-\infty}^{+\infty} \mathrm{e}^{\beta x}\mathrm{d}F_Z(x) < \infty. \qquad \triangle$$

Thus, the Esscher transform corresponds to an exponential tilting of the PDF, if available, and a subsequent re-normalization. This requires that the β-th exponential moment of Z under $\mathbb{P}$ is well-defined. Gerber and Shiu (1994b) extend this approach to a Lévy process $X = \{X_t : t \in [0, T^*]\}$ by applying an exponential tilting to the PDF of X_t at all points in time $t \in [0, T^*]$. Analogous to Definition IV.7, this is still possible in terms of a Riemann-Stieltjes integral, even when the distribution function of X_t is not differentiable. Definition IV.8 generalizes this approach to additive processes. The non-stationarity now calls for a time-dependent transform parameter. We refer to Kallsen and Shiryaev (2002) for an application to semimartingales, where the change of measure process takes a similar structure.

Definition IV.8 (Esscher Transform Process).
The Esscher transform process $\hat{X} = \left\{\hat{X}_t : t \in [0, T^*]\right\}$ of the additive process $X =$

$\{X_t : t \in [0, T^*]\}$ with deterministic transform parameter $\beta : [0, T^*] \to \mathbb{R}$ is given by

$$\hat{X}_t \quad = \quad \exp\left\{(\beta \circ X)_{[0,t]}\right\} \left(\mathbb{E}_{\mathbb{P}}\left[\exp\left\{(\beta \circ X)_{[0,t]}\right\}\right]\right)^{-1},$$

conditional on

$$\int_0^{T^*} \left(|\beta(u)\gamma(u)| + \beta^2(u)\sigma^2(u)\right) \mathrm{d}u < \infty$$

and

$$\int_0^{T^*} \int_{-\infty}^{+\infty} \mathrm{e}^{\beta(u)x} \mu(\mathrm{d}u \times \mathrm{d}x) < \infty. \qquad \triangle$$

Lemma IV.7 ($\hat{X}$ Is a Radon-Nikodým Derivative Process).
The Esscher transform process $\hat{X} = \left\{\hat{X}_t : t \in [0, T^*]\right\}$ in Definition IV.8 constitutes a valid Radon-Nikodým derivative process.

Proof For $\hat{X}$ to be a valid Radon-Nikodým derivative process, it has to be a $(\mathbb{P}, \mathbb{F})$-martingale starting at $\hat{X}_0 = 1$. The latter property is obvious from Definition IV.8. Next, we factor $\hat{X}$ into two terms linked to the continuous and jump components X^c and X^j, respectively. We can show that each of these independent processes is a $(\mathbb{P}, \mathbb{F})$-martingale and, thus, their product is as well. All details are provided in Appendix IV.B.1. $\square$

Definition IV.9 (Esscher Transform Probability Measure).
Let $X = \{X_t : t \in [0, T^*]\}$ be an AJD process. The ETPM $\hat{\mathbb{P}}(X, \beta)$ equivalent to $\mathbb{P}$ on $[0, T^*]$ is defined through the Radon-Nikodým derivative process $\hat{X} = \left\{\hat{X}_t : t \in [0, T^*]\right\}$ in Definition IV.8. For all $0 \leq t \leq T^*$, we have

$$\begin{aligned} \xi_t\big(\mathbb{P}, \hat{\mathbb{P}}\big) = \left.\frac{\mathrm{d}\hat{\mathbb{P}}}{\mathrm{d}\mathbb{P}}\right|\mathfrak{F}_t \quad &= \quad \exp\left\{\int_0^t \beta(u)\sigma(u)\mathrm{d}W_u - \frac{1}{2}\int_0^t \beta^2(u)\sigma^2(u)\mathrm{d}u\right\} \\ &\quad\ \exp\left\{\int_0^t \int_{-\infty}^{+\infty} \beta(u)x J_X(\mathrm{d}u \times \mathrm{d}x)\right. \\ &\quad\ \left. - \int_0^t \int_{-\infty}^{+\infty} \left(\mathrm{e}^{\beta(u)x} - 1\right) \lambda(u) f(u, x)\mathrm{d}x\mathrm{d}u\right\} \qquad \mathbb{P}\text{-a.s..} \end{aligned}$$

We denote the set of all ETPM by $\mathcal{P}(X)$. $\triangle$

Again, the Radon-Nikodým derivative process factors into a change of measure process for the continuous and jump parts of X, respectively, because of the independence of X^c and X^j. The following standard result characterizes the drift of X^c under the new probability measure $\hat{\mathbb{P}}(X,\beta)$.

Lemma IV.8 (Dynamics of X^c under $\hat{\mathbb{P}}(X,\beta)$).
Let $X^c = \{X_t^c : t \in [0,T^*]\}$ be the continuous component of an AJD process $X = \{X_t : t \in [0,T^*]\}$. Then

$$X_t^c = \int_0^t \big(\gamma(u) + \beta(u)\sigma^2(u)\big)\,\mathrm{d}u + \int_0^t \sigma(u)\mathrm{d}\hat{W}_u,$$

where the process $\hat{W} = \{\hat{W}_t : t \in [0,T^*]\}$ is a standard one-dimensional Brownian motion under $\hat{\mathbb{P}}(X,\beta)$.

Proof This is a direct consequence of the Girsanov theorem for Brownian motions; see for example Theorem III.5.1 in Karatzas and Shreve (1991), p. 191. In particular, it entails that the process

$$\hat{W}_t = W_t - \int_0^t \beta(u)\sigma(u)\mathrm{d}u.$$

is a one-dimensional standard Brownian motion under $\hat{\mathbb{P}}(X,\beta)$ and the result follows by substitution. □

Note that the conditions imposed on the transform parameter in Definition IV.8 are sufficient for the Lebesgue integral in the dynamics of X^c under $\hat{\mathbb{P}}(X,\beta)$ to be well-defined. In the following sections, we discuss the effect of the measure transformation on the ACP process in detail. We start by finding the characteristic function of X^j under $\hat{\mathbb{P}}(X,\beta)$.

Proposition IV.3 (Dynamics of X^j under $\hat{\mathbb{P}}(X,\beta)$ I).
Let $X^j = \{X_t^j : t \in [0,T^*]\}$ be the ACP pure jump component of an AJD process $X = \{X_t : t \in [0,T^*]\}$ under $\mathbb{P}$. Let $\beta : \mathbb{R}_+ \to \mathbb{R}$ be such that

$$\int_0^{T^*}\int_{-\infty}^{+\infty} \mathrm{e}^{\beta(u)x} f(u,x)\mathrm{d}x\mathrm{d}u < \infty.$$

Then X^j is also an ACP process under the ETPM $\hat{\mathbb{P}}(X,\beta)$ with intensity measure $\hat{\mu}(\mathrm{d}t \times \mathrm{d}x) = \hat{\lambda}(t)\hat{f}(t,x)\mathrm{d}t\mathrm{d}x$, where

$$\begin{aligned} \hat{\lambda}(t) &= \lambda(t)\phi_Y(t,-\mathrm{i}\beta(t)), \\ \hat{f}(t,x;\beta(t)) &= \frac{\mathrm{e}^{\beta(t)x} f(t,x)}{\phi_Y(t,-\mathrm{i}\beta(t))} \end{aligned}$$

and $\phi_Y(t,\omega)$ is the characteristic function of the PDF $f(t,x)$ under $\mathbb{P}$ as defined in Proposition IV.1.

Proof This is shown by computing the characteristic function $\hat{\phi}_{X_t^j}(\omega)$ of X_t^j under $\hat{\mathbb{P}}(X,\beta)$. We start by making a change of measure to represent $\hat{\phi}_{X_t}(\omega)$ as an expectation under $\mathbb{P}$, which can be computed using Proposition IV.1. The resulting expression resembles the characteristic function of an ACP process given in Corollary IV.1, but the PDF needs to be renormalized. All details can be found in Appendix IV.B.2. □

We observe that, for each time $0 \leq t \leq T^*$, the jump size distribution under the ETPM $\hat{\mathbb{P}}(X,\beta)$ is given by the Esscher transform of the corresponding jump size distribution under the original probability measure $\mathbb{P}$ with transform parameter $\beta(t)$; compare to Definition IV.7.

Corollary IV.2 (Characteristic Function of $\hat{f}(t,x)$).
The characteristic function of the jump size PDF $\hat{f}(t,x)$ is given by

$$\hat{\phi}_Y(t,\omega) = \frac{\phi_Y(t,\omega - \mathrm{i}\beta(t))}{\phi_Y(t,-\mathrm{i}\beta(t))}.$$

Proof This is shown as part of the proof to Proposition IV.3 in Appendix IV.B.2. □

In the context of contingent claim valuation, the ETPM has two main applications. First, it is used to construct the risk-neutral probability measure. As discussed in the literature review in Section IV.1, the ETMM naturally arises as the pricing kernel in different model economies, where the representative agent has iso-elastic utility of consumption; see for example Naik and Lee (1990), Milne and Madan (1991) and Gerber and Shiu (1994b). Second, the Radon-Nikodým derivative process linked to the change of numéraire from the bank account to the spot asset corresponds to an Esscher transform of the logarithmic return process with a constant transform parameter function $\beta(t) = 1$; see for example Gerber and Shiu (1994b) and Geman et al. (1995).

We proceed by defining and characterizing the ETMM.

Definition IV.10 (Esscher Transform Martingale Measure).

An ETPM $\mathbb{P}^* \in \mathcal{P}(X)$ is the ETMM, if the discounted asset price process S/B is a $(\mathbb{P}^*, \mathbb{F})$-martingale. $\triangle$

Lemma IV.9 (Characterization of the ETMM).

The discounted asset price process S/B is a $(\mathbb{P}^*, \mathbb{F})$-martingale if the transform parameter $\beta^* : [0, T^*] \to \mathbb{R}$ satisfies

$$\gamma(t) - r(t) + \sigma^2(t)\left(\beta^*(t) + \frac{1}{2}\right) + \lambda(t)\left(\phi_Y\left(t, -\mathrm{i}\left(1 + \beta^*(t)\right)\right) - \phi_Y\left(t, -\mathrm{i}\beta^*(t)\right)\right) = 0$$

for all $t \in [0, T^*]$.

Proof The martingale condition $S_0 = \mathbb{E}_{\mathbb{P}^*}\left[S_t/B_t\right]$ for all $t \in [0, T^*]$ can equivalently be expressed as $\phi^*_{X_t}(-\mathrm{i}) = B_t$. Using Propositions IV.2 and IV.3, we obtain

$$\int_0^t \left(\gamma(u) - r(u) + \sigma^2(u)\left(\beta^*(u) + \frac{1}{2}\right) + \lambda^*(u)\left(\phi^*_Y(u, -\mathrm{i}) - 1\right)\right) \mathrm{d}u = 0.$$

We substitute for the jump frequency and the characteristic function of the jump size distribution under $\mathbb{P}$ using Proposition IV.3 and Corollary IV.1 to obtain the result. $\square$

Note that the above characterization does not mean to imply the existence of the ETMM. For any fixed $t \in [0, T^*]$, the conditions under which this problem has a solution are very similar to the standard time-homogeneous case. We refer to the proof of Proposition 9.9 in Cont and Tankov (2004), pp. 310–310, who discuss the existence of the ETMM for Lévy processes; see also Section 2 in Gerber and Shiu (1994a), pp. 197–200. Delbaen and Schachermayer (1994) generalize the fundamental theorem of asset pricing due to Harrison and Pliska (1981) by showing that in general semimartingale markets, the existence of a risk-neutral probability measure is equivalent to the absence of arbitrage. It should be noted that the non-existence of the ETMM does not imply the existence of an arbitrage, as the ETMM is only one possible construction of the risk-neutral probability measure.

The condition in Lemma IV.9 has one interesting consequence. Assume that logarithmic returns follow a THJD process under the physical probability measure. If the risk-free interest rate is a non-constant deterministic function of time, then Lemma IV.9 implies that $\beta^*(t)$ is non-constant as well. Thus, by Proposition IV.3, both the jump intensity and the jump size distribution become time-dependent under the ETMM and we obtain a strictly ACP process. The connection between the risk-free rate and the risk-neutral jump dynamics seems surprising at first. By assumption, X follows a THJD process under $\mathbb{P}$. Thus, a non-constant instantaneous risk-free rate implies a time-varying excess return. Since the jump risk is priced under the Esscher transform, this yields a non-constant market price of jump risk and, consequently, also a time-varying jump intensity and jump size distribution under the ETMM. We illustrate this by giving an example based on the Merton (1976) jump-diffusion model.

Example IV.1 (Merton (1976) with a Term-Structure of Interest Rates). Following Merton (1976), we assume that the physical dynamics of the logarithmic returns exhibit normally distributed jumps, that is

$$X_t = \left(\mu - \frac{1}{2}\sigma^2 - \lambda\left(\phi_Y(-\mathrm{i}) - 1\right)\right) t + \sigma W_t + \sum_{i=1}^{N_t} Y_i,$$

where $N = \{N_t : t \in [0, T^*]\}$ is a one-dimensional Poisson process with a constant intensity $\lambda \in \mathbb{R}_+$ under $\mathbb{P}$, and $(Y_i)_{i\in\mathbb{N}}$ is a sequence of i.i.d. $\mathcal{N}\left(\gamma, \delta^2\right)$ normal random variables. Assume that we estimate $\mu = 10\%$, $\sigma = 20\%$, $\lambda = 15$, $\gamma = -0.50\%$ and $\delta = 2.50\%$ from the historical time series of returns. Let the instantaneous interest rate be given by a Nelson and Siegel (1987) exponential polynomial of the form

$$r(t) = \zeta_0 + \zeta_1 \mathrm{e}^{-t/\eta}.$$

The corresponding term-structure of zero-coupon yields is then given by

$$\begin{aligned} y(t) &= \frac{1}{t}\int_0^t r(u)\mathrm{d}u \\ &= \zeta_0 + \zeta_1\left(\frac{\eta}{t}\right)\left(1 - \mathrm{e}^{-t/\eta}\right). \end{aligned}$$

Assume that, by calibrating the parameters to the current term-structure of interest rates, we obtain $\zeta_0 = 5.00\%$, $\zeta_1 = -2.00\%$ and $\eta = 1.50$. This yields a strictly increasing and concave term-structure of instantaneous forward rates with $r(0) = 3.00\%$ and $\lim_{t\to\infty} r(t) = 5.00\%$.

Using Lemma IV.9, we numerically solve for the transform parameter function $\beta^*(t)$ using a root-search routine. Figure IV.1 shows the time-dependence of the jump-diffusion parameters under the ETMM. Since the risk premium under the physical probability measure is positive for all time horizons, the expected return from jumps over any fixed time interval is lower under the ETMM than under the physical probability measure. This corresponds to a lower mean jump return $\gamma^*(t)$ and a higher jump frequency $\lambda^*(t)$. ■

Now assume that the logarithmic returns follow a TCCP process under the physical probability measure and the risk-free interest rate is constant. By a similar argument, it follows from Lemma IV.9 that the transform function $\beta^*(t)$ becomes time-dependent. Consequently, a TCCP process under the physical probability measures is rendered into a strictly ACP process under the ETMM.

These two examples provide further justification for considering ACP processes. They show that ACP processes can arise quite naturally under a measure transformation from common asset dynamics.

IV.4 Natural Exponential Families

In this section, we define two subclasses of ACP processes, where, at each time $0 \leq t \leq T^*$, the jump size distribution is a natural exponential (NE) family or a finite mixture thereof. The important property of these special types of ACP processes is that they are closed under an Esscher transform measure change. To be able to better focus on the key idea, we start by deriving the main results for the simpler case of no mixing before moving on to the more general case.

IV.4.1 One-Parameter Natural Exponential Families

We start by recalling the following two definitions; see for example Chapter 1.6 in Bickel and Doksum (2001), pp. 49–66.

Definition IV.11 (Exponential Family).
An exponential family is a class of probability distributions indexed by a parameter vector $\boldsymbol{\eta} \in \mathbb{R}^n$ for some $n \in \mathbb{N}$ whose PDF admits the representation

$$f(x;\boldsymbol{\eta}) = a(x) \exp\left\{\boldsymbol{\eta} \cdot \boldsymbol{T}(x) - b(\boldsymbol{\eta})\right\},$$

where $\boldsymbol{T} : \mathbb{R} \to \mathbb{R}^n$ is the sufficient statistic, $\beta : \mathbb{R}^n \to \mathbb{R}$ and $a : \mathbb{R} \to \mathbb{R}_+$. △

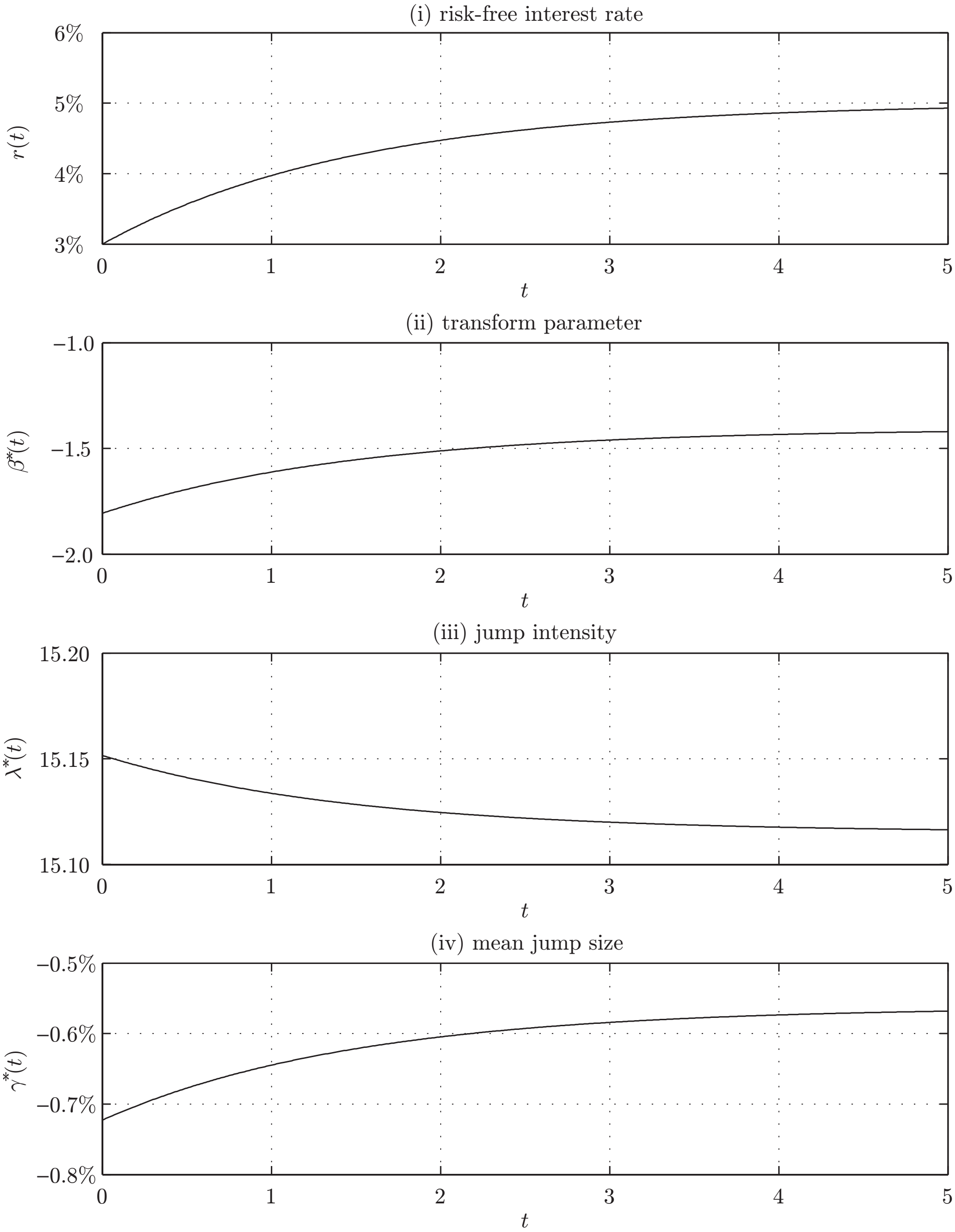

Figure IV.1: Sample parameters of the Merton (1976) model under the ETMM when the instantaneous risk-free interest rate is time-dependent.

Definition IV.12 (Natural Exponential Family).

An NE family is a class of probability distributions indexed by a parameter $\theta \in \mathbb{R}$, whose PDF admits the representation

$$f(x;\theta) = a(x) \exp\{\theta x - b(\theta)\}.$$

We define $\mathcal{D}_{\mathrm{NE}}(b(\cdot))$ as the class of NE families characterized by the function $b(\theta)$ and formally write $f(x;\theta) \in \mathcal{D}_{\mathrm{NE}}(b(\cdot))$ to indicate that the PDF $f(x;\theta)$ is a member of $\mathcal{D}_{\mathrm{NE}}(b(\cdot))$. $\triangle$

Thus, an NE family is a one-parameter exponential family, whose sufficient statistic $T(x) = x$ is the identity function. Given the class of exponential families $\mathcal{D}_{\mathrm{NE}}(b(\cdot))$ that a PDF belongs to, it is fully characterized by the particular value of the parameter θ. Note that many multi-parameter classes of distributions are NE families when considering all but one parameter as fixed; see also the examples following Proposition IV.4.

Lemma IV.10 (Characteristic Function of Natural Exponential Families).

Let Z be a random variable whose distribution under $\mathbb{P}$ is a $\mathcal{D}_{NE}(b(\cdot))$ NE family with parameter θ. Then the characteristic function $\phi_Z(\omega)$ of Z under $\mathbb{P}$ is given by

$$\phi_Z(\omega) = \exp\{b(\theta + \mathrm{i}\omega) - b(\theta)\}.$$

Proof This follows from a completion of the exponent in the integrand defining the characteristic function; see Appendix IV.C.1 for details. $\square$

Note that the characteristic function of a random variable following an NE family only depends on the functional form of $b(\theta)$ but not on $a(x)$. Since the characteristic function uniquely identifies a distribution, see for example Theorem 3.1.1 in Lukacs (1970), p. 28, it follows that $b(\theta)$ fully characterizes any NE family. This justifies the notation $\mathcal{D}_{\mathrm{NE}}(b(\cdot))$ introduced in Definition IV.12.

Definition IV.13 (Natural Exponential Additive Compound Poisson Processes).

Let $X^j = \left\{X_t^j : t \in [0, T^*]\right\}$ be an ACP process. It is an NE-ACP process, if the intensity measure can be represented as

$$\mu(\mathrm{d}t \times \mathrm{d}x) = \lambda(t) f(t, x; \theta(t)) \mathrm{d}t \mathrm{d}x,$$

where, for each time $0 \le t \le T^*$, $f(t, \cdot; \theta(t)) \in \mathcal{D}_{\mathrm{NE}}(b(t, \cdot)) : \mathbb{R} \to \mathbb{R}_+$ is an NE family characterized by the function $b(t, \cdot)$ and with parameter $\theta(t)$. Thus, any NE-ACP process is fully characterized by the system of triplets

$$(\lambda, \theta, b) = \{(\lambda(t), \theta(t), b(t, \cdot)) : t \in [0, T^*]\}. \qquad \triangle$$

The system of triplets (λ, θ, b) used to uniquely identify an NE-ACP process is not be confused with its system of generating triplets, as discussed in Lemma IV.3. The latter is a much more general concept and applies to all additive processes.

Proposition IV.4 (Dynamics of X^j under $\hat{\mathbb{P}}(X, \beta)$ II).
Let $X^j = \left\{X_t^j : t \in [0, T^*]\right\}$ be the ACP pure jump component of an AJD process $X = \{X_t : t \in [0, T^*]\}$. Assume that X^j is an NE-ACP process under $\mathbb{P}$ with system of triplets $(\lambda, \theta, b) = \{(\lambda(t), \theta(t), b(t, \cdot)) : t \in [0, T^*]\}$. Then X^j is also an NE-ACP process under the ETPM $\hat{\mathbb{P}}(X, \beta)$ with system of triplets $\left(\hat{\lambda}, \hat{\theta}, b\right) = \left\{\left(\hat{\lambda}(t), \hat{\theta}(t), b(t, \cdot)\right) : t \in [0, T^*]\right\}$, where

$$\begin{aligned} \hat{\lambda}(t) &= \lambda(t) \phi_Y(t, -\mathrm{i}\beta(t)), \\ \hat{\theta}(t) &= \theta(t) + \beta(t) \end{aligned}$$

and

$$\phi_Y(t, \omega) = \exp\{b(t, \theta(t) + \mathrm{i}\omega) - b(t, \theta(t))\}$$

as in Lemma IV.10. In particular, for each time $0 \le t \le T^*$, the jump size PDFs $f(t, x; \theta(t))$ and $\hat{f}\left(t, x; \hat{\theta}(t)\right)$ are the same NE family $\mathcal{D}_{NE}(b(t, \cdot))$.

Proof It follows from Proposition IV.3, that X^j is also an ACP process under $\hat{\mathbb{P}}(X, \beta)$ with the given jump intensity. Therefore, it only remains to show that, if, for each $0 \le t \le T^*$, the jump size PDF $f(t, x; \theta(t))$ is an NE family under $\mathbb{P}$, then, $\hat{f}\left(t, x; \hat{\theta}(t)\right)$ is the same NE family under $\hat{\mathbb{P}}(X, \beta)$ with the given parameter. Using Proposition IV.3 again, in conjunction with Definition IV.12, and substituting for $\phi_Y(t, -\mathrm{i}\beta(t))$ using Lemma IV.10, we obtain

$$\hat{f}\big(t, x; \theta(t), \beta(t)\big) = a(t, x) \exp\left\{(\theta(t) + \beta(t))\, x - b(t, \theta(t) + \beta(t))\right\},$$

which justifies setting $\hat{\theta}(t) = \theta(t) + \beta(t)$. We see that $\hat{f}\big(t, x; \hat{\theta}(t)\big)$ is also an NE family. Since the function $b(\theta)$ is unaffected by the change of measure, it follows by Lemma IV.10 and the discussion succeeding it that, for each $0 \leq t \leq T^*$, the jump size distributions under $\mathbb{P}$ and $\hat{\mathbb{P}}(X, \beta)$ are the same NE family.

Alternatively, we can use Corollary IV.2 in conjunction with the representation of the characteristic function for NE families in Lemma IV.10 to obtain

$$\hat{\phi}_Y(t, \omega) = \exp\left\{b\left(t, \theta(t) + \beta(t) + \mathrm{i}\omega\right) - b\left(t, \theta(t) + \beta(t)\right)\right\}.$$

By Lemma IV.10, we recognize this as the characteristic function of an NE family $\mathcal{D}_{\mathrm{NE}}(b(t, \cdot))$ with parameter $\hat{\theta}(t)$ and the claim follows. □

This result is important because it shows that, for any choice of $\beta(t)$, the class of NE-ACP processes with a jump size distribution in $\mathcal{D}_{\mathrm{NE}}(b(t, \cdot))$ is closed under a measure change given by an Esscher transform. In Section IV.4.2, we show that there exists a broader class of jump size distributions, given by a finite mixture of NE distributions, that still preserves this property. Next, we provide some examples of common NE families and their parameters under the original probability measure $\mathbb{P}$ and the ETPM $\hat{\mathbb{P}}(X, \beta)$. To keep the presentation as simple as possible, we consider the case of time-homogeneous jump size distributions as in Definition IV.4. The extension to time-dependent parameters is straightforward but complicates the notation. The examples are of a purely illustrative nature and we do not mean to imply that these distributions are good choices to model the jumps of logarithmic asset returns.

Example IV.2 (Normal Distribution).
Let $(Y_i)_{i\in\mathbb{N}}$ be a sequence of i.i.d. $\mathcal{N}\left(\gamma, \delta^2\right)$ normally distributed random variables under $\mathbb{P}$ with PDF

$$f\left(x; \gamma, \delta^2\right) = \frac{1}{\sqrt{2\pi\delta^2}} \exp\left\{-\frac{(x-\gamma)^2}{2\delta^2}\right\}.$$

If we consider the variance δ^2 as being fixed, then we see that $f\left(x; \gamma\right)$ is an NE family with

$$\theta = \frac{\gamma}{\delta^2}, \qquad a(x) = \frac{1}{\sqrt{2\pi\delta^2}} \exp\left\{-\frac{x^2}{2\delta^2}\right\}, \qquad b(\theta) = \frac{(\theta\delta)^2}{2}.$$

From Proposition IV.3, it follows that each Y_i is $\mathcal{N}\left(\hat{\gamma}, \delta^2\right)$ normally distributed under $\hat{\mathbb{P}}(X, \beta)$ with $\hat{\gamma} = \gamma + \beta\delta^2$ since

$$\theta + \beta = \frac{\gamma + \beta\delta^2}{\delta^2} = \frac{\hat{\gamma}}{\delta^2} = \hat{\theta}. \qquad \blacksquare$$

Example IV.3 (Gamma Distribution).
Let $(Y_i)_{i\in\mathbb{N}}$ be a sequence of i.i.d. $\Gamma(a, b)$ gamma distributed random variables under $\mathbb{P}$ with PDF

$$f(x; a, b) = \frac{1}{\Gamma(a)b^a} x^{a-1} \mathrm{e}^{-x/b} 1\{x \geq 0\}.$$

If we consider the shape parameter a as being fixed, then we see that $f(x; b)$ is an NE family with

$$\theta = -\frac{1}{b}, \qquad a(x) = \frac{1}{\Gamma(a)} x^{a-1} 1\{x \geq 0\}, \qquad b(\theta) = a \ln\left(-\frac{1}{\theta}\right).$$

From Proposition IV.3, it follows that each Y_i is $\Gamma\big(a, \hat{b}\big)$ gamma distributed under $\hat{\mathbb{P}}(X, \beta)$ with $\hat{b} = b/(1 - b\beta)$ since

$$\theta + \beta = -\frac{1}{b/(1 - b\beta)} = -\frac{1}{\hat{\beta}} = \hat{\theta}. \qquad \blacksquare$$

Example IV.4 (Exponential Distribution).
Let $(Y_i)_{i\in\mathbb{N}}$ be a sequence of i.i.d. $\mathcal{E}(\lambda)$ exponentially distributed random variables under $\mathbb{P}$ with PDF

$$f(x; \lambda) = \lambda \mathrm{e}^{-\lambda x} 1\{x \geq 0\}.$$

Since the exponential distribution is a special case of the gamma distribution with $\mathcal{E}(\lambda) \sim \Gamma(1, 1/\lambda)$, it follows from Example IV.3 that each Y_i is $\mathcal{E}\big(\hat{\lambda}\big)$ exponentially distributed under $\hat{\mathbb{P}}(X, \beta)$ with $\hat{\lambda} = \lambda - \beta$. $\blacksquare$

IV.4.2 Natural Exponential Mixture Families

Definition IV.14 (Natural Exponential Mixture Family).
An NEM family is a class of probability distributions indexed by an n-dimensional parameter vector $\boldsymbol{\theta} = (\theta_1, \theta_2, \ldots, \theta_n)^T$ and weight vector $\boldsymbol{w} = (w_1, w_2, \ldots, w_n)^T$ whose PDF admits the representation

$$f(x; \boldsymbol{\theta}, \boldsymbol{w}) = \sum_{i=1}^{n} w_i f_i(x; \theta_i).$$

Here, the weights satisfy $w_i \geq 0$ for all $i \in \{1, 2, \ldots, n\}$ and $\sum_{i=1}^{n} w_i = 1$. Each $f_i(x; \theta_i) \in \mathcal{D}_{\mathrm{NE}}(b_i(\cdot))$ is an NE family. We define $\mathcal{D}_{\mathrm{NEM}}(\boldsymbol{b}(\cdot))$ to be the class of NEM families characterized by the vector valued function $\boldsymbol{b}(\boldsymbol{\theta}) = (b_1(\theta_1), b_2(\theta_2), \ldots, b_n(\theta_n))^T$.
$\triangle$

Consequently, a random variable Z follows an NEM distribution if it is defined by a finite mixture of n random variables $\{A_i\}$, the i-th of which is a $\mathcal{D}_{\mathrm{NE}}(b_i(\cdot))$ NE family with parameter θ_i and PDF $f_i(x; \theta_i)$. A realization of Z has the same distribution as A_i with probability w_i. We refer to the $\{A_i\}$ as the mixture components of Z. Note that each A_i is allowed to follow a different NE family. Since an NE family can be considered a special case when we mix over a single distribution with unit weight, all the following results generalize the ones previously obtained. We refer to, for example, Section 1.1 in McLachlan and Peel (2000), pp. 22–23, for a definition of general finite mixture distributions.

Lemma IV.11 (Characteristic Function of Natural Exponential Mixture Families).
Let Z be a random variable whose distribution under $\mathbb{P}$ is a $\mathcal{D}_{NEM}(\boldsymbol{b}(\cdot))$ NEM family with parameter vector $\boldsymbol{\theta}$ and weight vector $\boldsymbol{w}$. Then, the characteristic function $\phi_Z(\omega)$ of Z under $\mathbb{P}$ is given by

$$\phi_Z(\omega) = \sum_{i=1}^{n} w_i \exp\{b_i(\theta_i + \mathrm{i}\omega) - b_i(\theta_i)\}.$$

Proof This follows immediately from Lemma IV.10 and the linearity of the Fourier transform. $\square$

Definition IV.15 (Natural Exponential Mixture Additive Compound Poisson Processes).
Let $X^j = \left\{X_t^j : t \in [0, T^*]\right\}$ be an ACP process. It is an NEM-ACP process if the intensity measure can be represented as

$$\mu(\mathrm{d}t \times \mathrm{d}x) = \lambda(t) f(t, x; \boldsymbol{\theta}(t), \boldsymbol{w}(t))\mathrm{d}t\mathrm{d}x,$$

where, for each time $0 \le t \le T^*$, $f(t, \cdot; \boldsymbol{\theta}(t), \boldsymbol{w}(t)) \in \mathcal{D}_{\text{NEM}}(\boldsymbol{b}(t, \cdot)) : \mathbb{R} \to \mathbb{R}_+$ is an NEM family characterized by the function $\boldsymbol{b}(t, \cdot)$ with parameter vector $\boldsymbol{\theta}(t)$ and weight vector $\boldsymbol{w}(t)$. Here, $\boldsymbol{b} : \mathbb{R}_+ \times \mathbb{R}^n \to \mathbb{R}^n$, $\boldsymbol{\theta} : \mathbb{R}_+ \to \mathbb{R}^n$ and $\boldsymbol{w} : \mathbb{R}_+ \to [0, 1]^n$ such that $\sum_{i=1}^n w_i(t) = 1$. Thus, any NEM-ACP process is fully characterized by the system of quadruplets

$$(\lambda, \boldsymbol{\theta}, \boldsymbol{w}, \boldsymbol{b}) = \{(\lambda(t), \boldsymbol{\theta}(t), \boldsymbol{w}(t), \boldsymbol{b}(t, \cdot)) : t \in [0, T^*]\}. \qquad \triangle$$

Proposition IV.5 below is our main result. It shows for any choice of $\boldsymbol{b}(t, \cdot)$, the class of NEM-ACP processes with jump size distribution in $\mathcal{D}_{\text{NEM}}(\boldsymbol{b}(t, \cdot))$ is closed under a measure change given by an Esscher transform.

Proposition IV.5 (Dynamics of $\boldsymbol{X^j}$ under $\hat{\mathbb{P}}(\boldsymbol{X}, \boldsymbol{\beta})$ III).
Let $X^j = \left\{X_t^j : t \in [0, T^*]\right\}$ be the ACP pure jump component of an AJD process $X = \{X_t : t \in [0, T^*]\}$. Assume that X^j is an NEM-ACP process under $\mathbb{P}$ with system of quadruplets $(\lambda, \boldsymbol{\theta}, \boldsymbol{w}, \boldsymbol{b}) = \{(\lambda(t), \boldsymbol{\theta}(t), \boldsymbol{w}(t), \boldsymbol{b}(t, \cdot)) : t \in [0, T^*]\}$. Then X^j is also an NEM-ACP process under the ETPM $\hat{\mathbb{P}}(X, \beta)$ with system of quadruplets $\left(\hat{\lambda}, \hat{\boldsymbol{\theta}}, \hat{\boldsymbol{w}}, \boldsymbol{b}\right) = \left\{\left(\hat{\lambda}(t), \hat{\boldsymbol{\theta}}(t), \hat{\boldsymbol{w}}(t), \boldsymbol{b}(t, \cdot)\right) : t \in [0, T^*]\right\}$, where

$$\begin{aligned}
\hat{\lambda}(t) &= \lambda(t)\phi_Y(t, -\mathrm{i}\beta(t)), \\
\hat{w}_i(t) &= \frac{w_i(t)\phi_{A_i}(t, -\mathrm{i}\beta(t))}{\phi_Y(t, -\mathrm{i}\beta(t))}, \\
\hat{\theta}_i(t) &= \theta_i(t) + \beta(t),
\end{aligned}$$

and

$$\begin{aligned}
\phi_Y(t, \omega) &= \sum_{i=1}^n w_i(t)\phi_{A_i}(t, \omega), \\
\phi_{A_i}(t, \omega) &= \exp\left\{b_i\left(t, \theta_i(t) + \mathrm{i}\omega\right) - b_i\left(t, \theta_i(t)\right)\right\}
\end{aligned}$$

as in Lemmata IV.10 and IV.11. Here, $\phi_{A_i}(t,\omega)$ is the time $0 \le t \le T^*$ characteristic function of the i-th mixing component under the original probability measure $\mathbb{P}$. In particular, for each time $0 \le t \le T^*$, the jump size PDFs $f(t,x;\boldsymbol{\theta}(t),\boldsymbol{w}(t))$ and $\hat{f}\big(t,x;\hat{\boldsymbol{\theta}}(t),\hat{\boldsymbol{w}}(t)\big)$ are the same NEM family $\mathcal{D}_{NEM}(\boldsymbol{b}(t,\cdot))$.

Proof It follows from Proposition IV.3, that X^j is also an ACP process under $\hat{\mathbb{P}}(X,\beta)$ with the given jump intensity. Therefore, it only remains to show that, if, for each $0 \le t \le T^*$, the jump size PDF $f(t,x;\boldsymbol{\theta}(t),\boldsymbol{w}(t))$ is an NEM family under $\mathbb{P}$, then $\hat{f}\big(t,x;\hat{\boldsymbol{\theta}}(t),\hat{\boldsymbol{w}}(t)\big)$ is the same NEM family under $\hat{\mathbb{P}}(X,\beta)$ with the given parameter. The proof is very similar to that of Proposition IV.4. Again, it is based on explicitly computing the jump size distribution using Proposition IV.3 in conjunction with Lemmata IV.10 and IV.11. Care must be taken when defining the weight vector $\hat{\boldsymbol{w}}(t)$ such that it satisfies Definitions IV.14 and IV.15. Alternatively, we can employ Corollary IV.1 and Lemmata IV.10 and IV.11 again to find the characteristic function $\hat{\phi}_Y(t,\omega)$. All details are provided in Appendix IV.C.2. □

Proposition IV.5 shows that not only the parameters of the mixture components but also their weights change under the ETPM. Each weight w_i is scaled by the percentage that the i-th mixture component contributes to the total β-th exponential moment of the jump size distribution under $\mathbb{P}$. The main insight is, that for any choice of $\beta(t)$, the class of NEM-ACP processes with a jump size distribution in $\mathcal{D}_{\text{NEM}}(\boldsymbol{b}(t,\cdot))$ is closed under a measure change given by an Esscher transform.

Examples IV.5 and IV.6 below illustrate how Proposition IV.5 can be used to find the logarithmic return dynamics under both the ETMM and the corresponding asset price probability measure.

Example IV.5 (Displaced Mixed Exponential Distribution).
Following Cai and Kou (2011), we consider the case where the jump sizes follow a mixed exponential distribution. Their model augments the Kou (2002) double exponential jump-diffusion model by adding additional exponential tails; see also Kou and Wang (2003) and Kou and Wang (2004). The authors motivate this model by showing that a wide variety of heavy-tailed distributions can be closely approximated through a mixture of two to four exponential distributions. We consider a further generalization, where each of the exponential tails is allowed to be displaced away from the origin. See also Chapter II for a

discussion of and closed-form solutions for European plain vanilla options under displaced double exponential jump size distributions.

Let $(Y_i)_{i\in\mathbb{N}}$ be a sequence of i.i.d. M-$\mathcal{E}\left(\boldsymbol{p}_+, \boldsymbol{\eta}_+, \boldsymbol{\kappa}_+, \boldsymbol{p}_-, \boldsymbol{\eta}_-, \boldsymbol{\kappa}_-\right)$ displaced mixed exponentially distributed random variables under $\mathbb{P}$ with PDF

$$f_Y(x) = \sum_{i=1}^{m} p_{+,i}\eta_{+,i}\mathrm{e}^{-\eta_{+,i}(x-\kappa_{i,+})}1\left\{x \geq \kappa_{+,i}\right\} + \sum_{i=1}^{n} p_{-,i}\eta_{-,i}\mathrm{e}^{\eta_{-,i}(x-\kappa_{-})}1\left\{x \leq \kappa_{-,i}\right\}.$$

Here, $\boldsymbol{p}_+ \in [0,1]^m$, $\boldsymbol{\eta}_+ \in \mathbb{R}_+^m$, $\boldsymbol{\kappa}_+ \in \mathbb{R}_+^m$, $\boldsymbol{p}_- \in [0,1]^n$, $\boldsymbol{\eta}_- \in \mathbb{R}_+^n$ and $\boldsymbol{\kappa}_- \in \mathbb{R}_-^n$. As usual, the weight vectors $\boldsymbol{p}_+$ and $\boldsymbol{p}_-$ satisfy $\sum_{i=1}^m p_{+,i} + \sum_{i=1}^n p_{-,i} = 1$. Cai and Kou (2011) allow for the individual weights to be negative, conditional on the resulting PDF being non-negative everywhere. The authors formulate the model dynamics directly under the risk-neutral probability measure and, thus, are not concerned with the measure transformation discussed in this chapter. However, they mention that the mixed exponential dynamics can be embedded in a Naik and Lee (1990) type general equilibrium economy, thus, giving rise to an Esscher transform as the Radon-Nikodým derivative process.

From the above representation of the PDF, we see that each Y_i is an NEM family, where the mixing components correspond to m positive and n negative displaced exponential random variables. In the notation introduced in Definition IV.14, we have

$$\begin{aligned}\boldsymbol{w} &= \left(\boldsymbol{p}_+, \boldsymbol{p}_-\right)^T, \\ \boldsymbol{\theta} &= \left(-\boldsymbol{\eta}_+, \boldsymbol{\eta}_-\right)^T.\end{aligned}$$

Given the characteristic function for displaced double exponential jumps in Chapter II, we immediately obtain

$$\phi_Y(\omega) = \sum_{i=1}^{m} \frac{p_{+,i}\eta_{+,i}}{\eta_{+,i} - \mathrm{i}\omega}\mathrm{e}^{\mathrm{i}\omega\kappa_{+,i}} + \sum_{i=1}^{n} \frac{p_{-,i}\eta_{-,i}}{\eta_{-,i} + \mathrm{i}\omega}\mathrm{e}^{\mathrm{i}\omega\kappa_{-,i}}.$$

From Proposition IV.4, it follows that each Y_i is M-$\mathcal{E}\left(\hat{\boldsymbol{p}}_+, \hat{\boldsymbol{\eta}}_+, \boldsymbol{\kappa}_+, \hat{\boldsymbol{p}}_-, \hat{\boldsymbol{\eta}}_-, \boldsymbol{\kappa}_-\right)$ displaced mixed exponentially distributed under $\hat{\mathbb{P}}(X, \beta)$ with

$$\begin{aligned}\hat{p}_{+,i} &= \frac{p_{+,i}\eta_{+,i}}{\eta_{+,i} - \beta}\mathrm{e}^{\beta\kappa_{+,i}}\left(\sum_{i=1}^{m} \frac{p_{+,i}\eta_{+,i}}{\eta_{+,i} - \beta}\mathrm{e}^{\beta\kappa_{+,i}} + \sum_{i=1}^{n} \frac{p_{-,i}\eta_{-,i}}{\eta_{-,i} + \beta}\mathrm{e}^{\beta\kappa_{-,i}}\right)^{-1}, \\ \hat{p}_{-,i} &= \frac{p_{-,i}\eta_{-,i}}{\eta_{-,i} + \beta}\mathrm{e}^{\beta\kappa_{-,i}}\left(\sum_{i=1}^{m} \frac{p_{+,i}\eta_{+,i}}{\eta_{+,i} - \beta}\mathrm{e}^{\beta\kappa_{+,i}} + \sum_{i=1}^{n} \frac{p_{-,i}\eta_{-,i}}{\eta_{-,i} + \beta}\mathrm{e}^{\beta\kappa_{-,i}}\right)^{-1}, \\ \hat{\eta}_{+,i} &= \eta_{+,i} - \beta, \\ \hat{\eta}_{-,i} &= \eta_{-,i} + \beta. \qquad \blacksquare\end{aligned}$$

Example IV.6 (Gaussian Mixture Distribution).
We now propose to model the jump size as following a Gaussian mixture distribution. Our model embeds the Merton (1976) jump-diffusion model with normally distributed jumps as a special case.

Let $(Y_i)_{i\in\mathbb{N}}$ be a sequence of i.i.d. M-$\mathcal{N}\left(\boldsymbol{w},\boldsymbol{\gamma},\boldsymbol{\delta}^2\right)$ Gaussian mixture random variables under $\mathbb{P}$ with PDF

$$f_Y(x) = \sum_{i=1}^{n} \frac{w_i}{\sqrt{2\pi\delta_i^2}} \exp\left\{-\frac{(x-\gamma_i)^2}{2\delta_i^2}\right\},$$

where $\boldsymbol{w} \in [0,1]^n$, $\boldsymbol{\gamma} \in \mathbb{R}^n$ and $\boldsymbol{\delta} \in \mathbb{R}_+^n$. The weight vector $\boldsymbol{w}$ satisfies $\sum_{i=1}^n w_i = 1$. Consequently, each Y_i follows an NEM distribution, where each of the n mixing random variables follows a normal distribution. In the notation of Definition IV.14, we have

$$\boldsymbol{\theta} = \left(\frac{\gamma_1}{\delta_1^2}, \frac{\gamma_2}{\delta_2^2}, \ldots, \frac{\gamma_n}{\delta_n^2}\right)^T;$$

compare to Example IV.2. The corresponding characteristic function is given by

$$\phi_{Y_i}(\omega) = \sum_{i=1}^{n} w_i \exp\left\{\mathrm{i}\omega\gamma_i - \frac{1}{2}\omega^2\delta_i^2\right\}.$$

From Proposition IV.4 and the result obtained in Example IV.2, it follows that each Y_i is a M-$\mathcal{N}\left(\hat{\boldsymbol{w}},\hat{\boldsymbol{\gamma}},\boldsymbol{\delta}^2\right)$ Gaussian mixture random variable under $\hat{\mathbb{P}}(X,\beta)$ with

$$\begin{aligned} \hat{w}_i &= w_i \exp\left\{\beta\gamma_i + \frac{1}{2}\beta^2\delta_i^2\right\}\left(\sum_{i=1}^{n} w_i \exp\left\{\beta\gamma_i + \frac{1}{2}\beta^2\delta_i^2\right\}\right)^{-1}, \\ \hat{\gamma}_i &= \gamma_i + \beta\delta_i^2. \quad \blacksquare \end{aligned}$$

Until now, we only considered discrete mixtures of NE families. In the limit, when $n \to \infty$, we obtain a continuous mixture. The previous results can be seamlessly generalized to this case. Instead of re-iterating the previous definitions and results, we only provide an informal discussion of this case and illustrate it through an example. The mixing weights now correspond to a PDF $w : \mathcal{A} \to \mathbb{R}_+$ on some domain $\mathcal{A}$. Let $f(x; y, \theta(y)) \in \mathcal{D}_{\mathrm{NE}}\left(b(y,\cdot)\right)$ be an NE family for each $y \in \mathcal{A}$. A continuous NEM family can be represented as

$$f(x;\theta,w) = \int_{\mathcal{A}} w(y) f(x; y, \theta(y))\mathrm{d}y.$$

Note that Definition IV.14 corresponds to the special case when $w(y)$ is a discrete PDF of the form

$$w(y) = \sum_{i=1}^{n} w_i \delta(y - i),$$

where $\delta(x)$ is the Dirac delta function. The following example based on student's t-distribution considers a jump size distribution that is not an NE family but can be represented as a continuous NEM family.

Example IV.7 (Student's *T*-Distribution).
Let $(Y_i)_{i\in\mathbb{N}}$ be a sequence of i.i.d. $\mathcal{N}$-$\Gamma^{-1}(\mu, \xi, \sigma, \gamma, \delta)$ normal inverse gamma random variables under $\mathbb{P}$. That is, each Y_i is a normal mean-variance mixture, where the mixing density is an inverse gamma distribution. It can be represented as

$$Y_i \sim \mu + \xi W + \sigma\sqrt{W}Z,$$

where $Z \sim \mathcal{N}(0,1)$ and $W \sim \Gamma^{-1}(\gamma, \delta)$ are independent random variables and the parameters satisfy $\mu, \xi \in \mathbb{R}$, $\sigma, \gamma, \delta \in \mathbb{R}_+$. The PDF is given by

$$\begin{aligned} f_Y(x) &= \int_0^\infty f_W(y;\gamma,\delta) f_Z\left(x; \mu + \xi y, \sigma^2 y\right) \mathrm{d}y \\ &= \int_0^\infty \frac{\delta^\gamma}{\Gamma(\gamma)} y^{-\gamma-1} \exp\left\{-\frac{\delta}{y}\right\} \frac{1}{\sqrt{2\pi\sigma^2 y}} \exp\left\{-\frac{(x-\mu-\xi y)^2}{2\sigma^2 y}\right\} \mathrm{d}y. \end{aligned}$$

Consider the special case when $\mu = \xi = 0$, $\sigma = 1$ and $\gamma = \delta = \nu/2$. Then, as shown in Appendix IV.C.3,

$$f_Y(x) = \frac{\Gamma((\nu+1)/2)}{\sqrt{\nu\pi}\Gamma(\nu/2)} \left(1 + \frac{x^2}{\nu}\right)^{-(\nu+1)/2}.$$

We recognize this as the PDF of a student's t-distribution with ν degrees of freedom, that is $X \sim T(\nu)$. Thus, while each Y_i follows a continuous NEM family, it does not follow an NE family. Nevertheless, we can apply the general result in Proposition IV.3 to find its PDF under $\hat{\mathbb{P}}(X,\beta)$, assuming that it does exist. After some simple algebraic manipulations, we obtain

$$\begin{aligned} \hat{f}_Y(x) &= \int_0^\infty \frac{(\nu/2)^{\nu/2}}{\phi_Y(-\mathrm{i}\beta)\Gamma(\nu/2)} y^{-(\nu/2)-1} \exp\left\{-\frac{\nu-\beta^2y^2}{2y}\right\} \\ &\qquad \frac{1}{\sqrt{2\pi y}} \exp\left\{-\frac{(x-\beta y)^2}{2y}\right\} \mathrm{d}y. \end{aligned}$$

We observe that each Y_i is still a normal mean-variance mixture under $\hat{\mathbb{P}}(X,\beta)$ and consequently follows a continuous NEM family. However, the mixing density $\hat{w}(y)$ is now given by

$$\hat{w}(y) = \frac{(\nu/2)^{\nu/2}}{\phi_Y(-\mathrm{i}\beta)\Gamma(\nu/2)} y^{-(\nu/2)-1} \exp\left\{-\frac{\nu - \beta^2 y^2}{2y}\right\}$$

and, in particular, it no longer follows an inverse gamma distribution. Consequently, each Y_i no longer follows a normal inverse gamma distribution, in general, and a student's t-distribution, in particular, under $\hat{\mathbb{P}}(X,\beta)$ either. To find the jump size PDF under $\hat{\mathbb{P}}(X,\beta)$, we can just apply Proposition IV.3 to obtain

$$\hat{f}_Y = \frac{\Gamma((\nu+1)/2)}{\phi_Y(-\mathrm{i}\beta)\sqrt{\nu\pi}\Gamma(\nu/2)} \left(1 + \frac{x^2}{\nu}\right)^{-(\nu+1)/2} \mathrm{e}^{\beta x}.$$

■

We choose this example because it illustrates an important property of continuous NEM distributions. In principle, any continuous distribution can be approximated through a Gaussian mixture to an arbitrary precision; see for example Section 1.5.2 in McLachlan and Peel (2000), pp. 11–14. However, as is the case in Example IV.7, the PDF of the continuous NEM distribution is not necessarily an NE or finite NEM family. It is for this reason that we use the terminology "class of probability distributions" to refer to parametric distributions or finite mixtures thereof only.

For the moment, assume that we would also include continuous mixtures. By this definition, the jump size distribution of any ACP process would either be closed under the Esscher transform or could be approximated to an arbitrary precision by one that is. However, the representation of the jump size distribution as a continuous NEM family does not provide additional insights or enhance tractability. As with any ACP process, the jump size PDF can simply be found using the general Proposition IV.3.

IV.4.3 Relation to Conjugate Distributions

It is tempting to think that the results in Sections IV.4.1 and IV.4.2 are somewhat related to the concept of conjugate priors in Bayesian statistics; see for example Box and Tiao (1973) for a standard reference. Both problems analyze under which conditions a class of distributions is closed under some operation and, in both cases, (natural) exponential families and their mixtures play key roles. Thus, we briefly discuss why these two problems are quite distinct, while similar at the first glance. Consider a random sample $\mathcal{X} = \{X_1, X_2, \ldots X_n\}$ obtained from a one-parameter sampling distribution $f(x;\theta)$. Denote the prior distribution of the parameter θ by $\pi : \mathcal{D} \to \mathbb{R}_+$. By Bayes' theorem, the posterior distribution of θ, conditional on the sample $\mathcal{X}$, is given by

$$\pi(\theta; \mathcal{X}) = \frac{f(\mathcal{X}; \theta)\, \pi(\theta)}{\int_{\mathcal{D}} f(\mathcal{X}; \theta)\, \pi(\theta) \mathrm{d}\theta},$$

where we write $f(\mathcal{X}; \theta)$ to denote the likelihood of the sample, conditional on the parameter θ. A class of prior distributions $\mathcal{A}$ is a conjugate family for a class of sampling distributions $\mathcal{B}$, if the posterior distribution is in $\mathcal{A}$ for all $\pi(\theta) \in \mathcal{A}$, all $f(x; \theta) \in \mathcal{B}$, and for any random sample $\mathcal{X}$. The key difference between the above expression for the posterior distribution and the Esscher transform is that the exponential tilting in the latter is not a PDF. While it resembles an exponential distribution, it is unnormalized and, thus, does not integrate to one.

Assume that the samples are drawn from an exponential distribution and the prior distribution is an NE family, that is $f(x; \theta) = \theta \mathrm{e}^{-\theta x}$ and $\pi(\theta) = \alpha(\theta) \exp\{\eta\theta - \beta(\eta)\}$. Then, ignoring the normalization term, we obtain

$$\begin{aligned} \pi(\theta; \mathcal{X}) &\propto \prod_{i=1}^{n} f(X_i; \theta)\, \pi(\theta) \\ &\propto \alpha(\theta) \exp\left\{ \left(\eta - \sum_{i=1}^{n} X_i \right) \theta + n \ln \theta - \beta(\eta) \right\}. \end{aligned}$$

The gamma distribution has a sufficient statistic $T(\theta) = (\theta, \ln\theta)^T$ and, thus, is the conjugate prior. Other distributions that nest the gamma distribution as special cases are also conjugate priors when considering some of their parameters fixed. One such example is the generalized inverse Gaussian distribution. Similar to the result in Section IV.4.2, a mixture of gamma distributions is also a conjugate prior.

Now, consider the Esscher transform parameterized by $\xi = -\beta$ when the $f_Z(x; \theta)$ follows an NE family under $\mathbb{P}$. We have

$$\begin{aligned} \hat{f}_Z(x; \theta) &\propto \mathrm{e}^{-x\xi} f_Z(x; \theta) \\ &\propto a(x) \exp\{(\theta - \xi)x - b(\theta)\}. \end{aligned}$$

Any distribution with sufficient statistic $T(x) = x$ is closed under the Esscher transform because of the lack of a normalization term in the exponential tilting.

IV.4.4 Implications for Minimal Entropy Martingale Measures

While Gerber and Shiu (1994b) only explicitly consider measure changes defined by the Esscher transform of the Lévy dynamics governing the logarithm of the underlying asset, it is clear that alternative choices of the risk process are equally possible. In a series of papers, Miyahara (1999, 2004), Fujiwara and Miyahara (2003) and Fujiwara (2009) identify the ETMM of the simple return process as the MEMM under increasingly general dynamics. See also Chan (1999), Kallsen and Shiryaev (2002) and Hubalek and Sgarra (2006) for related works. The MEMM is the equivalent martingale measure that minimizes the relative entropy or Kullback-Leibler divergence to the physical probability measure and, thus, is closest to it in terms of its information content. In Miyahara (1999), the MEMM is motivated economically through its link to utility indifference pricing when the agent has exponential utility; see also Frittelli (2000).

Formally, the MEMM $\mathbb{P}^*$ is defined as the solution to the problem

$$\mathbb{P}^* = \arg \inf_{\mathbb{Q} \in \mathcal{M}(\mathbb{P})} \mathbb{E}_{\mathbb{P}} \left[\frac{\mathrm{d}\mathbb{Q}}{\mathrm{d}\mathbb{P}} \ln \left(\frac{\mathrm{d}\mathbb{Q}}{\mathrm{d}\mathbb{P}} \right) \right],$$

where $\mathcal{M}(\mathbb{P})$ denotes the set of martingale measures equivalent to $\mathbb{P}$ on $[0, T^*]$. As shown in Theorem 3.1 in Fujiwara (2009), pp. 77–78, the MEMM is given by the ETPM of the simple return process $R = \{R_t : t \in [0, T^*]\}$, defined as

$$R_t = \int_0^t \frac{\mathrm{d}S_u}{S_{u-}}.$$

Using the Itō formula, see for example Proposition 8.15 in Cont and Tankov (2004), p. 276, we obtain

$$R_t = \int_0^t \left(\gamma(u) + \frac{1}{2}\sigma^2(u) \right) \mathrm{d}u + \int_0^t \sigma(u) \mathrm{d}W_u + \int_0^t \int_{-\infty}^{+\infty} (\mathrm{e}^x - 1)\, J_X(\mathrm{d}x \times \mathrm{d}u).$$

We observe that R also follows an AJD process under $\mathbb{P}$. When the process X jumps by ΔX_t at some time $t \in [0, T^*]$, then the process R jumps by $\mathrm{e}^{\Delta X_t} - 1$ at the same time. Thus, we set $h(x) = \mathrm{e}^x - 1$ ($h^{-1}(x) = \ln(x+1)$) and define a new intensity measure $\nu(\mathrm{d}t \times \mathrm{d}x) = \mu\left(\mathrm{d}t \times h^{-1}(\mathrm{d}x)\right)$ with corresponding Poisson random measure $J_R(\mathrm{d}t \times \mathrm{d}x)$. Then,

$$R_t = \int_0^t \left(\gamma(u) + \frac{1}{2}\sigma^2(u) \right) \mathrm{d}u + \int_0^t \sigma(u) \mathrm{d}W_u + \int_0^t \int_{-\infty}^{+\infty} x J_R(\mathrm{d}x \times \mathrm{d}u).$$

The MEMM is then given by the ETPM $\mathbb{P}^* \in \mathcal{P}(R)$ that satisfies Definition IV.10. It follows from Proposition IV.5 that the jump size distributions of X under $\mathbb{P}$ and $\mathbb{P}^*$ fall into the same parametric class if R follows an NEM-ACP process.

Most jump-diffusion processes proposed in the literature and considered thus far in this chapter are such that the jump size distribution of the logarithmic return process X is an NEM family, while that of the simple return process R is not. Example IV.8 below shows that, when each Y_i follows a negative Gumbel distribution with unit scale parameter under the physical probability measure, then R exhibits displaced exponential jumps. Consequently, the jump sizes of X under the MEMM also follow a negative Gumbel distribution but with a different location parameter. Again, this example is purely of an illustrative nature.

Example IV.8 (Gumbel Distribution).
Let $(Y_i)_{i\in\mathbb{N}}$ be a sequence of i.i.d. $\mathcal{G}_-(\mu, \sigma)$ negative Gumbel random variables under $\mathbb{P}$ with PDF

$$f(x; \mu, \sigma) = \frac{1}{\sigma} \exp\left\{\frac{x+\mu}{\sigma} - \exp\left\{\frac{x+\mu}{\sigma}\right\}\right\}.$$

Let $(Z_i)_{i\in\mathbb{N}}$ be the corresponding sequence of jumps in the simple return process R. It has the PDF

$$g(x; \mu, \sigma) = \frac{1}{\sigma}(x+1)^{1/\sigma - 1} \exp\left\{\frac{\mu}{\sigma} - (x+1)^{1/\sigma} \exp\left\{\frac{\mu}{\sigma}\right\}\right\} 1\{x \geq -1\}.$$

Assume that the scale parameter is fixed at $\sigma = 1$ and define $\lambda = \mathrm{e}^{\mu}$. Then,

$$g(x; \mu, 1) = \lambda \mathrm{e}^{-\lambda(x+1)} 1\{x \geq -1\}.$$

We recognize this as the PDF of a D-$\mathcal{E}(\lambda, \kappa)$ displaced exponential distribution with displacement term $\kappa = -1$. Its characteristic function under $\mathbb{P}$ is given by

$$\phi_Z(\omega) = \frac{\lambda}{\lambda - \mathrm{i}\omega} \mathrm{e}^{\mathrm{i}\omega\kappa}.$$

It follows from Proposition IV.4 and Example IV.4 that each Z_i is D-$\mathcal{E}\big(\hat{\lambda}, -1\big)$ distributed under $\hat{\mathbb{P}}(R, \beta)$ with $\hat{\lambda} = \lambda - \beta$. Consequently, each Y_i follows a $\mathcal{G}_-\left(\hat{\mu}, 1\right)$ negative Gumbel distribution under $\hat{\mathbb{P}}(R, \beta)$ with $\hat{\mu} = \ln\left(\mathrm{e}^{\mu} - \beta\right)$. ■

IV.5 Conclusion

This chapter shows that the class of NEM-AJD processes is closed under an Esscher transform measure change. This result is important since it ensures that jump sizes under the physical probability measure and the ETMM fall into the same distributional class. It thus allows for a direct comparison of the corresponding two asset dynamics based on their parameter vectors. Furthermore, we fully characterize the model parameters under the new probability measure in terms of the parameters under the original probability measure and the transform parameter. A second application of this result is the change of numéraire from the bank account to the spot asset. For all NEM-AJD processes, being able to evaluate the tail probability of logarithmic asset prices under the risk-neutral probability measure is sufficient to be able to price European plain vanilla options. We show that several well-known models represent special cases of NEM-AJD processes and provide further examples.

Bibliography

Abramowitz, Milton and Irene A. Stegun eds. (1972) *Handbook of Mathematical Functions*, Applied Mathematics Series: National Bureau of Standards, 10th edition.

Aït-Sahalia, Yacine (2002) "Maximum Likelihood Estimation of Discretely Sampled Diffusions: A Closed-Form Approximation Approach," *Econometrica*, Vol. 70, No. 1, pp. 223–262.

——— (2004) "Disentangling Diffusion from Jumps," *Journal of Financial Economics*, Vol. 74, No. 3, pp. 487–528.

Bakshi, Gurdip, Charles Cao, and Zhiwu Chen (1997) "Empirical Performance of Alternative Option Pricing Models," *Journal of Finance*, Vol. 52, No. 5, pp. 2003–2049.

Ball, Clifford A. and Walter N. Torous (1983) "A Simplified Jump Process for Common Stock Returns," *Journal of Financial and Quantitative Analysis*, Vol. 18, No. 1, pp. 53–65.

Bates, David S. (2006) "Maximum Likelihood Estimation of Latent Affine Processes," *Review of Financial Studies*, Vol. 19, No. 3, pp. 909–965.

Bickel, Peter J. and Kjell A. Doksum (2001) *Mathematical Statistics*, Vol. 1: Prentice-Hall, 2nd edition.

Black, Fischer and Myron S. Scholes (1973) "The Pricing of Options and Corporate Liabilities," *Journal of Political Economy*, Vol. 3, No. 3, pp. 637–654.

Box, George E. P. and George C. Tiao (1973) *Bayesian Inference in Statistical Analysis*: John Wiley & Sons.

Cai, Ning and Steven G. Kou (2011) "Option Pricing under a Mixed-Exponential Jump Diffusion Model," *Management Science*, Vol. 57, No. 11, pp. 2067–2081.

Chan, Terence (1999) "Pricing Contingent Claims on Stocks Driven by Lévy Processes," *The Annals of Applied Probability*, Vol. 9, No. 2, pp. 504–528.

Cont, Rama and Peter Tankov (2004) *Financial Modelling with Jump Processes*: Chapman & Hall.

Cox, David (1955) "Some Statistical Methods Connected with Series of Events," *Journal of the Royal Statistical Society*, Vol. 17, No. 2, pp. 129–164.

Delbaen, Freddy and Walter Schachermayer (1994) "A General Version of the Fundamental Theorem of Asset Pricing," *Mathematische Annalen*, Vol. 300, No. 1, pp. 463–520.

Esscher, Frederik (1932) "On the Probability Function in the Collective Theory of Risk," *Scandinavian Actuarial Journal*, Vol. 15, No. 3, pp. 175–195.

Folland, Gerald B. (1984) *Real Analysis: Modern Techniques and Their Applications*: John Wiley & Sons.

Frittelli, Marco (2000) "The Minimal Entropy Martingale Measure and the Valuation Problem in Incomplete Markets," *Mathematical Finance*, Vol. 10, No. 1, pp. 39–52.

Fujiwara, Tsukasa (2009) "The Minimal Entropy Martingale Measures for Exponential Additive Processes," *Asia-Pacific Financial Markets*, Vol. 16, No. 1, pp. 65–95.

Fujiwara, Tsukasa and Yoshio Miyahara (2003) "The Minimal Entropy Martingale Measure for Geometric Lévy Processes," *Finance and Stochastics*, Vol. 7, pp. 509–531.

Geman, Hélyette, Nicole El Karoui, and Jean-Charles Rochet (1995) "Changes of Numéraire, Changes of Probability Measure and Option Pricing," *Journal of Applied Probability*, Vol. 32, No. 2, pp. 443–458.

Gerber, Hans U. and Elias S. W. Shiu (1994a) "Martingale Approach to Pricing Perpetual American Options," *Astin Bulletin*, Vol. 24, No. 2, pp. 195–220.

——— (1994b) "Option Pricing by Esscher Transforms," *Transactions of Society of Actuaries*, Vol. 46, pp. 99–191.

Harrison, J. Michael and Stanley R. Pliska (1981) "Martingales and Stochastic Integrals in the Theory of Continuous Trading," *Stochastic Processes and Their Applications*, Vol. 11, pp. 215–260.

Hubalek, Friedrich and Carlo Sgarra (2006) "Esscher Transforms and the Minimal Entropy Martingale Measure for Exponential Lévy Models," *Quantitative Finance*, Vol. 6, No. 2, pp. 125–145.

Jacod, Jean and Albert N. Shiryaev (2003) *Limit Theorems for Stochastic Processes*: Springer, 2nd edition.

Kallsen, Jan and Albert N. Shiryaev (2002) "The Cumulant Process and Esscher's Change of Measure," *Finance and Stochastics*, Vol. 6, No. 4, pp. 397–428.

Karatzas, Ioannis and Steven E. Shreve (1991) *Brownian Motion and Stochastic Calculus*: Springer, 2nd edition.

Kou, Steven G. (2002) "A Jump-Diffusion Model for Option Pricing," *Management Science*, Vol. 48, No. 8, pp. 1086–1101.

Kou, Steven G. and Hui Wang (2003) "First Passage Times of a Jump-Diffusion Process," *Advances in Applied Probability*, Vol. 35, pp. 504–531.

——— (2004) "Option Pricing under a Double Exponential Jump-Diffusion Model," *Management Science*, Vol. 50, No. 9, pp. 1178–1192.

Lucas, Robert E., Jr. (1978) "Asset Prices in an Exchange Economy," *Econometrica*, Vol. 46, No. 6, pp. 1429–1445.

Lukacs, Eugene (1970) *Characteristic Functions*: Griffin London, 2nd edition.

McLachlan, Geoffrey and David Peel (2000) *Finite Mixture Models*, Wiley Series in Probability and Statistics: John Wiley & Sons.

Merton, Robert C. (1976) "Option Pricing When Underlying Stock Returns Are Discontinuous," *Journal of Financial Economics*, Vol. 3, No. 1-2, pp. 125–144.

Milne, Frank and Dilip B. Madan (1991) "Option Pricing with V.G. Martingale Components," *Mathematical Finance*, Vol. 1, No. 4, pp. 39–55.

Miyahara, Yoshio (1999) "Minimal Entropy Martingale Measure of Jump Type Price Processes in Incomplete Asset Markets," *Asia-Pacific Financial Markets*, Vol. 6, pp. 97–113.

——— (2004) "A Note on Esscher Transformed Martingale Measures for Geometric Lévy Processes," Discussion Paper in Economics 329, Faculty of Economics, Nagoya City University.

Naik, Vasanttilak and Moon Lee (1990) "General Equilibrium Pricing of Options on the Market Portfolio with Discontinuous Returns," *Review of Financial Studies*, Vol. 3, No. 4, pp. 493–521.

Nelson, Charles R. and Andrew F. Siegel (1987) "Parsimonious Modeling of Yield Curves," *The Journal of Business*, Vol. 60, No. 4, pp. 473–489.

Ramezani, Cyrus A. and Yong Zeng (1999) “Maximum Likelihood Estimation of Asymmetric Jump-Diffusion Processes: Application to Security Prices,” Working Paper, Department of Statistics, University of Wisconsin, Madison.

——— (2007) “Maximum Likelihood Estimation of the Double Exponential Jump-Diffusion Process,” *Annals of Finance*, Vol. 3, No. 4, pp. 487–507.

Sato, Ken-iti (1999) *Lévy Processes and Infinitely Divisible Distributions*: Cambridge University Press.

Sørensen, Michael (1991) *Statistical Inference in Stochastic Processes*, Chap. Likelihood Methods for Diffusions with Jumps, pp. 67–105: Marcel Dekker.

IV.A Appendix for Section IV.2

IV.A.1 Martingale Property of Z^j

This appendix contains the detailed proof of Lemma IV.4. It is almost identical to that for Lévy processes; see for example Proposition 3.17.(i) in Cont and Tankov (2004), p. 97. Let $0 \leq s \leq t \leq T^*$, then

$$\begin{aligned}
& \mathbb{E}_{\mathbb{P}}\left[\exp\left\{\mathrm{i}\left(\alpha \circ X^j\right)_{[0,t]}\right\}\middle|\,\mathfrak{F}_s\right] \\
= \; & \exp\left\{\mathrm{i}\left(\alpha \circ X^j\right)_{[0,s]}\right\}\mathbb{E}_{\mathbb{P}}\left[\exp\left\{\mathrm{i}\left(\alpha \circ X^j\right)_{[s,t]}\right\}\right] \\
= \; & \exp\left\{\mathrm{i}\left(\alpha \circ X^j\right)_{[0,s]} + \int_s^t \lambda(u)\left(\phi_Y(u,\alpha(u)) - 1\right)\mathrm{d}u\right\}.
\end{aligned}$$

Here, we used the independence of $\left(\alpha \circ X^j\right)_{[s,t]}$ of $\mathfrak{F}_s$ in the second and Proposition IV.1 in the third step. We divide this expression by

$$\mathbb{E}_{\mathbb{P}}\left[\exp\left\{\mathrm{i}\left(\alpha \circ X^j\right)_{[0,t]}\right\}\right] = \exp\left\{\int_0^t \lambda(u)\left(\phi_Y(u,\alpha(u)) - 1\right)\mathrm{d}u\right\}$$

and use the linearity of the integral to obtain the result.

IV.A.2 $\hat{X}^j$ Is an Additive Process

This appendix contains the detailed proof of Lemma IV.1. It only remains to establish the stochastic continuity of X^j. For any interval we can bound the probability of the absolute change in X^j being greater than some value ϵ by the probability of observing at least one jump during this time.

$$\begin{aligned}
\mathbb{P}\left\{\left|X^j_{t+h} - X^j_t\right| > \epsilon\right\} & \leq 1 - \mathbb{P}\left\{\int_t^{t+h}\int_{-\infty}^{\infty} J_X(\mathrm{d}u \times \mathrm{d}x) = 0\right\} \\
& = 1 - \exp\left\{-\mu([t,t+h] \times \mathbb{R})\right\}.
\end{aligned}$$

Here, we used that by Definition IV.2 the total number of jumps on the set $A = [t, t+h] \times \mathbb{R}$ follows a Poisson distribution with mean $\mu(A)$. Taking the limit as $h \downarrow 0$, the right-hand side converges to zero and the stochastic continuity of X^j follows.

IV.A.3 Time-Changed Compound Poisson Representation

This appendix contains the detailed proof of Lemma IV.5. Just like for standard compound Poisson processes, we use iterated conditional expectations to obtain

$$\begin{aligned}
\phi_{X_t^j}(\omega) &= \sum_{n=0}^{\infty} \{N_t = n\} \left(\phi_Y(\omega)\right)^n \mathbb{P} \\
&= \sum_{n=0}^{\infty} \frac{\mathrm{e}^{-\zeta(t)} \left(\zeta(t)\phi_Y(\omega)\right)^n}{n!} \\
&= \exp\left\{\int_0^t \lambda(u) \left(\phi_Y(\omega) - 1\right) \mathrm{d}u\right\}.
\end{aligned}$$

Here, $\zeta(t)$ is the total jump intensity over the interval $[0, t]$ as previously defined in Section IV.2.1. This expression is equal to the one given in Corollary IV.1 when the jump size distribution is time-homogeneous. The result then follows from the uniqueness of the characteristic function; see for example Theorem 3.1.1 in Lukacs (1970), p. 28.

IV.B Appendix for Section IV.3

IV.B.1 $\hat{X}$ Is a Radon-Nikodým Derivative Process

This appendix contains the detailed proof of Lemma IV.7. First, the independence of X^c and X^j and the linearity of the stochastic integral allow us to decompose $\hat{X}$ into two factors $\hat{X}_t^c = \left\{\hat{X}_t^c : t \in [0, T^*]\right\}$ and $\hat{X}_t^j = \left\{\hat{X}_t^j : t \in [0, T^*]\right\}$, that is $\hat{X}_t = \hat{X}_t^c \hat{X}_t^j$. Here,

$$\hat{X}_t^i = \exp\left\{\left(\beta \circ X^i\right)_{[0,t]}\right\} \left(\mathbb{E}_{\mathbb{P}}\left[\exp\left\{\left(\beta \circ X^i\right)_{[0,t]}\right\}\right]\right)^{-1},$$

where $i \in \{c, j\}$. If we can show that both $\hat{X}_t^c$ and $\hat{X}_t^j$ are $(\mathbb{P}, \mathbb{F})$-martingales then it follows that $\hat{X}$ is one as well. First, note that by Proposition IV.2 with $\alpha(t) = -\mathrm{i}\beta(t)$

$$\begin{aligned}
\hat{X}_t^c &= \exp\left\{\int_0^t \beta(u)\sigma(u)\mathrm{d}W_u - \frac{1}{2}\int_0^t \beta^2(u)\sigma^2(u)\mathrm{d}u\right\} \\
&= \mathcal{E}_t\left(\int_0^{\cdot} \beta(u)\sigma(u)\mathrm{d}W_u\right),
\end{aligned}$$

where $\mathcal{E}$ denotes the Doléans-Dade exponential. The Novikov condition, see for example Proposition III.5.12 in Karatzas and Shreve (1991), p. 198, states that a sufficient condition for $\hat{X}^c$ to be a martingale is given by

$$\exp\left\{\frac{1}{2}\int_0^t \beta^2(u)\sigma^2(u)\mathrm{d}u\right\} < \infty.$$

This is ensured to hold for all $0 \leq t \leq T^*$ by the restriction imposed on the parameter functions in Definition IV.8. Next, again from Proposition IV.1 with $\alpha(t) = -\mathrm{i}\beta(t)$ we get

$$\begin{aligned} X_t^j &= \exp\left\{\int_0^t \int_{-\infty}^{+\infty} \beta(u)xJ_X(\mathrm{d}u\times \mathrm{d}x) - \int_0^t \int_{-\infty}^{+\infty} \left(\mathrm{e}^{\beta(u)x} - 1\right)\lambda(u)f(u,x)\mathrm{d}x\mathrm{d}u\right\} \\ &= \mathcal{E}_t\left(\int_0^{\cdot} \int_{-\infty}^{+\infty} \beta(u)xJ_X(\mathrm{d}u\times \mathrm{d}x)\right). \end{aligned}$$

Once more, it follows from the restriction imposed on the transform parameter and the intensity measure that X^j is a $(\mathbb{P},\mathbb{F})$-martingale; see for example Proposition 3.6 in Cont and Tankov (2004), p. 78.

IV.B.2 Characteristic Function of X^j under $\hat{\mathbb{P}}(X,\beta)$ Part I

This appendix contains the detailed proof of Proposition IV.3. We start by computing the characteristic function $\hat{\phi}_{X_t^j}(\omega)$ of X^j under $\hat{\mathbb{P}}(X,\beta)$. We change the probability measure to $\mathbb{P}$ and get

$$\begin{aligned} \hat{\phi}_{X_t^j}(\omega) &= \mathbb{E}_{\hat{\mathbb{P}}}\left[\exp\left\{\mathrm{i}\omega X_t^j\right\}\right] \\ &= \mathbb{E}_{\mathbb{P}}\left[\xi_t\big(\mathbb{P},\hat{\mathbb{P}}\big)\exp\left\{\mathrm{i}\omega X_t^j\right\}\right] \\ &= \mathbb{E}_{\mathbb{P}}\left[\exp\left\{\int_0^t (\mathrm{i}\omega+\beta(u))\,\mathrm{dX}_u^j - \int_0^t\int_{-\infty}^{+\infty}\left(\mathrm{e}^{\beta(u)x}-1\right)\lambda(u)f(u,x)\mathrm{d}x\mathrm{d}u\right\}\right]. \end{aligned}$$

Note, that due to the independence of X^c and X^j, the characteristic functions of X^j under $\hat{\mathbb{P}}(X,\beta)$ and under $\hat{\mathbb{P}}\left(X^j,\beta\right)$ coincide. Formally, we substituted for $\xi_t\big(\mathbb{P},\hat{\mathbb{P}}\big)$ in the last equality, using that

$$\mathcal{E}_t\left(\int_0^{\cdot}\beta(u)\mathrm{d}X_u^c\right) = \exp\left\{\int_0^t \beta(u)\mathrm{d}X_u^c - \frac{1}{2}\int_0^t \beta^2(u)\mathrm{d}\langle X^c\rangle_t\right\}$$

is a $(\mathbb{P},\mathbb{F})$-martingale starting at one. Continuing with the computation of $\hat{\phi}_{X_t^j}(\omega)$, we obtain

$$\begin{aligned} \hat{\phi}_{X_t^j}(\omega) &= \exp\left\{\int_0^t\int_{-\infty}^{+\infty}\left(\mathrm{e}^{(\mathrm{i}\omega+\beta(u))x} - \mathrm{e}^{\beta(u)x}\right)\lambda(u)f(u,x)\mathrm{d}x\mathrm{d}u\right\} \\ &= \exp\left\{\int_0^t\int_{-\infty}^{+\infty}\left(\mathrm{e}^{\mathrm{i}\omega x}-1\right)\lambda(u)\mathrm{e}^{\beta(u)x}f(u,x)\mathrm{d}x\mathrm{d}u\right\}. \end{aligned}$$

Here, we again used Proposition IV.1 to compute the remaining expectation. This last expression already closely resembles the characteristic function of an ACP process given in Corollary IV.1. However, the term $\mathrm{e}^{\beta(u)x} f(u,x)$ is in general not a valid PDF but requires re-normalization. Let $\xi : \mathbb{R}_+ \to \mathbb{R}_+$ be a deterministic normalizing function such that for every $0 \le t \le T^*$ we have

$$\frac{1}{\xi(t)} \int_{-\infty}^{+\infty} \mathrm{e}^{\beta(t)x} f(t,x)\mathrm{d}x = 1 \qquad \Leftrightarrow \qquad \begin{aligned} \xi(t) &= \int_{-\infty}^{+\infty} \mathrm{e}^{\beta(t)x} f(t,x)\mathrm{d}x \\ &= \phi_Y(t, -\mathrm{i}\beta(t)). \end{aligned}$$

The condition imposed on $\beta(t)$ ensures that the $\beta(t)$-th exponential moment of $f(t,x)$ exists for all $0 \le t \le T^*$. Here, we defined $\phi_Y(t,\omega)$, in analogy to the representation of the TCCP process in Lemma IV.5, to be the characteristic function of the PDF $f(t,x)$. Then

$$\hat{\phi}_{X_t^j}(\omega) = \exp\left\{ \int_0^t \int_{-\infty}^{+\infty} \left(\mathrm{e}^{\mathrm{i}\omega x} - 1\right) \hat{\lambda}(u) \hat{f}(u,x)\mathrm{d}x\mathrm{d}u \right\},$$

where for all $0 \le t \le T^*$

$$\begin{aligned} \hat{\lambda}(t) &= \lambda(t)\phi_Y(t, -\mathrm{i}\beta(t)), \\ \hat{f}(t,x) &= \frac{\mathrm{e}^{\beta(t)x} f(t,x)}{\phi_Y(t, -\mathrm{i}\beta(t))}. \end{aligned}$$

Again, the condition imposed on $\beta(t)$ ensures that

$$\int_0^{T^*} \hat{\lambda}(u)\mathrm{d}u < \infty.$$

Thus, $\hat{\lambda}(t)$ is a valid jump intensity function as required by Definition IV.3. Simplifying further gives

$$\begin{aligned} \hat{\phi}_{X_t^j}(\omega) &= \exp\left\{ \int_0^t \hat{\lambda}(u) \left(\frac{\phi_Y(t, \omega - \mathrm{i}\beta(t))}{\phi_Y(t, -\mathrm{i}\beta(t))} - 1 \right) \mathrm{d}u \right\} \\ &= \exp\left\{ \int_0^t \hat{\lambda}(u) \big(\hat{\phi}_Y(t,\omega) - 1 \big) \mathrm{d}u \right\}, \end{aligned}$$

where

$$\hat{\phi}_Y(t,\omega) = \frac{\phi_Y(t, \omega - \mathrm{i}\beta(t))}{\phi_Y(t, -\mathrm{i}\beta(t))}.$$

The Proposition follows by the uniqueness of the characteristic function. Note that the last step was not necessary for the proof but yields the characteristic function $\hat{\phi}_Y(t,\omega)$ of the PDF $\hat{f}(t,x)$ as a useful side result.

IV.C Appendix for Section IV.4

IV.C.1 Characteristic Function of Natural Exponential Families

This appendix contains the detailed proof of Lemma IV.10. We have

$$\begin{aligned}
\phi_Z(\omega;\theta) &= \int_{-\infty}^{+\infty} \mathrm{e}^{\mathrm{i}\omega x} f(x;\theta)\mathrm{d}x \\
&= \int_{-\infty}^{+\infty} a(x) \exp\left\{(\theta+\mathrm{i}\omega)x - b(x)\right\} \mathrm{d}x \\
&= \exp\left\{b(\theta+\mathrm{i}\omega) - b(\theta)\right\} \int_{-\infty}^{+\infty} a(x) \exp\left\{(\theta+\mathrm{i}\omega)x - b(\theta+\mathrm{i}\omega)\right\} \mathrm{d}x \\
&= \exp\left\{b(\theta+\mathrm{i}\omega) - b(\theta)\right\} \int_{-\infty}^{+\infty} f(x;\theta+\mathrm{i}\omega)\mathrm{d}x.
\end{aligned}$$

To compute the remaining integral, we notice that if $\omega \in \mathbb{C}$ was a strictly complex number with $\mathfrak{Re}(\omega) = 0$, then the integrand would be real valued and we would recognize this expression as an integral over the full support of a PDF. It would thus evaluate to one. However, the transform parameter $\omega \in \mathbb{R}$ is a real number and thus this argument cannot be directly employed. Instead, we can expand the exponent as a Taylor series around $\omega = 0$ to obtain

$$\begin{aligned}
\mathrm{e}^{-b(\theta+\mathrm{i}\omega)} \int_{-\infty}^{+\infty} a(x)\mathrm{e}^{(\theta+\mathrm{i}\omega)x}\mathrm{d}x &= \mathrm{e}^{-b(\theta+\mathrm{i}\omega)} \int_{-\infty}^{+\infty} \sum_{n=0}^{\infty} a(x)\frac{(\mathrm{i}\omega x)^n}{n!}\mathrm{e}^{\theta x}\mathrm{d}x \\
&= \mathrm{e}^{-b(\theta+\mathrm{i}\omega)} \sum_{n=0}^{\infty} \frac{(\mathrm{i}\omega)^n}{n!} \int_{-\infty}^{+\infty} a(x)x^n\mathrm{e}^{\theta x}\mathrm{d}x.
\end{aligned}$$

Furthermore it follows from the definition of the NE family that

$$\begin{aligned}
\frac{\partial^n}{\partial\xi^n}\mathrm{e}^{b(\xi)} &= \frac{\partial^n}{\partial\xi^n}\int_{-\infty}^{+\infty} a(x)\mathrm{e}^{\xi x}\mathrm{d}x \\
&= \int_{-\infty}^{+\infty} a(x)x^n\mathrm{e}^{\xi x}\mathrm{d}x.
\end{aligned}$$

Consequently,

$$\frac{\partial}{\partial\omega^n}\left\{\mathrm{e}^{b(\theta+\mathrm{i}\omega)}\right\}(0) = \mathrm{i}^n \int_{-\infty}^{+\infty} a(x)x^n\mathrm{e}^{\theta x}\mathrm{d}x,$$

which shows that the sum is a Taylor series expansion of the reciprocal of the first term around $\omega = 0$. As a result, the remaining integral does vanish and we obtain

$$\phi_Z(\omega;\theta) = \exp\left\{b(\theta+\mathrm{i}\omega) - b(\theta)\right\}.$$

IV.C.2 Characteristic Function of $\boldsymbol{X}^j$ under $\hat{\mathbb{P}}(\boldsymbol{X}, \boldsymbol{\beta})$ Part III

This appendix contains the detailed proof of Proposition IV.5. Using Proposition IV.3 in conjunction with Definitions IV.12 and IV.14 we get

$$\begin{aligned}
& \hat{f}\left(t, x; \boldsymbol{\theta}(t), \boldsymbol{w}(t), \beta(t)\right) \\
= & \sum_{i=1}^{n} \frac{w_i(t)}{\phi_Y(t, -\mathrm{i}\beta(t))} a_i(t,x) \exp\left\{\left(\theta_i(t) + \beta(t)\right) x - b_i\left(t, \theta_i(t)\right)\right\}.
\end{aligned}$$

While this expression already resembles the structure of an NEM family, we observe that the exponentials in the summands are not properly normalized; compare to Definition IV.12. We thus substitute for $\hat{\theta}_i(t) = \theta_i(t) + \beta(t)$ and add and subtract the normalization term to obtain

$$\begin{aligned}
\ldots = & \sum_{i=1}^{n} \frac{w_i(t)}{\phi_Y(t, -\mathrm{i}\beta(t))} a_i(t,x) \exp\left\{\hat{\theta}_i(t)x - b_i\left(t, \theta_i(t)\right) \pm b_i\big(t, \hat{\theta}_i(t)\big)\right\} \\
= & \sum_{i=1}^{n} \frac{w_i(t)\phi_{A_i}(t, -\mathrm{i}\beta)}{\phi_Y(t, -\mathrm{i}\beta(t))} a_i(t,x) \exp\left\{\hat{\theta}_i(t)x - b_i\big(t, \hat{\theta}_i(t)\big)\right\},
\end{aligned}$$

where we define

$$\phi_{A_i}(t, \omega) = \exp\left\{b_i\left(t, \theta_i(t) + \mathrm{i}\omega\right) - b_i\left(t, \theta_i(t)\right)\right\}$$

to be the time $0 \leq t \leq T^*$ characteristic function of the i-th mixing component under the original probability measure $\mathbb{P}$; see also the discussion following Definition IV.14. We thus set

$$\hat{w}_i(t) = \frac{w_i(t)\phi_{A_i}(t, -\mathrm{i}\beta(t))}{\phi_Y(t, -\mathrm{i}\beta(t))}$$

and it remains to show that $\hat{\boldsymbol{w}}(t)$ is a vector of non-negative real numbers that sum to one. First, we recognize $\phi_{A_i}(t, -\mathrm{i}\beta(t))$ and $\phi_Y(t, -\mathrm{i}\beta(t))$ as the time $0 \leq t \leq T^*$ moment generating functions of the i-th mixing density and the jump size distribution under $\mathbb{P}$, evaluated at $\beta(t)$. Their existence is ensured by the assumption made in Proposition IV.3. Since a moment generating function is the expected value of a strictly positive random variable, it follows that it is strictly positive itself; see for example Theorem 7.1.4 in Lukacs (1970), p. 197. From $w_i(t) \geq 0$ for all $i = 1, 2, \ldots, n$ it then follows that $\hat{w}_i(t) \geq 0$ as well.

Finally, it is not hard to see that

$$\begin{aligned}\sum_{i=1}^{n} \hat{w}_i(t) &= \frac{1}{\phi_Y(t, -\mathrm{i}\beta(t))} \sum_{i=1}^{n} w_i \phi_{A_i}(t, -\mathrm{i}\beta(t)) \\ &= \frac{\phi_Y(t, -\mathrm{i}\beta(t))}{\phi_Y(t, -\mathrm{i}\beta(t))} \\ &= 1,\end{aligned}$$

where we use Lemma IV.11.

Alternatively, we can use Corollary IV.2 in conjunction with the representation of the characteristic function for NEM families in Lemma IV.11 to obtain

$$\hat{\phi}_Z(t, \omega) = \sum_{i=1}^{n} \frac{w_i(t)}{\phi_Y(t, -\mathrm{i}\beta(t))} \exp\left\{b_i\left(t, \theta_i(t) + \beta(t) + \mathrm{i}\omega\right) - b_i\left(t, \theta_i(t)\right)\right\}.$$

Again, by multiplying and dividing through $\phi_{A_i}\left(t, -\mathrm{i}\beta(t)\right)$, we obtain the characteristic function of an NEM distribution with the given weights $\hat{w}_i(t)$.

IV.C.3 Student's *T*-Distribution as a Gaussian Mean Variance Mixture

This appendix contains additional details for Example IV.7. Setting $\mu = \xi = 0$, $\sigma = 1$ and $\gamma = \delta = \nu/2$ in the normal inverse gamma distribution function yields

$$\begin{aligned}f_X(x) &= \int_0^\infty \frac{(\nu/2)^{\nu/2}}{\Gamma(\nu/2)} y^{-\nu/2-1} \exp\left\{-\frac{\nu}{2y}\right\} \frac{1}{\sqrt{2\pi y}} \exp\left\{-\frac{x^2}{2y}\right\} \mathrm{d}y \\ &= \frac{(\nu/2)^{\nu/2}}{\sqrt{2\pi}\Gamma(\nu/2)} \int_0^\infty y^{-(\nu+1)/2-1} \exp\left\{-\frac{x^2+\nu}{2y}\right\} \mathrm{d}y.\end{aligned}$$

We make a change of variables by setting $y = 1/z$ to obtain

$$\begin{aligned}\ldots &= \frac{(\nu/2)^{\nu/2}}{\sqrt{2\pi}\Gamma(\nu/2)} \int_0^\infty z^{(\nu+1)/2-1} \exp\left\{-\frac{\left(x^2+\nu\right) z}{2}\right\} \mathrm{d}z \\ &= \frac{(\nu/2)^{\nu/2}\Gamma((\nu+1)/2)}{\sqrt{2\pi}\Gamma(\nu/2)} \left(\frac{x^2+\nu}{2}\right)^{-(\nu+1)/2}.\end{aligned}$$

See Section 6.1.1 in Abramowitz and Stegun (1972), p. 251, for the solution of the integral used in the second equality. Another simplification finally yields

$$\ldots = \frac{\Gamma((\nu+1)/2)}{\sqrt{\nu\pi}\Gamma(\nu/2)} \left(1 + \frac{x^2}{\nu}\right)^{-(\nu+1)/2}.$$

IV.D Parameters for Common Natural Exponential Families

This appendix contains an alphabetically sorted overview of common NE families that might be used in mixture models for the jump size distribution. This list is by no means exhaustive. Often, however, the distributions listed here nest other NE families as special cases such that the results still apply. For each distribution, we state the parametrization under $\mathbb{P}$ and $\hat{\mathbb{P}}(X,\beta)$, the PDF $f(x)$ under $\mathbb{P}$, the natural parameter θ as well as the two functions $a(x)$ and $b(\theta)$.

IV.D.1 Exponential Distribution

$$\begin{aligned}
\mathcal{E}(\lambda) &\Rightarrow \mathcal{E}(\lambda-\beta) \\
f(x) &= \lambda e^{-\lambda x} 1\{x>0\} \\
\theta &= -\lambda \\
a(x) &= 1\{x>0\} \\
b(\theta) &= -\ln(-\theta)
\end{aligned}$$

IV.D.2 Gamma Distribution

$$\begin{aligned}
\Gamma(a,b) &\Rightarrow \Gamma\left(a, \frac{b}{1-b\beta}\right) \\
f(x) &= \frac{1}{\Gamma(a)b^a} x^{a-1} e^{-x/b} 1\{x>0\} \\
\theta &= -\frac{1}{b} \\
a(x) &= \frac{1}{\Gamma(a)} x^{a-1} 1\{x>0\} \\
b(\theta) &= a \ln\left(-\frac{1}{\theta}\right)
\end{aligned}$$

IV.D.3 Generalized Inverse Gaussian Distribution

$$
\begin{aligned}
\mathrm{GIG}(a,b,p) &\Rightarrow \mathrm{GIG}(a-2\beta,b,p) \\
f(x) &= \frac{(a/b)^{p/2}}{2K_p(\sqrt{ab})}x^{p-1}\exp\left\{-\frac{ax+b/x}{2}\right\}1\{x>0\} \\
\theta &= -\frac{a}{2} \\
a(x) &= \frac{1}{2b^{p/2}}x^{p-1}\exp\left\{-\frac{b}{2x}\right\}1\{x>0\} \\
b(\theta) &= \ln\left(K_p(-2\theta b)\right) - \frac{p}{2}\ln(-2\theta)
\end{aligned}
$$

IV.D.4 Hyperbolic Distribution

$$
\begin{aligned}
\mathrm{Hyp}(\mu,a,b,\delta) &\Rightarrow \mathrm{Hyp}(\mu,a,b+\beta,\delta) \\
f(x) &= \frac{\sqrt{a^2-b^2}}{2a\delta K_1(\delta\sqrt{a^2-b^2})}\exp\left\{-a\sqrt{\delta^2+(x-\mu)^2}+b(x-\mu)\right\} \\
\theta &= b \\
a(x) &= \frac{\sqrt{a^2-b^2}}{2a\delta K_1(\delta\sqrt{a^2-b^2})}\exp\left\{-a\sqrt{\delta^2+(x-\mu)^2}\right\} \\
b(\theta) &= \mu b
\end{aligned}
$$

IV.D.5 Inverse Gaussian Distribution

$$
\begin{aligned}
\mathrm{IG}(\mu,\lambda) &\Rightarrow \mathrm{IG}\left(\sqrt{\frac{\mu^2\lambda}{\lambda-2\mu^2\beta}},\lambda\right) \\
f(x) &= \sqrt{\frac{\lambda}{2\pi x^3}}\exp\left\{-\frac{\lambda(x-\mu)^2}{2\mu^2 x}\right\}1\{x>0\} \\
\theta &= -\frac{\lambda}{2\mu^2} \\
a(x) &= \sqrt{\frac{\lambda}{2\pi x^3}}\exp\left\{-\frac{\lambda}{2x}\right\}1\{x>0\} \\
b(\theta) &= -\sqrt{-2\theta\lambda}
\end{aligned}
$$

IV.D.6 Normal Distribution

$$
\begin{aligned}
\mathcal{N}\left(\mu, \sigma^2\right) &\Rightarrow \mathcal{N}\left(\mu + \beta\sigma^2, \sigma^2\right) \\
f(x) &= \frac{1}{\sqrt{2\pi}\sigma} \exp\left\{-\frac{(x-\mu)^2}{2\sigma^2}\right\} \\
\theta &= \frac{\mu}{\sigma^2} \\
a(x) &= \frac{1}{\sqrt{2\pi}\sigma} \exp\left\{-\frac{x^2}{2\sigma^2}\right\} \\
b(\theta) &= \frac{(\theta\sigma)^2}{2}
\end{aligned}
$$

IV.E Glossary of Notation

$\square$	end of a proof
$\blacksquare$	end of an example
$\triangle$	end of a definition
$1\{A\}$	indicator of the set A
ACP	additive compound Poisson
AJD	additive jump-diffusion
$\mathbb{P}^A$-a.s.	almost surely under $\mathbb{P}^A$
$\mathcal{B}(A)$	Borel σ-algebra on the set A
$\beta(t)$	Esscher transform parameter function
$\mathcal{D}_{\mathrm{NE}}(b(\cdot))$	class of NE families
$\mathcal{D}_{\mathrm{NEM}}(b(\cdot))$	class of NEM families
D-$\mathcal{E}(\cdot)$	displaced exponential distribution
$\mathcal{E}$	Borel σ-algebra on the set E
$\mathcal{E}(\lambda)$	exponential distribution with rate parameter λ
$\mathcal{E}_t(X_\cdot)$	Doléans-Dade exponential of the process X
$\mathbb{E}_{\mathbb{P}^A}$	expectation under $\mathbb{P}^A$
ETMM	Esscher transform martingale measure
ETPM	Esscher transform probability measure
$\mathbb{F}$	sigma algebra
$\mathfrak{F}_t$	filtration at time t
$f(t,x)$	ACP jump size PDF
$\mathcal{G}(\mu,\sigma)$	Gumbel distribution with local parameter μ and scale parameter σ
$\gamma(t)$	ACP drift function
$\Gamma(a,b)$	gamma distribution with shape parameter a and scale parameter b
i	imaginary unit
i.i.d.	independent and identically distributed
J_X	Poisson random measure of the process X
$\lambda(t)$	ACP jump intensity function
$\mathcal{M}(\mathbb{P})$	set of martingale measures equivalent to $\mathbb{P}$
M-$\mathcal{E}(\cdot)$	displaced mixed exponential distribution
MEMM	minimal entropy martingale measure

μ	intensity measure
N^A	one-dimensional Poisson process under $\mathbb{P}^A$
$\mathcal{N}\left(\gamma, \delta^2\right)$	normal distribution with mean γ and variance δ^2
$\mathcal{N}\text{-}\Gamma^{-1}(\cdot)$	normal inverse gamma distribution
NE	natural exponential
NEM	natural exponential mixture
Ω	probability space
$\mathbb{P}^*$	bank account martingale measure/risk-neutral measure
$\mathcal{P}(X)$	set of all ETPM with respect to X
$\hat{\mathbb{P}}(X, \beta)$	ETPM of the risk process X with parameter β
PDF	probability density function
$\phi_X^A(\omega)$	characteristic function of the random variable X under $\mathbb{P}^A$
$r(t)$	continuously compounded risk-free interest rate
$\sigma(t)$	AJD diffusion function
T^*	terminal time
$T(\nu)$	student's t-distribution with ν degrees of freedom
$\theta(t)$	NE parameter function
THJD	time-homogeneous jump-diffusion
W^A	standard one-dimensional Brownian motion under $\mathbb{P}^A$
$w(t)$	NEM-ACP weight function
$\xi\left(\mathbb{P}^A, \mathbb{P}^B\right)$	Radon-Nikodým derivative process between $\mathbb{P}^A$ and $\mathbb{P}^B$
$\zeta(t)$	ACP total jump intensity over the interval $[0, t]$

Chapter V

Conclusion

This dissertation discusses three contemporary topics in financial engineering. Here, we briefly summarize the main contributions of Chapters II through IV and propose potential avenues of future research.

Chapter II proposes the most general jump-diffusion model yet that admits closed-form solutions for European plain vanilla option prices. The corresponding valuation functions are both numerically robust and computationally fast to evaluate. Empirical estimations provide strong evidence that our newly introduced asymmetrical displacement terms are both jointly and individually highly statistically significant. In particular, we can reject the Kou (2002) double exponential jump-diffusion model for all assets. We find that the empirical jump size distribution of most assets in the sample is consistent with exponential tails. The additional flexibility offered by gamma tails with an inter-valued shape parameter only improves the empirical fit for a single asset.

We approach the model selection problem by choosing the dynamics that provide the best fit to the historical time series of logarithmic returns conditional on the availability of closed-form solutions for European plain vanilla options. However, other selection criteria are equally reasonable. Following Bakshi et al. (1997), future research could investigate whether and by how much our model improves the robustness of the corresponding replication portfolios.

Chapter III introduces a novel framework that jointly addresses the pricing and risk management of deferred start barrier options. We consider markets where the implied volatility exhibits a smile pattern and a the underlying asset dynamics are discontinuous. We formulate an adjusted valuation problem in terms of a deferred start piecewise exponential barrier option on a constant coefficient geometric Brownian motion asset. It is solved iteratively by introducing the image operator for exponential barriers. These results are novel and further applications to another well-known problem are proposed below. A Monte Carlo simulation study confirms the improved robustness of our approach.

Future research could explore further applications of piecewise exponential barrier options. Following Omberg (1987), the valuation function for a down & out put with a piecewise exponential barrier could be applied to find an improved approximation to the value of American put options. In addition to the results obtained in this dissertation, this requires the valuation of a slightly different rebate structure and the characterization of the optimal parameters defining the early exercise boundary.

Chapter IV shows that the class of natural exponential mixture additive compound Poisson processes is closed under an Esscher transform measure change. This result is important when not only the risk-neutral but also the physical model dynamics are of interest. Furthermore, it reduces the European plain vanilla option pricing problem to finding the tail probabilities under the risk-neutral probability measure.

Bibliography

Bakshi, Gurdip, Charles Cao, and Zhiwu Chen (1997) "Empirical Performance of Alternative Option Pricing Models," *Journal of Finance*, Vol. 52, No. 5, pp. 2003–2049.

Kou, Steven G. (2002) "A Jump-Diffusion Model for Option Pricing," *Management Science*, Vol. 48, No. 8, pp. 1086–1101.

Omberg, Edward (1987) "The Valuation of American Put Options with Exponential Exercise Policies," *Advances in Futures and Options Research*, Vol. 2, pp. 117–142.